UNIVERSITY OF SEVILLE

FACULTY OF PHARMACY

DEPARTMENT OF PHARMACOLOGY

Antioxidant, antitumor, and anti-inflammatory activity of natural products obtained from the brown alga *Cystoseira usneoides*

Thesis submitted in fulfillment of the requirements for the award of the degree of

DOCTOR in PHARMACY (Ph.D.)

Hanaa Zbakh

Seville, June 2019

VIRGINIA MOTILVA SÁNCHEZ**,** Catedrática de Universidad del Departamento de Farmacología de la Universidad de Sevilla, y EVA ZUBÍA MENDOZA, Catedrática de Universidad del Departamento de Química Orgánica de la Universidad de Cádiz,

CERTIFICAN:

Que la presente Tesis Doctoral titulada "Antioxidant, antitumor, and anti-inflammatory activity of natural products obtained from the brown alga *Cystoseira usneoides*", ha sido realizada bajo su dirección por HANAA ZBAKH para aspirar al grado de Doctor en Farmacia.

Sevilla, 24 de junio de 2019

Fdo.: Virginia Motilva Sánchez Fdo.: Eva Zubía Mendoza

MARÍA CONCEPCIÓN PÉREZ GUERRERO**,** Directora del Departamento de Farmacología de la Universidad de Sevilla,

CERTIFICA:

Que la presente Tesis Doctoral titulada "Antioxidant, antitumor, and anti-inflammatory activity of natural products obtained from the brown alga *Cystoseira usneoides*", realizada por HANAA ZBAKH para aspirar al grado de Doctor en Farmacia, ha sido dirigida por la Dra. Virginia Motilva Sánchez y la Dra. Eva Zubía Mendoza, cumpliendo los requisitos para este tipo de trabajo.

Sevilla, 24 de junio de 2019

Fdo.:María Concepción Pérez Guerrero

ACKNOWLEDGMENTS

With passion and curiosity about science, I traveled from Morocco to Spain to pursue my Ph.D at Faculty of Pharmacy-University of Seville in collaboration with the University of Cadiz. My research life in my new lab and new working atmosphere was new and different for me, but very exciting. During this long journey, there was happy and sadness, excitement and depression, encourage and disappointment, progress and retrogress, success and failure, gain and loss, all these feelings allowed me continue my destiny without despair or frustration till I've reached my goals and achieved my greatest dream.

First and foremost, I have been lucky to have two supervisors who are real supervisors with high sense of responsibility and whose personalities and areas of expertise and supervising styles harmoniously complement each other. **Virginia Motilva**, I am very grateful for believing in me, supporting, and inspiring me throughout my studies. I am amazed by your energy, drive, and dedication to, not only science, but also family. I am so grateful that I get to be part of your second family, the research family.

Eva Zubia, my brilliant co-supervisor, full of energy, thank you for leading me to the fantastic world of chemistry. Thanks for all the professional meetings and discussions and time you took out of your busy schedules to revise my manuscript and thesis. Our discussions were a great pleasure, and it was wonderful to be inspired by your critical-thinking and deep knowledge.

Special mention goes to my Professor **Hassane Riadi,** who has been a truly dedicated mentor. I would like to express my special appreciation and to thank you for encouraging my research and for allowing me to grow as a research scientist. Your advice on both research as well as on my career have been invaluable.

Elena Talero, you are such a kind and caring person, thank you for your tremendous support. Thank you for your patience and for teaching me everything about the in vivo experiment. Your knowledge and laboratory skills have been such a great asset.

My sincere thanks to **Carolina De los Reyes** from the Department of Organic Chemistry, Faculty of Marine and Environmental Sciences, University of Cádiz, for her great help and her contributions to the phytochemical work.

Thank you, **Javier Avila**, for supporting and helping me, especially with the cell experiments. You have a fantastic enthusiasm, never let anyone take it away!

To my colleagues, my co-authors and my friends from **FARMOLAP** group: **Antonio**, **Azahara**, **Jose Antonio**, **Jesus**, **Bui**: I couldn't have asked for a better team to work with. I miss you all and I hope to have the opportunity to meet you in the future.

Many thanks to all professors and members of the department of Pharmacology, you have jointly created an open and friendly work environment, to talk about research, to have lunch together and for sharing with me the fun of lab work.

I am so grateful to **Carmen Claro**, for making work at the Lab so much easier with all your support and help, you are truly valued.

I am also very grateful to all technicians at CITIUS, especially to **Modesto** who was always so helpful and provided me the technical support to analyze Flow cytometry throughout my dissertation.

I truly appreciate my lovely friends, **Hanaa**, **Houda**, **Ghizlane** and **Mustapha**, for cheering me on throughout this journey. I wouldn't have made it without you.

A big thanks to all my colleagues and professors of the Department of Biology at University of Abdelmalek Essaadi in Morocco, for being like a friend and for giving me considerate advice both in career and life.

تعجز الكلمات عن التعبير لمدى شكري، امتناني وحبي لأغلى الناس في قلبي أمي وأبي، هما سندي في الحياة، سر قوتي وسبب عزيمتي لتحقيق أحلامي، كل كلمات الشكر لا تفي حقكم...
أخي، أخواتي العزيزات، أنتم كنزي في هذه الحياة، شكرا لكم على دعمي ومساندتي دائما وأبدا، أحبكم...

TABLE OF CONTENTS

LIST OF ABBREVIATIONS

A2780	Human ovarian carcinoma cell line
A431	Human epidermoid carcinoma cell line
A549	Human carcinomic alveolar basal epithelial cell line
ABTS	2,2'-azinobis (3-ethylbenzothiazoline-6-sulphonic acid)
AGS	Human gastric adenocarcinoma cell line
AKT	Aerine/threonine protein kinase
AMT	Algal meroterpenoid
APCI	Atmospheric Pressure Chemical Ionization
ATCC	American Type Culture Collection
B16	Murine melanoma cell line
B16F10	Murine melanoma cell line
Bad	Bcl-2-associated death promoter
Bak	Bcl-2 homologous antagonist killer
Bax	Bcl-2–associated X protein
Bcl-2	B-cell leukemia/lymphoma 2-like proteins
Bcl-xL	B-cell lymphoma-extra large
BCRP	Breast cancer resistance protein
BE2-C	Human neuroblastoma cell line
BHT	Butylated hydroxytoluene
^{13}C NMR	Carbon-13 Nuclear Magnetic Resonance
Caco-2	Human epithelial colorectal adenocarcinoma cells
CADO-ES-1	Human Ewing's sarcoma cell line
Caspase	Cysteinyl-aspartate-cleaving proteases
CC	Column Chromatography
CDK (Cdc)	Cyclin-dependent kinases
Chk2	Checkpoint kinase 2
COLO205	Human Caucasian colon adenocarcinoma cell line
COX-2	Cyclooxygenase 2
d	In NMR: doublet
dd	In NMR: double doublet
DMEM	Dulbecco's Modified Eagle's Medium
δ_C	Carbon chemical shift
δ_H	Proton chemical shift
DCC841CON	Primary human colon epithelial cell line
DMAPP	Dimethylallyl diphosphate
DMEM	Dulbecco's modified Eagle's medium
DMSO	Dimethyl sulfoxide
DPPH	1,1-diphenyl-2-picrylhydrazyl
Du145	Human prostate cancer cell line
DXP	1-deoxyxylulose 5-phosphate or 1-deoxy-D-xylulose 5-phosphate
EC_{50}	Half maximal effective concentration
ED_{50}	Effective dose for 50% of the population
EDTA	Ethylenediaminetetraacetic acid
EGF	Endothelial growth factor
EGTA	Ethylene glycol tetraacetic acid
ELISA	Enzyme-Linked-ImmunoSorbent-Assay
ERK	Extracellular signal-regulated kinase
ESI	Electrospray
FITC	Fluorescein Isothiocyanate
FPP	Farnesyl diphosphate
GFPP	Geranylfarnesyl diphosphate
GGPP	Geranylgeranyl diphosphate
GPP	Geranyl diphosphate
^{1}H NMR	Proton Nuclear Magnetic Resonance

H2AX	H2A histone family member X
H460	Human lung cancer cell line
HeLa	Human cervical cancer cell line
Hep-G2	Human liver cancer cell line
HIF-1	Hypoxia-inducible factor 1
HL-60	Human promyelocytic leukemia cell line
HPLC	High Performance Liquid Chromatography
HRMS	High Resolution Mas Spectrometry
Hs683	Human Neuronal Glioma cell line
HT-1080	Human fibrosarcoma cell line
HT-29	Human colorectal adenocarcinoma cell line
IC_{50}	50% inhibitory concentration
IL	Interleukine
iNOS	Inductible nitric oxide synthase
IPP	Isopentenyl diphosphate
J	coupling constant
JNK	C-Jun NH_2-terminal kinase
Jurkat	Immortalized line of human T lymphocyte cell line
K562	Human immortalised myelogenous leukemia cell line
KB	Human epidermoid carcinoma cell line
L-1210	Mouse lymphocytic leukemia cell line
L929	Mouse fibroblast cell line
LOVO	Human colon adenocarcinoma cell line
LPS	Lipopolysaccharide
LS174	Human colon cancer cell line
m	In NMR: multiplet
MAPK	Mitogen-activated protein kinase
MBA-MD468	Human triple-negative breast cancer cell line
MCF-7	Human adenocarcinoma cell line
MCP-1	Monocyte chemoattractant protein-1
MDA-MB-231	Human breast carcinoma cell line
MIA	Human pancreatic cancer cell line
MM144	Human myeloma cell line
MMP	Matrix metallopeptidase
MRC-5	Human fetal lung fibroblast
MS	Mass Spectrometry
mTOR	Mammalian target of rapamycin
MTT	3-(4,5-Dimethylthiazol-2-yl)-2,5-diphenyltetrazolium bromide
mult.	Multiplicity
m/z	Mass-charge relationship
NCI-H187	Human lung cancer cell line
NCI-H460	Non-small-cell lung cancer cell line
NF-κB	Nuclear factor-kappa B
NMR	Nuclear Magnetic Resonance
NO	Nitric oxide
NOS	Nitric oxide synthases
NPs	Natural products
OE21	Human oesophageal squamous cell carcinoma
P-388	Murine lymphocytic leukemia cell
P38	Mitogen-activated protein kinase
P53	Tumor protein 53
PA-1	Human ovarian teratocarcinoma cell line
PARP	Poly ADP ribose polymerase
PC-3	Human prostate cancer cell lines
PG	Prostaglandin
PI	Propidium Iodide

PI3K	Phosphatidyl inositol-3 kinase
PMA	Phorbol myristate acetate
pRb	Retinoblastoma protein
PS	Phosphatidylserine
Raf	Rapidly accelerated fibrosarcoma
Ras	Rat sarcoma
Raw 264.7	Mouse leukaemic monocyte macrophage cell line
RBL-2H3	Basophilic leukemia cell line
Ref-1	Redox factor-1
RNase	Ribonuclease
RONS	Reactive oxygen and nitrogen species
ROS	Reactive oxygen species
s	In NMR: singlet
S17	Clonal stromal cell line
SDS	Sodium dodecyl sulfate
SDS-PAGE	SDS-polyacrylamide gel electrophoresis
SF-268	Human tumor glioblastoma cell line
SH-SY5Y	Human neuroblastoma cell line
SJ-G2	Human glioblastoma cell line
SKMEL-28	Human melanoma cell line
SRB	Sulforhodamine B
STAT-3	Signal transducer and activator of transcription 3
t	in NMR: triplet
T47D-T.R	Human breast cancer cell line
TBARS	Thiobarbituric acid reactive substances
TBS-T	Tris-buffered saline Tween
TCA	Trichloroacetic acid
TGF-β	Transforming growth factor beta
THP-1	Human monocytic leukemia cell line
TNBC	Triple-negative breast cancer
TNF-α	Tumor necrosis factor alpha
Tris	Tris(hydroxymethyl)aminomethane
Tris-HCl	Tris (hydroxymethyl)aminomethane hydrochloride
Trolox	6-hydroxy-2,5,7,8-tetramethylchroman-2-carboxylic acid
U373	Human glioblastoma astrocytoma cell line
U87	Human primary glioblastoma cell line
U937	Pro-monocytic, human myeloid leukaemia cell line
V79	Chinese hamster lung fibroblast cell line
VEGF	Vascular endothelial growth factor
Vero	African green monkey kidney normal cell line
WHCO1	Oesophageal cancer cell line
γH2AX	Phosphorylation of the histone H2AX

LIST OF FIGURES

LIST OF TABLES

Abstract

Macroalgae are an inexhaustible source of natural products that display a variety of pharmacological and biological activities. Among marine algae, the genus *Cystoseira* has proven to produce a wide variety of secondary metabolites that could benefit human health. However, studies on the natural products of the species *Cystoseira usneoides* and their respective biological properties are scarce. Hence, in this thesis, the extract of the brown alga *Cystoseira usneoides* and the natural products isolated therefrom were tested for antioxidant, anticancer, and anti-inflammatory activities.

The extract of *C. usneoides* exhibited potent radical-scavenging and inhibited the proliferation of HT-29 cancer cells by inducing apoptotis and G2/M arrest of the cell cycle. The extract was also found to inhibit the production of TNF-α in LPS-stimulated THP-1 human macrophages.

The chemical study of the extract yielded six known algal meroterpenoids (AMTs): usneoidone Z (**1**), 11-hydroxy-1´-*O*-methylamentadione (**2**), cystomexicone B (**3**), cystomexicone A (**4**), 6-*cis*-amentadione-1′-methyl ether (**5**), and amentadione-1′-methyl ether (**6**), together with six new compounds: cystodiones A-F (**7-12**).

AMTs **1-10** showed radical-scavenging activity in the ABTS assay. The most active were compounds **5**, **6**, **7**, and **8**, which exhibited antioxidant capacity equal or superior to that of the Trolox standard.

AMTs **1-8** displayed significant cytotoxic activity against HT-29 human colon cancer cells, whereas lower cytotoxicity was observed against non-tumor cells CCD 841 CoN. Flow cytometry analysis revealed that AMTs **2**, **3**, and **5** caused apoptosis in HT-29 cells and compounds **1**, **2**, **3**, **4**, **5**, and **7** induced cell cycle arrest in G2/M phase. Furthermore, AMTs **1-8** also inhibited the migration and invasion of colon cancer cells. Interestingly, exposure of HT-29 cells to different concentrations of AMTs **1-8** correlated with the down-regulation of p-ERK, p-JNK, and p-AKT pathways. Regarding to the anticancer effect of AMTs **1-8** against A549 human lung cancer cells, the cytotoxicity of all compounds was selective for A549 cells when compared to the non-tumor MRC-5 cells. Moreover, treatment of A549 cancer cells with AMTs **1-8** also led to cell cycle arrest in S and G2/M phases.

In the *in vitro* anti-inflammatory assays, AMTs **1-8** showed significant activity as inhibitors of the production of the pro-inflammatory mediators TNF-α, IL-1β, IL-6, COX-2 and iNOS in LPS-stimulated THP-1 human macrophages. The *in vivo* study clearly demonstrated that the compound 11-hydroxy-1´-*O*-methylamentadione (AMT-E, **2)** significantly ameliorated DSS colitis (seven days), including the reduction of weight loss, disease activity, macroscopic and microscopic colonic injury. The levels of TNF-α, IL-1β, IL-10, COX-2 and iNOS expression were also significantly decreased in AMT-E treated DSS colitis.

Taken together, these findings strengthen the potential of the natural products isolated from *C. usneoides* as leads for novel antioxidant, anticancer, and anti-inflammatory agents.

Keywords: *Cystoseira usneoides*; marine natural products; meroterpenes; biological activities; antioxidant; anticancer; anti-inflammatory; cytokines; DSS-colitis

1. General introduction

1.1. Algae as source of natural products

Algae are a heterogeneous group of photoautotrophic organisms that have chlorophyll *a* as main photosynthetic pigment and lack a covering of sterile cells around their reproductive cells (Lee, 2008; Barsanti and Gualtieri, 2006a). Algae usually occur in aquatic habitats including fresh, marine, or brackish waters, although they can also grow in almost every terrestrial environment.

Algae can be divided into two main groups, prokaryotes and eukaryotes (Lee, 2008; Bold and Wynne, 1985). According to their morphological, physiological, and chemical differences, prokaryotic algae are classified into two divisions, Cyanophyta and Prochlorophyta, while the eukaryotic algae are classified into nine divisions: Glaucophyta, Rhodophyta, Heterokontophyta, Haptophyta, Cryptophyta, Dinophyta, Euglenophyta, Chlorarachniophyta, and Chlorophyta (Graham and Wilcox, 2000; Van Den Hoek et al., 1995).

Nonetheless, a common and useful classification considers two groups of algae depending on their size: unicellular microscopic algae or microalgae (Figure 1.1.A) and multicellular macroscopic algae or macroalgae (Figure 1.1.B).

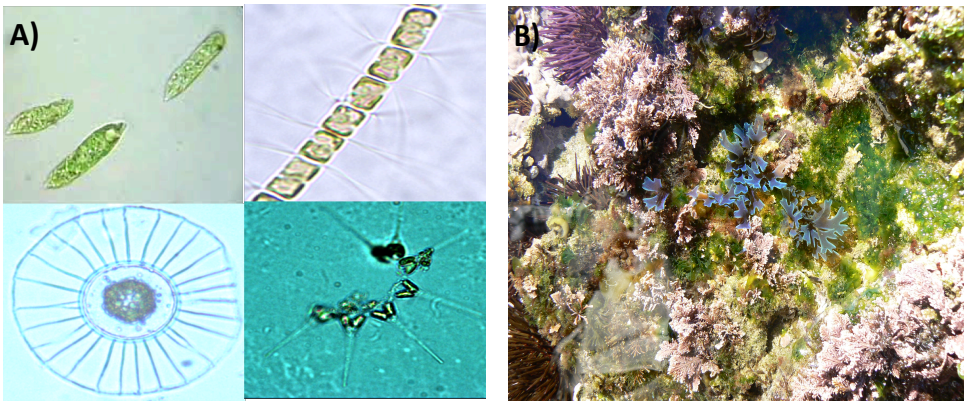

Figure 1.1. (**A**) Microalgae species from the Mediterranean coast of Morocco (photos by Applied Algology-Mycology research group). **(B)** Macroalgae species during low tide at the Mediterranean coast of Morocco (photo by H. Zbakh).

Macroalgae, commonly known as seaweeds, are thallophytes with a wide variety of life cycles, fertilization processes, and cell morphologies (Charrier et al., 2017). They can

be subdivided into green algae (Chlorophyta, Figure 1.2.A), red algae (Rhodophyta, Figure 1.2.B), and brown algae (Phaeophyta, Figure 1.2.C), according to the occurrence of specific photosynthetic pigments and the evolution of chloroplasts (Bold and Wynne, 1985). In their natural environment, macroalgae grow attached to rock substrates (epilithic) and on mud or sand (epipelic), although some species can also grow on other algae or plants (epiphytic) or on animals (epizoic) (Barsanti and Gualtieri, 2006a).

Figure 1.2. Green alga *Ulva lactuca* **(A)**, red alga *Asparagopsis armata* **(B)**, and brown alga *Cystoseira tamariscifolia* **(C)**, during low tide at the Mediterranean coast of Morocco (photos by H. Zbakh).

Since ancient times to nowadays seaweeds have been used for food, in traditional medicine, and for diverse consumer products, due to their low content in lipids and high concentration in vitamins, minerals, proteins, dietary fiber, and polysaccharides (Wells et al., 2017; Pereira 2012; Barsanti and Gualtieri 2006b).

In addition, macroalgae biosynthetize an array of secondary metabolites or natural products (NPs), which have been shown to possess health-promoting effects, including antioxidative (Roohinejad et al., 2017; Sonani et al., 2017), anti-inflammatory (Fernando et al., 2016; Lee et al., 2013), antimicrobial (Roohinejad et al., 2017; Shannon et al., 2016), and anticancer properties (Ruan et al., 2018; Hussain et al., 2016).

The systematic research on NPs from macroalgae started in the sixties of the XX century (Faulkner, 1984) and since then macroalgae have accounted for more than 3000 NPs, which represents about 13% of the compounds reported from marine organisms (Blunt et al., 2015, Leal et al., 2013). In particular, the review due to Leal et al. (2013) shows that most of the seaweed-derived NPs have been isolated from Rhodophyta (53% of the total in the period 1965-2012), followed by Pheophyta (39%), and Chlorophyta (8%). Moreover, from a structural point of view, most of the NPs obtained from macroalgae are

terpenoids, which in the period 1965-1912 represented 59% of the isolated macroalgal metabolites (Leal et al., 2013).

1.2. Terpenoids: biosynthesis and classification

Terpenoids are a large and structurally diverse group of NPs derived from five-carbon (C_5) isoprenoid units joined in a head to tail fashion (Dewick, 2002). The biochemically active isoprenoid units are isopentenyl diphosphate (IPP) and dimethylallyl diphosphate (DMAPP) (Figure 1.3). Based on the number of isoprenoid units that are combined, the terpenoids are classified into monoterpenes ($2xC_5$), sesquiterpenes ($3xC_5$), diterpenes ($4xC_5$), sesterterpenes ($5xC_5$), triterpenes ($6xC_5$) and tetraterpenes ($8xC_5$).

Two biogenetic pathways have been described for the biosynthesis of the C_5 isoprenoid units, the mevalonate pathway, and the mevalonate-independent pathway *via* deoxyxylulose phosphate (Dewick, 2002).

In the mevalonate pathway, which operates in eucaryotes, archaebacteria, and cytosols of higher plants (Kuzuyama et al., 2002), three molecules of acetyl-Coenzyme A condense successively to form mevalonic acid (Figure1.3).

The nonmevalonate pathway, more recently discovered, is used by many eubacteria, green algae, and the chloroplasts of higher plants (Kuzuyama et al., 2002). The first step in this pathway is the formation of 1-deoxy-D-xylulose 5-phosphate (DXP) by the condensation of pyruvate and D-glyceraldehyde 3-phosphate, catalyzed by DXP synthase (Figure 1.3).

Combination of one IPP molecule with one DMAPP molecule leads to geranyl diphosphate (GPP), which is the precursor of the monoterpenes (Figure 1.3). Successive addition of one IPP unit leads to farnesyl diphosphate (FPP), geranylgeranyl diphosphate (GGPP), and geranylfarnesyl diphosphate (GFPP), which are the precursors of the sesqui-, di-, and sesterterpenes, respectively. The link tail to tail of two FPP molecules yields squalene, precursor of the triterpenes, and the link tail to tail of two GGPP molecules yields phytoene, precursor of the carotenoids.

An extraordinary variety of terpenoids arise from the precursors above mentioned through multistep sequences of transformations, which include the loss of the diphosphate

group, the introduction of a variety of functional groups (alcohol, ketone, carboxylic groups, etc) and very often cyclization reactions, although the C_5 units are recognized in the carbon skeleton of the final terpenoid. In many instances rearrangement reactions also occur, leading to carbon skeletons where all the C_5 units cannot be recognized or even some carbons have been lost.

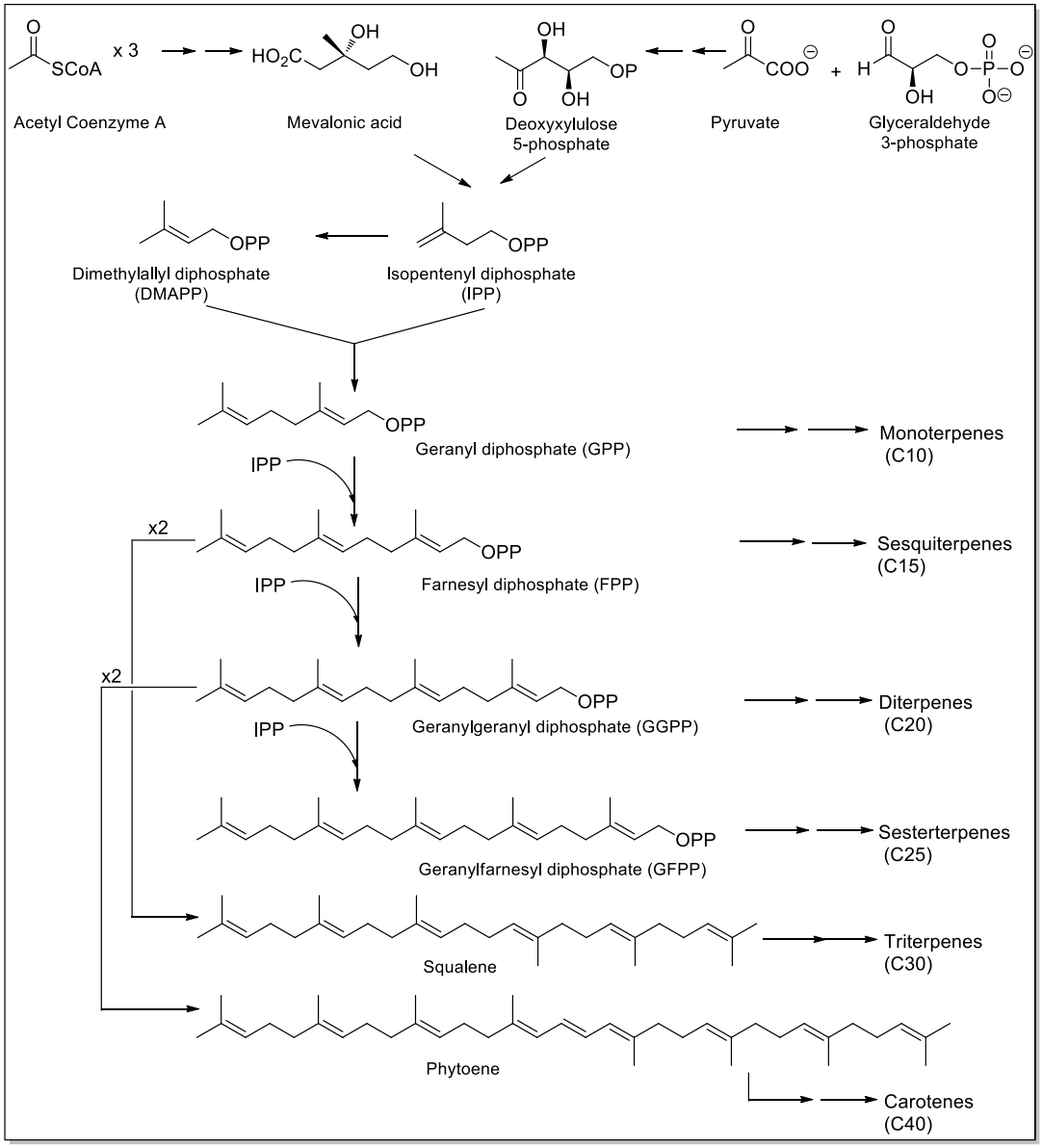

Figure 1.3. Biosynthesis of terpenoids and carotenoids.

On the other hand, there are many NPs of mixed biogenesis, which combine a terpenoid moiety with a portion derived through another biosynthetic route, such as the acetate or the shikimate pathways; these metabolites are usually referred as meroterpenoids (Dewick, 2002).

Some examples of algal terpenoids possessing a regular isoprenoid carbon skeleton are shown in Figure 1.4-A. In these compounds the C_5 isoprenoid units can be easily recognized. An example of a terpenoid with a rearranged skeleton where all the C_5 units cannot be identified is shown in Figure 1.4-B. An example of a meroterpene consisting of a diterpenoid chain linked to an aromatic ring derived through the shikimate pathway is shown in Figure 1.4-C.

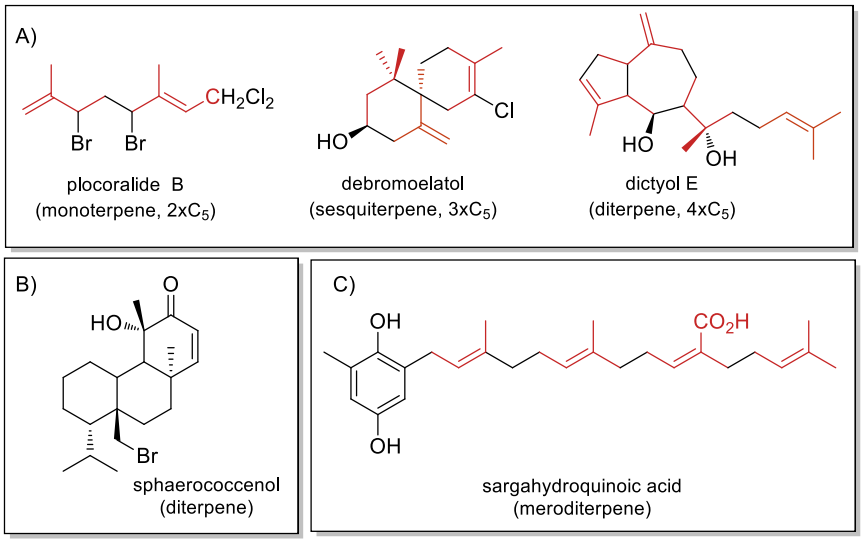

Figure 1.4. Examples of algal terpenoids: **(A)** three terpenoids with regular isoprenoid carbon skeleton (the C_5 isoprenoid units of the skeleton are depicted in red); **(B)** a diterpenoid with rearranged carbon skeleton; **(C)** a meroterpenoid.

1.3. Antioxidant, antitumor, and anti-inflammatory properties of terpenoids and meroterpenoids isolated from macroalgae

The evidences accumulated along the last two decades suggest that continued oxidative stress and oxidative damage can lead to chronic inflammation, which in turn is associated with increased risk of cancer development (Reuter et al., 2010; Federico et al., 2007).

Oxidative stress is involved in the activation of multiple transcription factors, which lead to the differential expression of over 500 different genes, including those of growth factors, cytokines, chemokines, cell cycle regulatory molecules, and anti-inflammatory molecules (Imbesi et al., 2013; Reuter et al., 2010). These mediator players activate complex mechanisms and signalling pathways that characterise inflammation (Imbesi et al., 2013; Federico et al., 2007; Reuter et al., 2010).

Chronic inflammation contributes to tumour development at all three phases: initiation, promotion, and progression (Gonda et al., 2009). Thus, inflammatory cells liberate a number of reactive oxygen species leading to DNA damage and reducing DNA repair. On the other hand, inflammation also favors carcinogenesis by further recruiting inflammatory cells to the site of damage and activating and producing many mediators, including transcription factors (NF-κB, STAT-3, and HIF-1), chemokines (MCP-1, IL-8, CXC chemokine receptor), and cytokines (TNF-α, IL-6, IL-10, *TGF-*β). These promoters influence the whole tumour and impact on the different stages of tumorigenesis such as initiation, promotion, and progression, as well as on the angiogenesis (Landskron et al., 2014; Multhoff et al., 2012; Reuter et al., 2010; Coussens and Werb, 2002). Therefore, discovering natural drugs that target redox-sensitive pathways, and transcription factors offers great promise for cancer prevention and therapy.

In this context, bioactive terpenoids from marine algae could be used as scaffolds in the design of novel compounds for pharmacological purposes. Herein, we provide a comprehensive overview of the terpenoids and meroterpenoids with antioxidant, antitumor, and anti-inflammatory activities that have been described from macroalgae during the last twelve years (2007-2018).

1.3.1. Antioxidant properties of terpenoids and meroterpenoids isolated from macroalgae

Oxidative stress is defined as an imbalance between the production and accumulation of oxygen reactive species (ROS) in cells and tissues and the ability of a biological system to detoxify these reactive products (Pizzino et al., 2017). ROS are products of the normal cellular metabolism (Birben, et al., 2012) and play important physiological roles, especially in the maintenance of cell homeostasis and in the regulation of functions such as proliferation, signal transduction, gene expression, and activation of

receptors (Dröge, 2002). However, when the production of ROS exceeds the cellular protective mechanisms (oxidative stress) the excessive ROS levels can cause damage to DNA, lipids, and proteins (Wu et al., 2013).

The cellular antioxidant defense mechanisms include enzymatic (enzymes that reduce lipid peroxidation) and non-enzymatic pathways (*e.g.* glutation, L-arginine, coenzyme Q) (Kumar and Pandey, 2015; López-Alarcón and Denicola, 2013). In addition to these endogenous antioxidants, a variety of exogenous antioxidants can be obtained through the diet and nutritional supplements (*e.g.* vitamins C and E, flavonoids, carotenoids) (Pizzino et al., 2017; Nimse and Palb, 2015).

It has been noted that although marine macroalgae are exposed to intense light and oxygen concentrations they do no show oxidative damages in their structural components, suggesting the presence of metabolites with antioxidative defense functions (Jiménez-Escrig et al., 2001). In this line, the extracts from a great variety of macroalgae and some pure compounds have been shown to possess significant antioxidant properties in different assays (Balboa et al., 2013; Farvin and Jacobsen, 2013). Herein we present the terpenoids and meroterpenoids with antioxidant activity described from macroalgae during the last twelve years (2007-2018).

Most of the algal NPs with antioxidant properties are meroterpenoids containing a phenolic ring and have been isolated from brown algae. Thus, sargahydroquinoic acid (**St-1**), sargaquinoic acid (**St-2**), sargachromenol (**St-3**) and sargathunbergol (**St-4**) (Figure 1.5) from *Sargassum thunbergii* showed the capacity to scavenge the DPPH free radical with ED_{50} values in the range 20-38 μg/mL, which were similar to those of the reference compounds BHT (42 μg/mL) and α-tocopherol (23 μg/mL) (Seo et al., 2007).

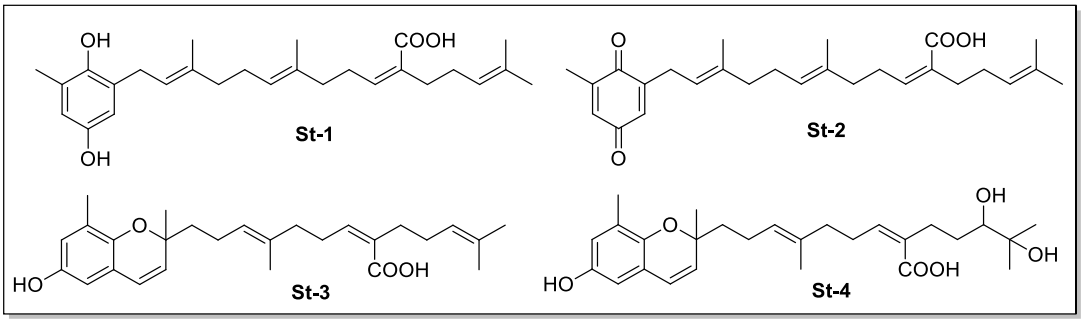

Figure 1.5. Antioxidant meroterpenoids from the brown alga *Sargassum thunbergii*.

The chemical study of *S. siliquastrum* led to the isolation of twenty meroterpenoids most of which showed radical scavenging activity in the DPPH assay (EC_{50} values in the range 0.10-23.23 μg/mL) (Jung et al., 2008). The more active compounds were the known compounds sargahydroquinoic acid (**St-1**, Figure 1.5), isonahocol D_1 (**Ss-1)** and isonahocol D_2 (**Ss-2)** (Figure 1.6), together with the new compounds **Ss-3**, **Ss-4**, **Ss-5**, **Ss-6**, and **Ss-7** (Figure 1.6), that showed ED_{50} values in the range 0.10-0.33 μg/mL. Another study of this species yielded the new chromene mojabanchromanol (**Ss-8**, Figure 1.6), which at 500 μg/mL caused 84.08% decrease of TBARS formation and 96.07% radical elimination in the DPPH assay (Cho et al., 2008).

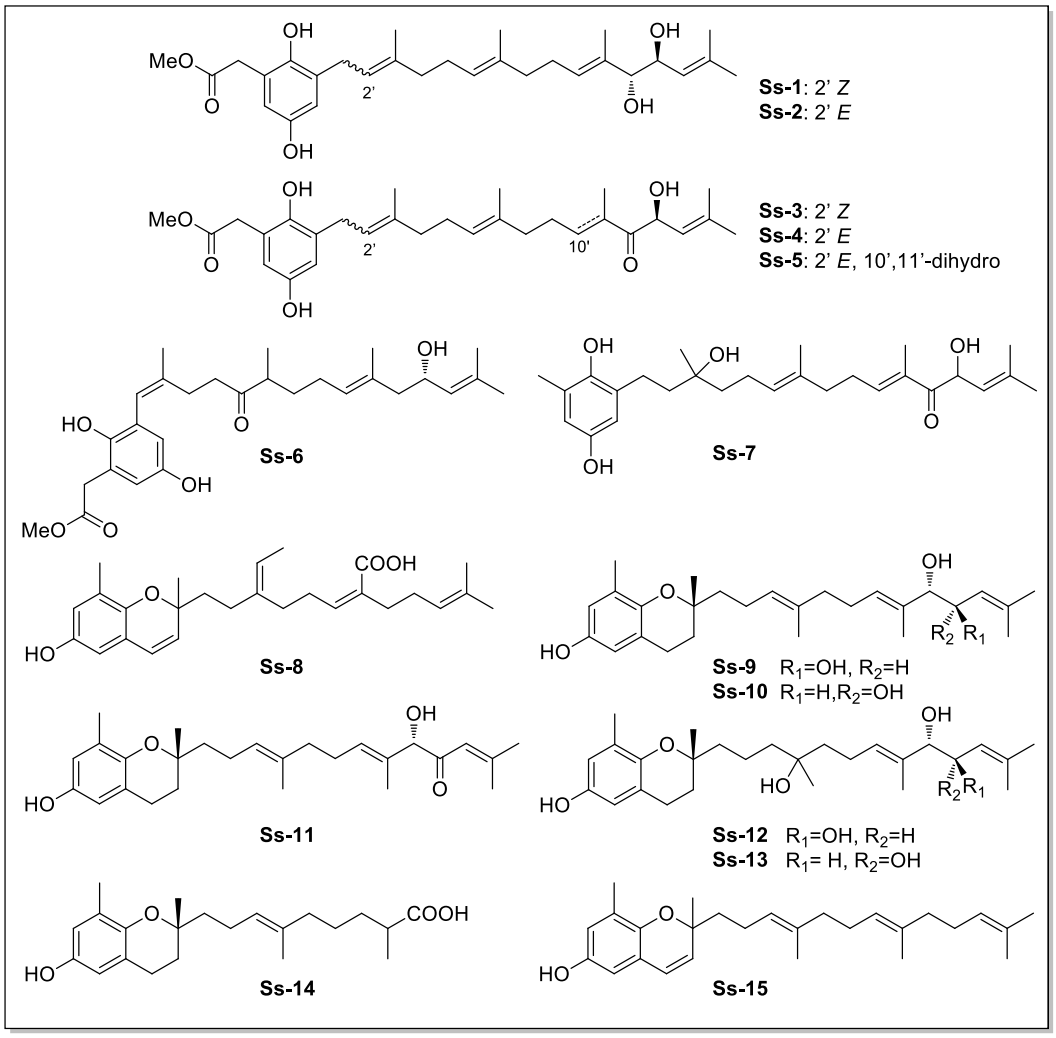

Figure 1.6. Antioxidant meroterpenoids from the brown algae *Sargassum siliquastrum* (**Ss-1** to **Ss-14**) and *Stypopodium zonale* (**Ss-15**).

A third report on *S. siliquastrum* described six chromanols, the known sargachromanols D (**Ss-9**), E (**Ss-10**), and K (**Ss-11**) and the new **Ss-12**, **Ss-13**, and **Ss-14** (Figure 1.6) whose antioxidant effects were evaluated in different assays (Lee and Seo 2011). At 5 μg/mL all the compounds decreased by more than 67.2% the intracellular generation of ROS in HT1080 cells and increased the intracellular level of glutathione. The most active was sargachromanol E (**Ss-10**), which caused 87.2% decrease of ROS levels. In addition, at 50 μg/mL all the compounds inhibited the lipid peroxidation, in particular the new compounds **Ss-12** and **Ss-13**, which caused 43.2 and 38.9% inhibition, respectively. The related compound sargaol (**Ss-15**, Figure 1.6), isolated from *Stypopodium zonale*, was also described to scavenge 86% of the DPPH radical at 50 μg/mL (Penicooke et al., 2013).

The meroterpenes cystoazorol A (**Cab-1**) and cystoazorol B (**Cab-2**) (Figure 1.7), isolated from *Cystoseira abies-marina,* were described to cause 29% and 30% scavenging of the DPPH radical at 500 μg/mL, respectively; these are values rather lower than those observed for the reference compounds quercetin and trolox (78% and 75 % scavenging, respectively) at the same concentration (Gouveia et al., 2013b).

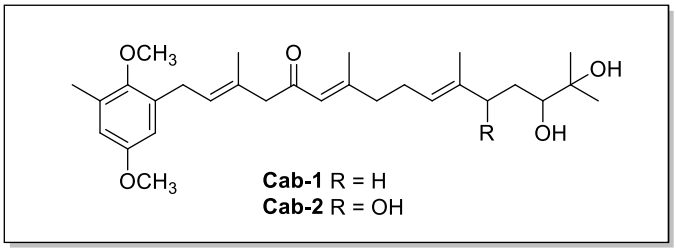

Figure 1.7. Antioxidant meroterpenoids isolated from the brown alga *Cystoseira abies-marina*.

After a screening of the extracts of thirteen species of algae from the Aegean Sea using chemiluminescence (CL) and DPPH assays, the extract of the brown alga *Taonia atomaria* showed the highest levels of antioxidant activity (Nahas et al., 2007). The isolation guided by radical scavenging activity led to the obtention of six polycyclic meroditerpenes active in the CL and DPPH assays. The highest levels of activity were observed for taondiol (**Ta-1**) and isoepitaondiol (**Ta-2**) (Figure 1.8), which were more active than the reference compounds trolox and ascorbic acid.

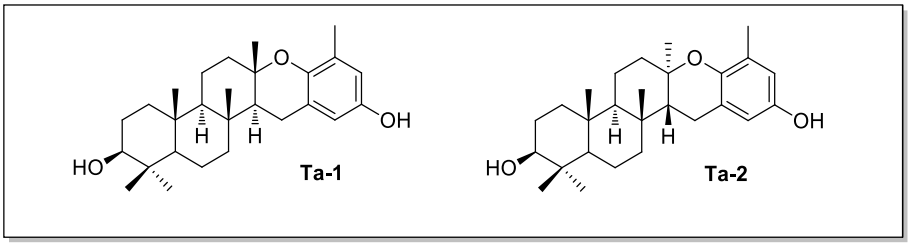

Figure 1.8. Antioxidant meroditerpenoids isolated from the brown alga *Taonia atomaria*.

A few terpenoids lacking a phenolic ring have ben reported to possess antioxidant activity, such as the diterpenes amijiol acetate (**Dd-1**) and amijiol-7,10-diacetate (**Dd-2**) (Figure 1.9) isolated from *Dictyota dichotoma* (Ayyad et al., 2011). These compounds, at 100 μM, caused 83.35 and 80.24% inhibition of the ABTS radical, respectively, while another seven diterpenes isolated in the same study were less active.

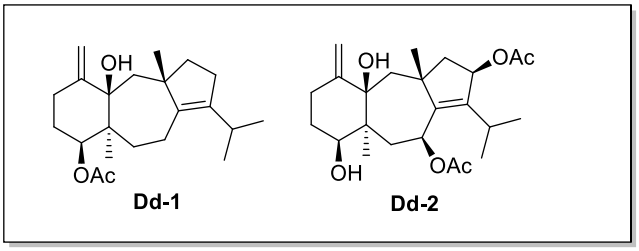

Figure 1.9. Antioxidant diterpenoids isolated from the brown alga *Dictyota dichotoma*.

The only example of antioxidant meroterpenoids from red algae has been found in the arylterpenoids isolated from *Hypnea musciformis* (Chakraborty et al., 2016). Among the isolated compounds, **Hm-1** (Figure 1.10) showed IC_{50} = 25.05 μM in the DPPH assay and IC_{50} = 350.7 μM in the Fe^{2+} ion chelating activity assay, which were similar to those shown by gallic acid (IC_{50} 32.3 μM and 646.6 μM, respectively).

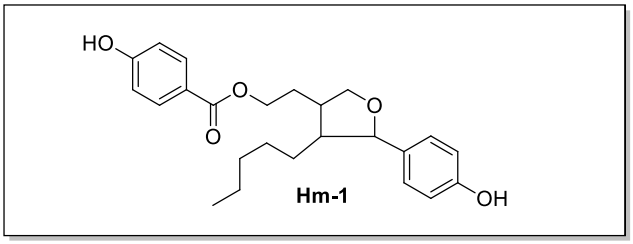

Figure 1.10. Antioxidant arylterpenoid isolated from the red alga *Hypnea musciformis*.

1.3.2. Antitumor properties of terpenoids and meroterpenoids isolated from macroalgae

Cancer is a worldwide leading cause of mortality (Torre et al., 2015). In spite of the therapeutic progresses achieved during the last decades, the fail of various types of chemotherapies, mainly because of side effects or drugs resistance, evidence the need and importance of the research for new molecules with anticancer activity, more effective and with smaller adverse effects. NPs have great potential in cancer therapy (Cragg and Pezzuto, 2015; Cragg et al., 2009) as demonstrates the fact that 77% of the anti-cancer drugs (excluding biologicals and vaccines) developed from 1930 to 2014 are derived from NPs (Newman and Cragg, 2016). Therefore, the search for novel therapeutic agents from NPs that target specific, novel, or so far not investigated molecular signaling pathways, in order to arrest the growth and metastasis of tumors, continues to be an active research area (Harvey et al., 2015). Although historically plant-derived compounds have played a prominent role in the discovery and development of anticancer drugs (Seca and Pinto, 2018), more recently marine NPs have also led to new anticancer drugs and several compounds are currently in clinical trials (Ruiz-Torres et al., 2017; Newman and Cragg, 2014).

Marine macroalgae have been shown to contain a variety of compounds with interesting antitumor properties, including polysaccharides, polyphenols, and small molecules such as terpenoids and steroids, among others (Murphy et al., 2014). Herein we present the structures and antitumor properties of the terpenoids and meroterpenoids reported from macroalgae during the last twelve years (2007-2018). The data are organized by class of algae, and within each class, by type of terpenoid, from mono- to triterpenes.

Green algae

During the last years only two sesquiterpenes from green algae, caulerpenyne (**Cp-1**) from *Caulerpa taxifolia* and **Uf-1** from *Ulva fasciata* (Figure 1.11), have been studied for their antitumor properties. In particular, research on the mechanism of action of caulerpenyne (**Cp-1**), which is cytotoxic for several cancer cell lines and inhibits the polymerization of tubulin, have shown that **Cp-1** neither interact to colchicine, taxol, and vinka-alkaloid binding domain, not bind covalently to tubulin (Bourdron et al., 2009).

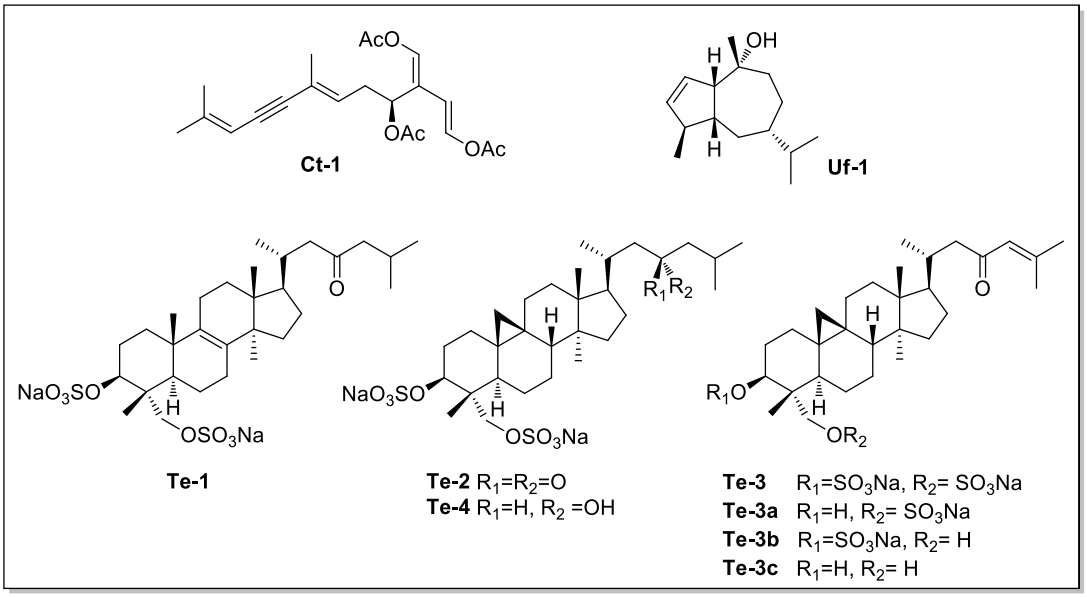

Figure 1.11. Cytotoxic terpenoids isolated from the green algae *Caulerpa taxifolia* (**Ct-1**), *Ulva fasciata* (**Uf-1**), and *Tydemania expeditionis* (**Te-1 – Te-4**) and cytotoxic derivatives prepared from **Te-3** (**Te-3a**, **Te-3b**, **Te-3c**).

More recently, the novel guaiane sesquiterpene **Uf-1** has shown cytotoxic activity against triple-negative breast cancer (TNBC) cell line MDA MB-231 with IC_{50} =17.35 μM at 24h of treatment (Lakshmi et al., 2018). More advanced studies showed that **Uf-**1 was capable of inducing apoptosis and cell cycle arrest in G1 phase, via regulation of EGFR/PI3K/Akt pathway, in human TNBC cells (Lakshmi et al., 2018).

On the other hand, four triterpenoid disulfates, one of lanostane-type (**Te-1)** and three of cycloartane type (**Te-2**, **Te-3** and **Te-4**) isolated from *Tydemania expeditionis*, along with the monosulfated derivatives **Te-3a** and **Te-3b,** and the desulfated **Te-3c** prepared from **Te-3** (Figure 1.11), were tested against a panel of 12 tumor cell lines including breast (BT-549, DU4475, MDA-MB-468, MDA-MB-231), colon (HCT116), lung (NCI-H446, SHP-77), prostate (PC-3, LnCaP-FGC, Du145), ovarian (A2780/DDPS), and leukemia (CCRF-CEM) cancer cell lines. Compounds **Te-1**, **Te-2**, **Te-3**, and **Te-4** displayed antitumor effects with mean IC_{50} values ranging from 31 to 38 μM, while the derivatives **Te-3a**, **Te-3b** and **Te-3c** were more active with IC_{50} values from 6.0 to 11 μM (Jiang et al., 2008).

Red algae

Several species of red algae of the genus *Plocamium*, *Laurencia*, *Sphaerococcus*, and *Callophycus* have been source of a variety of terpenoids with interesting antitumor properties.

Thus, the studies of three *Plocamium* species from the South African coasts have led to the isolation of several polyhalogenated monoterpenes cytotoxic against WHCO1 esophageal cancer cell line (Antunes et al., 2011; Mann et al., 2007). The highest activity levels were observed for **Pcr-1** (Figure 1.12) (IC_{50} = 7.5 μM), isolated from *Plocamium corallorhiza* (Mann et al., 2007), and for **Ps-1**, **Ps-2**, **Ps-3**, **Ps-4**, **Ps-5**, and **Ps-6** (Figure 1.12) (IC_{50} = 6.6–9.9 μM), isolated from *P. suhrii,* which were more active than the known anticancer drug cisplatin (IC_{50} = 13 μM) (Antunes et al., 2011). However, the monoterpenoids isolated from *P. cornutum* were less active and only compounds **Pco-1**, **Pco-2**, **Pco-3** (Figure 1.12) displayed IC_{50} values lower than 50 μM (17.8, 47.3, and 40.2 μM, respectively) (Antunes et al., 2011).

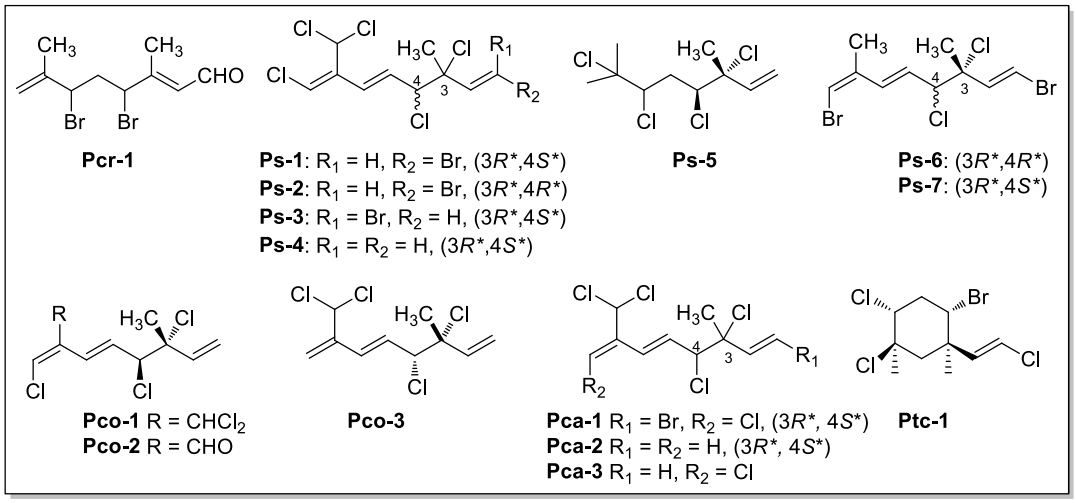

Figure 1.12. Cytotoxic monoterpenoids from the red algae *Plocamium corallorhiza* (**Pcr-1**), *P. suhrii* (**Ps-1** – **Ps-7**), *P. cornutum* (**Pco-1** – **Pco-3**), *P. cartilagineum* (**Pca-1** – **Pca-3**), and *Pterocladiella capillacea* (**Ptc-1**).

Later, the monoterpene **Pca-1**, isolated from *P. cartilagineum*, together with **Pca-2**, **Ps-4** and **Pco-1**, obtained by synthesis, were assayed against a panel of 9 cancer cell lines, including colon (H116), lung (H125), breast (MCF-7, MDA-MB-231), prostate (LNCap),

ovary (OVC-5), glioblastoma (U251N), pancreas (PANC-1), and liver (HepG2) tumors, and showed mean IC_{50} values of 1.3, 15, 3.6, and 1.3 μg/mL, respectively (Vogel et al., 2014). More recently, the species *P. cartilagineum* has also yielded the monoterpene **Pca-3**, whose configuration at C-3 and C-4 has not been assigned. This compound was cytotoxic against the NCI-H460 tumor cell line with IC_{50}= 4 μg/mL (Sabry et al., 2017).

On the other hand, a chemical report on the red macroalga *Pterocladiella capillacea* described the new halogenated monoterpene mertensene (**Ptc-1**, Figure 1.12), which exhibited antiproliferative activity against the human colorectal adenocarcinoma cell lines HT29 and LS174 with IC_{50} of 56.50 μg/mL and 49.77 μg/mL, respectively. The compound **Ptc-1** induced G2/M cell cycle arrest in HT29 cells through a negative modulation of phosphorylated forms of p53, retinoblastoma protein (Rb), cdc2, and chkp2, and also reduced the expression level of cyclin-dependent kinases CDK2 and CDK4. Moreover, the cytotoxicity of **Ptc-1** was associated with the induction of cell apoptosis via modulation of ERK-1/-2, AKT and NF-κB pathways (Tarhouni-Jabberi et al., 2017).

Red algae of the genus *Laurencia* have been a prolific source of bioactive sesqui-, di-, and triterpenoids. Among the sesquiterpenes, the new aromatic derivatives **Lmi-1** and **Lmi-2**, along with the known metabolites dibromophenol (**Lmi-3**), (+)-α-isobromocuparene (**Lmi-4**) and (-)-α-bromocuparene (**Lmi-5**) (Figure 1.13), isolated from *Laurencia microcladia*, exhibited weak inhibitory effect against the human cancer cell lines HT-29, MCF7, PC3, HeLa, and A431 with IC_{50} values in the range 75.2-287.3 μM (Kladi et al., 2007). On the other hand, the chamigrane-type sesquiterpene elatol (**Lmi-6**) (Figure 1.13**)** also obtained from *L. microcladia* was reported to show significant cytotoxic activity against the murine cell lines B16F10 (melanoma) and L929 (fibroblast), and against the human tumor cell lines MCF7 (breast), DU145 (prostate), and A549 (lung), with IC_{50} values between 1.1 and 10.1 μM (Campos et al., 2012). Further studies showed that elatol (**Lmi-6**) exhibited cytotoxicity against murine melanoma B16F10 cells (IC_{50} 10.1 μM) by promoting the activation of the apoptotic process and inducing cell cycle arrest in the G1/S phase, *via* the reduction of cyclin-D1, cyclin-E, cyclin-A, cdk-4, cdk-2, and pRb expression. In an *in vivo* experiment, treatments of C57Bl6 mice bearing B16F10 cells with elatol (**Lmi-6**) at 3, 10, and 30-mg/kg p.o. caused 50.4, 41.3, and 61.2% reduction of tumor

volume, respectively. Higher reductions of 51.8, 61.4, and 71,4% were observed in 1, 3, and 10 mg/kg i.p.-treated mice, respectively, while cisplatin at 4 mg/kg (i.p.) caused 85% reduction of tumor growth (Campos et al., 2012).

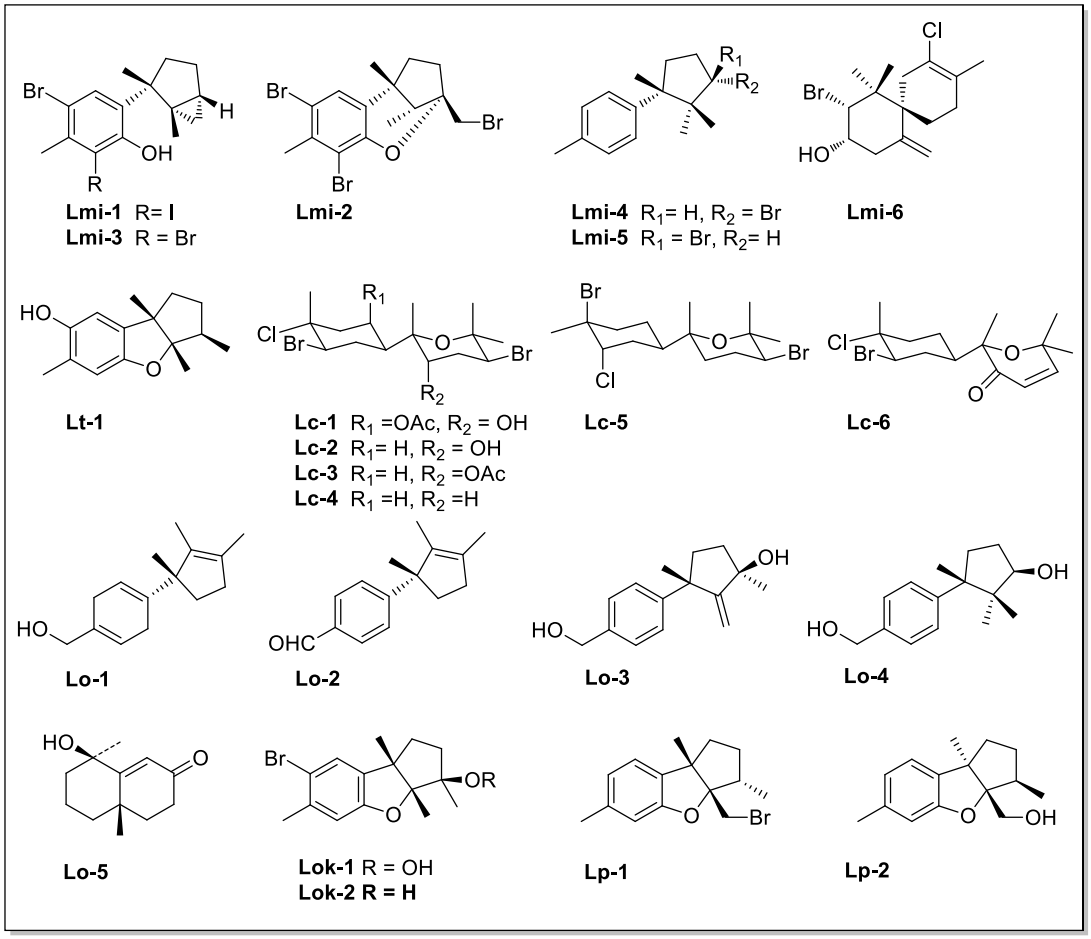

Figure 1.13. Cytotoxic sesquiterpenes from the red algae *Laurencia microcladia* (**Lmi-1** –**Lmi-6**), *L. tristicha* (**Lt-1**), *L. catarinensis* (**Lc-1** − **Lc-6**), *L. obtusa* (**Lo-1** – **Lo-5**), *L. okamurai* (**Lok-1**, **Lok-2**) and *L. pacifica* (**Lp-1**, **Lp-2**).

Among the nineteen sesquiterpenoids isolated from *Laurencia tristicha*, the new compound debromoepiaplysinol (**Lt-1**, Figure 1.13) showed selective cytotoxicity against the HeLa cell line with IC_{50} of 15.5 µM (Sun et al., 2007).

The *in vitro* cytotoxicity of seven new and seven known halogenated sesquiterpenoids isolated from *Laurencia catarinensis* was evaluated against the human tumor cell lines HT-29 (colon carcinoma), MCF7 (breast carcinoma), and A431

(epidermoid carcinoma) (Lhullier et al., 2010). The compounds (5*S*)-5-acetoxycaespitol (**Lc-1**), caespitol (**Lc-2**), acetylcaespitol (**Lc-3**), deoxycaespitol (**Lc-4**), deoxyisocaespitol (**Lc-5**), and caespitenone (**Lc-6**) (Figure 1.13) showed cytotoxicity against all the tested cells with IC_{50} values in the range 7.6-31.7 μM. The most active compound was **Lc-2** with IC_{50} = 7.6, 9.7, and 10.2 μM for HT29, MCF7, and A431 cells, respectively (Lhullier et al., 2010).

A chemical study of the red alga *Laurencia obtusa* led to the isolation of three laurene-type sesquiterpenes among which 8,11-dihydro-12-hydroxyisolaurene (**Lo-1**) and isolaureldehyde (**Lo-2**) (Figure 1.13) showed *in vitro* antitumor activity in the Ehrlich ascites assay. Although **Lo-1** and **Lo-2** were reported to cause 79.9% and 83.2% cytotoxic activity, the concentration of compounds that cause those effects was not reported (Alarif et al., 2012). The related sesquiterpene alcohols, laur-2-ene-3,12-diol (**Lo-3**), and cuparene-3,12-diol (**Lo-4**) (Figure 1.13), isolated from the same macroalga, were tested against KB, HepG2, and MCF-7 human tumor cell lines. The compound **Lo-3** showed cytotoxicity towards KB and MCF-7 cells, with IC_{50} values of 0.171 and 0.184 μM respectively, while **Lo-4** was only active against KB cell line with IC_{50} of 0.213 μM (Angawi et al., 2014). More recently *L. obtusa* has also yielded the trinor-sesquiterene teuhetenone (**Lo-5**, Figure 1.13), which showed higher cytotoxic activity towards MCF-7 cells (IC_{50} = 22 μM) than the reference compound cisplatin (IC_{50} = 59 μM) (Alarif et al., 2016).

Another two laurane-type sesquiterpenes, the new 3β-hydroperoxyaplysin (**Lok-1**) and the known 3β-hydroxyaplysin (**Lok-2**) (Figure 1.13), isolated from *Laurencia okamurai*, showed moderate cytotoxic activity against A-549 cell line with IC_{50} values of 35.3 and 15.4 μM, respectively (Yu et al., 2014).

The sesquiterpenes isoaplysin (**Lp-1**), and debromoaplysinol (**Lp-2**) (Figure 1.13), isolated from *Laurencia pacifica,* showed cytotoxicity against a panel of cancer-derived cell lines of human colon (HT29), glioblastoma (U87, SJ-G2), breast (MCF-7), ovarian (A2780), lung (H460), skin (A431), prostate (Du145), neuroblastoma (BE2-C), and pancreas (MIA), and also of murine glioblastoma (SMA), with average GI_{50} values of 23 and 14 μM, respectively (Zaleta-Pinet et al., 2014). The higher levels of cytotoxicity were observed against Du145 cells (GI_{50} = 12 and 6.8 μM, respectively). In addition, both

compounds were less cytotoxic against normal breast cells MCF10A (GI_{50} = 46 and 28 μM, respectively).

Algae of the genus *Laurencia* have also yielded several cytotoxic diterpenes. Thus, the compound kahukuen-10-ol (**Lo-6**) (Figure 1.14), isolated from *L. obtusa*, exhibited high cytotoxic activity against KB, HepG2, and MCF-7 cell lines with IC_{50} values of 0.1, 0.057 and 0.054 μM, respectively, comparable to those of the reference compound 5-fluorouracil (Angawi et al., 2014).

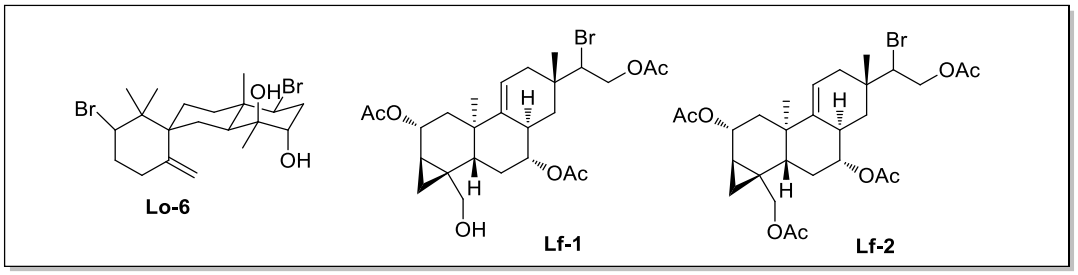

Figure 1.14. Cytotoxic diterpenoids isolated from the red algae *Laurencia obtusa* (**Lo-6**) and *L. filiformis* (**Lf-1** and **Lf-2**).

On the other hand, two rare bromoditerpenes, parguerenes I (**Lf-1**) and II (**Lf-2**) isolated from the macroalga *L. filiformis* (Figure 1.14) have been described to exert inhibitory effects on the ABC transporter P-glycoprotein (P-gp) (Huang et al., 2013). The compounds **Lf-1** and **Lf-2** were non-cytotoxic, dose-dependent inhibitors of P-gp mediated drug efflux, and caused reversal of P-gp mediated vinblastine, doxorubicin, and paclitaxel resistence. The inhibitory properties span both to P-gp and multidrug resistant protein 1 (MRP1), but do not extend to breast cancer resistance protein (BCRP). Moreover, parguerene II (**Lf-2**) (10 μM) was more potent than the reference compound verapamil (30 μM).

Several chemical investigations of the red alga *Sphaerococcus coronopifolius* have led to the isolation of an array of brominated diterpenes. The study of *S. cororonopifolius* from the Greek coasts yielded sixteen diterpenes that were tested against four human apoptosis-resistant (U373, A549, SKMEL-28, OE21) and two human apoptosis-sensitive (PC-3, LoVo) cancer cell lines (Smyrniotopoulos et al., 2010). The compounds exhibited different levels of growth inhibitory activity with IC_{50} values in the range 2.8-97 μM. The

more potent compounds were sphaerococcenol A (**Sc-1**) (IC_{50} 2.8-5.2 μM), 12*S*-hydroxybromosphaerol (**Sc-2**) (IC_{50} 9-22 μM), and 14*R*-hydroxy-13,14-dihydrosphaerococcenol A (**Sc-3**) (IC_{50} 5.3-21 μM) (Figure 1.15).

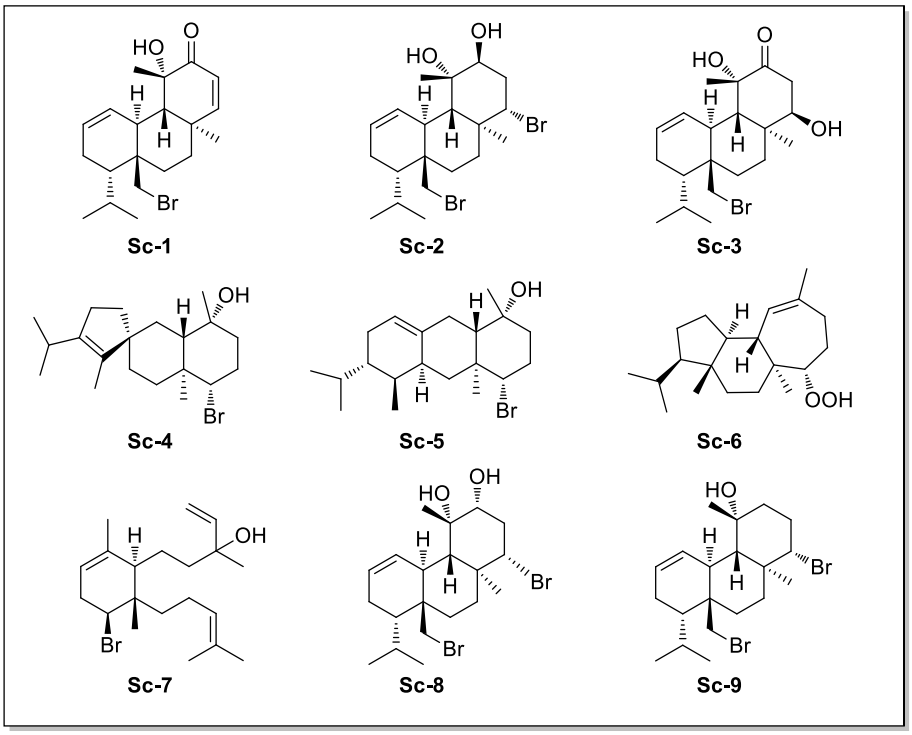

Figure 1.15. Antitumor diterpenoids isolated from the red alga *Sphaerococcus coronopifolius* (**Sc-1** – **Sc-9**).

A reinvestigation of this species yielded another three new diterpenoids, spirosphaerol (**Sc-4**), anthrasphaerol (**Sc-5**) and corfusphaeroxide (**Sc-6**) (Figure 1.15) that were evaluated against one murine (B16F10) and five human cancer cell lines (A549, Hs683, U373, MCF-7, and SKMEL28) (Smyrniotopoulos et al., 2015). The three compounds displayed moderate antitumor activity against the cell lines B16F10, A549, Hs683, and MCF-7, (IC_{50} 46 to 93 μM), and **Sc-6** showed also slight effect against U373 and SKMEL28. In the same line, the study on *S. coronopifolius* from the Portuguese coasts yielded the new sphaerodactylomelol (**Sc-7**), along with the four already reported sphaerane bromoditerpenes sphaerococenol (**Sc-1**), 12*S*-hydroxybromosphareol (**Sc-2**), 12*R*-hydroxybromosphareol (**Sc-8**), and bromosphareol (**Sc-9**) (Figure 1.15) (Rodrigues et al.,

2015). All compounds were reported to possess anti-proliferative activity on human hepatocellular cancer cell line Hep2G, at sub-toxic concentrations, with IC_{50} values in the range 42.9-291.4 μM. The highest activity was exhibited by **Sc-1** (IC_{50} = 42.9 μM).

Another interesting group of bioactive NPs from red algae are the meroditerpenes isolated from *Callophycus serratus*. The callophycoic acids A (**Cs-1**), B (**Cs-2**), C (**Cs-3**), and D (**Cs-4**) (Figure 1.16a) were reported to exhibit modest anticancer activity against a panel of eleven human tumor cell lines including breast, colon, lung, prostate and ovarian cancer cells, with IC_{50} values in the range 20.6-24.5 μM (Lane et al., 2007).

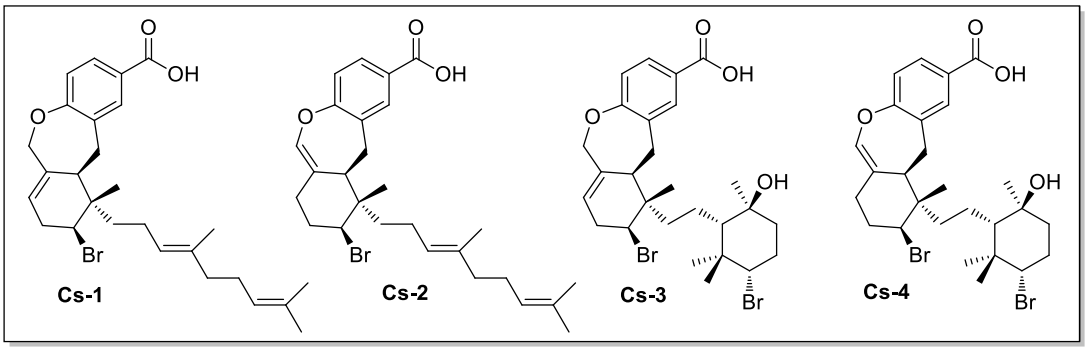

Figure 1.16a. Cytotoxic meroditerpenes isolated from the red alga *Callophycus serratus*.

Later, another seven metabolites isolated from the same species, the bromophycolides J (**Cs-5**), K (**Cs-6**), and M-Q (**Cs-7** – **Cs-11**) (Figure 1.16b), were shown to be cytotoxic toward a panel of twelve cell lines with mean IC_{50} values in the range 2.0-31 μM (Lane et al., 2009). The most potent compound was bromophycolide Q (**Cs-11**) (mean IC_{50} 2.0 μM) while bromophycolide N (**Cs-8**) displayed some selectivity towards the breast tumor cell line DU4475 (mean IC_{50} = 8.6 μM, IC_{50} against DU4475 = 2.0 μM). The bromophycolides R (**Cs-12**), S (**Cs-13**), T (**Cs-14**), and U (**Cs-15**) (Figure 1.16b) were less active with mean IC_{50} values of 16-24 μM (Lin et al., 2010). The last study of this species has yieled another eight halogenated meroditerpenes, among which the known bromophycolides A (**Cs-14**) and T (**Cs-15**) and the new iodocallophycol E (**Cs-16**) (Figure 1.16b) showed moderate cytotoxicity against the human leukemia HL-60 cell line, with IC_{50} values of 6.2, 6.0, and 5.1 μM (Woolner et al., 2018).

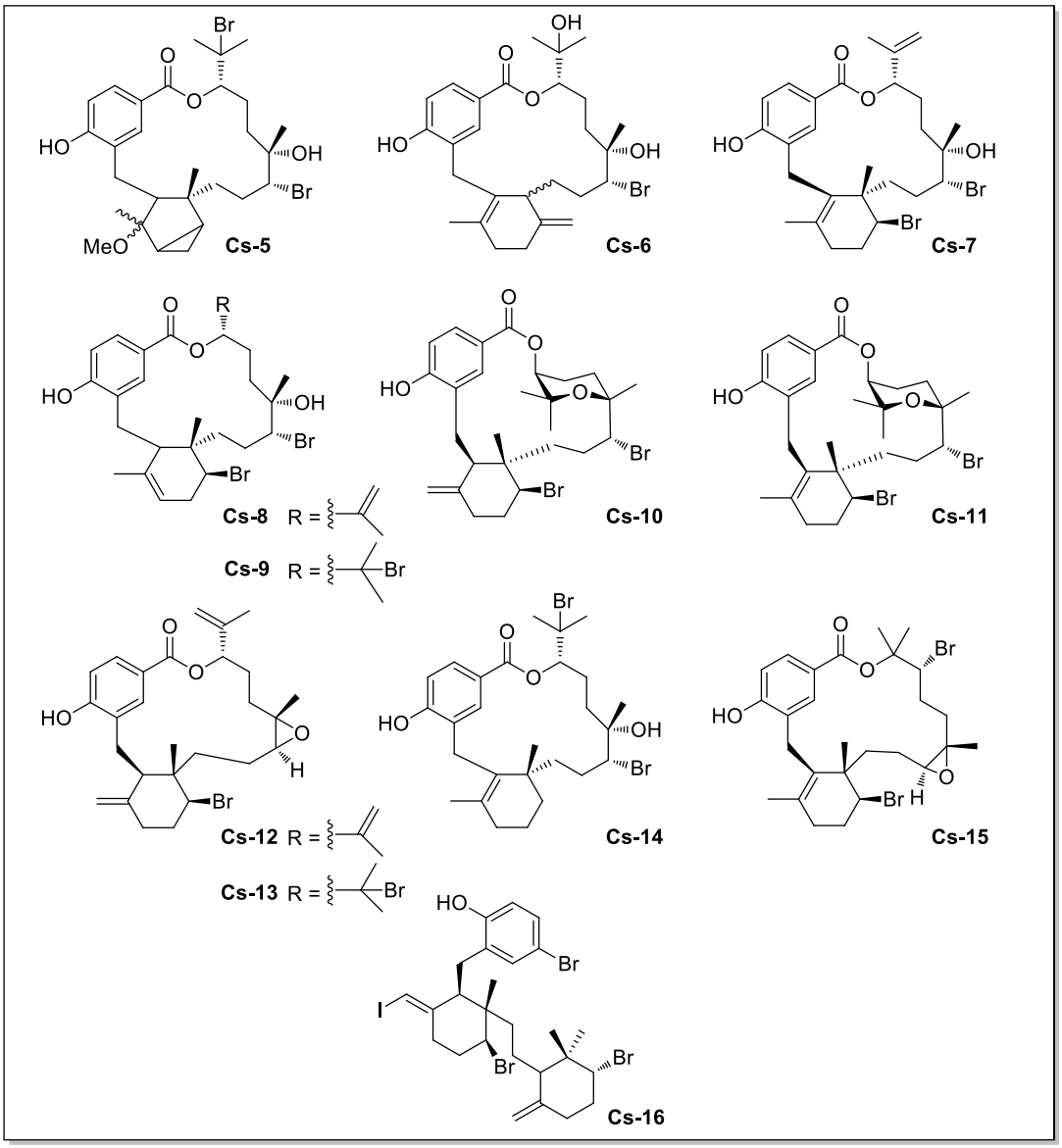

Figure 1.16b. Cytotoxic meroditerpenes isolated from the red alga *Callophycus serratus*.

An unidentified species of the genus *Callophycu*s yielded the new bromophycoic acids A (**Csp-1**), B (**Csp-2**), C (**Csp-3**) D (**Csp-4**) and E (**Csp-5**) (Figure 1.17) that were active against a panel of fourteen tumor cell lines including breast, colon, lung, prostate, and ovarian cancer cells, with average IC_{50} values in the range 6.8-36 μM (Teasdale et al., 2012). Bromophycoic acid D (**Csp-4**) was the only compound to exhibit an average

cytotoxity in the low micromolar range (average IC_{50} 6.8 μM) and proved to be most active against the human ovarian teratocarcinoma PA-1, with IC_{50} = 2.0 μM.

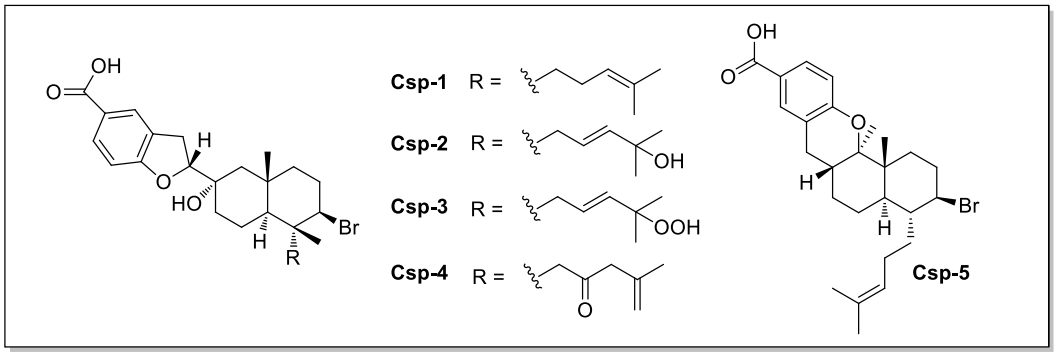

Figure 1.17. Cytotoxic meroditerpenes isolated from the red alga *Callophycus* sp.

All the triterpenes with cytotoxic properties isolated from red algae have been obtained from species of the genus *Laurencia*. Laurenmariannol (**Lm-1**) and (21α)-21-hydroxythyrsiferol (**Lm-2**) (Figure 1.18) are polyether triterpenoids isolated from *L. mariannensis* that have exhibited cytotoxcity against P-388 tumor cells with IC_{50} values of 0.6 and 6.6 μg/mL, respectively, while the positive control etoposide had IC_{50} = 0.30 μg/mL (Ji et al., 2008).

A series of three reports focused on *Laurencia viridis* have also described the isolation of squalene-derived polyethers. In particular, the new compounds 15-dehydroxythyrsenol A (**Lv-1**), prethyrsenol A (**Lv-2**), 13-hydroxyprethyrsenol A (**Lv-3**), together with the known dehydrothyrsiferol (**Lv-4**), and the derivatives **Lv-4a**, **Lv-4b**, **Lv-4c**, and **Lv-4d,** prepared from **Lv-4** (Figure 1.18), showed cytotoxic effects against Jurkat (T-cell acute leukaemia), MM144 (multiple myeloma), HeLa (epitheloid cervix carcinoma), and CADO-ES-1 (Ewing's sarcoma) cell lines (IC_{50} values in the range 3.10-35.5 μM) (Cen-Pacheco et al., 2011a). The Jurkat leukaemic cells were the more sensitive (IC_{50} = 4.6-13.5 μM) although the highest effectiveness was exhibited by **Lv-3** against CADO-ES-1 cell line (IC_{50} 3.10 μM). Moreover, the cell cycle analysis performed with **Lv-4** and **Lv-4a** showed that both compounds induced apoptosis in Jurkat cells. The related triterpenoids iubol (**Lv-5**), 22-hydroxy-15(28)-dehydrovenustatriol (**Lv-6**), 1,2-dehydropseudo-dehydrothyrsiferol (**Lv-7**), and secodehydrothyrsiferol (**Lv-8***)* (Figure 1.18) also displayed

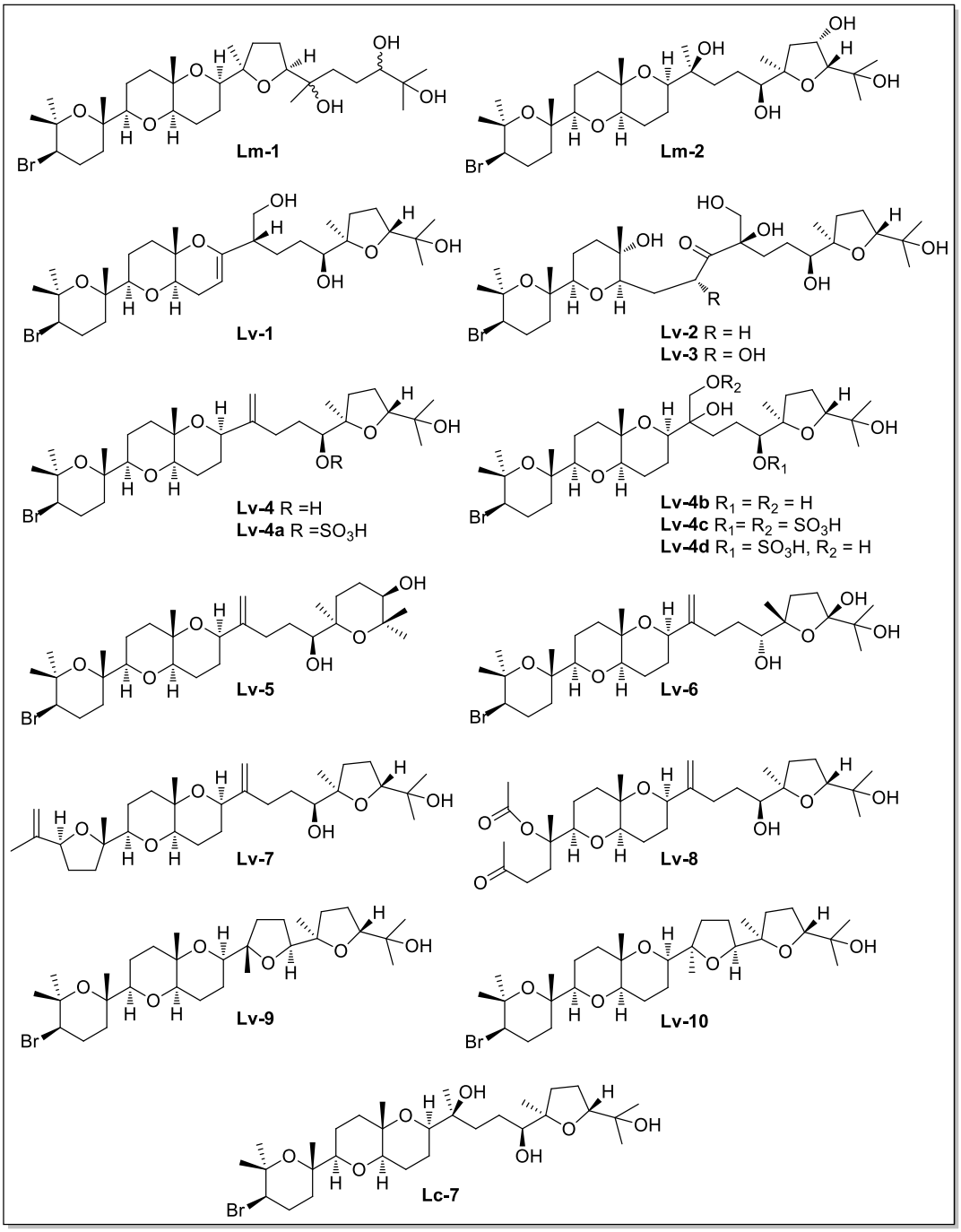

Figure 1.18. Cytotoxic triterpenoids isolated from the red algae *Laurencia mariannensis* (**Lm-1**, **Lm-2**), *L. viridis* (**Lv-1** – **Lv-10**) and *L. catarinensis* (**Lc-7**) together with the antitumor derivatives **Lv-4a**, **Lv-4b**, **Lv-4c**, and **Lv-4d** prepared from **Lv-4.**

significant cytotoxic activity against the same panel of cancer cell lines (IC_{50} = 2.0-30.0 μM) (Cen-Pacheco et al., 2011b). The highest inhibitory activity was observed for **Lv-5**, **Lv-6,** and **Lv-8** against the Jurkat leukemic cells, with IC_{50} values of 3.5, 2.0, and 2.5 μM, respectively. In addition, secodehydrothyrsiferol (**Lv-8**) at 20 μM induced apoptosis, as inferred from the appearance of a sub-G1/G0 subpopulation in cell cycle analysis (Cen-Pacheco et al., 2011b). The last report of this series on *L. viridis* described two new triterpenoids, saiyacenols A (**Lv-9**) and B (**Lv-10**) (Figure 1.18), that inhibited the proliferation of the same four cell lines with IC_{50} values in the range 2.7-27.5 μM. Again, the highest effect was observed against Jurkat cells and it was caused by compound **Lv-10** (IC_{50} 2.7 μM) (Cen-Pacheco et al., 2012).

On the other hand, studies on the mechanism of action of the cytotoxic triterpene thyrsiferol (**Lc-7**, Figure 1.18), obtained from *Laurencia catarinensis*, showed that **Lc-7** at 3μM caused 66% inibition of the hypoxia-inducible factor-1 (HIF-1) activation in T47D human breast cancer cells (Mahdi et al., 2011). Moreover, thyrsiferol suppressed mitocondrial respiration by selectively inhibiting ETC complex I (IC_{50} 3 μM).

Brown algae

A few studies have investigated the antitumor potential of terpenoids and meroterpenoids isolated from brown macroalgae. The new *bis*-prenylated quinone **Pc-1** (Figure 1.19) isolated from *Perithalia capillaris* showed potent antiproliferative activity against HL60 cells with IC_{50} = 0.34 μM (Sansom et al., 2007), while the phenol **Pc-2** and the new chromane **Pc-3** were less active (IC_{50} = 2.7 and 5.6 μM, respectively). The compounds **Pc-1** and **Pc-2** were later isolated from *Sporochnus comosus* together with four new *bis*-prenylated phenols, comosusols A (**Sco-1**), B (**Sco-2**), C (**Sco-3**), and D (**Sco-4**), and the *bis*-prenylated cyclohexenone comosone A (**Sco-5**) (Figure 1.19). All these compounds showed cytotoxic activity against the human tumor cell lines MCF-7 (breast), SF-268 (CNS), H460 (lung), and HT-29 (colon) with GI_{50} values ranging from 5 to 59 μM (Ovenden et al., 2011). The most active was comosusol B (**Sco-2**) with IC_{50} values of 5, 6, 6, and 6 μM, respectively.

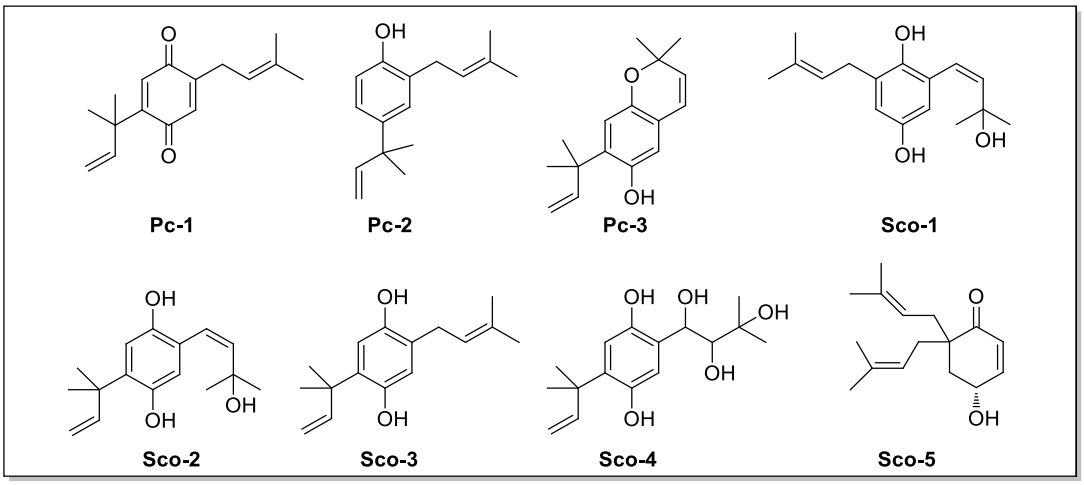

Figure 1.19. Antitumor *bis*-prenylated compounds isolated from the brown algae *Perithalia capillaris* (**Pc-1** – **Pc-3**) and *Sporochnus comosus* (**Pc-1**, **Pc-2**, **Sco-1** – **Sco-5**).

The meroditerpenoids sargaquinoic acid (**St-1**), sargahydroquinoic acid (**St-2**), and sargaquinone (**St-3**) (Figure 1.20), isolated from the seaweed *Sargassum fallax*, proved to have moderate antitumor activity against P388 murine leukaemia cell line (IC_{50} = 17, 14 and 32 μM, respectively) (Reddy and Urban 2009).

The antitumor activity of the chromane sargachromanol E (**Ss-10**) (Figure 1.20) isolated from *Sargassum siliquastrum* was investigated against the HL-60 cell line (Heo et al., 2011). The meroditerpene **Ss-10** inhibited tumor cell proliferation (68.9% at 25 μM) and induced apoptosis by mechanisms involving the downregulation of Bcl-xL, upregulation of Bax, activation of caspase-3, and cleavage of poly-ADP-ribose-polymerase (PARP). Another chemical investigation of *S. siliquastrum* yielded the known meroterpenoid sargachromanol J (**Ss-16**), and the new sargachromanols Q (**Ss-17**) and R (**Ss-18**) (Figure 1.20), which were described to inhibit the proliferation of a panel of human cancer cell lines including AGS (gastric adenocarcinoma), HT-29 (colon adenocarcinoma), HT-1080 (fibrosarcoma), and MCF-7 (breast adenocarcinoma) (Lee et al., 2014). Sargachromanol R (**Ss-18**) displayed the strongest activity against AGS, HT-29, and HT-1080 cell lines with IC_{50} values of 6.5, 3.4, and 13.9 μg/mL, respectively. Sargachromanol J (**Ss-16**) was active againts the four cells (IC_{50} 27.8-31.3 μg/mL) and sargachromanol Q (**Ss-17**) was only active against AGS (IC_{50} 42.8 μg/mL).

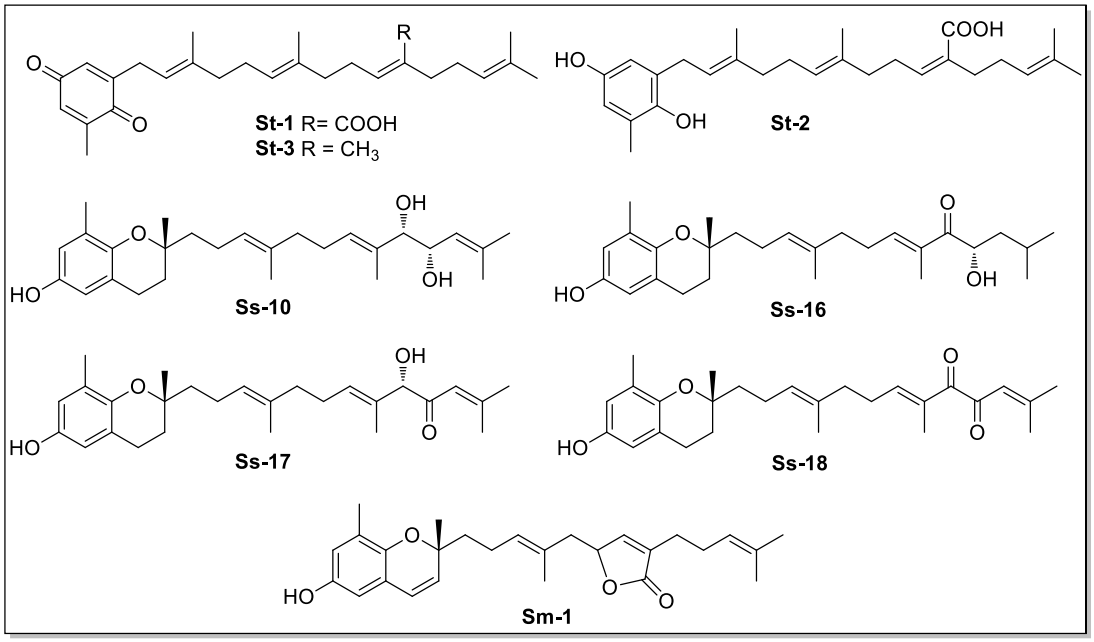

Figure 1.20. Cytotoxic meroterpenoids isolated from the brown algae *Sargassum fallax* (**St-1**, **St-2**, and **St-3**), *S. siliquastrum* (**Ss-10**, **Ss-16**, **Ss-17**, and **Ss-18**) and *S. macrocarpum* (**Sm-1**).

The meroterpenoid tuberatolide B (**Sm-1**), isolated from *Sargassum macrocarpum*, has been shown to inhibit tumor growth on breast, lung, colon, prostate, and cervical cancer cells by inducing apoptosis (Choi et al., 2017). Tuberatolide B (**Sm-1**) enhanced DNA damage by inducing γH2AX foci formation and the phosphorylation of DNA damage-related proteins such as Chk2 and H2AX. Furthermore, **Sm-1** selectively inhibited STAT3 activation, which resulted in a reduction in cyclin D1, MMP-9, survivin, VEGF, and IL-6.

The activity of six meroditerpenoids isolated from *Stypopodium flabelliforme*, epitaondiol (**Sf-1**), epitaondiol diacetate (**Sf-2**), epitaondiol monoacetate (**Sf-3**), stypotriol triacetate (**Sf-4**), 14-ketostypodiol diacetate (**Sf-5**), and stypodiol (**Sf-6**) (Figure 1.21) as inhibitors of cell proliferation was investigated against a panel of human (Caco-2 and SH-SY5Y), and non-human (RBL-2H3 and RAW.267) cancer cell lines, as well as against the non-cancer cells V79 (Pereira et al., 2011). Overall, all compounds showed significant activity against the tested cancer cell lines. The compounds **Sf-1**, **Sf-3** and **Sf-4** displayed nearly 100% inhibition of RAW.267 cells at all the tested concentrations (12.5, 25, 50 μM for **Sf-1** and **Sf-4**; 6.25, 12.5 and 25 μM for **Sf-3**). The cells SH-SY5Y were the most susceptible and except for **Sf-2** all compounds caused nearly 100% inhibition of SH-SY5Y

at the highest tested dose (50 μM). For Caco-2 and RBL-2H3 cell lines, all meroterpenes showed a concentration-dependent inhibitory effect, with **Sf-1**, **Sf-3,** and **Sf-4** being the most actives. On the other hand, **Sf-2**, **Sf-5**, and **Sf-6** had no effect on the non-cancer cell line.

A related compound, zonaquinone acetate (**Sz-1**) isolated from *Stypopodium zonale* (Figure 24) was described to inhibit the proliferation of MCF-7 (breast) and HT-29 (colon) cancer cell lines with IC_{50} values of 20.4 μM and 17.7 μM respectively, which were comparable to the values shown by the standard drugs tamoxifen (17.3 μM for MCF-7) and fluorouracil (29.3 μM for HT-29) (Penicooke et al., 2013); however, no activity was observed against HepG2 cells.

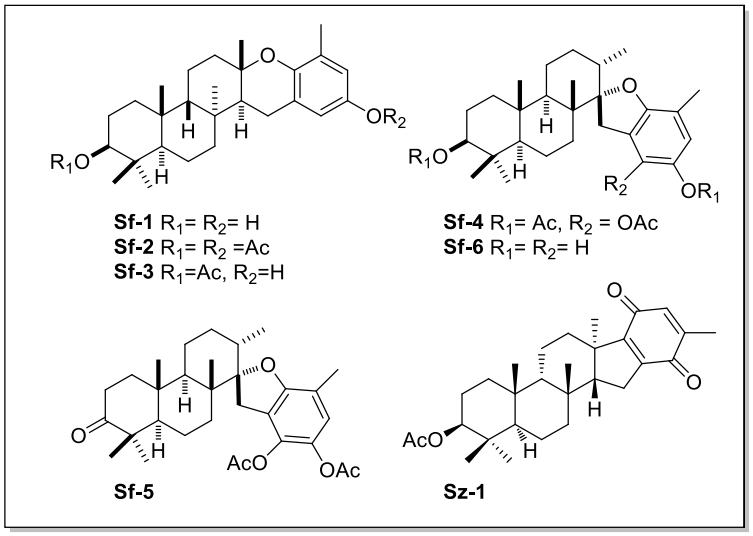

Figure 1.21. Cytotoxic terpenoids isolated from the brown algae *Stypopodium flabelliforme* (**Sf-1** – **Sf-6**) and *Stypopodium zonale* (**Sz-1**).

The new meroditerpene cystoazorol A (**Cab-1**), along with the new meronorsesquiterpenes cystoazorones A (**Cab-2**) and B (**Cab-3**) (Figure 1.22), were isolated from *Cystoseira abies-marina* and tested for their cytotoxicity toward tumor (HeLa) and non-tumor (Vero) cell lines (Gouveia et al., 2013b). The most active compound was cystoazorol A (**Cab-1**), with IC_{50} values of 10.2 μg/mL against cells in lag phase and 2.8 μg/mL against cells in log phase. The compound was less cytotoxic against non-tumor cells, displaying selectivity index (SI = IC_{50}Vero/ IC_{50}HeLa) of 1.64 and 2.46 for cells in

lag and log phases, respectively, which are superior to those shown by taxol (1.5 and 0.5, respectively). Cystoazorones **Cab-2** and **Cab-3** were also cytotoxic (IC_{50} of 14.3-32.0 μg/mL) against HeLa, but less selective.

More recently, the compound **Ct-1** (Figure 1.22), a derivative of the meroditerpenoid cystoketal isolated from *Cystoseira tamariscifolia*, was shown to display a significant inhibition of HepG2 cells (IC_{50} 14.77 μg/ml), and less activity towards the non-tumor S17 cells (IC_{50} 48.46 μg/ml, SI = 3.28) (Vizetto-Duarte et al., 2016).

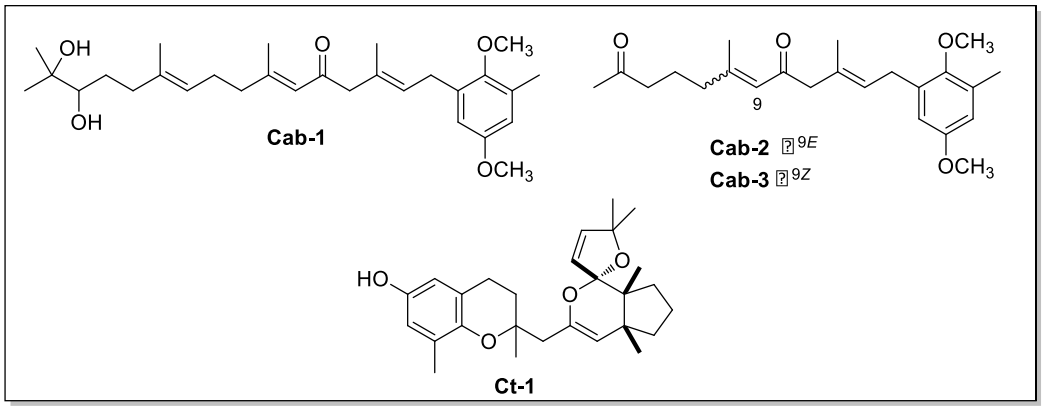

Figure 1.22. Cytotoxic meroterpenoids from the brown algae *Cystoseira abies-marina* (**Cab-1** – **Cab-3**) and *C. tamariscifolia* (**Ct-1**).

Among the NPs isolated from *Homoeostrichus formosana*, the known compound methylfarnesylquinone (**Hf-1**) together with the new chromene derivative **Hf-2** and its acetyl derivative **Hf-2a** (Figure 1.23), displayed moderate to weak cytotoxicity on HepG2 (liver), A549 (lung) and MDA-MB-231 (breast) cancer cell lines, with IC_{50} values ranging from 20.2 to 43.1 μM (Fang et al., 2015).

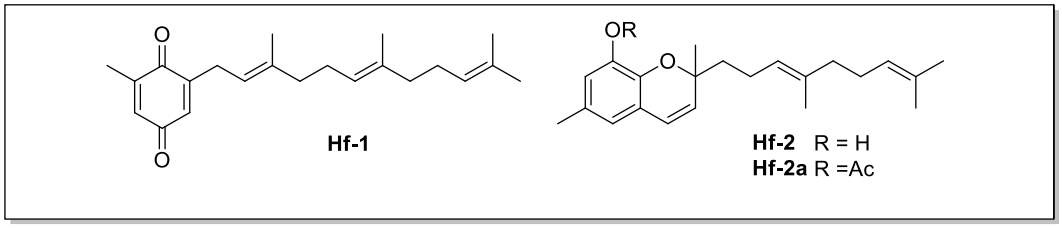

Figure 1.23. Cytotoxic meroterpenoids isolated from the brown alga *Homoeostrichus formosana*.

Brown algae belonging to the family Dictyotaceae represent a rich source of biologically active terpenoids. The new compound 8α,11-dihydroxypachydictyol A (**Dsp-1**), isolated from an unidentified species of the genus *Dictyota* (Figure 1.24) showed cytotoxicity against the lung cancer cell line NCI-H187 (IC_{50} 5 μg/ml) and moderate activity against KB oral carcinoma cell (IC_{50} 14.1 μg/ml) (Jongaramruong and Kongkam 2007). The related compound pachydictyol A (**Dd-1**), isolated from *Dictyota dichotoma,* (Figure 1.24), exhibited cytotoxicity against a panel of 12 human tumor cell lines with a mean IC_{50} of 23.6 μM (Abou-El-Wafa et al., 2013).

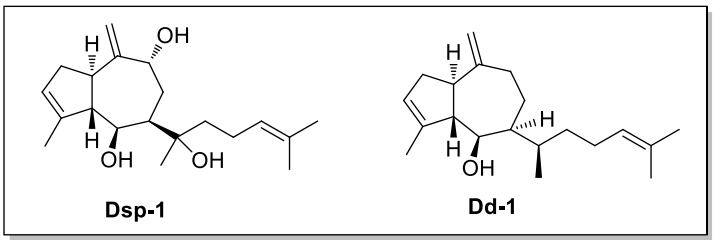

Figure 1.24. Cytotoxic diterpenoids isolated from the brown algae *Dictyota* sp. (**Dsp-1**) and *Dictyota dichotoma* (**Dd-1**).

A chemical study of *Stoechospermum marginatum* led to the isolation of ten terpenoids that were used to synthetize seven derivatives. The compounds were assayed against the cancer cell lines U937 (histocytic lymphoma), THP-1 (acute monocytic leukemia), COLO205 (colon adenocarcinoma), B16F10 (mouse melanocarcinoma), and HL60 (promyelocytic leukemia). Although many compounds were active against most of the cell lines, the highest levels of cytotoxicity were described for the natural spatane diterpenoid **Sma-1**, and the semi synthetic derivatives **Sma-1a**, **Sma-2a**, and **Sma-3a** (Figure 1.25). These exibited cytotoxic activity against U937 cells with IC_{50} values of 5.60, 8.80, 7.52, and 9.58 μg/mL, respectively, and against B16F10 with IC_{50} values of 3.45, 4.11, 3.62 and 3.28 μg/mL, respectively, which are comparable to those of the standard drug etoposide (IC_{50} = 2.27 and 4.12 μg/mL against U937 and B16F10, respectively) (Chinnababu et al., 2015). The apoptotic mechanism of the compound **Sma-1** was investigated on B16F10 cancer cells, and the results indicated that **Sma-1** induced intrinsic mitochondrial apoptosis pathway by generating ROS and deregulating the PI3K/Akt pathway (Velatooru et al., 2016). In addition, the *in vivo* antitumor activity of **Sma-1** was

investigated in C57BL/6 mice bearing B16F10 melanoma. At doses of 4, 10, and 15 mg/ kg (i.p.), the compound **Sma-1** caused an effective inhibition of tumor volume (up to 70 %) in a dose dependent manner without apparent toxic effects.

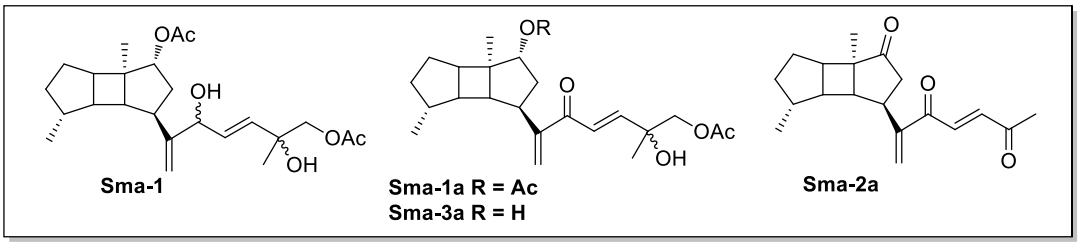

Figure 1.25. Cytotoxic diterpenoids isolated from the brown alga *Stoechospermum marginatum* (**Sma-1**, **Sma-1a**, **Sma-2a**, and **Sma-3a**).

1.3.3. Anti-inflammatory properties of terpenoids and meroterpenoids isolated from macroalgae

Inflammation is a natural defense mechanism against exogenous and endogenous noxious stimuli (Okin et al., 2012). The purpose of inflammation is to protect the area of injury or infection by eliminating the injurious agent and removing the damaged tissue components (Khanna et al., 2014). During the process of inflammation, different cell types are recruited, including macrophages, which are involved in the production of various pro- and anti-inflammatory mediators such as the cytokines (tumor necrosis factor TNF-α and interleukins), the enzymes cyclooxygenase-2 (COX-2) and inducible nitric oxide synthase (iNOS), nitric oxide (NO), the prostaglandins and leukotrienes (Duque and Descoteaux 2014). Thus, the inhibition of the pro-inflammatory mediators produced by macrophages is believed to be crucial for managing inflammatory diseases. Moreover, the expression of most of the pro-inflammatory cytokines is controlled through the activation of NF-κB; this is a key regulator of immune system and inflammatory response (Biswas, 2016), and therefore an important target for the discovery of anti-inflammatory compounds.

Many investigations have been focused on the identification of anti-inflammatory agents from natural sources, mainly terrestrial plants, using a variety of *in vitro* and *in vivo* assays (Azab et al., 2016). These studies have also shown that many NPs with anti-inflammatory effects, including terpenoids, target and modulate the NF-κB signaling pathway (Salminen et al., 2008; Folmer et al., 2008).

Macroalgae have been shown to possess different types of compounds with anti-inflammatory potential, such as polyphenols, sulfated polysaccharides, terpenoids, and fatty acids (Fernando et al., 2016; Jaswir and Monsur 2011; Park et al., 2011). Herein we present the data reported during the last twelve years (2007-2018) on the terpenoids and meroterpenoids from macroalgae with anti-inflammatory properties, organized by class of algae and type of terpenoids.

Red algae

Among the five sesquiterpenoids isolated from *Laurencia dendroidea*, the new chamigrane-type sesquiterpenes debromoelatol (**Ld-1**) and obtusane (**Ld-2)**, and the known compound **Ld-3** (Figure 1.26) inhibited the release of the inflammatory mediator NO in LPS-stimulated RAW 264.7 macrophages (Machado et al., 2014). Debromoelatol **Ld-2** (IC_{50} 44.9 μM) was more active than the reference compound LNMNA (L-monomethylarginine, IC_{50} = 71.3 μM), while the IC_{50} values of **Ld-1** and **Ld-3** (69.1 μM and 74.6 μM, respectively) were similar to that of LNMMA. In addition, **Ld-1** also caused moderate inhibition of the TNF-α levels (IC_{50} 133.8 μM).

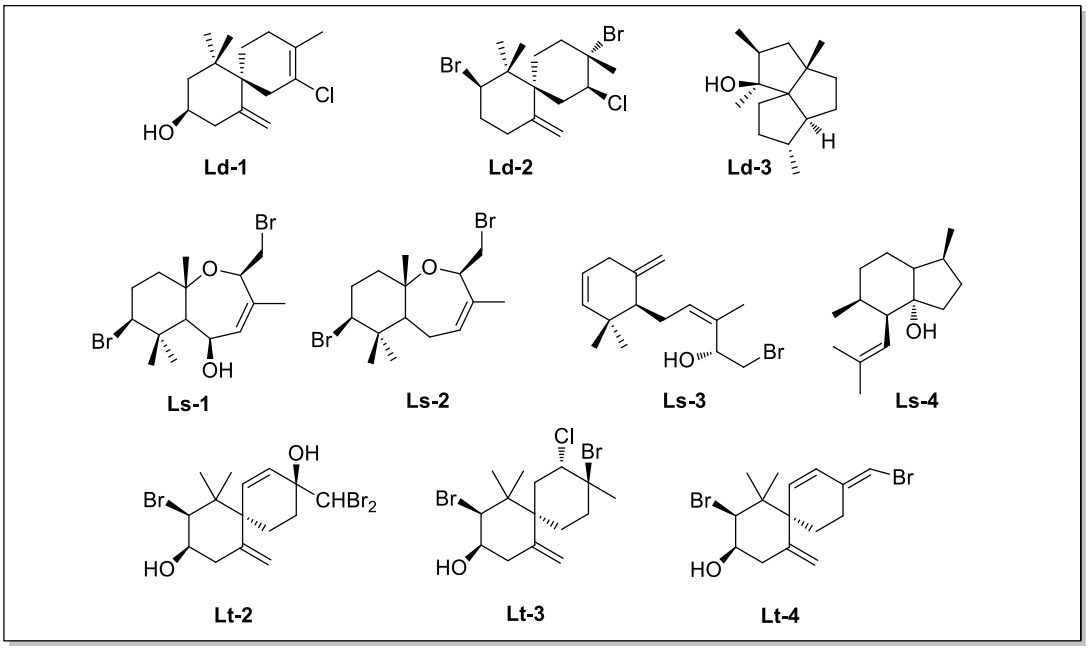

Figure 1.26. Anti-inflammatory sesquiterpenoids isolated from the algae *Laurencia dendroidea* (**Ld-1 − Ld-3**), *L. snackeyi* (**Ls-1 −Ls-4**), and *L. tristicha* (**Lt-1− Lt-4**).

The sesquiterpene 5β-hydroxypalisadin B (**Ls-1**), along with another three compounds, palisadin (**Ls-2**), palisol (**Ls-3**), and pacifigorgiol (**Ls-4**) (Figure 1.26) isolated from the red alga *Laurencia snackeyi* also showed *in vitro* inhibition of the NO production in LPS-stimulated RAW 264.7 cells (Wijesinghe et al., 2014a). The most active compound was **Ls-1**, which caused 90% inhibition at 50 μM (IC_{50}=17.56 μM). This compound also decreased the LPS-induced release of prostaglandin E2 (PGE_2, 37.4% inhibition at 50 μM), markedly suppressed the iNOS and COX-2 expression at 25-50 μM, and diminished the production of the pro-inflammatory cytokines TNF-α, IL-1β, and IL-6 (38%, 52%, and 30%, respectively, at 20 μM). Furthermore, the compound **Ls-1** was tested for its anti-inflammatory effect on zebrafish embryo in an *in vivo* model (Wijesinghe et al., 2014b). At concentrations in the range 0.25-1 μg/mL the compound showed protective effect against stress-induced ROS formation and effectively inhibited the LPS-induced nitric oxide (NO) production in zebrafish embryos. Moreover, all the protective effects observed for **Ls-1** were comparable to those caused by the reference compound dexamethasone (0.5 μg/mL).

The chemical investigation of *Laurencia tristicha* led to the isolation of eighteen metabolites among which the new chamigrane sesquiterpene **Lt-2** and the two known chamigranes **Lt-3** and **L-4** (Figure 1.26) caused at 20 μM significant inhibition of elastase release (33%, 60%, and 69%, respectively) (Chen et al., 2016). In addition, **Lt-2** and **Lt-3** at 20 μM significantly inhibited the *N*-formylmethionyl-leucyl-phenylalanine /cytochalasin B (fMLP/CB)-induced superoxide anion ($O_2^{-\bullet}$) secretion (32% and 48%, respectively).

Only one diterpene with anti-inflammatory properties has been described from red algae in the last years, neorogioltriol (**Lg-1**) (Figure 1.27) (Chatter et al., 2011).

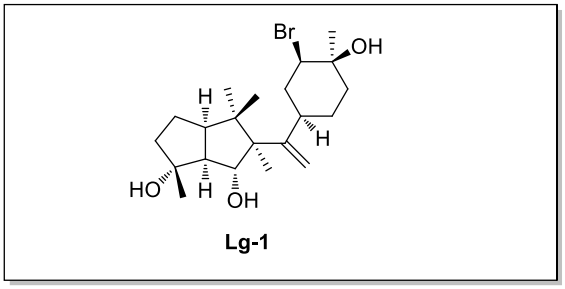

Figure 1.27. Anti-inflammatory diterpene from the red alga *Laurencia glandulifera*.

Neorogioltriol (**Lg-1**) was isolated from *Laurencia glandulifera* and showed anti-inflammatory effects *in vivo* and *in vitro*. In the carregeenan-induced rat edema model, the administration of 1 mg/kg of **Lg-1** produced about 28% reduction of edema after the first hour and a maximum redution of 58% after three hours. *In vitro* assays showed that **Lg-1** at concentrations of 0.125 to 62.5 μM inhibited the production of TNF-α in LPS-stimulated RAW264.7 cells. **Lg-1** also decreased the release of NO and the expression of COX-2, although the anti-inflammatory effects decreased and even were lost at concentrations higher than 25 μM. **Lg-1** was also shown to inhibit the NF-κB activation, and the loss of anti-inflammatory efficacy at high doses was sugested to be independent of NF-κB inhibition.

Brown algae

The new *bis*-prenylated quinone **Pc-1** and the known *bis*-prenylated phenol **Pc-2** (Figure 1.28) isolated from *Perithalia capillaris* were described to inhibit the superoxide production by human neutrophils with IC_{50} values of 2.1 μM and 29 μM, respectively (Sansom et al., 2007).

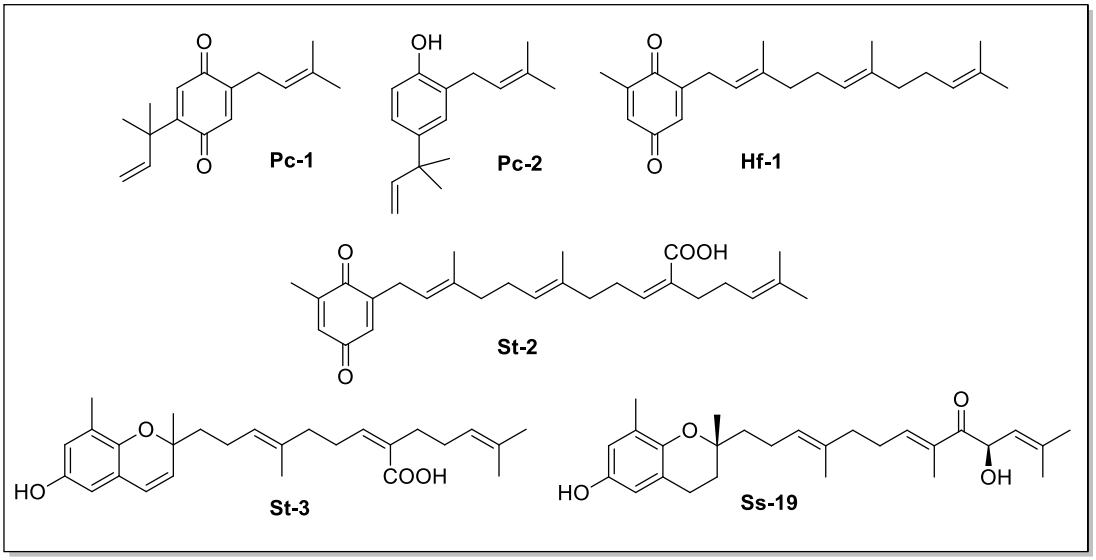

Figure 1.28. Anti-inflammatory meroterpenoids isolated from the brown algae *Perithalia capillaris* (**Pc-1**, **Pc-2**), *Homoeostrichus formosana* (**Hf-1**), *Sargassum siliquastrum* (**St-2** and **Ss-19**) and *Sargassum micracanthum* (**St-3**).

The related compound methylfarnesylquinone (**Hf-1**) isolated from the brown alga *Homoeostrichus formosana* (Figure 1.28), was found to inhibit the production of FMLP/CB-induced superoxide anion (IC_{50} 0.22 μg/mL) and the elastase release (IC_{50} 0.48 μg/mL) in human neutrophils (Fang et al., 2015).

On the other hand, sargaquinoic acid (**St-2**) (Figure 1.28) isolated from *Sargassum siliquastrum* was described to inhibit in a dose dependent manner (6.5, 12.5, 25 μM) the production of NO and, at 25 μM, the expression of iNOS in LPS-stimulated RAW264.7 macrophages (Kang et al., 2013). In addition, sargaquinoic acid (**St-2**) inhibited the degradation of IκB and the subsequent nuclear translocation of NF-κB, and also influenced the LPS-stimuated phosphorylation of JNK 1/2 MAPK.

Similar results have been described for the meroterpenoids sargachromanol G (**Ss-19**) and sargachromenol (**St-3**) (Figure 1.28), isolated from *Sargassum siliquastrum* and *S. micracanthum*, respectively. Both compounds were shown to inhibit in a dose dependent manner (10, 20, and 40 μM for **Ss-19** and 12.5, 25, 50, 100 μM for **St-3**) the production of various inflammatory mediators including, NO, iNOS, PGE 2, and COX-2 in LPS-stimulated RAW 264.7 cells (Yoon et al., 2012; Yang et al., 2013). Sargachromanol G (**Ss-19**) was also demonstrated to inhibit the pro-inflammatory cytokines TNF-α, IL-1β, and IL-6 (Yoon et al., 2012). The anti-inflammatory properties of **Ss-19** and **St-3** were mediated through the inhibition of NF-κB (Yoon et al., 2012, Yang et al., 2013). For **Ss-19,** the down-regulation of MAPK (ERK1/2, JNK, and p38) signalling pathway was also demonstrated (Yoon et al., 2012).

Finally, two studies on the bioactive metabolites of *Dictyota plectens* led to the identification of four anti-inflammatory diterpenoids: dictyol E (**Dp-1**), 4β-hydroxydictyodial A (**Dp-2**)**,** 4-hydroxydictyolactone **(Dp-3),** and 4α-hydroxypachylactone **(Dp-4)** (Figure 1.29) (Zhao et al., 2015; Cheng et al., 2014). At 10 μM, these compounds caused 90%, 86%, 76% and 53.2% inhibition, respectively, of LPS-induced NO production in mouse peritoneal macrophages (PEMΦ).

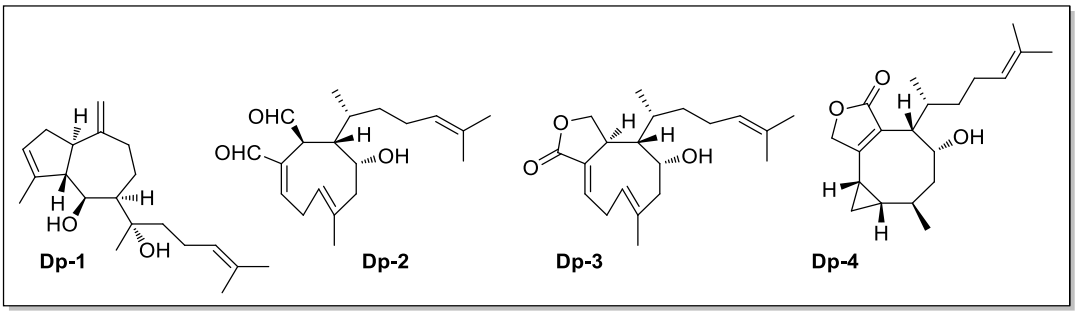

Figure 1.29. Anti-inflammatory diterpenoids isolated from the brown alga *Dictyota plectens*.

1.4. Algae of the genus *Cystoseira*

Cystoseira C. Agargh is a polyphyletic genus of marine algae of the Sargassaceae family, which currently encompasses 46 species worldwide distributed through subtropical waters (Guiry, 2019). Most of the species live in the Mediterranean Sea and the northeastern Atlantic coasts, from Cape Verde to the British Islands (Draisma et al., 2010; Amico, 1995).

The chemical research of algae of the genus *Cystoseira*, which was especially intense during the period between 1980 and 1995, has led to the isolation and structural characterization of an array of novel NPs of meroterpenoid type (Gouveia et al., 2013a; Amico et al., 1995; Valls and Piovetti, 1995).

Despite the high number and structural variety of the meroterpenoids obtained from *Cystoseira* algae, the biological properties of these metabolites have been scarcely explored. This can be in part explained because at the years when most the compounds were isolated there were not bioactivity assays easily accessible. Nonetheless, a few meroterpenoids from algae of the genus *Cystoseira* have been shown to possess *in vitro* cytotoxic activity, either by using the fertilized sea-urchin eggs assay (Mesguiche et al., 1997; Fadli et al., 1991; Francisco et al., 1986) or by using tumor cell lines (Gouveia et al., 2013a; Norte et al., 1993; Urones et al., 1992a; Urones et al., 1992b). Another few compounds have also been shown to possess antimicrobial (Bennamara et al., 1999; Amico et al., 1988), antiviral (Urones et al., 1992a and 1992b), or antioxidant (Fisch et al., 2003; Foti et al., 1994) activities. These data suggest that the meroterpenoids produced by *Cystoseira* algae possess a great biomedical potential that remains almost unexplored.

The coasts of the Gibraltar Strait harbour several species of algae of the genus *Cystoseira*, among which *C. usneoides* (Figure 1.30) is one of the most abundant species.

Figure 1.30. Brown alga *Cystoseira usneoides*.

A survey of the literature revealed that the only data on the NPs of the species *C. usneoides* were published in 1992 and refer to a study of specimens collected at the Portuguese coasts, near Sesimbra (Setubal district, Lisbon area) (Urones et al., 1992a, 1992b). The chemical study of those specimens yielded four meroditerpenoids which exhibited cytotoxicity against several tumor cell lines (P388, A-549, HeLa, B16 or L-1210) and activity in preliminary antiviral assays.

The alga *C. usneoides* that grows in the Gibraltar Strait could be expected to contain the same four meroterpenoids above mentioned, although it should not be descarded the possible presence of other related compounds, due to intraspecific variations in the natural product profile of the alga, and of minor metabolites not previously isolated. Therefore, the alga *C. usenoides* from the Gibraltar Strait could be an interesting source of NPs of meroterpenoid type for performing more advanced studies on the antitumor activity of this class of algal metabolites and for investigating their antioxidant and anti-inflammatory properties, which remain almost unexplored. Moreover, the study of these properties could contribute to the understanding of both the relationship between the three processes oxidative stress/inflammation/cancer, and the benefice of the pharmacological control of the oxidative stress and the inflammatory processes to reduce cancer development.

1.5. References

Abou-El-Wafa, H.G.S.E.; Shaaban, M.; Shaaban, K.A.; El-Naggar, M.E.E.; Maier, A.; Fiebig, H.H.; Laatsch, H. Pachydictyols B and C: New diterpenes from *Dictyota dichotoma*. *Mar. Drugs* **2013**, *11*, 3109–3123.

Alarif, W.M.; Al-Footy, K.O.; Zubair, M.S.; Halid, M.; Ghandourah, M.A.; Basaif, S.A.; Al-Lihaibi, S.S.; Ayyad, S.E.; Badria, F.A. The role of new eudesmane-type sesquiterpenoid and known eudesmane derivatives from the red alga *Laurencia obtusa* as potential antifungal-antitumour agents. *Nat. Prod. Res*. **2016**, *30*, 1150–1155.

Alarif, W.M.; Al-Lihaibi, S.S.; Ayyad, S.N.; Abdel-Rhman, M.H.; Badria, F.A. Laurene-type sesquiterpenes from the Red Sea red alga *Laurencia obtusa* as potential antitumor-antimicrobial agents. *Eur. J. Med. Chem.* **2012**, *55,* 462–466.

Amico, V. Marine brown algae of family Cystoseiraceae: Chemistry and chemotaxonomy. *Phytochemistry* **1995**, *39*, 1257−1279.

Amico, V.; Cunsolo, F.; Neri, P.; Piattelli, M.; Ruberto, G. Antimicrobial tetraprenyltoluquinol derivatives from *Cystoseira spinosa* var. *squarrosa*. *Phytochemistry* **1988**, *27*, 1327-1331.

Angawi, R.F.; Alarif, W.M.; Hamza, R.I.; Badria, F.A.; Ayyad, S.N. New cytotoxic laurene-, cuparene-, and laurokamurene-type sesquiterpenes from the red alga *Laurencia obtuse*. *Helv. Chim. Acta.* **2014**, *97*, 1388–1395.

Antunes, E.M.; Afolayan, A.F.; Chiwakata, M.T.; Fakee, J.; Knott, M.G.; Whibley, C.E.; Hendricks, D.T.; Bolton, J.J.; Beukes, D.R. Identification and *in vitro* anti-esophageal cancer activity of a series of halogenated monoterpenes isolated from the South African seaweeds *Plocamium suhrii* and *Plocamium cornutum*. *Phytochemistry* **2011**, *72*, 769–772.

Ayyad, S.N.; Makki, M.S.; Al-kayal, N.S.; Basaif, S.A.; El-Foty, K.O.; Asiri, A.M.; Alarif, W.M.; Badri, F.A. Cytotoxic and protective DNA damage of three new diterpenoids from the brown alga *Dictoyota dichotoma*. *Eur. J. Med. Chem.* **2011**, *46*, 175–182.

Azab, A.; Nassar, A.; Azab, A.N. Anti-inflammatory activity of natural products. *Molecules* **2016**, *21*,1321. doi: 10.3390/molecules21101321.

Balboa, E.M.; Conde, E.; Moure, A.; Falqué, E.; Domínguez, H. In vitro antioxidant properties of crude extracts and compounds from brown algae. *Food. Chem.* **2013,** *138*, 1764–1785.

Barsanti, L.; Gualtieri, P. Algae and men. In *Algae: anatomy, biochemistry, and biotechnology.* CRC Press: Boca Raton, **2006b;** pp. 251-291.

Barsanti, L.; Gualtieri, P. General overview. In *Algae: anatomy, biochemistry, and biotechnology.* CRC Press: Boca Raton, **2006a**; pp. 1-34

Bennamara, A.; Abourriche, A.; Berrada, M.; Charrouf, M.; Chaib, N.; Boudouma, M.; Garneau, F. X. *Phytochemistry* **1999**, *52*, 37–40.

Birben, E.; Sahiner, U.M.; Sackesen, C.; Erzurum, S.; Kalayci, O. Oxidative stress and antioxidant defense. *World Allergy Organ. J.* **2012**, *5*, 9–19.

Biswas, S.K. Does the interdependence between oxidative stress and inflammation explain the antioxidant paradox? *Oxid. Med. Cell Longev.* **2016**, *2016*, article 5698931, dx.doi.org/10.1155/2016/5698931.

Blunt, J.W.; Copp, B.R.; Keyzers, R.A.; Munro, M.H.G.; Prinsep, M.R. Marine natural products. *Nat. Prod. Rep*. **2015**, *32*, 116–211.

Bold, H.C.; Wynne, M.J. *Introduction to the algae: structure and reproduction*. Prentice-Hall: Englewood Cliffs, **1985**; p. 706**.**

Bourdron, J.; Barbier, P.; Allegro, D.; Villard, C.; Lafitte, D.; Commeiras, L.; Parrain, J.L.; Peyrot, V. Caulerpenyne binding to tubulin: structural modifications by a non conventional pharmacological agent. *Med. Chem.* **2009**, *5*, 182–190.

Campos, A.; Souza, C.B.; Lhullier, C.; Falkenberg, M.; Schenkel, E.P.; Ribeiro-do-Valle, R.M.; Siqueira, J.M. Anti-tumour effects of elatol, a marine derivative compound obtained from red algae *Laurencia microcladia*. *J. Pharm. Pharmacol.* **2012**, *64*, 1146-1154.

Cen-Pacheco, F.; Mollinedo, F.; Villa-Pulgarin, J.A.; Norte**,** M.; Fernández, J.J.; Daranas, A.H. Saiyacenols A and B: the kay to solve the controversy about the configuration of aplysiols. *Tetrahedron* **2012**, *68*, 7275–7279

Cen-Pacheco, F.; Villa-Pulgarin, J.A.; Mollinedo, F.; Martín, M.N.; Fernández, J.J.; Daranas, A.H. New polyether triterpenoids from *Laurencia viridis* and their biological evaluation. *Mar. Drugs* **2011b**, *9*, 2220–2235.

Cen-Pacheco, F.; Villa-Pulgarin, J.A.; Mollinedo, F.; Norte, M.; Daranas, A.H.; Fernández, J.J. Cytotoxic oxasqualenoids from the red alga *Laurencia viridis*. *Eur. J. Med. Chem.* **2011a**, *46*, 3302–3308.

Chakraborty, K.; Joseph, D.; Joy, M.; Raola, V.K. Characterization of substituted aryl meroterpenoids from red seaweed *Hypnea musciformis* as potential antioxidants. *Food Chem.* **2016**, *212*, 778–788.

Charrier, B.; Abreu, M.H.; Araujo, R.; Bruhn, A.; Coates, J.C.; De Clerck, O.; Katsaros, C.; Robaina, R.R.; Wichard, T. Furthering knowledge of seaweed growth and development to facilitate sustainable aquaculture. *New Phytol*. **2017**, *216,* 967–975.

Chatter, R.; Othman, R.B.; Rabhi, S.; Kladi, M.; Tarhouni, S.; Vagias, C.; Roussis, V.; Guizani-Tabbane, L.; Kharrat, R. In *vivo* and in vitro anti-Inflammatory activity of neorogioltriol, a new diterpene extracted from the red algae *Laurencia glandulifera*. *Mar. Drugs* **2011**, *9*, 1293–1306.

Chen, J.Y.; Huang, C.Y.; Lin, Y.S.; Hwang, T.L.; Wang, W.L.; Chiou, S.F.; Sheu, J.H. Halogenated sesquiterpenoids from the red alga *Laurencia tristicha* collected in Taiwan. *J. Nat. Prod*. **2016**, *79*, 2315–2323.

Cheng, S.; Zhao, M.; Sun, Z.; Yuan, W.; Zhang, S.; Xiang, Z.; Cai, Y.; Dong, J.; Huang, K.; Yan, P. Diterpenes from a chinese collection of the brown alga *Dictyota plectens*. *J. Nat. Prod.* **2014**, *77*, 2685−2693.

Chinnababu, B.; Purushotham Reddy, S.; Sankara Rao, P.; Loka Reddy, V.; Sudheer Kumar, B.; Rao, J.V.; Prakasham, R.S.; Suresh Babu, K. Isolation, semi-synthesis and bio-evaluation of spatane derivatives from the brown algae *Stoechospermum marginatum*. *Bioorg. Med. Chem. Lett.* **2015**, *25*, 2479–2483.

Cho, S.H.; Cho, J.Y.; Kang, S.E.; Hong, Y.K.; Ahn, D.H. Antioxidant activity of mojabanchromanol, a novel chromene, isolated from brown alga *Sargassum siliquastrum. J. Environ. Biol.* **2008**, *29*, 479–484.

Choi, Y.K.; Kim, J.; Lee, K.M.; Choi, Y.J.; Ye, B.R.; Kim, M.S.; Ko, S.G.; Lee, S.H.; Kang, D.H.; Heo, S.J. Tuberatolide B suppresses cancer progression by promoting ROS-mediated inhibition of STAT3 signaling. *Mar. Drugs* **2017**, *15*, 55.

Coussens, L.M.; Werb, Z. Inflammation and cancer. *Nature* **2002**. *420*, 860–867.

Cragg, G.M.; Grothaus, P.; Newman, D.J. Impact of natural products on developing new anti-cancer agents. *Chem. Rev.* **2009**, *109*, 3012–3043.

Cragg, G.M.; Pezzuto, J.M. Natural products as a vital source for the discovery of cancer chemotherapeutic and chemopreventive agents. *Med. Princ. Pract.* **2016**, *25,* 41–59.

Dewick, P.M. The mevalonate and deoxyxylulose phosphate pathway. In *Medicinal Natural Products: a biosynthetic approach*, 2nd Ed. John Wiley and Sons: Chichester, **2002**; pp.167-232.

Draisma, S.G.A.; Ballesteros, E.; Rousseau, F.; Thibaut, T.J. DNA sequence data demonstrate the polyphyly of the genus *Cystoseira* and *Sargassaceae* genera (Phaeophyceae*). J. Phycol.* **2010**, *46*, 1329−1345.

Dröge, D. Free radicals in the physiological control of cell function. *Physiol. Rev*. **2002**, *82*, 47–95.

Duque, G.A.; Descoteaux, A. Macrophage cytokines: involvement in immunity and infectious diseases. *Front. Immunol*. **2014**, *5*, 491.

Fadli, M.; Aracil, J.M.; Jeanty, G.; Banaigs, B.; Francisco, C. Novel meroterpenoids from *Cystoseira mediterranea*: use of the crown-gall bioassay as a primary screen for lipophilic antineoplastic agents. *J. Nat. Prod*. **1991**, *54*, 261−264.

Fang, H.Y.; Chokkalingam, U.; Chiou, S.F.; Hwang, T.S.; Chen, S.L.; Wang, W.L.; Sheu, J.H. Bioactive chemical constituents from the brown alga *Homoeostrichus formosana*. *Int. J. Mol. Sci.* **2015**, *16*, 736–746.

Farvin, K.H.S.; Jacobsen, C. Phenolic compounds and antioxidant activities of selected species of seaweeds from Danish coast. *Food Chem.* **2013**, *138*, 1670–1681.

Faulkner, D.J. Marine Natural products: metabolites of marine algae and herbivorous marine molluscs. *Nat. Prod. Rep*. **1984**, *1*, 251–280.

Federico, A.; Morgillo, F.; Tuccillo, C.; Ciardiello, F.; Loguercio, C. Chronic inflammation and oxidative stress in human carcinogenesis. *Int. J. Cancer* **2007,** *121*, 2381–2386.

Fernando, I.P.S.; Nah, J.W.; Jeon, Y.J. Potential anti-inflammatory Natural products from marine algae. *Environ. Toxicol. Pharmacol*. **2016**, *48*, 22–30.

Fisch, K.M.; Bohm, V.; Wright, A.D.; Konig, G.M. Antioxidative meroterpenoids from the brown alga *Cystoseira crinita*. *J. Nat. Prod.* **2003**, *66*, 968-975.

Folmer, F.; Jaspars, M.; Dicato, M.; Diederich, M. Marine Natural products as targeted modulators of the transcription factor NF-κB. *Biochem. Pharmacol.* **2008**, *75*, 603–617.

Foti, M.; Piattelli, M.; Amico, V.; Ruberto, G. Antioxidant activity of phenolic meroditerpenoids from marine algae. *J. Photochem. Photobiol. B.* **1994**, *26*, 159−164.

Francisco, C.; Banaigs, B.; Teste, J.; Cave, A. Mediterraneols: a novel biologically active class of rearranged diterpenoid metabolites from *Cystoseira mediterranea* (Pheophyta). *J. Org. Chem.* **1986**, *51*, 1115−1120.

Gonda, T.A.; Tu, S.; Wang, T.C. Chronic inflammation, the tumor microenvironment and carcinogenesis. *Cell Cycle* **2009**, *8*, 2005–2013.

Gouveia, V.; Seca, A.M.L.; Barreto, M.C.; Pinto, D.C.G.A. Di- and sesquiterpenoids from *Cystoseira* genus: Structure, intra-molecular transformations and biological activity. *Mini-Rev. Med. Chem.* **2013a**, *13*, 1150−1159.

Gouveia, V.L.M.; Seca, A.M.L.; Barreto, M.C.; Neto, A.I.; Kijjoa, A.; Silva, A.M.S. Cytotoxic meroterpenoids from the macroalga *Cystoseira abies-marina*. *Phytochemistry Lett.* **2013b**, *6*, 593–597.

Graham, L.E.; Wilcox, L.W. *Algae*. Prentice Hall: Upper Saddle River, **2000**; p. 640.

Guiry, M.D. In Guiry, M.D. & Guiry G. *AlgaeBase*. World-wide electronic publication, National University of Ireland, Galway. http://www.algaebase.org; searched on 17 February 2019

Harvey, A.L.; Edrada-Eber, R.; Quinn, R.J. The re-emergence of Natural products for drug discovery in the genomics era. *Nature Rev. Drug. Discov.* **2015**, *14*, 111-129.

Heo, S.J.; Kim, K.N.; Yoon, W.J.; Oh, C.; Choi, Y.U.; Affan, A.; Lee, Y.J.; Lee, H.S.; Kang, D.H. Chromene induces apoptosis via caspase-3 activation in human leukemia HL-60 cells. *Food Chem. Toxicol*. **2011**, *49*, 1998–2004

Huang, X.; Sun, Y.-L.; Salim, A.A.; Chen, Z.-S.; Capon, R.J. Parguerenes: Marine red alga bromoditerpenes as inhibitors of P-glycoprotein (ABCB1) in multidrug resistant human cancer cells. *Biochem. Pharmacol.* **2013**, *85*, 1257–1268.

Hussain, E.; Wang, L.; Jiang, B.; Riaz, S.; Butt, G.Y.; Shi, D. A review of the components of brown seaweeds as potential candidates in cancer therapy. *RSC Adv.* **2016**, *6*, 12592–12610.

Imbesi, S.; Musolino, C.; Allegra, A.; Saija, A.; Morabito, F.; Calapai, G.; Gangemi, S. Oxidative stress in oncohematologic diseases: an update. *Expert Rev. Hematol.* **2013**, *6*, 317–325.

Jaswir, I.; Monsur, H.A. Anti-inflammatory compounds of macro algae origin: A review. *J. Med. Plant Res.* **2011,** *5*, 7146–7154.

Ji, N.-Y.; Li, X.-M.; Xie, H.; Ding, J.; Li, K.; Ding, L.-P.; Wang, B.-G. Highly oxygenated triterpenoids from the marine red alga *Laurencia mariannensis* (Rhodomelaceae). *Helv. Chim. Acta* **2008**, *91*, 1940–1946.

Jiang, R.W.; Lane, A.L.; Mylacraine, L.; Hardcastle, K.I.; Fairchild, C.R.; Aalbersberg, W.; Hay, M.E.; Kubanek, J. Structures and absolute configurations of sulfate-conjugated triterpenoids including an antifungal chemical defense of the green macroalga *Tydemania expeditionis*. *J. Nat. Prod.* **2008**, *71*, 1616–1619.

Jiménez-Escrig, A.; Jiménez-Jiménez, I.; Pulido, R.; Saura-Calixto, F. Antioxidant activity of fresh and processed edible seaweeds. *J. Sci. Food Agric.* **2001**, *81*, 530–534.

Jongaramruong, J.; Kongkam, N. Novel diterpenes with cytotoxic, anti-malarial and anti-tuberculosis activities from a brown alga *Dictyota sp. J Asian Nat. Prod. Res*. **2007**, *9*, 743–751.

Jung, M.; Jang, K.H., Kim, B.; Lee, B.H, Choi, B.W.; Oh, K.B., Shin, J. Meroditerpenoids from the brown alga *Sargassum siliquastrum*. *J. Nat. Prod.* **2008**, *71*, 1714-1719.

Kang, G.-J.; Han, S.-C.; Yoon, W.-J.; Koh, Y.-S.; Hyun, J.-W.; Kang, H.-K.; Cho, J.Y.; Yoo, E.-S. Sargaquinoic acid isolated from *Sargassum siliquastrum* inhibits lipopolysaccharide-induced nitric oxide production in macrophages *via* modulation of nuclear factor-κB and c-Jun *N*-terminal kinase pathways. *Immunopharm. Immunotox.* **2013**, *35*, 80-87.

Khanna, R.D.; Karki, K.; Pande, D.; Negi, R.; Khanna, R.S. Inflammation, free radical damage, oxidative stress and cancer. *Interdiscip. J. Microinflammation* **2014,** *1*, 109.

Kladi, M.; Vagias, C.; Papazafiri, P.; Furnari, G.; Serio, D.; Roussis, V. New sesquiterpenes from the red alga *Laurencia microcladia*. *Tetrahedron* **2007**, *63*, 7606–7611.

Kumar, S.; Pandey, A.K. Free radicals: health implications and their mitigation by herbals. *Br. J. Med. Med. Res.* **2015**, *7*, 438–457.

Kuzuyama, T. Mevalonate and non mevalonate pathways for the biosynthesis of isoprene units. *Biosci. Biotechnol. Biochem.* **2002**, *66*, 1619–1627.

Lakshmi, P.T.; Vajravijayan, S.; Moumita, M.; Sakthivel, N.; Gunasekaran, K.; Krishna, R. A novel guaiane sesquiterpene derivative, guai-2-en-10α-ol, from *Ulva fasciata* Delile inhibits EGFR/PI3K/Akt signaling and induces cytotoxicity in triple-negative breast cancer cells. *Mol. Cell Biochem.* **2018**, *438*,123–139.

Landskron, G.; De la Fuente, M.; Thuwajit, P.; Thuwajit, C.; Hermoso, M.A. Chronic inflammation and cytokines in the tumor microenvironment. *J. Immunol. Res*. **2014**, *2014*, 1–19.

Lane, A.L.; Stout, E.P.; Hay, M.E.; Prusak, A.C.; Hardcastle, K.; Fairchild, C.R.; Franzblau, S.G.; Le Roch, K.; Prudhomme, J.; Aalbersberg, W.; Kubanek, J. Callophycoic Acids and Callophycols from the Fijian Red Alga *Callophycus serratus*. *J. Org. Chem.* **2007**, *72*, 7343–7351.

Lane, A.L.; Stout, E.P.; Lin, A.S.; Prudhomme, J.; Le Roch, K.; Fairchild, C.R.; Franzblau, S.G.; Hay, M.E.; Aalbersberg, W.; Kubanek, J. Antimalarial bromophycolides J-Q from the Fijian red alga *Callophycus serratus*. *J. Org. Chem*. **2009**, *74*, 2736–2742.

Leal, M.C.; Munro, M.H.G.; Blunt, J.W.; Puga, J.; Jesus, B.; Calado, R.; Rosa, R.; Madeira, C. Biogeography and biodiscovery hotspots of macroalgal marine Natural products. *Nat. Prod. Rep*. **2013**, *30*, 1380–1390.

Lee, J.C.; Hou, M.F.; Huang, H.W.; Chang, F.R.; Yeh, C.C.; Tang, J.Y.; Chang, H.W. Marine algal Natural products with anti-oxidative, anti-inflammatory, and anti-cancer properties. *Cancer Cell Int*. **2013**, *13*, 1–7.

Lee, J.I.; Park, B.J.; Kim, H.; Seo, Y. Isolation of Two New Meroterpenoids from *Sargassum siliquastrum*. *Bull. Korean Chem. Soc.* **2014**, *35*, 2867–2869.

Lee, J.I.; Seo, Y. Chromanols from *Sargassum siliquastrum* and their antioxidant activity in HT1080 cells. *Chem. Pharm. Bull.* **2011**, *59*, 757–761.

Lee, R.E. Basic characteristics of the algae. In *Phycology*. Fourth ed. Cambridge University Press: Cambridge, **2008**; pp. 3–29.

Lhullier, C.; Falkenberg, M.; Ioannou, E.; Quesada, A.; Papazafiri, P.; Horta, P.A.; Schenkel, E.P.; Vagias, C.; Roussis, V. Cytotoxic halogenated metabolites from the Brazilian red alga *Laurencia catarinensis*. *J. Nat. Prod.* **2010**, *73*, 27–32.

Lin, A.S.; Stout, E.P.; Prudhomme, J.; Le Roch, K.; Fairchild, K.R.; Franzblau, S.G.; Aalbersberg, W.; Hay, M.E.; Kubanek, J. Bioactive bromophycolides R–U from the Fijian red alga *Callophycus serratus*. *J. Nat. Prod.* **2010,** *73*, 275–278.

López-Alarcón, C.; Denicola, A. Evaluating the antioxidant capacity of Natural products: A review on chemical and cellular-based assays. *Anal. Chim. Act*a **2013**, *763*, 1–10.

Machado F.L.S.; Ventura T.L.B.; Gestinari, L.M.S.; Cassano, V.; Resende J.A.L.C.; Kaiser, C.R.; Lasunkaia, E.B.; Muzitano, M.F.; Soares A.R. Sesquiterpenes from the brazilian red alga *Laurencia dendroidea.* J. Agardh. *Molecules* **2014**, *19*, 3181–3192.

Mahdi, F.; Falkenberg, M.; Ioannou, E.; Roussis, V.; Zhou, Y.D.; Nagle, D.G. Thyrsiferol inhibits mitochondrial respiration and HIF-1 activation. *Phytochemistry Lett.* **2011**, *4*, 75–78.

Mann, M.G.A.; Mkwananzi, H.B.; Antunes, E.M.; Whibley C.E.; Hendricks D-T.; Bolton, J.J.; Beukes, D.R. Halogenated monoterpene aldehydes from the South African marine alga *Plocamium corallorhiza*. *J. Nat. Prod.* **2007**, *70*, 596–599.

Mesguiche, V.; Valls, R.; Piovetti, L.; Banaigs, B. Meroditerpenes from *Cystoseira amentacea* var. stricta collected off the Mediterranean coasts. *Phytochemistry* **1997**, *45*, 1489−1494.

Multhoff, G.; Molls, M.; Radons, J. Chronic inflammation in cancer development. *Front. Immunol.* **2012**, *2*, 1–17.

Murphy, C.; Hotchkiss, S.; Worthington, J.; McKeown, S.R. The potential of seaweed as source of drugs for use in cancer therapy. *J. Appl. Phycol.* **2014**, *26*, 2211–2264.

Nahas, R.; Abatis, D.; Anagnostopoulou, M.A.; Kefalas, P.; Vagias, C.; Roussis, V. Radical-scavenging activity of Aegean Sea marine algae. *Food Chem.* **2007**, *102*, 577–581.

Newman, D.J.; Cragg, G.M. Marine-sourced anti-cancer and cancer pain control agents in clinical and late preclinical development. *Mar. Drugs* **2014**, *12*, 255–278.

Newman, D.J.; Cragg, G.M. Natural products as sources of new drugs from 1981 to 2014. *J. Nat Prod.* **2016**, *79*, 629-661.

Nimse, S.B.; Palb, D. Free radicals, natural antioxidants, and their reaction mechanisms. *RSC Adv.* **2015**, *5*, 27986–28006.

Norte, M., Sánchez, A., González, G. Claraenone, a new meroditerpene from brown alga. *Tetrahedron Lett.* **1993**, *24*, 3485–3486.

Okin, D.; Medzhitov, R. Evolution of Inflammatory Diseases. *Curr. Biol.* **2012**, *22*, 733–740.

Ovenden, S.P.; Nielson, J.L.; Liptrot, C.H.; Willis, R.H.; Wright, A.D.; Motti, C.A.; Tapiolas, D.M. Comosusols A-D and comosone A: cytotoxic compounds from the brown alga *Sporochnus comosus*. *J. Nat. Prod.* **2011**, *74*, 739–743.

Park, H.Y.; Min, H.H.; Cheol, P.; Jin, C.Y., J.; Kim, G.Y., Choi, I.W.; Kim, N.D.; Nam, T.J.; Kown, T.K.; Choi, Y.H. Anti-inflammatory effects of fucoidan through inhibition of NF-

κB, MAPK and Akt activation in lipopolysaccharide-induced BV2 microglia cells. *Food Chem. Toxicol.* **2011**, *49*, 1745–1752.

Penicooke, N.; Walford, K.; Badal, S.; Delgoda, R.; Williams, L.A.; Joseph-Nathan, P.; Gordillo-Román, B.; Gallimore, W. Antiproliferative activity and absolute configuration of zonaquinone acetate from the Jamaican alga *Stypopodium zonale*. *Phytochemistry* **2013**, *87*, 96–101.

Pereira, D.M.; Cheel J.; Areche, C.; San-Martin, A.; Rovirosa, J.; Silva, L.R.; Valentao, P.; Andrade, P.B. Anti-`proliferative activity of meroditerpenoids isolated from the brown alga *Stypopodium flabelliforme* against several cancer cell lines. *Mar. Drugs* **2011**, *9*, 852–862.

Pereira, L.; A review of the nutrient composition of selected edible seaweeds. In *Seaweed: ecology, nutritional composition and medicinal uses*; Pomin, V.H., Ed.; Nova Sicence: New York, **2012**; pp.15–49.

Pizzino, G.; Irrera, N.; Cucinotta, M.; Pallio, G.; Mannino, F.; Arcoraci, V.; Squadrito, Altavilla, F.D.; Bitto, A. Oxidative Stress: Harms and benefits for human health. *Oxid. Med. Cell Longev.* **2017**, *2017*, 1–13.

Reddy, P.; Urban, S. Meroditerpenoids from the southern Australian marine brown alga *Sargassum fallax*. *Phytochemistry* **2009**, *70*, 250–255.

Reuter, S.; Gupta, S.C.; Chaturvedi, M.M.; Aggarwal, B.B. Oxidative stress, inflammation, and cancer: How are they linked? *Free Radic. Biol. Med*. **2010**, *49*, 1603–1616.

Rodrigues, D.; Alves, C.; Horta, A.; Pinteus, S.; Silva, J.; Culioli, G.; Thomas, O.P.; R. Antitumor and antimicrobial ptential of bromoditerpenes isolated from the red alga, *Sphaerococcus coronopifolius. Mar. Drugs* **2015***, 13,* 713–726.

Roohinejad, S.; Koubaa, M.; Barba, F.J.; Saljoughian, S.; Amid, M.; Greiner, R. Application of seaweeds to develop new food products with enhanced shelf-life, quality and health-related beneficial properties. *Food Res. Int*. **2017**, *99*, 1066–1083.

Ruan, B.F.; Ge, W.W.; Lin, M.X.; Li, Q.S. A Review of the components of seaweeds as potential candidates in cancer therapy. *Anticancer Agents Med. Chem*. **2018**, *18*, 354–366.

Ruiz-Torres, V.; Encinar, J.A.; Herranz-López, M.; Pérez-Sánchez, A.; Galiano, V.; Barrajón-Catalán, E.; Micol, V. An updated review on marine anticancer compounds: the use of virtual screening for the discovery of small-molecule cancer drugs. *Molecules* **2017**, *22*, article 1037.

Sabry, O.M.; Goeger, D.E.; Valeriote, F.A.; Gerwick, W.H. Cytotoxic halogenated monoterpenes from *Plocamium cartilagineum*. *Nat. Prod. Res.* **2017**, *31*, 261–267

Salminen, A.; Lehtonen, M.; Suuronen, T.; Kaarniranta, K.; Huuskonen, J. Terpenoids: natural inhibitors of NF-kB signaling with anti-inflammatory and anticancer potential. *Cell Mol. Life Sci.* **2008**, *65*, 2979–2999.

Sansom, C.E.; Larsen, L.; Perry, N.B.; Berridge, M.V.; Chia, E.W.; Jacquie L. Harper, J.K.; Webb V.L. An Antiproliferative bis-prenylated quinone from the New Zealand brown alga *Perithalia capillaris*. *J. Nat. Prod.* **2007**, *70*, 2042–2044.

Seca, A.M.L.; Pinto, D.C.G.A. Plant secondary metabolites as anticancer agents: successes in clinical trials and therapeutic application. *Int. J. Mol. Sci.* **2018**, *19*, 263; doi:10.3390/ijms19010263.

Seo, Y.; Park, K.E.; Nam, T.J. Isolation of a new chromene from the brown alga *Sargassum thunbergii*. *Bull. Korean Chem. Soc.* **2007**, *28*, 1831–1833.

Shannon, E.; Abu-Ghannam, N. Antibacterial derivatives of marine algae: An overview of pharmacological mechanisms and applications. *Mar. Drugs* **2016**, *14*, 1–23.

Smyrniotopoulos, V.; Kiss, R.; Mathieu, V.; Vagias, C.; Roussis, V. Diterpenes with unprecedented skeletons from the red alga *Sphaerococcus coronopifolius*. *Eur. J. Org. Chem.* **2015**, *13*, 2848–2853.

Smyrniotopoulos, V.; Vagias, C.; Bruyère, C.; Lamoral-Theys, D.; Kiss, R.; Roussis, V. Structure and in vitro antitumor activity evaluation of brominated diterpenes from the red alga *Sphaerococcus coronopifolius*. *Bioorg. Med. Chem.* **2010**, *18*, 1321–1330.

Sonani, R.R.; Rastogi, R.P.; Madamwar, D. Natural antioxidants from algae. *Algal Green Chem*. **2017**, 91–120; https://doi.org/10.1016/B978-0-444-63784-0.00005-9.

Sun, J.; Shi, D.Y.; Li, S.; Wang, S.J.; Han, L.J.; Fan, X.; Yang, Y.C.; Shi, J.G. Chemical constituents of the red alga *Laurencia tristicha*. *J. Asian Nat. Prod. Res*. **2007**, *9*, 725–734.

Tarhouni-Jabberi, S.; Zakraoui, O.; Ioannou, E.; Riahi-Chebbi, I.; Haoues, M.; Roussis, V.; Kharrat, R.; Essafi-Benkhadir, K. Mertensene, a Halogenated monoterpene, induces G2/M cell cycle arrest and caspase dependent apoptosis of human colon adenocarcinoma HT29 cell line through the modulation of ERK-1/-2, AKT and NF-κB signaling. *Mar. Drugs* **2017**, *15*, E221.

Teasdale, M.E.; Shearer, T.L.; Engel, S.; Alexander, T.S.; Fairchild, C.R.; Prudhomme, J.; Torres, M.; Le Roch, K.; Aalbersberg, W.; Hay, M.E.; Kubanek, J. Bromophycoic acids: bioactive natural products from a Fijian red alga *Callophycus sp*. *J. Org. Chem*. **2012**, *77*, 8000–8006.

Torre, L.A.; Siegel, R.L.; Ward, E.M.; Jemal, A. Global cancer incidence and mortality rates and trends—An Update. *Cancer Epidemiol. Biomarkers Prev.* **2015**, *25*, 16–27.

Urones, J.G.; Araújo, M.E.M.; Brito Palma, F.M.S.; Basabe, P.; Marcos, I. S.; Moro, R. F.; Lithgow, A. M.; Pineda, J. Meroterpenes from *Cystoseira usneoides* II. *Phytochemistry* **1992a**, *31*, 2105−2109.

Urones, J.G.; Basabe, P.; Marcos, I.S.; Pineda, J.; Lithgow, A.M.; Moro, R.F.; Brito Palma, F.M.S.; Araújo , M.E.M.; Graválos, M.D.G. Meroterpenes from *Cystoseira usneoides*.

Phytochemistry **1992b**, *31*, 179−182.

Valls, R.; Piovetti, L. The chemistry of the Cystoseiraceae (Fucales: Pheophyceae): Chemotaxonomic relationships. *Biochem. Syst. Ecol.* **1995**, *23*, 723−745.

Van den Hoek, C.; Mann, D.G.; Jahns, H.M. *Algae — An introduction to phycology*. Cambridge University Press: Cambridge, **1995**; p. 158.

Velatooru, L.R.; Baggu, C.B.; Janapala, V.R. Spatane diterpinoid from the brown algae, *Stoechospermum marginatum* induces apoptosis via ROS induced mitochondrial mediated caspase dependent pathway in murine B16F10 melanoma cells. *Mol. Carcinog*. **2016**, *55*, 2222–2235.

Vizetto-Duarte, C.; Custódio, L.; Acosta, G.; Lago, J.H.G.; Morais, T.R.; Bruno de Sousa, C.; Gangadhar, K.N.; Rodrigues, M.J.; Pereira, H.; Lima, R.T.; Vasconcelos, M.H.; Barreira, L.; Rauter, A.P.; Albericio, F.; Varela, J. Can macroalgae provide promising anti-tumoral compounds? A closer look at *Cystoseira tamariscifolia* as a source for antioxidant and anti-hepatocarcinoma compounds. *Peer J.* **2016**, *4*, 1704.

Vogel, C.V.; Pietraszkiewicz, H.; Sabry, O.M.; Gerwick, W.H.; Valeriote, F.A. Enantioselective divergent syntheses of several polyhalogenated *Plocamium* monoterpenes and evaluation of their selectivity for solid tumors. *Angew. Chem. Int. Ed.* **2014**, *53*, 12205–12209.

Wells, M.L.; Potin, P.; Craigie, J.S.; Raven, J.A.; Merchant, S.S.; Helliwell, K.E.; Smith, A.G.; Camire, M.E.; Brawley, S.H. Algae as nutritional and functional food sources: revisiting our understanding. *J. Appl. Phycol*. **2017**, *29*, 949–982.

Wijesinghe, W.A.J.P.; Kang, M.N.; Lee, W.W.; Lee, H.S.; Kamada, T.; Vairappan, C.S.; and Jeon, Y.J. 5β-Hydroxypalisadin B isolated from red alga *Laurencia snackeyi* attenuates inflammatory response in lipopolysaccharide-stimulated RAW 264.7 macrophages. *Algae* **2014**a, *29*, 333–341.

Wijesinghe, W.A.; Kim, E.A.; Kang, M.C.; Lee, W.W.; Lee, H.S.; Vairappan, C.S.; Jeon, Y.J. Assessment of anti-inflammatory effect of 5β-hydroxypalisadin B isolated from red seaweed *Laurencia snackeyi* in zebrafish embryo in vivo model. *Environ. Toxicol. Pharm*. **2014**b, *37*, 110–117.

Woolner, V.H.; Gordon, R.M.A.; Miller, J.H.; Lein, M.; Northcote, P.T.; Keyzers, R.A. Halogenated meroditerpenoids from a South Pacific collection of the red alga *Callophycus serratus*. *J. Nat. Prod.* **2018**, *81*, 2446–2454.

Wu, J.Q.; Kosten, T.R.; Zhang, X.Y. Free radicals, antioxidant defense system, and schizophrenia. *Prog. Neuropsychopharmacol. Biol. Psychiatry* **2013**, *46*, 200–206.

Yang, E.-J.; Ham, Y.M.; Yang, K.-W.; Lee, N.H.; Hyun, C.-G. Sargachromenol from *Sargassum micracanthum* inhibits the lipopolysaccharide-induced production of inflammatory mediators in RAW 264.7 macrophages. *Sci. World J.* **2013**, 712303.

Yoon, W.J.; Heo, S.J.; Han, S.C.; Lee, H.J.; Kang, G.J.; Kang, H.K.; Hyun, J.W.; Koh, Y.S.; Yoo, E.S. Anti-inflammatory effect of sargachromanol G isolated from *Sargassum siliquastrum* in RAW 264.7 Cells. *Arch. Pharm. Res.* **2012,** *35*, 1421–1430.

Yu, X.Q.; He, W.F.; Liu, D.Q.; Feng, M.T.; Fang, Y.; Wang, B.; Feng, L.H.; Guo, Y.W.; Mao, S.C. A seco-laurane sesquiterpene and related laurane derivatives from the red alga *Laurencia okamurai* Yamada. *Phytochemistry* **2014**, *103*, 162–170.

Zaleta-Pinet, D.A.; Holland, I.P.; Muñoz-Ochoa, M.; Murillo-Alvarez, J.I.; Sakoff, J.A.; van Altena, I.A.; McCluskey, A. Cytotoxic compounds from *Laurencia pacifica*. *Org. Med. Chem. Lett*. **2014**, *4*, 8.

Zhao, M.; Cheng, S.; Yuan, W.; Dong, J.; Huang, K.; Sun, Z.; Yan, P. Further new xenicanes from a chinese collection of the brown alga *Dictyota plectens*. *Chem. Pharm. Bull.* **2015**, *63*, 1081–1086.

2. Objectives

While acute inflammatory response has therapeutic benefits, chronic inflammation is associated with multitude of diseases. In this line, several epidemiological, pre-clinical, and clinical studies over the last years have established the close relationship between the process of chronic inflammation and cancer.

The search for lead compounds from natural resources continues to be an important strategy for the discovery and development of new drugs. The marine environment is a rich source of functional compounds and promising bioactive molecules for a wide range of applications, including not only new therapeutics, but also cosmetics, and biotechnology. Among marine organisms, macroalgae have proven to be a valuable source of structurally diverse compounds exhibiting a variety of biological activities, including antioxidant, antitumor, and anti-inflammatory properties. Therefore, the search for novel therapeutic agents from macroalgae has aroused great interest among scientific groups and pharmaceutical industrialists. In this context, brown algae of the genus *Cystoseira* are characterized by containing a variety of natural products of the class of the meroterpenoids (AMTs) whose pharmacological potential has been scarcely explored.

This thesis is aimed to study the antioxidant, anticancer, and anti-inflammatory activities of the AMTs produced by the brown alga *Cystoseira usneoides,* by using *in vitro* and *in vivo* assays of inflammation and cancer.

This main objective comprises the following specific objectives:

1. To extract specimens of the brown alga *C. usneoides* collected in the Moroccan coasts of the Gibraltar Strait and to evaluate the antioxidant, anticancer, and anti-inflammatory activities of the extract.
2. To isolate the natural products of the class of AMTs from the algal extract.
3. To evaluate the antioxidant properties of the isolated AMTs by using radical scavenging assays.

4. To study the anticancer properties of the AMTs using several approaches, including the analysis of cytotoxic effects on selected cancer cell lines, apoptosis, cell cycle analysis, and cell migration and invasion abilities.
5. To investigate the anticancer mechanisms through the study of ERK 1/2, JNK, and AKT signaling pathways.
6. To determine the *in vitro* anti-inflammatory properties of the isolated AMTs through the analysis of the levels of pro-inflammatory cytokines (TNF-α, IL-1ß and IL-6) and to determine the effect of these AMTs on important molecular targets for the prevention of inflammatory diseases, including COX-2 and iNOS expressions.
7. To investigate the *in vivo* anti-inflammatory effects of selected bioactive AMTs in an animal model of acute intestinal inflammation by dextran sodium sulphate (DSS)-induced colitis.

3. Preliminary biological evaluation of the extract of *Cystoseira usneoides*

In order to achieve the first objective of this thesis, the first part of the research was focused on the evaluation of the biological properties of the extract obtained from specimens of the brown alga *Cystoseira usneoides*, in particular its antioxidant, anticancer, and anti-inflammatory properties.

Abstract: The aim of this study was to evaluate the antioxidant, antitumor, and anti-inflammatory properties of the acetone/methanol extract of the marine alga *Cystoseira usneoides* collected in the Gibraltar Strait. The extract was tested by the $ABTS^{+\bullet}$ radical scavenging assay to assess its antioxidant activity. The anticancer effect of the extract on human colon cancer cells HT-29 was investigated *via* cell viability, apoptosis assay, and cell cycle analysis. The anti-inflammatory activity was investigated by TNF-α inhibition assay in LPS-stimulated THP-1 differentiated macrophages from monocytic cell line. We found that the acetone/methanol extract of *C. usneoides* showed significant radical-scavenging activity (IC_{50} = 94.05 µg/mL). The extract of *C. usneoides* also inhibited the growth of HT-29 cells in a dose- and time-dependent manner (IC_{50} = 25.28 µg/mL at 72 h). Moreover, after treatment of HT-29 cells with the extract, the apoptotic rate was significantly increased, and a time- and concentration-dependent G2/M arrest of the cell cycle was induced. Finally, the production of TNF-α by THP-1 culture treated with LPS was found to be significantly inhibited by *C. usneoides* extract. These results support the significant pharmacological potential of the macroalga *C. usneoides*.

3.1. Introduction

Seaweeds are a potential renewable marine resource for obtaining compounds with interesting biomedical properties and functional ingredients to improve human health (Wells et al., 2017, Murphy et al., 2014). In this regard, the screening of the biological properties of extracts from marine algae is a common approach to detect the presence of bioactive compounds and to select the most interesting species for further studies or developments (Vizetto-Duarte et al., 2016; Nahas et al., 2007).

It is well recognized that antioxidants may have positive effects on human health, since they can protect the human body against reactive oxygen species (ROS) damage. ROS cause oxidative damage to lipids, proteins, and DNA, eventually leading to several human diseases including cancer (Caputo et al., 2012; Halliwell, 2007). Cancer constitutes a main cause of mortality in the world, according to the World Health Organization (WHO, 2018), with colon cancer being one of the most malignant types of neoplasia (Shen et al., 2019). Furthermore, chronic inflammation predisposes tissues to various types of cancer and the development of powerful anti-inflammatory agents may play a role in cancer prevention or treatment (Todoric et al., 2016). Besides, the inhibition of inflammatory mediators produced by macrophages is believed to be crucial for managing inflammatory diseases (Dinarello, 2010).

In this context, research efforts on the biological properties of algal extracts have experienced great increase in recent years and have revealed the promising potential of an array of algal species to provide bioactive compounds with various activities, including antioxidant (Agregán et al., 2018; Namvar et al., 2018; Neethu et al., 2017), anticancer (Alves et al., 2018; Namvar et al., 2018; Neethu et al., 2017) and anti-inflammatory properties (Song et al., 2018; Shih et al., 2017).

The present study was aimed to assess the antioxidative, anticancer, and anti-inflammatory capabilities of the extract of the brown alga *Cystoseira usneoides* settled along the Mediterranean coasts of Morocco. Herein, we describe the radical scavenging activity of the acetone/methanol extract of *C. usneoides*, its cytotoxicity against HT29 colon cancer cells and its effects on cell cycle, as well as its inhibitory activity on the production of the proinflammatory cytokine TNF-α in THP-1 macrophages.

3.2. Material and Methods

3.2.1. Chemicals

Ethanol, acetone, and methanol were obtained from Merck (Darmstadt, Germany). 2,2-azino-bis(3-ethylbenzothiazoline-6-sulfonic acid) diammonium salt (ABTS), 6-hydroxy-2,5,7,8-tetramethylchroman-2-carboxylic acid (Trolox) and propidium iodide were purchased from Sigma Chemical Co. (St. Louis, MO, USA). Potassium persulfate was

procured from Fluka Chemical Co. (Buchs, Swizerland) and sulforhodamine-B (SRB) was purchased from Sigma-Aldrich (Taufkirchen, Germany). The RNase A for cell cycle analysis was obtained from AppliChem and the Annexin-FITC kit for apoptosis from eBioscience.

3.2.2. Collection of the alga

Samples of *Cystoseira usneoides* (class Phaeophyceae, order Fucales, family Sargassaceae) were collected by hand (1−4 m depth) in the Mediterranean coast of Morocco, at the Gibraltar Strait (35°50′52.58″ N, 5°33′39.04″ W). Voucher specimens (HTET.Phyc 545) were deposited in the herbarium of the Laboratory of Applied Algology-Mycology, Department of Biology, Faculty of Sciences at Abdelmalek Essaadi University, 93002 Tetouan, Morocco.

After collection, epiphytes were removed from the alga and the samples were rinsed with sterile seawater to remove associated debris and necrotic parts. In the laboratory, the samples were shade dried, cut into small pieces and powdered in a mixer grinder (IKA R A11 basic, Sigma-Aldrich). The obtained powder was cold-preserved (−12 °C).

3.2.3. Extraction of the alga

The powder of *C. usneoides* (150 g) previously prepared was extracted with acetone/methanol (1:1, 2L). After filtration, the solution was evaporated under reduced pressure to obtain an extract that was weighed (4.63 g) and stored in sealed vials in a freezer (-20 ºC) until being used.

3.2.4. Antioxidant assay

The antioxidant activity of the extract was determined by using the $ABTS^{+\bullet}$ free radical decolorization assay (Re et al., 1999). ABTS (2.9 mM) solution was mixed with potassium persulfate (final concentration of 0.98 mM) and kept overnight in dark for generation of the blue colored $ABTS^{+\bullet}$ radical. The solution was then diluted with ethanol to obtain the absorbance of 0.7 ± 0.2 units at 734 nm. To determine the radical scavenging activity, 100 µL of $ABTS^{+\bullet}$ solution was mixed with 90 µL of ethanol and 10 µL of different solutions of seaweed extract in ethanol (final concentrations of 3.125, 6.25, 12.5, 25, 50, 100, 150 and 200 µg/mL). Controls were prepared by mixing 100 µL of $ABTS^{+\bullet}$

solution with 100 µL of ethanol. The absorbance, monitored for 6 min, was measured spectrophotometrically at 734 nm using a microtiter plate reader. Trolox (6-hydroxy-2,5,7,8-tetramethylchroman-2-carboxylic acid) was used as standard. The percentage of inhibition of absorbance caused by each concentration of extract or Trolox was calculated using the following equation: % Inhibition = $[(A_0 – A_1)/A_0] \times 100$, where A_0 expresses the absorbance of the control and A_1 expresses the absorbance of the tested seaweed extract or Trolox.

3.2.5. Anticancer assays

Cell culture

HT-29 human colon carcinoma cells were obtained from ATCC (American Type Culture Collection) and grown on McCoy's medium supplemented with 10% heat-inactivated fetal bovine serum (FBS), 100 U/mL penicillin and 100 µg/mL streptomycin. Cultures were maintained at 37°C in a 5% CO_2 incubator.

Sulforhodamine B assay

Viability of HT-29 cells was determined by the SRB assay. The cells were seeded into 96 well plates in the growth medium at a concentration of 5000 cells/well. After 24 h of incubation, the cells were exposed to various concentrations of extract of *C. usneoides* dissolved in DMSO. The final concentrations were 0, 6.25, 12.5, 25, 50 and 100 µg/mL and less than 0.05 % of DMSO. The cells were then incubated for 48 h and 72 h. Afterwards, the cells were fixed with TCA by gently adding 50 µl TCA (50%) to each well for 1 h at 4°C, and processed as described in the literature (Skehan et al., 1990). Results are expressed as % of cell viability *vs* control (time 0).

Apoptosis detection by flow cytometry

The percentage of apoptotic cells was determined by flow cytometry using an Annexin V-FITC Apoptosis Detection Kit (eBiosciences). In brief, HT-29 cells were seeded in 6-well plates ($1x10^6$ cells /well) and incubated for 24 h before treatment with 0, 30 and 60 µg/mL of algal extract. After being incubated for 24 h, cells were harvested by trypsinization and rinsed with cold PBS twice. After centrifugation (4℃, 1500 rpm) for 5 min, cells were suspended in 195 µL of 1×Annexin buffer and then treated with 5 µL of

Annexin V-FITC and 10 µL of propidium iodide for 10 min at room temperature in the dark. To this mixture 200 µL of 1×Annexin buffer were added before analysis using Bekhman Coulter FC500 flow cytometer. 10,000 cellular events in each sample were analyzed using DML program.

Cell cycle analysis

HT-29 cells were seeded in 6-well plates ($1x10^6$ cells per well) and incubated for 24 h. After addition of various doses of the extract dissolved in DMSO (final concentrations of 0, 30 and 60 µg/mL and less than 0.05 % of DMSO), the cells were incubated for 24 h. Cells were harvested after trypsinization and washed once with PBS. Then, the cells were centrifuged at 1500 rpm for 5 min (25ºC), the pellet was fixed with 1 mL of ice-cold 70% ethanol, and the samples stored at -4ºC overnight. The cells were then washed with PBS and incubated in the darkness with PBS containing 5 mg/mL of RNase A for 48 h at 4°C. Subsequently, 50 µL of 0.1 mg/mL of propidium iodide was added to the cells and they were incubated for 1 h at 4°C. The relative DNA content per cell was analyzed using a Bekhman Coulter FC500 flow cytometer. The data acquisition was performed with the DML program. The analysis of the acquired data was performed with the CXP cytometer.

3.2.6. Anti-inflammatory assay

Cell culture

The THP-1 human monocytic leukemia cell line was obtained from the American Type Culture Collection (TIB-202, ATCC, USA) and cultured in RPMI 1640 medium containing 10% heat-inactivated fetal bovine serum, 100 U/mL penicillin, and 100 µg/ mL streptomycin in a humidified atmosphere containing 5% CO2 at 37 °C.

Cell viability Assay

The viability of THP-1 cells was measured by the SRB assay. The cells were seeded into 96-well plates in the growth medium at a density of 1×10^4 cells per well, and differentiation into macrophages was induced by 0.2 µM phorbol myristate acetate (PMA). Three days after differentiation into macrophages, the cells were treated with various concentrations of algal extract in fresh medium and incubated for another 48 and 72 h. The cells were fixed with 50 µL of trichloroacetic acid (TCA, 50%) and processed as described

in the literature (Skehan et al., 1990).

Determination of TNF-α production

THP-1 cells were plated at a density of 3×10^5 cells/mL in 24-well plates and incubated with PMA (0.2 μM) for 72 h in a humidified atmosphere of 5% CO_2 at 37°C. The macrophages were then treated with 10 μg/mL of the algal extract for 24 h (the viability of cells was greater than 95% throughout the experiment), then stimulated with lipopolysaccharide (LPS, 1 μg/mL) and incubated for another 24 h. Dexamethasone was used as positive reference compound. The levels of TNF-α in the cultured medium (supernatant) were measured with enzyme-linked immunosorbent assay (ELISA) kits (Diaclone GEN-PROBE) according to the manufacturer's protocols. The absorbance was determined at 450 nm using a microplate reader. To calculate the concentration of cytokines, a standard curve was constructed using serial dilutions of cytokine standards provided with the kit.

3.2.7. Statistical analysis

The results were expressed as means ± standard deviations (S.D.). Differences between two groups were analyzed by the Student's *t-test*. One-way analysis of variance (ANOVA) was used in multiple group comparisons. Difference with $p < 0.05$ (*), $p < 0.01$ (**) or $p < 0.001$ (***) was considered statistically significant.

3.3. Results and Discussion

3.3.1. Antioxidant effects of the extract of C. usneoides

The antioxidant capacity of the acetone/methanol extract of *C. usneoides* was determined by the $ABTS^{+\bullet}$ radical cation decolorization assay. This is one of the most commonly employed methods for measuring antioxidant activity, which determines the radical scavenging activity of an extract, fraction or compound toward the radical cation $ABTS^{+\bullet}$. This method has been strongly recommended for analysing plant and algae extracts, because the maximum absorption of the radical cation at 734 nm prevents the color interference usually found when working with plant extracts (Awika et al., 2003).

The extract of *C. usneoides* was assayed at concentrations between 3.125 and 200 µg/mL, causing decreases of the absorbance of the $ABTS^{+\bullet}$ solution between 6.67 and 60.55%, which were lower than the decreases caused by the reference compound Trolox® (between 23 and 97.78% at concentrations between 3.125 and 25 µg/mL) (Figure 3.1). The reaction of the extract with the radical $ABTS^{+\bullet}$ was dose-dependent, and the concentration that caused 50% decrease of the absorbance (IC_{50}) was 94.05 ± 6.3 µg/mL. The Trolox standard was more active, showing IC_{50} = 7.36 ± 0.6 µg/mL.

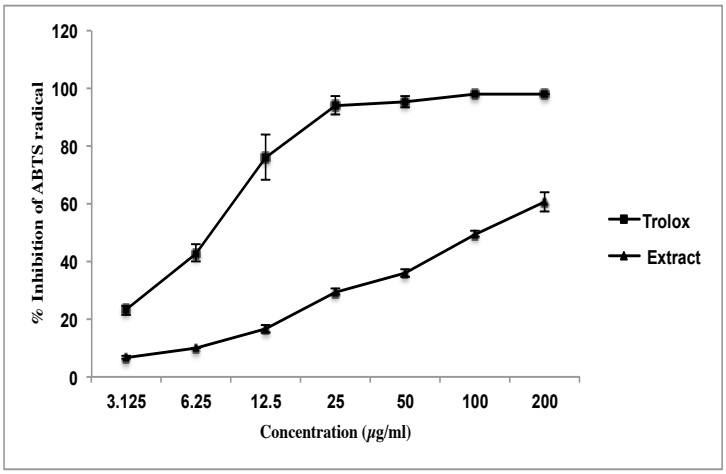

Figure 3.1. Effect of the extract of *C. usneoides* at different concentrations (3.125 – 200 µg/mL) on the $ABTS^{+\bullet}$ radical compared to Trolox.

The antioxidant activity measured for our acetone/methanol extract of *C. usneoides* is much higher than that reported in the same assay for the extracts of this species collected in the Portuguese coasts (Vizetto-Duarte et al., 2016) (Table 3.1). In that study, the hexane, diethyl ether, ethyl acetate, and methanol extracts obtained by sequential extraction of lyophilised samples of *C. usneoides* were tested in the ABTS assay, and only the hexane and the diethyl ether extracts displayed significant radical-scavenging activity. Moreover, the antioxidant activity of our extract of *C. usneoides* was also stronger than that reported for the extracts of *C. humilis* and *C. tamariscifolia* (Vizetto-Duarte et al- 2016) (Table 3.1).

A number of recent reports, which are summarized in Table 3.2, have also described the antioxidant activities of extracts of *C. usneoides* and of other algae of the genus *Cystoseira* by using the DPPH assay (Tenorio-Rodriguez et al., 2017; Custodio et al., 2016;

Çelenk et al., 2016; Vizzeto-Duarte et al., 2016; Güner et al., 2015; Mhadhebi et al., 2014; Airanthi et al., 2011; Zubia et al., 2009).

The significant antioxidant activity detected in our study of the acetone/methanol extract of *C. usneoides* reinforces the potential of this marine genus of brown algae as a new and alternative source of antioxidant components, which could be suitable for exploitation in the food and cosmetic sectors.

Table 3.1. Antioxidant activity of extracts of algae of the genus *Cystoseira* in the ABTS assay.

Species (collection coast)	Solvent of extraction	Radical scavenging activit in the ABTS assay	Reference
C. usneoides (Morocco)	acetone/methanol	IC_{50} = 94.05 μg/mL Control:Trolox, IC_{50} = 7.36μg/mL	Present study
C. usneoides (Portugal))	hexane diethyl ether ethyl acetate methanol	IC_{50} = 5.54 mg/mL IC_{50} = 600 μg/mL IC_{50} > 10 mg/mL IC_{50} > 10 mg/mL Control: BHT, IC_{50} = 110 μg/mL	Vizetto-Duarte et al., 2016
C. humilis (Portugal)	hexane diethyl ether ethyl acetate methanol	IC_{50} >10 mg/mL IC_{50} = 8.85 mg/mL IC_{50} = 9.25 mg/mL IC_{50} > 10 mg/mL Control: BHT, IC_{50} = 110 μg/mL	Vizetto-Duarte et al., 2016
C. tamariscifolia (Portugal)	hexane diethyl ether ethyl acetate methanol	IC_{50} = 520 μg/mL IC_{50} = 470 μg/mL IC_{50} = 250 μg/mL IC_{50} = 2.93 mg/mL Control: BHT, IC_{50} = 110 μg/mL	Vizetto-Duarte et al., 2006

Table 3.2. Antioxidant activity of extracts of algae of the genus *Cystoseira* in the DPPH assay

Species (collection coast)	Solvent of extraction	Radical scavenging activity in the DPPH assay	Reference
C. baccata (Portugal)	methanol	21.6% inhibition at 1 mg/mL 90.4% inhibition at 10 mg/mL	Custodio et al., 2016
C. barbata (Turkey)	methanol	58.22% inhibition at 1 mg/mL	Çelenk et al., 2016
C. compressa (Tunisia)	water	IC_{50} = 12 μg/mL Control: Trolox, IC_{50} = 90 μg/mL	Mhadhebi et al., 2014
C. compressa (Turkey)	methanol chloroform hexane	IC_{50} = 15.94 mg/mL IC_{50} = 7.46 mg/mL IC_{50} = 5.0 mg/mL	Güner et al., 2015
C. compressa (Turkey)	methanol	65% inhibition at 1 mg/mL	Çelenk et al., 2016
C. crinita (Tunisia)	water	IC_{50} = 20 μg/mL Control: Trolox, IC_{50} = 90 μg/mL	Mhadhebi et al., 2014

C. crinita (Turkey)	methanol	79.3% inhibition at 1 mg/mL	Çelenk et al., 2016
C. hakodatensis (Japan)	methanol	65.32 μg α- tocopherol equivalent per mg extract	Airanthi et al., 2011
C. humilis (Portugal)	methanol	8.8 % inhibition at 1 mg/mL 41.1 % inhibition at 10 mg/mL	Custodio et al., 2016
C. humilis (Portugal)	hexane diethyl ether ethyl acetate metanol	IC_{50} >10 mg/mL IC_{50} = 8.28 mg/mL IC_{50} = 5.04 mg/mL IC_{50} > 10 mg/mL Control: BHT, IC_{50} = 70 μg/mL	Vizzeto-Duarte et al., 2016
C. nodicaulis (Portugal)	methanol	39.6% inhibition at 1 mg/mL 95.1 % inhibition at 10 mg/mL	Custodio et al., 2016
C. osmundacea (Baja California, Mexico)	ethanol	IC_{50} = 69 μg/mL	Tenorio-Rodriguez et al., 2017
C. sedoides (Tunisia)	chloroform ethyl acetate	IC_{50} = 120 μg/mL IC_{50} = 121 μg/mL Control: Trolox, IC_{50} = 90 μg/mL	Mhadhebi et al., 2011
C. sedoides (Tunisia)	water	IC_{50} = 75 mg/mL Control: Trolox, IC_{50} = 90 μg/mL	Mhadhebi et al., 2014
C. tamariscifolia (Brittany)	dichloromethane/ methanol	EC_{50} = 490 μg/mL Control compounds: BHA, EC_{50} = 40 μg/mL BHT, EC_{50} = 60 μg/mL Ascorbic acid, EC_{50} = 60 μg/mL α-tocopherol, EC_{50} = 140 μg/mL	Zubia et al., 2009
C. tamariscifolia (Portugal)	hexane diethyl ether ethyl acetate metanol	IC_{50} = 630 μg/mL IC_{50} = 300 μg/mL IC_{50} = 170 μg/mL IC_{50} = 1.08 mg/mL Control: BHT, IC_{50} = 70 μg/mL	Vizetto-Duarte et al., 2016
C. tamariscifolia (Portugal)	methanol	92% inhibition at 1 mg/mL	Custodio et al., 2016
C. usneoides (Portugal)	hexane diethyl ether ethyl acetate metanol	IC_{50} = 4.37 mg/mL IC_{50} = 650 μg/mL IC_{50} = 7.73 mg/mL IC_{50} = 7.16 mg/mL Control:BHT, IC_{50} = 70 μg/mL	Vizetto-Duarte et al., 2006
C. usneoides (Portugal)	methanol	37.1 % inhibition at 1 mg/mL	Custodio et al., 2016

3.3.2. Anticancer effects of the extract of C. usneoides

Effect of the extract of *C. usneoides* on the viability of HT-29 cells

The effect of the extract of *C. usneoides* (0, 6.25, 12.5, 25, 50 and 100 μg/mL) on the viability of HT-29 cells was determined by the SRB assay after 48 and 72 h of incubation (Figure 3.2). As shown in Figures 3.2a and 3.2b, the extract of *C. usneoides*

decreased cell viability in a dose- and time-dependent manner and the IC_{50} values were 33.05 µg/mL and 25.28 µg/mL, after 48 and 72 h of incubation, respectively.

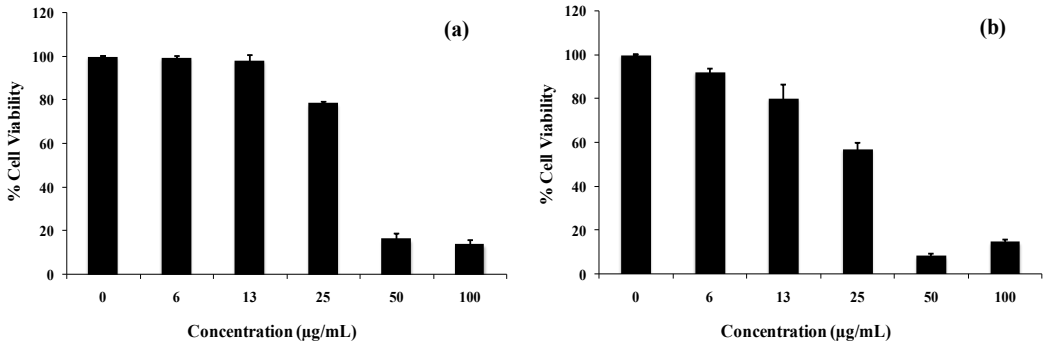

Figure 3.2. Effect of the acetone/methanol extract of *C. usneoides* on HT-29 cells proliferation. Cells were treated with different concentrations of extract (6.25, 12.5, 25, 50, and 100 µg/mL) for 48 h **(a)** and 72 h **(b)**. Cell viability was determined by SRB assay (n = 6).

Induction of apoptosis in HT29 cells by treatment with the extract of *C. usneoides*

In an attempt to explore the effects of the extract of *C. usneoides* on apoptosis, the HT-29 cells were treated with the extract and then analyzed by flow cytometry, using Annexin V-FITC as a marker of phosphatidylserine exposure and propidium iodide as a marker of dead cells. Figure 3.3 shows the results of the Annexin V-FITC binding and propidium iodide staining on HT-29 cells, after exposure for 24 h either to the extract (two different doses) or to curcumin as positive control.

The treatment with the extract significantly increased the proportion of apoptotic cells. Thus, in the vehicle treated samples, 0.35 ± 0.01% of cells stained positive for Annexin V-FITC, while the treatment with the extract of *C. usneoides* at 30 µg/mL caused an increase up to 12.52 ± 3.12% of cells in late stage apoptosis and 5.32± 0.21% in early apoptosis ($p<0.05$). When HT-29 cells were treated with 60 µg/mL of extract for 24 h, the percentage of cells in late apoptosis was 17.71 ± 0.01%, although no significant difference with early stage apoptosis was observed. These results demonstrate the ability of the extract of *C. usneoides* to induce apoptosis, mainly late stage apoptosis in HT-29 cells.

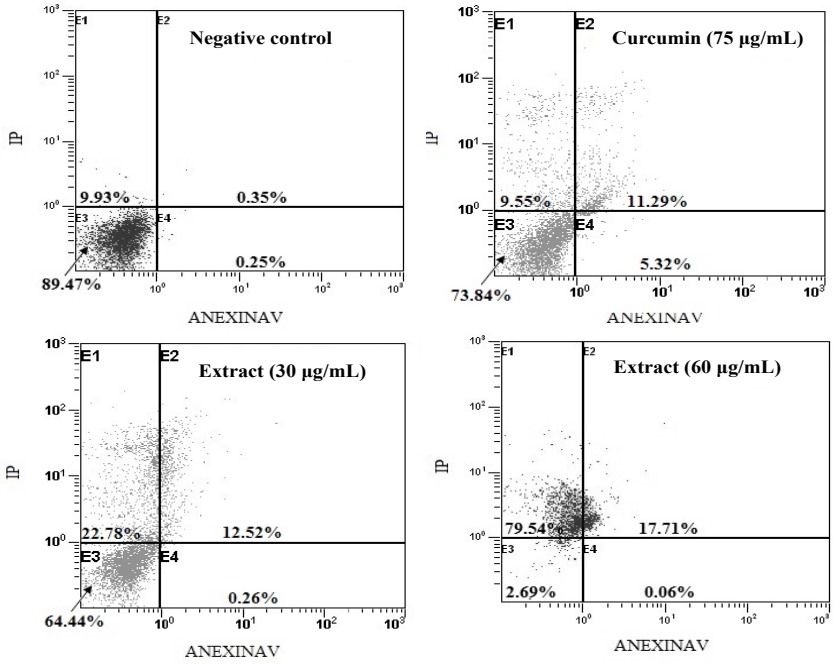

Figure 3.3. Effects of *C. usneoides* on the apoptosis of HT-29 cells. Cells were treated without and with different concentrations of *C. usneoides* extract (30 µg/mL and 60 µg/mL, for 24 h), then stained with annexin V-FITC, and evaluated by flow cytometry. Curcumin was used as positive reference compound at 75 µM. (E1: Necrotic, E2: Late apoptotic, E3: Live and E4: Early apoptotic).

Effect of the extract of *C. usneoides* on cell cycle progression in HT-29 cells

To investigate the possible mechanism(s) involved in the cytotoxic effect caused by the extract of *C. usneoides* on colon cancer cells HT-29, we examined whether such reduction was associated with cytostatic effects due to changes in cell cycle progression. Figure 3.4 shows the cell cycle distribution of HT-29 cells incubated for 24 h in the absence or in the presence of different concentrations of extract. In the absence of the extract, most HT-29 cells (about 70%) were in G0/G1 phase. However, after 24 h incubation with the algal extract (60 µg/mL) there was an increase in the percentage of cells in the G2/M phase, while the percentage of cells in the other phases decreased. These data markedly suggest that the extract of *C. usneoides* interferes with cell cycle progression.

The present study has demonstrated for the first time that the extract of the alga *C. usneoides* inhibits the proliferation of colon cancer cells by arresting cell cycle progression at the G2/M phase and inducing apoptosis. As shown in Figure 3.2, the extract of *C.*

usneoides inhibited cell growth in a dose- and time-dependent manner and this inhibition seems to be associated with apoptosis (Fig. 3.3) and accumulation of cells at the G2/M region (Figure 3.4).

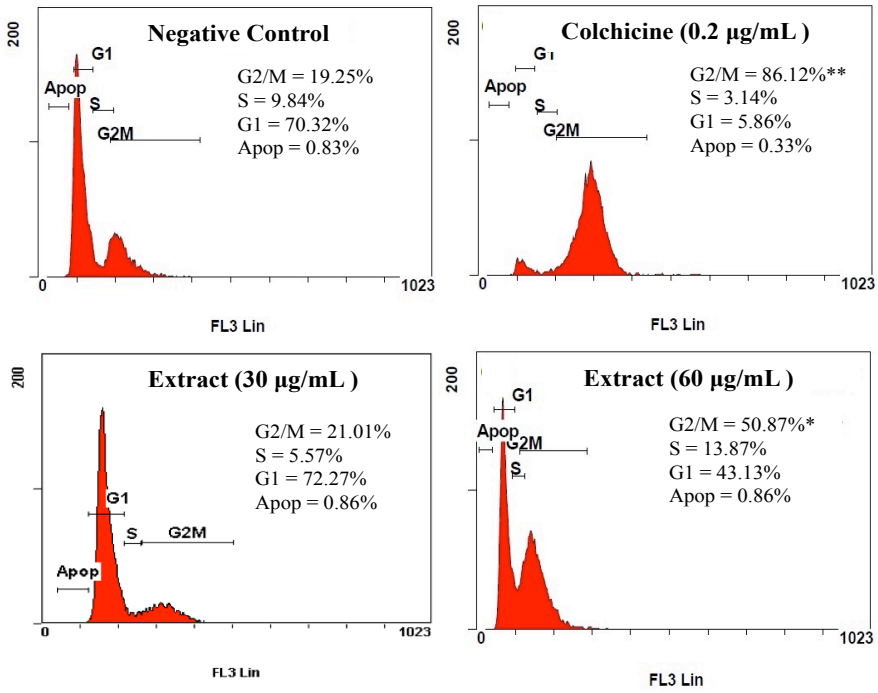

Figure 3.4. Effects of the extract of *C. usneoides* on HT-29 cell cycle distribution. Cells were incubated with or without extract for the indicated concentrations (30 and 60 µg/mL) for 24 h. Then, the cells were fixed and stained with propidium iodide to analyze DNA content by FAC Scan flow cytometer. Colchicine was used as positive reference compound at 0.2 µg/mL; (*$p < 0.05$, **$p < 0.01$, ***$p < 0.001$).

Previous reports have described the cytotoxicity of the hexane and the diethyl ether extracts of *C. usneoides* towards HepG2 cells (IC_{50} = 31.4 µg/mL and 52.0 µg/mL, respectively) (Vizetto-Duarte et al., 2016). In the present study, we have shown that the acetone/methanol extract of *C. usneoides* is cytotoxic for HT-29 cells with an IC_{50} of 25.28 µg/mL against HT-29 cells. This activity is comparable to that reported for aqueous extracts of *C. crinita*, *C. sedoides,* and *C. compressa* against the colon cancer cells HCT-15 (IC_{50} = 26.4, 10.5, 20.3 µg/mL, respectively) (Mhadhebi *et al.,* 2014) and much better than those described for the hexane fraction of *C. myrica* against the colon cancer cells HT-29 and Caco-2 (IC_{50}= 328.7 µg/mL and 254.92 µg/mL, respectively) (Khanavi et al., 2010) and for

the chloroform and the ethyl acetate fractions of *C. sedoides* against HCT-15 (IC_{50} = 250.6 and 255.3 µg/mL, respectively) (Mhadhebi *et al.,* 2011).

Several recent researches have dealt with the anticancer properties of the extracts of other brown algae of the genus *Cystoseira*, showing that these extracts cause cell growth inhibition in various cancer cell lines. Thus, the dichloromethane/methanol extract of *C. tamariscifolia* from the Brittany coasts, at 100 µg/mL was effective inhibiting by 60-80% the viability of the tumor cell lines Daudi (lymphoma), Jurkat (leukemia), and K562 (leukemia) (Zubia et al., 2009).

Another *in vitro* study showed that the hexane fraction obtained from the methanol extract of *C. myrica* was cytotoxic for the human breast carcinoma cells T47D, T47D-T.R and MBA-MD468 with IC_{50}= 99.9, 143.15 and 56.50 µg/mL, respectively (Khanavi et al., 2010). Moreover, this fraction was described to induce apoptosis in T47D cells with a proportion of apoptotic cells of 2.71%. Similarly, the methanol extract of *C. mediterranea* was cytotoxic toward the breast cancer cells MCF-7, causing at 100 µg/mL 55% of cell growth inhibition (Taskin et al., 2010).

The aqueous extracts and organic fractions derived from the methanol extracts of *C. sedoides, C. compressa,* and *C. crinita* have also shown antiproliferative properties against the cancer cell lines MCF-7 (IC_{50} from 17.9 to 130.0 µg/mL) and A-549 (IC_{50} from 33.0 to 110.0 µg/mL) (Mhadhebi *et al.,* 2011, 2012, and 2014) while the hexane extract of *C. tamariscifolia* has shown cytotoxic effects on HeLa, SH-SY5Y, AGS, HCT-15 and HepG2 cells, being specially potent on these latter cells (IC_{50} = 2.31 µg/mL) through apoptosis induction (Vizetto-Duarte et al. 2016). A meroditerpene, demethoxy cystoketal chromane, was identified in the same study as the active compound in the extract of *C. tamariscifolia*.

It is worth noting that along the studies on the antitumor potential of algae of the genus *Cystoseira*, a series of metabolites of the meroditerpene class have been isolated and identified as cytotoxic compounds in *C. crinita* (Fisch et al., 2003), *C. myrica* (Ayyad et al., 2003) and *C. usneoides* (Urones et al., 1992). These data suggest that the meroterpenes could also be responsible for the anticancer activity observed for the extract of *C. usneoides* tested in our study.

3.3.3. Anti-inflammatory activity of the extract of C. usneoides

The anti-inflammatory properties of the extract of *C. usneoides* was also investigated, in particular its activity as inhibitor of TNF-α. This is a potent pro-inflammatory cytokine mainly produced by monocytes and macrophages in immunologic and inflammatory responses (Iqbal et al., 2013). Assays were performed on the human THP-1 macrophages using lipopolysaccharide (LPS) to stimulate the TNF-α production. In order to rule out cytotoxic effects, the extract of *C. usneoides* was tested at a maximal concentration of 10 μg/mL, which did not affect THP-1 cell viability. To test the effects of the extract on TNF-α production, THP-1 macrophages were pretreated with the extract, then stimulated with LPS and finally analyzed to quantify TNF-α. As shown in Figure 3.5, the TNF-α production in THP-1 cells was increased about 4-fold, up to 282.05 ng/mL after LPS-stimulation. The pretreatment of cells with the extract of *C. usneoides* at 10 μg/mL significantly inhibited the production of TNF-α by 43% upon comparison with LPS-stimulated THP-1 control cells (Figure 3.5).

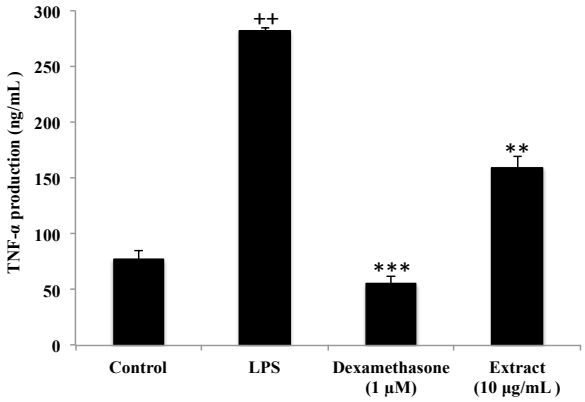

Figure 3.5. Effect of *C. usneoides* extract on TNF-α production in THP-1 macrophages stimulated with LPS. The cells were treated at concentration of 10 μg/mL for 24 h (the viability of cells was greater than 95% throughout the experiment), and then stimulated with LPS (1 μg/mL) for another 24 h. TNF-α concentration in the supernatants was measured using the ELISA assay. Dexamethasone was used as positive reference compound at 1 μM. Data were analyzed by one-way ANOVA followed by Tukey test for comparison between groups, (++) $p < 0.01$ *vs.* control; **$p < 0.01$, and ***$p < 0.001$ *vs.* LPS.

Previous accounts on the anti-inflammatory properties of extracts of algae of the genus *Cystoseira* have focused only on the carrageenan-induced rat paw edema model. In

particular, the chloroform and the ethyl acetate fractions of *C. sedoides* or *C. compressa* produced, at doses of 25 and 50 mg/kg i.p., marked inhibitions of edema (63.7-78.3% after 3h) when compared with the standard acetylsalicylic–lysine (ASL) (61.3-66.1% inhibition at 300 mg/kg i.p.) (Mhadhebi et al., 2011; Mhadhebi et al., 2012). A third report described the *in vivo* anti-inflammatory activity of the aqueous extracts of *C. crinita*, *C. sedoides,* and *C. compressa*, which at doses of 25 and 50 mg/kg i.p., exhibited significant anti-inflammatory activity in a dose dependent manner (70.9-82.1% inhibition of edema after 3h) upon comparison with the reference drugs ASL (61.2% at 300 mg/Kg) and dexamethasone (74.3% at 1 mg/kg) (Mhadhebi et al., 2014).

Therefore, the present study is the first description of the activity of an extract of algae of the genus *Cystoseira* as inhibitor of the production of proinflammatory cytokines, and the results suggest that this class of marine algae is worth of exploring in the anti-inflammatory area.

3.4. Conclusion

Marine algae have long been identified as valuable sources of metabolites with potent functional bioactivities. In this study, we have demonstrated that the extract of *C. usneoides* has a prominent radical-scavenging activity and an anti-proliferative effect on colon cancer cells by reducing cell viability through the apoptotic and cell cycle arrest pathways. Moreover, we have demonstrated for the first time that *C. usneoides* extract exhibits a significant activity as inhibitor of the production of the pro-inflammatory cytokine TNF-α in LPS-stimulated THP-1 human macrophages. The antioxidant activity together with the anticancer properties and the strong anti-inflammatory effects shown by the extract of *C. usneoides* make this alga an interesting candidate for further investigations. The prevalence of these properties in a single alga could be beneficial in terms of preventive and therapeutic purposes.

3.5. References

Agregán, R.; Munekata, P.E.S.; Franco, D.; Carballo, J.; Barba, F.J.; Lorenzo, J.M. Antioxidant potential of extracts obtained from macro- (*Ascophyllum nodosum*, *Fucus*

vesiculosus and *Bifurcaria bifurcata*) and micro-Algae (*Chlorella vulgaris* and *Spirulina platensis*) assisted by ultrasound. *Medicines (Basel)* **2018**, *5*, E33.

Airanthi, M.K.; Hosokawa, M.; Miyashita, K. Comparative antioxidant activity of edible Japanese brown seaweeds. *J. Food Sci.* **2011**, *76*, 104–11.

Alves, C.; Pinteus, S.; Rodrigues, A.; Horta, A.; Pedrosa, R. Algae from portuguese coast presented high cytotoxicity and antiproliferative effects on an in vitro model of human colorectal cancer. *Pharmacognosy Res*. **2018**,*10*, 24–30.

Awika, J.M.; Rooney, L.W.; Wu, X.L.; Prior, R.L.; Cisneros-Zevallos, L. Screening methods to measure antioxidant activity of sorghum (Sorghum bicolor) and sorghum products. *J. Agr. Food Chem.* **2003**, *51*, 6657–6662.

Ayyad, S.E.N.; Abdel-Halim, O.B.; Shier, W.T.; Hoye, T.R. Cytotoxic hydroazulene diterpenes from the brown alga *Cystoseira myrica*. *Z. Naturforsch. C.* **2003**, *58*, 33–38.

Caputo, F.; Vegliante, R.; Ghibelli, L. Redox modulation of the DNA damage response. *Biochem. Pharmacol.* **2012**, *84*, 292–306.

Çelenk, F.G.; Özkaya, A.B.; Sukatar, A. Macroalgae of Izmir Gulf: Dictyotaceae exhibit high in vitro anti-cancer activity independent from their antioxidant capabilities. *Cytotechnology* **2016**, *68*, 2667−2676.

Custódio, L.; Silvestre, L.; Rocha, M.I.; Rodrigues, M.J; Vizetto-Duarte, C.; Pereira, H.; Barreira, L.; Varela, J. Methanol extracts from *Cystoseira tamariscifolia* and *Cystoseira nodicaulis* are able to inhibit cholinesterases and protect a human dopaminergic cell line from hydrogen peroxide-induced cytotoxicity. *Pharm. Biol.* **2016**, *54*, 1687–1696.

Dinarello, C.A. Anti-inflammatory Agents: Present and Future. *Cell*. **2010**, *140*, 935–950.

Fisch, K.M.; Bohm, V.; Wright, A.D.; Konig, G.M. Antioxidative meroterpenoids from the brown alga *Cystoseira crinita*. *J. Nat. Prod.* **2003**, *66*, 968–975.

Güner, A.; Köksal, Ç.; Erel, Ş.B.; Kayalar, H.; Nalbantsoy, A.; Sukatar, A.; Karabay Yavaşoğlu, N.Ü. Antimicrobial and antioxidant activities with acute toxicity, cytotoxicity and mutagenicity of Cystoseira compressa (Esper) Gerloff & Nizamuddin from the coast of Urla (Izmir, Turkey). *Cytotechnology* **2015**, *67*, 135–143.

Halliwell, B. Oxidative stress and cancer: have we moved forward? *Biochem. J.* **2007**, 401, 1–11.

Iqbal, M.; Verpoorte, R.; Korthout, H.A.A.J.; Mustafa, N,R. Phytochemicals as a potential source for TNF-alpha inhibitors. *Phytochem. Rev.* **2013**, *12*, 65–93.

Khanavi, M.; Nabavi, M.; Sadati, N.; Ardekani, M.S.; Sohrabipour, J.; Nabavi, S.M.B.; Ghaeli, P.; Ostad, S.N. Cytotoxic activity of some marine brown algae against cancer cell lines. *Biol. Res.* **2010**, *43*, 31–37.

Liu, S.; Yamauchi, H. p27-Associated G1 arrest induced by hinokitiol in human malignant melanoma cells is mediated via down-regulation of pRb, Skp2 ubiquitin ligase, and impairment of Cdk2 function. *Cancer Lett.* **2009**, *286*, 240–249.

Mhadhebi, L.; Dellai, A.; Clary-Laroche, A.; Ben Said, R.; Robert, J.; Bouraoui, A. Anti-inflammatory and antiproliferative activities of organic fractions from the Mediterranean brown seaweed, *Cystoseira compressa*. *Drug. Dev. Res*. **2012**, *73*, 82–89.

Mhadhebi, L.; Laroche-Clary, A.; Robert, J.; Bouraoui, A. Antioxidant, anti-inflammatory, and antiproliferative activities of organic fractions from the Mediterranean brown seaweed *Cystoseira sedoides*. *Can. J. Physiol. Pharm.* **2011**, *89*, 911–921.

Mhadhebi, L.; Mhadhebi, A.; Robert, J.; Bouraouia, A. Antioxidant, anti-inflammatory and antiproliferative effects of aqueous extracts of three Mediterranean brown seaweeds of the genus Cystoseira. *Iran. J. Pharm. Res.* **2014**, *13*, 207–220.

Murphy, C.; Hotchkiss, S.; Worthington, J. McKeown, S.R. The potential of seaweed as a source of drugs for use in cancer chemotherapy. *J. Appl. Phycol*. **2014**, *26*, 2211–2264.

Nahas, R.; Abatis, D.; Anagnostopoulou, M.A.; Kefalasa, P.; Vagias, C.; Roussis, V. Radical-scavenging activity of Aegean Sea marine algae. *Food Chem*. **2007**, *102*, 577–581.

Namvar, F.; Baharara, J.; Mahdi, A.A. Antioxidant and anticancer activities of selected Persian gulf algae. *Indian J. Clin. Biochem*. **2014**, *29*, 13–20.

Neethu, P.V.; Suthindhiran, K.; Jayasri, M.A. Antioxidant and antiproliferative activity of *Asparagopsis taxiformis*. *Pharmacognosy Res.* **2017**, *9*, 238–246.

Re, R.; Pellegrini, N.; Proteggente, A.; Pannala, A.; Yang, M.; Rice-Evans, C. Antioxidant activity applying an improved ABTS+• radical cation decolorization assay. *Free Radical Biol. Med.* **1999**, *26*, 1231−1237.

Shen, M.Y.; Liu, T.I.; Yu, T.W.; Kv, R.; Chiang, W.H.; Tsai, Y.C.; Chen, H.H.; Lin, C.S; Chiu, H.G. Hierarchically targetable polysaccharide-coated solid lipid nanoparticles as T an oral chemo/thermotherapy delivery system for local treatment of colon cancer. *Biomaterials* **2019**, *197*, 86–100.

Shih, C.C.; Hwang, H.R.; Chang, C.I.; Su, H.M.; Chen, P.C.; Kuo, H.M.; Li, P.J.; Wang, H.D.; Tsui, K.H.; Lin, Y.C.; Huang, S.Y.; Wen, Z.H. Anti-inflammatory and antinociceptive effects of ethyl acetate fraction of an edible red macroalgae *Sarcodia ceylanica*. *Int. J. Mol. Sci.* **2017**, 18, pii: E2437.

Skehan, P.; Storeng, R.; Scudiero, D.; Monks, A.; McMahon, J.; Vistica, D.; et al., New colorimetric cytotoxicity assay for anticancer-drug screening. *J. Natl. Cancer. Inst.* **1990,** 82, 1107−1112.

Song, W.; Wang, Z.; Zhang, X.; Li, Y. Ethanol extract from *Ulva prolifera* prevents high-fat diet-induced insulin resistance, oxidative stress, and inflammation response in mice. *Biomed. Res. Int.* **2018**, *2018*,1374565

Taskin, E.; Caki, Z.; Ozturk, M.; Taskin, E. Assessment of in *vitro* anticanceral and antimicrobial activities of marine algae harvested from the eastern Mediterranean sea. *A. J. B*. **2010**, *9*, 4272–4277.

Tenorio-Rodriguez, P.A.; Murillo-Álvarez, J.I.; Campa-Cordova, Á.I.; Angulo, C. Antioxidant screening and phenolic content of ethanol extracts of selected Baja California Peninsula macroalgae. *J. Food Sci. Technol.* **2017**, *54*, 422−429.

Todoric, J.; Antonucci, L.; Karin, M. Targeting inflammation in cancer prevention and therapy. *Cancer Prev. Res. (Phila).* **2016**, *9*, 895–905.

Urones, J. G.; Araújo, M. E. M.; Brito Palma, F. M. S.; Basabe, P.; Marcos, I. S.; Moro, R. F.; Lithgow, A. M.; Pineda, J. Meroterpenes from *Cystoseira usenoides* II. *Phytochemistry* **1992a**, *31*, 2105−2109.

Urones, J. G.; Basabe, P.; Marcos, I. S.; Pineda, J.; Lithgow, A. M.; Moro, R. F.; Brito Palma, F. M. S.; Araújo, M. E. M.; Grávalos, M. D. G. Meroterpenes from *Cystoseira usenoides*. *Phytochemistry* **1992b**, *31*, 179−182.

Vizetto-Duarte, C.; Custódio, L.; Acosta, G.; Lago, J.H.G.; Morais, T.R.; Bruno de Sousa, C.; Gangadhar, K.N.; Rodrigues, M.J.; Pereira, H.; Lima, R.T.; Vasconcelos, M.H.; Barreira, L.; Rauter, A.P.; Albericio, F.; Varela, J. Can macroalgae provide promising anti-tumoral compounds? A closer look at *Cystoseira tamariscifolia* as a source for antioxidant and anti-hepatocarcinoma compounds. *Peer J.* **2016**, *4*, 1704, doi 10.7717/peerj.1704.

Wells, M.L.; Potin, P.; Craigie, J.S.; Raven, J.A.; Merchant, S.S.; Helliwell, K.E.; Smith, A.G.; Camire, M.E.; Brawley, S.H. Algae as nutritional and functional food sources: revisiting our understanding. *J. Appl. Phycol.* **2017**, *29*, 949–982.

Zubia, M.; Fabre, M.S.; Kerjean, V.; Le Lann, K.; Stiger-Pouvreau, V.; Fauchon, M. et al., Antioxidant and antitumoural activities of some Phaeophyta from Brittany coasts. *Food Chem.* **2009**, *116*, 693–701.

4. Chemical study of the brown alga *Cystoseira usneoides* and antioxidant activity of the isolated compounds

The findings described in the previous chapter on the antioxidant, antitumor, and anti-inflammatory activities of the crude extract of *C. usneoides* prompted us to perform a chemical study of the extract, aimed to identify the natural products of the alga and to isolate enough amounts of the compounds for the evaluation of their bioactivity. The results obtained were included in the article published in *The Journal of Natural Products* **2013**, *76*, 621-629.

Abstract: The chemical study of the extract of the brown alga *Cystoseira usneoides* has led to the isolation of twelve meroterpenes (**1**-**12**), six of which are new compounds: cystodiones A-F (**7**-**12**). From a structural point of view the isolated meroterpenes were characterized by containing a 1′-*O*-methyltoluhydroquinone ring that bears at C-2′ a regular C_{20} or C_{14} terpenoid chain with two or three double bonds and several oxygenated functions. In the antioxidant assays all the tested meroterpenes, and in particular the compounds 6-*cis*-amentadione-1′-methyl ether (**5**), amentadione-1′-methyl ether (**6**), cystodione A (**7**) and cystodione B (**8**), exhibited strong radical scavenging activity.

4.1. Introduction

Brown algae of the genus *Cystoseira* are widely distributed along the Mediterranean and the northeastern Atlantic coasts (Draisma et al., 2010). This group of algae has been subject of numerous chemical studies that have led to the isolation of an array of natural products consisting of a terpenoid residue linked to the position C-2 of a 6-methylhydroquinone ring (also known as toluhydroquinone or toluquinol ring) (Valls and Piovetti 1995; Amico et al., 1995; Gouveia et al., 2013a) (Figure 4.1).

Compounds such as cystoazorol A (Gouveia et al., 2013b), 1′-demethylcystalgerone (Amico et al., 1984) and mediterraneol A (Francisco et al., 1986) are examples of meroterpenoids isolated from various algae of the genus *Cystoseira* (Figure 4.1).

Biosynthetically, the meroterpenoids of *Cystoseira* are likely derived from a tetraprenyltoluquinol precursor (Figure 4.1), which through functionalization and cyclization reactions at the terpenoid chain could give rise to great structural variety, ranging from compounds with a regular isoprenoid framework, either linear (*e.g.* cystoazorol A in Figure 4.1) or cyclic (*e.g.* 1′-demethylcystalgerone in Figure 4.1), to rearranged derivatives (*e.g.* mediterraneol A in Figure 4.1).

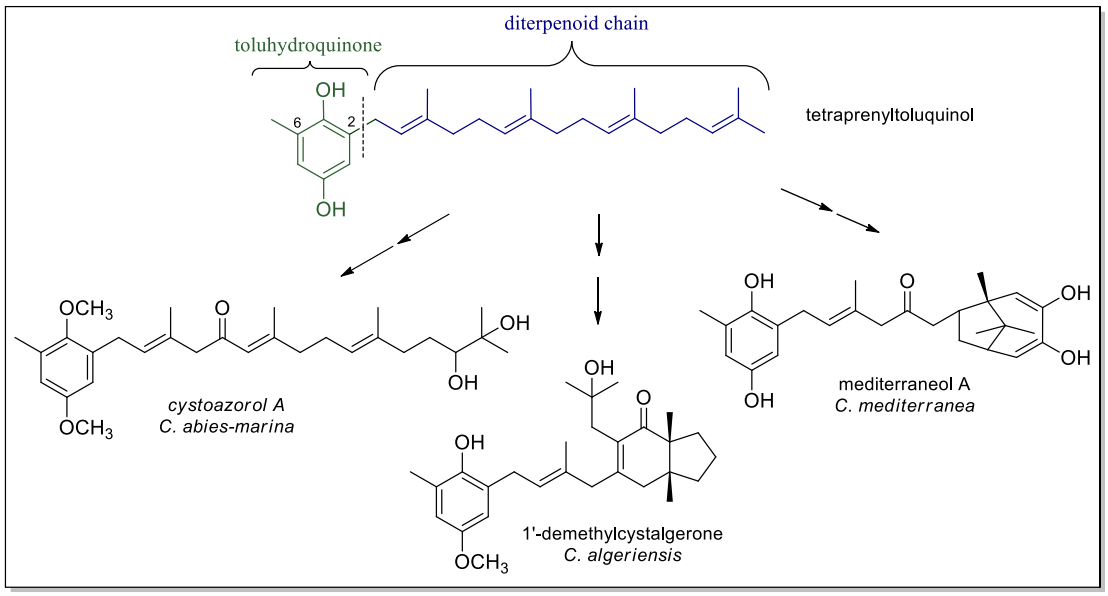

Figure 4.1. Examples of meroterpenoids isolated from algae of the genus *Cystoseira* and a tetraprenyltoluquinol as potential biosynthetic precursor.

The great number of phytochemical data obtained for algae of the genus *Cystoseira* early led to some chemotaxonomic conclusions (Valls and Piovetti 1995; Amico et al., 1995). Moreover, the classifications based on chemical data were found to be closely similar to those based on morphological features. Thus, algae of the genus *Cystoseira* were classified into three main groups: the first one includes species that do not contain diterpenoids, the second is formed by the species which produce linear diterpenoids and the third group consists of the species that produce meroterpenoids (Valls and Piovetti, 1995). This latter group was further subdivided into three categories depending on the presence of carbocycles in the terpenoid moiety. The first category includes the species that produce meroditerpenoids with a regular chain (*e.g. C. abies-marina* in Figure 4.1), the second is formed by the species that produce meroterpenoids that contain a regular terpenoid moiety

displaying one or various carbocyles (*e.g. C. algeriensis* in Figure 4.1), and the third category includes the species that contain compounds with a rearranged terpenoid moiety (*e.g. C. mediterranea* in Figure 4.1).

With regard to the species *C. usneoides*, in 1992 two reports described the isolation of four meroditerpenoids from specimens of this alga collected in the coasts of Sesimbra, Portugal (Urones et al., 1992a, 1992b). However, synthetic studies developed some years later demonstrated that the structures proposed for two of the compounds, usneoidones A and B, were incorrect (Danet et al., 2004). More recently, it has been suggested that the structures proposed for the other two isolated metabolites, usneoidols A and B, could also need to be revised (De los Reyes et al., 2016).

Herein we describe the chemical study of the bioactive extract of *C. usneoides* collected in the Moroccan coasts of the Gibraltar Strait that has led to the isolation of twelve meroterpenoids, whose antioxidant properties have also been evaluated.

4.2. Material and Methods

4.2.1. Solvents and reagents

Ethanol, acetone, and methanol were obtained from Merck (Darmstadt, Germany). CD_3OD and $CDCl_3$, 2,2-azino-bis(3-ethylbenzothiazoline-6-sulfonic acid) diammonium salt (ABTS), and 6-hydroxy-2,5,7,8-tetramethylchroman-2-carboxylic acid (Trolox) were purchased from Sigma Chemical Co. (St. Louis, MO, USA). Potassium persulfate was procured from Fluka Chemical Co.

4.2.2. Collection of the alga

Samples of *Cystoseira usneoides* (class Phaeophyceae, order Fucales, family Sargassaceae) were collected by hand (1−4 m depth) in the Mediterranean coast of Morocco at the Gibraltar Strait (35°50′52.58″ N, 5°33′39.04″ W). Voucher specimens of the specie (HTET.Phyc 545) were deposited in the herbarium of the Laboratory of Applied Algology-Mycology, Department of Biology, Faculty of Sciences at Abdelmalek Essaadi University, 93002 Tetouan, Morocco.

In the field, epiphytes were removed from the algae and the samples were rinsed with sterile seawater to remove associated debris and necrotic parts. In the laboratory, the

samples were shade dried, cut into small pieces and powdered in a mixer grinder (IKA R A11 basic, Sigma-Aldrich). The obtained powder was cold-preserved (−12 °C).

4.2.3. Extraction and isolation of natural products

The powder previously prepared of *C. usneoides* (150 g) was extracted with acetone/methanol (MeOH) (1:1, v/v, 400 mL) at room t[a]. The solution was filtered through paper and the residual solid material extracted five more times using the same procedure. The solutions were combined and the solvent evaporated at reduced pressure to yield a dark green oily extract (4.63 g).

The compounds were isolated from the extract by using column chromatography (CC) performed on Merck silica gel 60 (70−230 mesh) and HPLC separations that were performed on a LaChrom-Hitachi apparatus equipped with LiChrospher Si-60 (Merck, 250 × 10 mm, 10 μm) and Luna Si (2) (Phenomenex, 250 × 4.6 mm, 5 μm) columns, using an RI-71 differential refractometer or L-7400 UV detector (Merck) working at 254 nm. First the extract was subjected to CC eluting with *n*-hexane/diethyl ether (Et_2O) mixtures of increasing polarity (from 90:10 to 30:70, v/v), then Et_2O, $CHCl_3$/MeOH mixtures (95:5 and 80:20, v/v), and finally MeOH. The fractions eluted with n-hexane/Et_2O (30:70, v/v) and Et_2O were chromatographed over a silica gel column using *n*-hexane and *n*-hexane/ethyl acetate (EtOAc) mixtures (80:20 to 30:70, v/v) as eluents. Repeated HPLC separations of selected fractions using *n*-hexane/EtOAc (60:40, v/v) and *n*-hexane/isopropanol (90:10, v/v) yielded the compounds **4** (29.6 mg, 2.0 × 10−2 % dry wt), **3** (73.2 mg, 4.9 × 10−2 % dry wt), **11** (5.3 mg, 3.5 × 10−3 dry wt), **5** (86.6 mg, 5.8 × 10−2 % dry wt), and **6** (85.1 mg, 5.7 × 10−2 % dry wt). The fraction eluted with $CHCl_3$/MeOH (95:5) in the first column chromatography of the extract was further separated over a silica gel column using *n*-hexane/EtOAc mixtures (from 50:50 to 15:85, v/v) as eluents. Repeated separations of selected fractions by normal-phase HPLC using *n*-hexane/EtOAc (50:50, v/v) and *n*-hexane/isopropanol (90:10, v/v) as eluents afforded the compounds **1** (86.9 mg, 5.8×10^{-2} % dry wt), **12** (3.5 mg, 2.3×10^{-3} % dry wt), **2** (88.7 mg, 5.9 × 10−2 % dry wt), **9** (2.9 mg, 1.9 × 10−3 dry wt), **7** (29.5 mg, 2.0 × 10−2 % dry wt), **8** (16.7 mg, 1.1 × 10−2 % dry wt), **10** (4.9 mg, 3.3 × 10−3 % dry wt), and additional amounts of **6** (46.1 mg, total yield 8.7×10^{-2} % dry wt).

4.2.4. NMR and HRMS analysis

^{1}H and ^{13}C NMR spectra were recorded on a Varian INOVA 600 or on an Agilent 500 using CD_3OD or $CDCl_3$ as solvent. Chemical shifts were referenced using the corresponding solvent signals [δ_H 3.30 and δ_C 49.0 for CD_3OD, δ_H 7.26 and δ_C 77.0 for $CDCl_3$]. COSY, HSQC, HMBC, and NOESY experiments were performed using standard Varian pulse sequences. High-resolution mass spectra (HRMS) were obtained on a Waters SYNAPT G2 spectrometer.

4.2.5. ABTS radical scavenging activity

Antioxidant activity was determined by the ABTS (2,2′-azinobis(3-ethylbenzothiazoline-6-sulfonic acid)) free radical decolorization assay developed by Re et al., 1999 with slight modifications. ABTS was dissolved in H_2O to a 2.9 mM concentration. The $ABTS^{\bullet+}$ radical cation was produced by reacting the ABTS stock solution with 0.98 mM potassium persulfate (final concentration) and allowing the mixture to stand in the dark at room temperature for 12− 18 h before use. For the study of the algal compounds the $ABTS^{\bullet+}$ solution was diluted with EtOH to an absorbance of 0.7 ± 0.02 at 734 nm. Trolox (6-hydroxy-2,5,7,8-tetramethylchroman-2-carboxylic acid) was used as standard. After addition of 100 μL of $ABTS^{\bullet+}$ reagent to 90 μL of EtOH and 10 μL of the tested compound or Trolox standard (final concentration from 3.125 to 200 μM), the absorbance at 734 nm was taken 1 min after mixing and up to 6 min using a microtiter plate reader. Appropriate solvent blanks (controls) were run in each assay. All the determinations were carried out in triplicate. The percentage of inhibition of the absorbance was calculated by the following equation: % Inhibition = $[(A_0 - A_1)/A_0] \times 100$, where A_0 expresses the absorbance of the control and A_1 the absorbance of the tested compound.

4.2.6. Statistical analysis

The results were expressed as means ± standard deviations (S.D.). Differences between two groups were analyzed by the Student's *t-test*. One-way analysis of variance (ANOVA) was used in multiple group comparisons. Difference with $p < 0.05$ (*), $p < 0.01$ (**) or $p < 0.001$ (***) was considered statistically significant.

4.3. Results and Discussion

4.3.1. Isolation and identification of the natural products of C. usneoides

The separation of the acetone/methanol extract of *C. usneoides* by column chromatography (CC) over silica gel followed by repeated purification of selected fractions by CC and HPLC led to the isolation of twelve compounds. The analysis of each compound by spectroscopic techniques indicated that all the isolated metabolites were meroterpenoids and allowed to determining the chemical structures **1-12** shown in Figure 4.2. (De los Reyes et al., 2013).

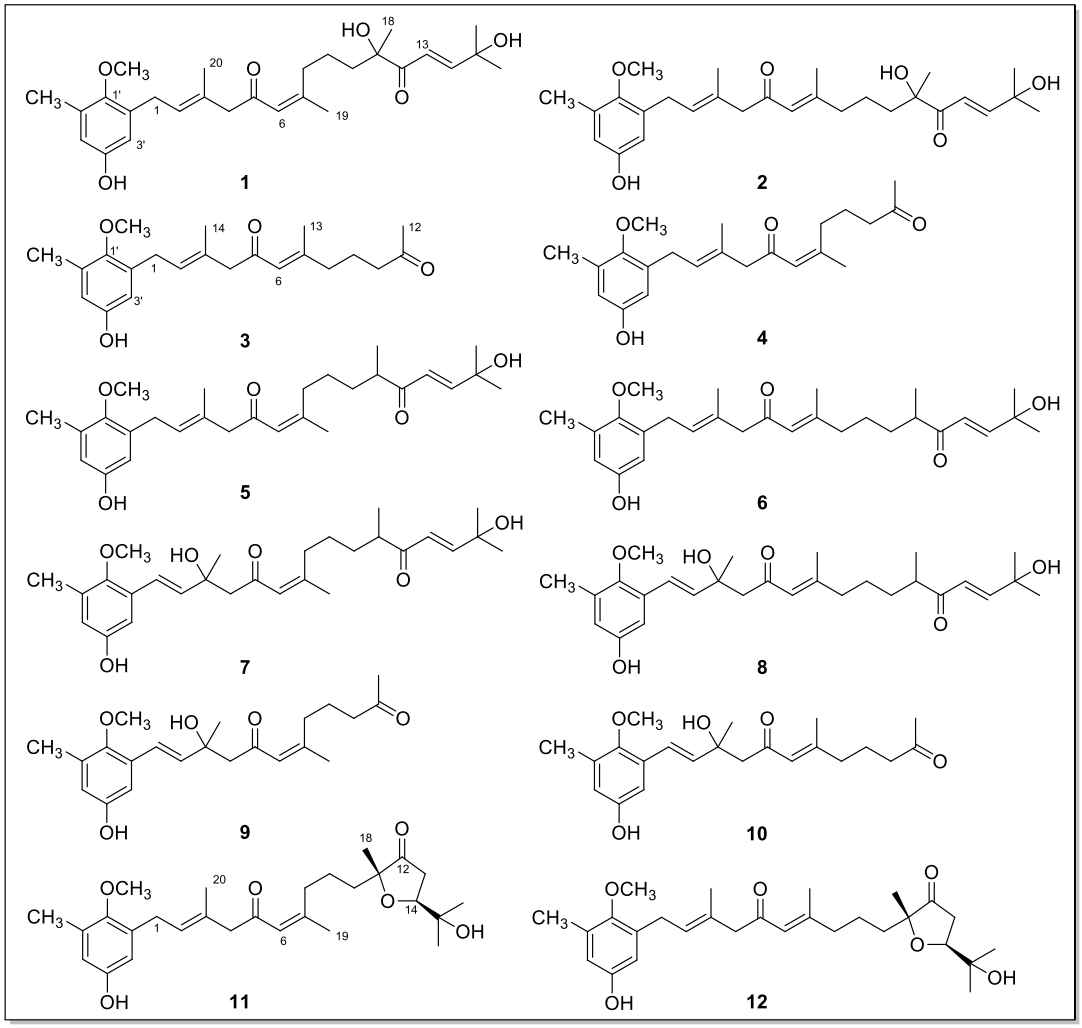

Figure 4.2. Chemical structures of the meroterpenoids **1-12** isolated from *C. usneoides* collected in the Moroccan coasts of the Gibraltar Strait.

From a structural point of view, all the isolated meroterpenoids consisted of a toluhydroquinone ring that possess *O*-methylated the phenolic group at C-1′ and bears at C-2′ a terpenoid moiety. Two main groups of compounds were obtained: compounds **1**, **2**, **5**, **6**, **7**, **8**, **11**, and **12** which possessed a regular diterpenoid moiety (twenty carbon atoms) derived from four isoprenoid C_5 units linked head to tail, and compounds **3**, **4**, **9**, and **10**, which contained a truncated isoprenoid chain of fourteen carbon atoms, where only two isoprenoid C_5 unis can be recognized. This C_{14} chain likely arises from a tetraprenyltoluquinol precursor by oxidative cleavage of a carbon-carbon double bond at C-11,C-12 of the diterpenoid chain.

Whithin each group of meroterpenoids, the structural differences among the compounds were found in the terpenoid residue. Thus, compounds **1**, **5**, and **7** possess a diterpenoid chain, which differ by the location of double bonds and/or the presence hydroxy groups in the chain, and compound **11** is characterized by containing an unusual tetrahydrofuran-3-one ring. Compounds **2**, **6**, **8**, and **12** differ from **1**, **5**, **7**, and **11**, respectively, by the configuration of the double bond at C-6,C-7.

Within the meroterpenoids with the C_{14} chain, compounds **4** and **9** differ by the presence of a hydroxy group and the location of a double bon in the terpenoid chain and compounds **3** and **10** are the 6*E* isomers of **4** and **9**, respectively.

A survey of literature revealed that the isolated compound **1** was usneoidone Z, a meroditerpene previously reported from *C. usneoides* collected in the Portuguese coasts (Urones et al., 1992a),[1] while compound **2** was identified as 11-hydroxy-1′-*O*-methylamentadione, a meroterpene that has been previously cited as a metabolite of *C. usneoides* (Valls and Piovetti 1995).

Compounds **3** and **4** were identified as cystomexicones B and A, respectively, previously described from *C. abies-marina* (Fernández et al., 1998).

Compounds **5** and **6** were identified as 6-*cis*-amentadione-1′-methyl ether and amentadione-1′-methyl ether, respectively, two meroditerpenoids that had been previously

[1] The structure assigned to usneoidone Z by Urones et al. (1992a) was not consistent with the spectroscopic data and was revised to **1** in De los Reyes et al., 2013.

reported from *C. tamariscifolia* (Amico et al. 1989).

Compounds **7-12** resulted to be new meroterpenoids and were given the names cystodiones A-F. The structures of these new compounds were determined by spectroscopic means, mainly NMR and MS, in particular through the analysis of the ^{1}H and ^{13}C NMR spectra and the correlations observed in the two-dimensional NMR spectra. The NMR data of compounds **7-12** are listed in Tables 4.1 and 4.2. The molecular formulae obtained for each new compound by HRMS are shown in Table 4.3.

Table 4.1. ^{13}C NMR data of cystodiones A-F (**7-12**) in CD_3OD.

	7[a]	**8**[a]	**9**[a]	**10**[a]	**11**[a]	**12**[b]
Position	δ_C, type	δ_C, type	δ_C, type	δ_C, type	δ_C, type	δ_C, type
1	123.3, CH	123.3, CH	123.3, CH	123.3, CH	29.4, CH_2	29.4, CH_2
2	137.7, CH	137.8, CH	137.7, CH	137.7, CH	129.5, CH	129.5, CH
3	73.5, C	73.5, C	73.5, C	73.5, C	131.4, C	131.5, C
4	56.2, CH_2	56.4, CH_2	56.2, CH_2	56.4, CH_2	56.2, CH_2	56.2, CH_2
5	201.7, C	202.1, C	201.7, C	202.2 C	201.4, C	202.0, C
6	126.4, CH	125.9, CH	126.8, CH	126.1, CH	124.4, CH	123.7, CH
7	161.5, C	160.6, C	160.9, C	160.2, C	161.5, C	160.6, C
8	34.6, CH_2	42.1, CH_2	33.8, CH_2	41.2, CH_2	34.6, CH_2	42.0, CH_2
9	26.8, CH_2	26.2, CH_2	23.1, CH_2	22.5, CH_2	23.0, CH_2	22.2, CH_2
10	34.2, CH_2	33.7, CH_2	43.7, CH_2	43.2, CH_2	36.2, CH_2	35.8, CH_2
11	44.9, CH	45.0, CH	211.8, C	211.3, C	84.5, C	84.4, C
12	206.9, C	206.7, C	29.7, CH_3	29.8, CH_3	219.5, C	219.5, C
13	125.6, CH	125.6, CH	25.4, CH_3	19.5, CH_3	37.7, CH_2	37.7, CH_2
14	155.2, CH	155.2, CH	28.7, CH_3	28.7, CH_3	81.1, CH	81.1, CH
15	71.3, C	71.3, C			71.7, C	71.7, C
16	29.3, CH_3	29.3, CH_3			25.8[c], CH_3	25.7[c], CH_3
17	29.3, CH_3	29.3, CH_3			25.6[c], CH_3	25.6[c], CH_3
18	17.0, CH_3	17.1, CH_3			22.3, CH_3	22.4, CH_3
19	25.6, CH_3	19.6, CH_3			25.5, CH_3	19.3, CH_3
20	28.6, CH_3	28.6, CH_3			16.6, CH_3	16.6, CH_3
1’	150.7, C	150.7, C	150.7, C	150.7, C	150.8, C	150.7, C
2’	131.9, C	131.9, C	131.9, C	131.9, C	135.6, C	135.6, C
3’	111.0, CH	111.0, CH	111.0, CH	111.0, CH	115.0, CH	114.9, CH
4’	154.4, C	154.4, C	154.3, C	154.3, C	154.3, C	154.3, C
5’	118.0, CH	118.0, CH	118.0, CH	118.0, CH	116.3, CH	116.3, CH
6’	133.1, C	133.1, C	133.1, C	133.1, C	132.7, C	132.7, C
6’-CH_3	16.2, CH_3	16.2, CH_3	16.1, CH_3	16.1, CH_3	16.4, CH_3	16.4, CH_3
-OCH_3	61.4, CH_3	61.4, CH_3	61.4, CH_3	61.4, CH_3	60.9, CH_3	61.0, CH_3

[a] At 150 MHz; [b] At 125 MHz; [c]Values may be interchanged

Table 4.2. ^{1}H NMR data of cystodiones A-F (**7-12**) in CD_3OD.

	7[a]	**8**[a]	**9**[a]	**10**[a]	**11**[a]	**12**[b]
Position	δ_H, m (*J* in Hz)	δ_H, m (*J* in Hz)	δ_H, m (*J* in Hz)	δ_H, m (*J* in Hz)	δ_H, m (*J* in Hz)	δ_H, m (*J* in Hz)
1	6.76, d (16.1)	6.76, d (16.1)	6.76, d (16.1)	6.77, d (16.2)	3.33, d (7.4)	3.33, d (7.0)
2	6.29, d (16.1)	6.30, d (16.1)	6.29, d (16.1)	6.30, d (16.2)	5.42, *br* t (7.4)	5.44, *br* t (7.3)
3						
4	2.79, d (14.2) 2.70, d (14.2)	2.80, d (13.9) 2.72, d (13.9)	2.80, d (14.4) 2.71, d (14.4)	2.81, d (14.2) 2.72, d (14.2)	3.09, s	3.11, s
5						
6	6.22, *br* s	6.20, *br* s	6.25, *br* s	6.21, *br* s	6.21, *br* s	6.21, *br* s
7						
8	2.55, m 2.51, m	2.11, t (7.5)	2.51, m	2.10, m	2.60, ddd (11.7, 9.1, 5.7) 2.54, m	2.15, t (6.6)
9	1.37, m	1.38, m	1.67, m	1.68, m	1.56, m 1.48, m	1.59, m 1.49, m
10	1.65, m 1.33, m	1.61, m 1.30, m	2.44, t (7.2)	2.43, t (7.2)	1.60, m 1.46, m	1.55, m 1.40, m
11	2.82, m	2.81, m				
12			2.07, s	2.08, s		
13	6.33, d (15.8)	6.34, d (15.9)	1.87, d (1.2)	206, d (1.2)	2.54, dd (18.2, 9.4) 2.43, dd (18.2, 6.6)	2.54, dd (18.3, 9.5) 2.41, dd (18.3, 6.6)
14	6.93, d (15.8)	6.93, dd (15.9, 1.2)	1.40, s	1.41, s	4.03, dd (9.4, 6.6)	4.00, dd (9.5, 6.2)
15						
16	1.31, s	1.32, s			1.12, s	1.12, s
17	1.31, s	1.32, s			1.24, s	1.24, s
18	1.02, d (6.8)	1.04, d (7.0)			1.18, s	1.18, s
19	1.85, d (1.0)	2.05, d (1.1)			1.87, d (1.1)	2.08, d (1.5)
20	1.40, s	1.40, s			1.70, *br* s	1.71, *br* s
1’						
2’						
3’	6.69, d (2.9)	6.70, d (3.1)	6.69, d (2.9)	6.70, (2.9)	6.43, d (2.9)	6.43, d (2.6)
4’						
5’	6.50, d (2.9)	6.51, d (3.1)	6.50, d (2.9)	6.50, d (2.9)	6.44, d (2.9)	6.44, d (2.6)
6’						
6’-CH_3	2.18, s	2.18, s	2.18, s	2.18, s	2.19, s	2.19, s
-OCH_3	3.60, s	3.60, s	3.60, s	3.60, s	3.64, s	3.64, s

[a] At 600 MHz; [b] At 500 MHz

Table 4.3. HRMS data of cystodiones A-F (**7-12**)

Compound	Molecular formula	Observed ion,[a] *m/z*	Calculated
7	$C_{28}H_{40}O_6$	[M − H], 471.2758	For $C_{28}H_{39}O_6$, 471.2747
8	$C_{28}H_{40}O_6$	[M − H], 471.2751	For $C_{28}H_{39}O_6$, 471.2747
9	$C_{22}H_{30}O_5$	[M + Na], 397.1981	For $C_{22}H_{30}O_5Na$, 397.1991
10	$C_{22}H_{30}O_6$	[M + Na], 397.1983	For $C_{22}H_{30}O_5Na$, 397.1991
11	$C_{28}H_{40}O_6$	[M − H], 471.2751	For $C_{28}H_{39}O_6$, 471.2747
12	$C_{28}H_{40}O_6$	[M + H], 473.2892	For $C_{28}H_{41}O_6$, 473.2903

[a] Ionization technique: ESI(-) for **7**, **8**,and **11**; ESI(+) for **9** and **10**; APCI for **12**.

4.3.2. Antioxidant activity of meroterpenoids isolated from *C. usneoides*

The meroterpenoids **1**−**10** isolated from *C. usneoides* were tested for their antioxidant activity by using the ABTS assay, which determines the radical-scavenging activity of compounds toward the $ABTS^{\bullet+}$ radical cation (Re et al., 1999). In this method, the ABTS is chemically or enzymatically oxidized to its radical cation $ABTS^{\bullet+}$, which is intensely blue-green colored, and the antioxidant capacity of a compound is measured as its ability to reduce the color by reacting with the $ABTS^{\bullet+}$ radical (Figure. 4.3).

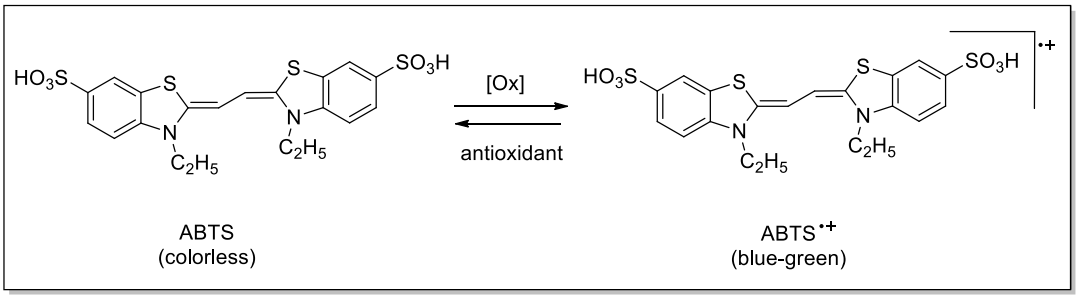

Figure 4.3. Interconversion between the ABTS and its radical.

The results are expressed relative to the activity of Trolox (Figure 4.4), a synthetic vitamin E analogue, measured under the same conditions.

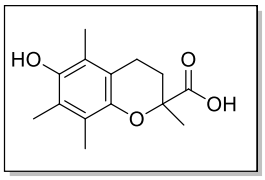

Figure 4.4. Chemical structure of Trolox®.

All the tested meroterpenoids exhibited strong radical-scavenging activity, as shown in Table 4.4.

The most active compounds were **5**, **6**, **7**, and **8,** which showed an antioxidant capacity equal or slightly superior to that of the Trolox standard. Compounds **2** and **3** were also strongly active, showing a potency of 78% that of Trolox, while compounds **1**, **4**, **9**, and **10** displayed an antioxidant activity about 50−60% that of Trolox.

Table 4.4. Antioxidant activities of compounds **1**−**10** in the ABTS assay.

Compound	EC_{50} (μM)[b]	TE[c]
Trolox[a]	25.9±0.5	1
1	43.1±3.1	0.60
2	33.1±5.1	0.78
3	33.3±2.3	0.78
4	51.6±4.8	0.50
5	26.3±2.3	0.98
6	24.5±1.6	1.06
7	22.5±2.1	1.15
8	24.4±0.9	1.06
9	55.9±9.9	0.46
10	44.7±1.1	0.58

[a]Standard compound: 6-hydroxy-2,5,7,8-tetramethylchroman-2-carboxylic acid.
[b]Concentration that caused a 50% reduction of the absorbance. Values are mean ± SD of three determinations.
[c]Trolox equivalents: EC_{50}(Trolox)/EC_{50}(compound).

From a structural point of view, except for compounds **7** and **8,** the compounds possessing a 6*E* configuration (**2**, **3**, **6**, **10**) were more active than the corresponding 6*Z* isomers (**1**, **4**, **5**, **9**).

On the other hand, compounds with a C_{20} side chain were in general more active than the corresponding analogues with a C_{14} side chain, as evidenced by the comparison of the activity of the meroditerpenes **5**, **6**, **7**, and **8** with that of the short chain analogues **4**, **3**, **9**, and **10**, respectively.

After an initial account on the properties of three *Cystoseira*-derived meroditerpenes as singlet oxygen and peroxyl radical scavengers (Foti et al., 1994), the antioxidant activities of a series of metabolites obtained from *C. crinita* have more recently been described (Fisch et al., 2003). The meroditerpenes of *C. crinita* were found to be less active than Trolox in the ABTS assay, with the most active compound displaying an antioxidant activity about 40% that of the Trolox standard. Our study of *C. usneoides* has allowed the identification of new members of this class of algal meroterpenoids provided of more potent antioxidative properties.

4.4. Conclusion

The chemical study herein described has shown than the brown alga *C. usneoides* contains a variety of meroterpenoids whose strcutures consist of a C_{20} or a C_{14} terpenoid moiety linked to an *O*-methyltoluhydroquinone. Six of the isolated meroterpenes are new natural products, the cystodiones A-F (**7**-**12**), while the compounds cystomexicone B (**3**), cystomexicone A (**4**), 6-*cis*-amentadione-1′-methyl ether (**5**), and amentadione-1′-methyl ether (**6**), are described for the first time in the species *C. usneoides*. In antioxidant assays the meroterpenes **5**, **6**, **7**, and **8** show potent radical-scavenging properties, further supporting the potential of algae of the genus *Cystoseira* as source of new natural antioxidants.

4.5. References

Amico, V. Marine brown algae of family Cystoseiraceae: chemistry and chemotaxonomy. *Phytochemistry* **1995**, *39*, 1257−1279.

Amico, V.; Cunsolo, F.; Piattelli, M.; Ruberto, G. Five novel tetraprenylhydroquinols from the brown alga *Cystoseira algeriensis*. *Phytochemistry* **1984**, *23*, 2017−2020.

Amico, V.; Piattelli, M.; Neri, P.; Ruberto, G. Metabolites of mixed biogenesis from *Cystoseira tamariscifolia*. *Gazz. Chim. Ital.* **1989**, *119*, 467−470.

Danet, M.; Normand-Bayle, M.; Mahuteau, J.; D'Angelo, J.; Morgant, G.; Desmaële, D. Enantioselective synthesis of the originally proposed usneoidone structure: evidence for a structural revision. *Eur. J. Org. Chem*. **2004**, *2004*, 1911−1922.

De los Reyes, C.; Ortega, M.; Zbakh, H.; Motilva, V.; Zubía, E. *Cystoseira usneoides*: A brown alga rich in antioxidant and anti-inflammatory meroditerpenoids. *J. Nat. Prod.*

2016, *79*, 395−405.

De los Reyes, C.; Zbakh, H.; Motilva, V.; Zubía, E. Antioxidant and anti-inflammatory meroterpenoids from the brown alga *Cystoseira usneoides*. *J. Nat. Prod.* **2013**, *76*, 621−629.

Draisma, S.G.A.; Ballesteros, E.; Rousseau, F.; Thibaut, T.J. DNA sequence data demonstrate the polyphyly of the genus *Cystoseira* and *Sargassaceae* genera (Phaeophyceae*). J. Phycol.* **2010**, *46*, 1329−1345.

Fernández, J.J.; Navarro, G.; Norte, M. Novel metabolites from the brown alga *Cystoseira abies-marina*. *Nat. Prod. Lett.* **1998**, *12*, 285−291.

Fisch, K.M.; Böhm, V.; Wright, A.D.; König, G.M. Antioxidative meroterpenoids from the brown alga *Cystoseira crinita*. *J. Nat. Prod.* **2003**, *66*, 968−975.

Foti, M.; Piattelli, M.; Amico, V.; Ruberto, G. J. Antioxidant activity of phenolic merodierpenoids from marine algae. *Photochem. Photobiol. B.* **1994**, *26*, 159−164.

Francisco, C.; Banaigs, B.; Teste, J.; Cave, A. Mediterraneols: a novel biologically active class of rearranged diterpenoid metabolites from *Cystoseira mediterranea* (Pheophyta). *J. Org. Chem.* **1986a**, *51*, 1115−1120.

Gouveia V.; Seca A.L.M.; Barreto M.C.; Pinto D.C.G.A. Di- and Sesquiterpenoids from *Cystoseira* Genus: Structure, intra-molecular, transformations and biological activity. *Mini-Rev. Med. Chem.* **2013a**, *13*, 1150−1159.

Gouveia, V.L.M.; Seca, A.M.L.; Barreto, M.C.; Neto, A.I.; Kijjoa, A.; Silva, A.M.S. Cytotoxic meroterpenoids from the macroalga *Cystoseira abies-marina*. *Phytochemistry Lett.* **2013b**, *6*, 593–597.

Mokrini, R.; Ben Mesaoud, M.; Daoudi, M.; Hellio, C.; Mare!chal, J.P.; El Hattab, M.; Ortalo-Magne, A.; Piovetti, L.; Culioli, G. J. Meroditerpenoids and derivatives from the brown alga *Cystoseira baccata* and their antifouling properties. *J. Nat. Prod.* **2008**, *71*, 1806−1811.

Re, R.; Pellegrini, N.; Proteggente, A.; Pannala, A.; Yang, M.; Rice-Evans, C. Antioxidant activity applying an improved ABTS radical cation decolorization assay. *Free Radical Biol. Med.* **1999**, *26*, 1231−1237.

Urones, J. G.; Araújo, M.E.M.; Brito Palma, F.M.S.; Basabe, P.; Marcos, I.S.; Moro, R.F.; Lithgow, A.M.; Pineda, J. Meroterpenes from *Cystoseira usenoides* II. *Phytochemistry* **1992a**, *31*, 2105−2109.

Urones, J.G.; Basabe, P.; Marcos, I.S.; Pineda, J.; Lithgow, A.M.; Moro, R.F.; Brito Palma, F. M.S.; Araújo, M.E.M.; Grávalos, M.D.G. Meroterpenes from *Cystoseira usenoides*. *Phytochemistry* **1992b**, *31*, 179−182.

Valls, R.; Piovetti, L. The chemistry of the Cystoseiraceae (Fucales: Pheophyceae): chemotaxonomic relationships. *Biochem. Syst. Ecol.* **1995**, *23*, 723−745.

5. Anticancer activities of meroterpenoids isolated from the brown alga *Cystoseira usneoides* against the human colon cancer cells HT-29

For the pharmacological screening of the AMTs isolated from the bioactive extract of *C. usneoides* we started by studying the anticancer activity in cellular models of colon cancer, in which our research group has experience, completing the investigation with mechanistic studies.

Abstract: The chemotherapy of different types of cancer, including colorectal cancers, remains disappointing at present. Unfortunately, most of current drugs are toxic and also attack healthy cells. Hence, the search for new anticancer agents, pharmacologically safe and effective, is needed. In the present study, we have investigated the anticancer effects of eight algal meroterpenoids (AMTs, **1-8)** isolated from the brown seaweed *Cystoseira usneoides* and their underlying mechanisms of action using HT-29, a highly metastatic human colon cancer cell line. All the tested meroterpenoids inhibited the growth of HT-29 malignant cells and were less toxic towards non-cancer colon cells, with the AMTs **1** and **5** exhibiting selectivity indexes of 5.26 and 5.23, respectively. Treatment of HT-29 cells with the AMTs **1**, **2**, **3**, **4**, **5**, and **7** induced cell cycle arrest in G2/M phase and, in some instances, apoptosis (compounds **2**, **3**, and **5**). Compounds **1**-**8** also exhibited significant inhibitory effects on the migration and/or invasion of colon cancer cells. Mechanistic analysis demonstrated that the AMTs **1**, **2**, **5**, **6**, **7**, and **8** reduced phosphorylation levels of extracellular signal-regulated kinase (ERK) and the AMTs **2**, **3**, **4**, **5**, **7**, and **8** decreased phosphorylation of c-JUN N-terminal kinase (JNK). Moreover, the AMTs **1**, **2**, **3**, **4**, **7**, and **8** inhibited phosphorylation levels of protein kinase B (AKT) in colon carcinoma cells. These results provide new insights into the mechanisms and functions of the meroterpenoids of *C. usneoides*, which exhibit anticancer effect on HT-29 colon cancer cells by inducing cell cycle arrest and apoptosis via the down-regulation of ERK/JNK/AKT signaling pathways.

5.1. Introduction

Colorectal cancer (CRC), also known as colon cancer or large bowel cancer, includes cancerous growths in the colon, rectum, anus, and appendix. CRC is the third most common type of cancer and the fourth leading cause of cancer-related death worldwide (Ferlay et al., 2015). Treatments such as surgical excision, chemotherapy using cytotoxic drugs, and radiotherapy constitute the major current therapeutic regimens for colon cancer (Kavousipour et al., 2017; Mayer, 2009). However, these therapeutic possibilities are only moderately successful for late-stage cancers and produce harmful side effects such as high toxicity or the increase of drug resistance and of the problems associated with metastasis. Therefore, novel therapeutic agents that target specific molecular signaling pathways in order to arrest CRC growth and metastasis are needed.

Traditionally, the search for novel drugs has largely relied on natural products (NPs) (Cragg et al., 2013) and the identification of antitumor constituents from plants has been essential for advancing the chemotherapy of cancer (Atanasov 2015). During the last decades, the marine macro- and microorganisms have also been a rich and diversified source of biologically active molecules with a broad range of health beneficial effects, including anticancer properties (Ruiz-Torres et al. 2017, Newman and Cragg 2014). Thus, numerous effective anticancer compounds have been discovered from natural sources and about 80% of chemotherapeutic agents so far developed for the treatment of cancer are based on NPs (Newman and Cragg, 2016).

Within the marine environment, macroalgae are a rich reservoir of structurally diverse secondary metabolites, mostly belonging to the class of the terpenoids (Leal et al., 2013,). NPs of this class have exhibited a wide spectrum of antitumor activities (Huang et al., 2012) expressed by their capacity to regulate a variety of pathophysiological processes, such as proliferation, migration, invasion, apoptosis, and cell cycle in different types of tumor cells (Rocha et al., 2018; Lisiak et al., 2017).

NPs of meroterpenoid type consisting of a terpenoid moiety attached to a toluquinone or a toluhydroquinone ring are widespread in brown algae of the family Sargassaceae (Sunasee and Davies-Coleman, 2012). In particular, algae of the genus *Cystoseira* have been the source of an array of meroditerpenoids (Gouveia et al., 2013a;

Amico, 1995; Valls and Piovetti, 1995). However, only a few of these compounds have been investigated for their biomedical properties, such as antioxidant, antibacterial or cytotoxic activities (Gouveia et al. 2013a). Regarding to the antitumor activity, the most recent reports have described the capacity of the meroterpenes cystoazorol A and cystoazorones A and B, isolated from *Cystoseira abies-marina*, to inhibit the growth of HeLa cells (Gouveia et al., 2013b) and the cytotoxicity of cystoketal, obtained from *Cystoseira tamariscifolia*, towards HepG2 cells (Vizetto-Duarte et al., 2016).

As a part of our research on bioactive metabolites from macroalgae, we observed that the extract of the seaweed *C.usneoides* exhibited significant activity as growth inhibitor of the colon cancer cells HT-29. In the present study, we have investigated the antitumor properties of AMTs **1-8** isolated from the extract of *C. usneoides* (Figure 5.1).

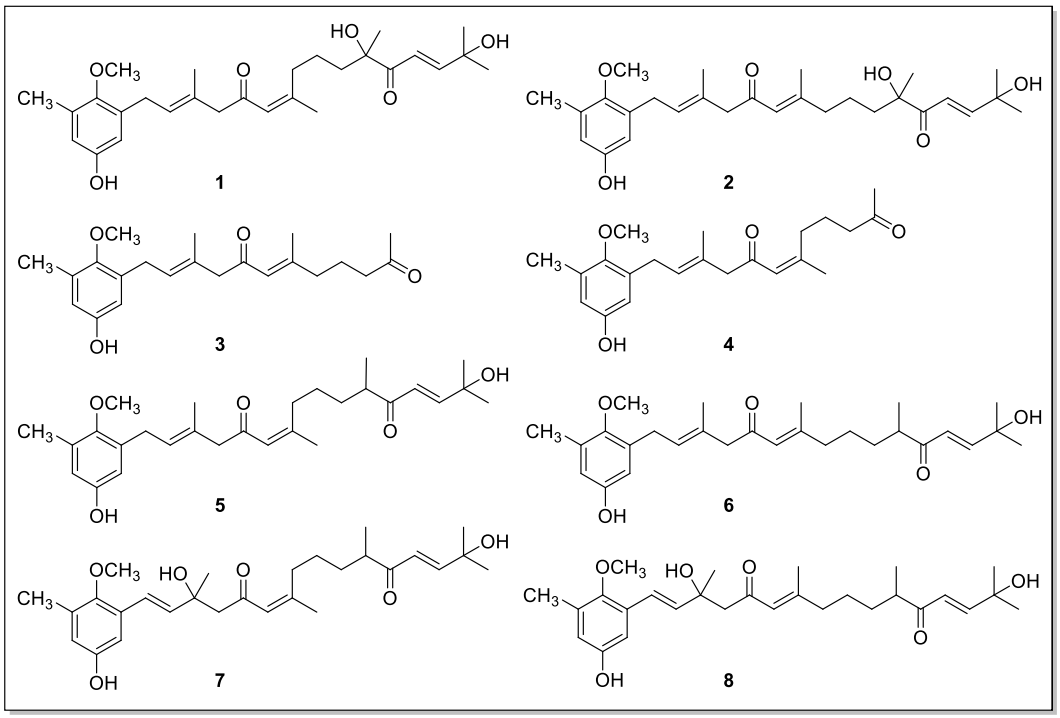

Figure 5.1. Chemical structures of AMTs **1-8** from *C. usneoides* subjected to anticancer studies.

In particular, we have examined the effects of the eight AMTs on the viability, apoptosis, cell cycle, and motility of HT-29 colon cancer cells and we have investigated the underlying mechanism of action. We have found that several of the AMTs possess

selectivity for colon cancer cells HT-29, showing lower toxicity on the normal colon cells CCD 841 CoN. Moreover, in *in vitro* assays, several of the tested AMTs increased apoptosis of HT29 colon cancer cells, caused cell cycle arrest at G2/M phase, and/or suppressed migration and invasion, which were associated with down-regulation of the ERK, JNK, and AKT signaling pathways. These results suggest the therapeutic potential of the AMTs produced by the alga *C. usneoides* in colorectal cancer.

5.2. Materials and methods

5.2.1. Isolation and identification of the meroterpenoids 1-8

The collection of the alga, the isolation, and the structural characterization of the AMTs were described in the previous chapter (De los Reyes et al., 2013). Briefly, shade-dried samples of *C. usneoides* collected at the Gibraltar Strait were ground and extracted with acetone/methanol (MeOH). The resulting extract was subjected to column chromatography (CC) eluting with *n*-hexane/diethyl ether (Et_2O) mixtures of increasing polarity, then Et_2O, chloroform/MeOH mixtures, and finally MeOH. Repeated separation of selected fractions by CC and HPLC afforded the pure compounds **1**-**8**, whose structures were determined by using NMR and MS.

5.2.2. Reagents for bioactivity assays

Sulforhodamine B (SRB), dimethylsulfoxide (DMSO), propidium iodide (PI) Tris-base, acetic acid, trichloroacetic acid (TCA), and RNase A were purchased from Sigma-Aldrich (Munich, Germany). Eagle's minimal essential medium (EMEM) and fetal bovine serum (FBS) were from GIBCO (USA). McCoy's medium was from Sigma-Aldrich (Saint Louis, MO, USA). Phosphate buffer saline (PBS), streptomycine, penicillin, and trypsine-EDTA were from PAA-Laboratories GmbH (Pasching, Austria). The Annexin V-FITC Apoptosis Detection Kit was purchased from eBiosciences Diagnostics (USA). Trevigen's Cultrex® 96 Well Cell Invasion Assays was purchased from R&D Systems (Gymea, NSW, Australia). For western blotting, primary and HRP-conjugated secondary antibodies anti-pERK1/2, anti-pJNK, and anti-pAKT were from Cell Signaling (Danvers, MA, USA), anti-

β-actin from Santa Cruz Biotechnology (Dallas, TX, USA), and goat anti-mouse or -rabbit antibody from Dako Cytomation (Hamburg, Germany).

5.2.3. Cell culture

HT-29 human colon carcinoma cells were obtained from the American Type Culture Collection (ATCC, USA). The cells were grown in McCoy's medium supplemented with 10% FBS, 100U/mL penicillin, and 100 mg/mL streptomycin, and the culture was maintained in a humidified incubator at 37°C under an atmosphere of 5% CO_2.

The normal human colonic epithelial cells CCD 841 CoN obtained from ATCC were grown in EMEM supplemented with 10% FBS, 100U/mL penicillin and 100 mg/mL streptomycin, and the culture was maintained in a humidified incubator at 37°C under an atmosphere of 5% CO_2.

5.2.4. Cell viability assay

Cell viability was quantified using the Sulforhodamine B assay described by Skehan et al. (1990). Cells were plated with a density of $5x10^3$ (HT-29) and $1x10^4$ (CCD 841 CoN) cells/well and allowed to attach at 37 °C in an atmosphere with 5% CO_2. After 24 h, the AMTs dissolved in DMSO were added to the cells (final concentrations of 10, 20, 30, and 50 μg/mL and less than 0.05 % of DMSO) and the plates were incubated for 72 h. Then, the cells were fixed by adding 50 μL of TCA (50%) to each well and the plates were maintained for 1 h at 4°C. The plates were washed five times with deionized water, air-dried, and stained for 30 min at room temperature with 100 μL of 0.4% (w/v) SRB prepared in 1% (v/v) acetic acid. The plates were rinsed quickly five times with 1% acetic acid to remove unbound dye, followed by air-drying. The bound dye was solubilized in 2 mM Tris base (100 μL/well) for 5 min. Optical densities were read on a microplate reader (Spectrophotometer LabsystemsMultiskan EX, λ 492 nm). Three independent assays were conducted, each one in duplicate. A standard curve was constructed for each experiment and used for converting the measured optical density values into numbers of viable cells/well. Cell survivals were expressed as percentage of viability (%) compared to the control and the half maximal inhibitory concentration (IC_{50}) was calculated. The selectivity index (SI) of each compound was calculated as described in the literature (Ibacache et al.,

2018): SI= IC_{50} value of the compound against a normal cell line/IC_{50} of the same compound against a cancer cell line.

5.2.5. Flow cytometric analysis for apoptosis induction assay

Quantitative assessment of apoptosis was performed by flow cytometry using an Annexin V-FITC Apoptosis Detection Kit (Vermes et al., 1995). Briefly, $1x10^6$ HT-29 cells were seeded per well in 6-well plates and incubated for 24 h, followed by the addition of the AMTs dissolved in DMSO (final concentrations of 10, 20, and 30 µg/mL for compounds **1**, **2**, **5**, **6**, **7**, and **8**, and 30, 60, and 90 µg/ml for compounds **3** and **4**, and less than 0.05 % DMSO) and incubation for 24 h. Curcumin (final concentrations of 50 and 75 µM) was used as a positive control. The cells were then washed, harvested with trypsin, and centrifuged at 1,500 rpm (5 min, 25 ºC). The pellet was resuspended in 195 µL of 1×Annexin buffer and then stained with 5 µL of Annexin V-FITC and 10 µL of PI for 10 min at room temperature, in the dark. To this mixture 200 µL of 1×Annexin buffer were added before analysis using a Cytomics FC500 flow cytometer (Beckman Coulter, Indianapolis, IN, USA). 10,000 cellular events in each sample were analyzed using DML program.

5.2.6. Cell cycle analysis by flow cytometry

HT-29 cells ($1x10^6$ cells/well) were seeded in 6-well plates and incubated for 24 h, followed by treatment with AMTs dissolved in DMSO (final concentrations of 10, 20, and 30 µg/mL for compounds **1**, **2**, **5**, **6**, **7**, and **8**, and 30, 60, and 90 µg/mL for compounds **3** and **4,** and always below 0.05 % DMSO) and 24 h of additional incubation (Nicoletti et al., 1991). Colchicine (final concentration of 0.2 µg/mL) was used as a positive control. The cells were then washed, harvested with trypsin, and centrifuged at 1,500 rpm (5 min, 25 ºC). The resulting pellet was fixed with ice-cold 70% ethanol (1 mL/10^6 cells) and the samples were stored at -4 ºC overnight. After fixation, the cells were washed with PBS, stained with PBS containing 5 mg/mL of RNase A, and incubated for 48 h at 4 °C. Subsequently, 50 µL of 0.1 mg/mL of IP was added and incubated for 1 h at 4 °C. The relative DNA content per cell was analyzed using a Cytomics FC500 flow cytometer (Beckman Coulter, Indianapolis, IN, USA). The data acquisition was performed with the DML program (DML, USA) and the analysis of the acquired data with the CXP Software (USA).

5.2.7. Wound migration assay

For cell migration assay, HT-29 cells were seeded in 6-well culture plates and allowed growing to 80–90% confluence for the experiment. After aspirating the medium, similar sized wounds were performed in the monolayer cells using a sterile micropipette tip. Wounded monolayer cells were washed three times with PBS to remove cell debris and then replaced with complete McCoy's medium. HT-29 cells were treated with the AMTs (10 µg/mL for compounds **1**, **2**, **5**, **6**, **7**, and **8**, and 30 µg/mL for compounds **3** and **4**) and incubated for 24h. For the image analysis of the effect of each treatment on cell migration, the wounded area was photographed immediately after scratching and after 24h. The level of cell migration was determined using NIH Image software (Image J 1.44g, Wayne Rasband, USA) and then expressed as a percentage of wound closure area using the equation: % of wound closure = $[(At_{0h} - At_{24h}) / At_{0h}] \times 100\%$, where, At_{0h} is the area of wound measured immediately after scratching and At_{24h} is the area of wound measured 24 h after scratching.

5.2.8. Cell invasion assay

The invasion activities were measured using Trevigen's Cultrex® 96 Well Cell Invasion Assays, as previously described (Moghadamtousi et al., 2014). Briefly, about 50 µL of basement membrane extract (BME, 1X) coat was added to each well. After incubation for 4 h at 37° in a 5% CO_2 atmosphere, the HT-29 cells at 50,000 cells/50µL in serum free McCoy's medium were added per well to the top chamber containing the tested compound (10 µg/mL for **1**, **2**, **5**, **6**, **7**, and **8**, and 30 µg/mL for compounds **3** and **4**). About 150 µL of McCoy's medium were then added to the lower chamber containing 10% FBS and penicillin/streptomycin as chemoattractants. Cells were allowed to migrate to the lower chamber in a humidified atmosphere containing 5% CO_2 at 37°C for 24 h. Afterwards, top and bottom chambers were aspirated and washed with washing buffer supplemented with the kit. About 100 µL of 1X Cell Dissociation Solution/Calcein-AM was added to each bottom chamber well and incubated for 1 h at 37 °C in CO_2 incubator. The cells internalized calcein-AM and the intracellular esterases cleaved the AM moiety to generate free calcein. Fluorescence of the samples was determined at 485 nm excitation, 520 nm emission, using ELISA plate reader (BioTek Instruments, USA). The number of cells that

had invaded through the BME coat was calculated using a standard curve. Results were expressed as percentage of invasion (%) compared to the control.

5.2.9. Preparation of cell lysates

Cells were cultured to 80% confluence at 37 °C. After 24 h of treatment with the compounds (10 and 20 µg/mL for compounds **1**, **2**, **5**, **6**, **7**, and **8**, and 30 and 60 µg/mL for compounds **3** and **4**), HT-29 cells were rinsed twice with ice-cold PBS, and then lysed immediately in lysis buffer (250 mM NaCl, 50 mM Tris (pH 7.5), 0.5 mM EDTA, 5 mM EGTA, 8 mM $MgCl_2$, 1 mM PMSF, 0.01 mg/mL pepstatin A, 0.01 mg/mL leupeptin, 0.01 mg/mL aprotinin, 1% Triton X-100). After centrifugation at 12,000 g for 3 min at 4 °C to separate the cellular debris, the supernatant was collected and stored at −80 °C until use. The protein concentrations were determined using Bio-Rad Protein Assay (BioRad, Richmond, CA, USA), according to the manufacturer's instructions.

5.2.10. Western blot analysis

Equal protein content (50 µg) samples of cell lysates were separated on 10% SDS–polyacrylamide gel and transferred to polyvinylidene difluoride membranes (Hybond-P, Amershan Biosciences, UK). The membranes were blocked with 5% (w/v) non-fat dry milk in Tris-buffered saline containing 0.1% Tween-20 buffer (pH 7.4) (TBST) for 1 h at room temperature and incubated with agitation with specific antibodies: anti-pERK1/2 (Cell Signaling; 1:1000), anti-pJNK (Cell Signaling; 1:1000), anti-pAKT (Cell Signaling; 1:1000), anti-β-actin (Sigma-Aldrich; 1:500). Membranes were incubated overnight at 4 °C with gentle shaking. The secondary antibody was a peroxidase-conjugated goat anti-mouse or -rabbit antibody (1:10,000; Dako Cytomation, USA). After washing the membrane three times in TBST buffer (10 min), the signals were detected using an enhanced chemiluminescence light-detecting kit (Super-Signal West Pico Chemiluminescent Substrate, Pierce, IL, USA), according to the manufacturer's instructions and exposed to an X-ray film (GE Healthcare Ltd., Amersham, UK). The protein band densities were analyzed and quantified with a Scientific Imaging Systems (Biophotonics Image J Analysis Software, USA). *β*-actin was used to confirm the equal loading and transfer of proteins.

5.2.11. Statistical analysis

The results were expressed as means ± Standard Error (SE). Data were evaluated with GraphPad Prism® Version 5.00 software. Differences between two groups were analyzed by the Student's *t*-test. Difference with $P < 0.05$ (*), $P < 0.01$ (**) or $P < 0.001$ (***) were considered statistically significant.

5.3. Results

5.3.1. *The AMTs 1-8 inhibit cell proliferation in human colon adenocarcinoma cells HT-29*

The AMTs usneoidone Z (**1**), 11-hydroxy-1′-*O*-methylamentadione (**2**), cystomexicone B (**3**), cystomexicone A (**4**), 6-*cis*-amentadione-1′-methyl ether (**5**), amentadione-1′-methyl ether (**6**), cystodione A (**7**), and cystodione B (**8**) (Figure 5.1) isolated from the alga *C. usneoides* have been investigated for their anticancer activity.

The ability of these compounds at different concentrations to inhibit the viability of cancer and non-cancer colon cells (HT-29 and CCD 841 CoN, respectively) was examined by the SRB assay. All compounds caused a dose-dependent decrease in cell survival for both, cancer and non-cancer cells, although at different extents (Figure 5.2).

Usneoidone Z (**1**) and 6-*cis*-amentadione-1′-methyl ether (**5**) showed the strongest growth inhibitory activity against colon cancer cells HT-29 (IC_{50} 8.81 and 7.83 µg/mL, respectively), while the effects of both compounds were much lower towards the normal colon cells CCD 841 CoN (IC_{50} 46.41 and 40.97 µg/mL, respectively) (Table 5.1).

The meroditerpenes **2**, **6**, **7**, and **8** also induced strong decreases of the viability of HT-29 cells, greater than those observed for CCD 841 CoN cells (IC_{50}, 9.14, 10.72, 14.00, and 9.14 µg/mL for HT-29 cells and IC_{50} 21.41, 48.38, >50, and 31.88 µg/mL for CCD 841 CoN cells, respectively).

Compounds **3** and **4** were the less cytotoxic towards both, the tumor and the normal cells.

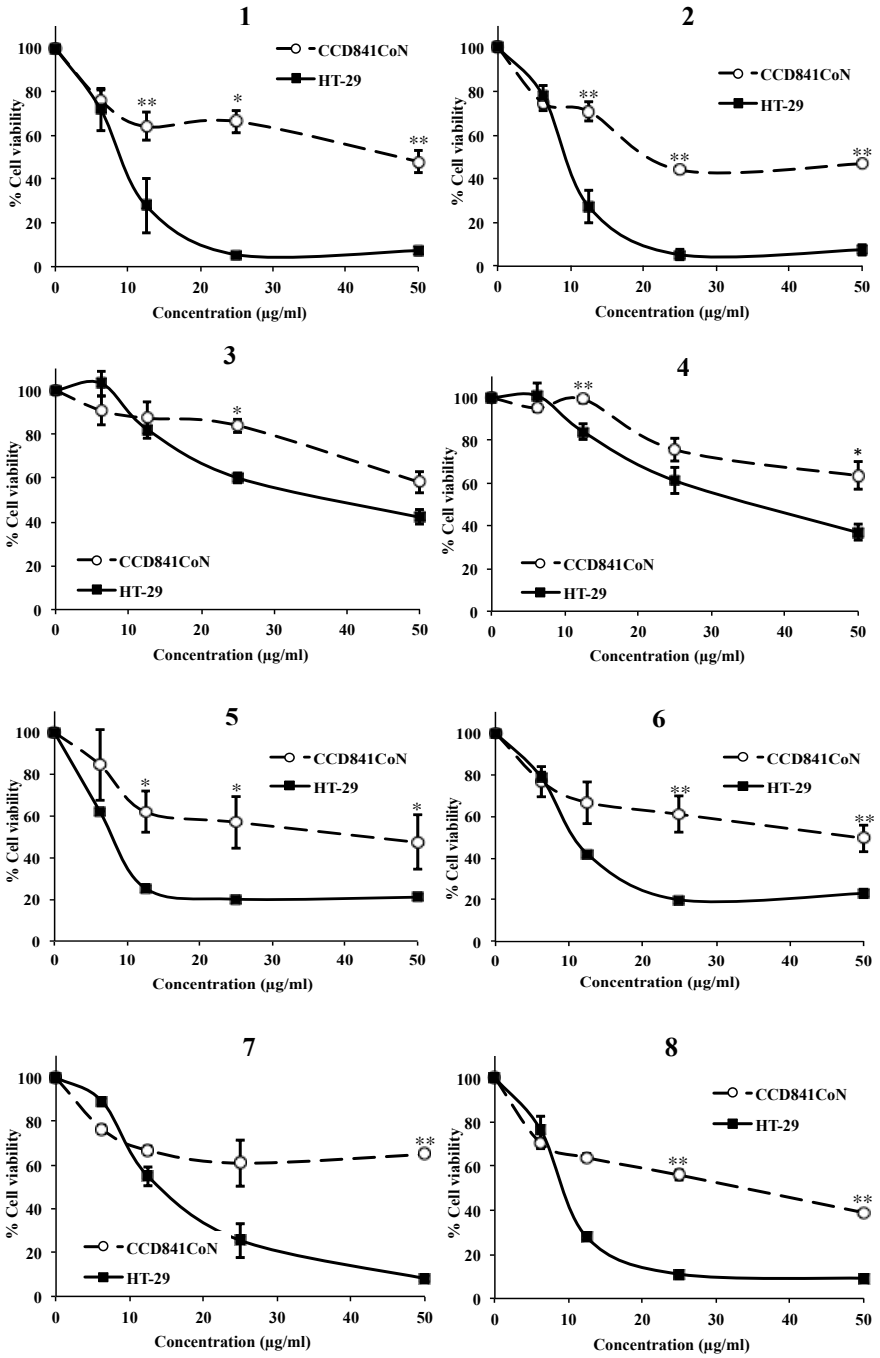

Figure 5.2. Effect of AMTs **1-8** at different concentrations on the viability of both HT-29 colon cancer cells and normal colonic epithelial cells CCD 841 CoN after 72 h of treatment. Results obtained by the SRB assay are reported as the percentage of viable cells (% cell viability). Data represent mean ± SE from three independent experiments. *$p<0.05$ and **$p<0.01$ compared with the untreated group.

Table. 5.1. IC_{50} values (μg/mL) obtained for AMTs **1**-**8** against the colon cancer cells HT-29 and the normal colon cells CCD 841 CoN after 72h of treatment (data are means ± SE of three experiments). SI = IC_{50} value for normal cells/ IC_{50} value for cancer cells.

Compound	Cell lines		Selectivity Index (SI)
	CCD 841 CoN	HT-29	
1	46.41±3.87	8.81±1.55	5.26
2	21.41±2.50	9.14±0.23	2.34
3	>50	34.34±1.81	>1.45
4	61.86±2.37	36.86±2.86	1.68
5	40.97±9.80	7.83±0.05	5.23
6	48.38±3.84	10.72±0.27	4.51
7	>50	14.00±1.33	>3.57
8	31.88±7.51	9,08±1.04	3.51

According to the literature, compounds with selectivity index (SI) values greater than 3 are considered highly selective (Bézivin et al., 2003), although other authors consider that compounds with a SI higher than or equal to 2.0 are also interesting (Suffness and Pezzuto, 1990). Treatments with the AMTs **1** and **5** afforded selectivity indexes higher that 5 (SI=5.26 and 5.23, respectively), indicating that these compounds are five times more toxic towards the cancer cells than towards the non-cancer cells (Table 5.1). The AMTs **6**, **7**, and **8** were also highly selective for cancer cells, affording SI higher than 3 (4.51, >3.57, and 3.51, respectively). However, the selectivity index observed for **2**, **3**, and **4** were more moderated (2.34, >1.45, and 1.68, respectively).

5.3.2. The AMTs 11-hydroxy-1'-O-methylamentadione (2), cystomexicone B (3), and 6-cis-amentadione-1'-methyl ether (*5) induce apoptosis of HT-29 colon cancer cells*

Flow cytometry analysis by annexin V/PI staining was performed in order to investigate the induction of apoptosis in HT-29 cells by AMTs **1**-**8**. Compounds **1**, **2**, **5**, **6**, **7**, and **8** were tested at concentrations of 10, 20, and 30 μg/mL, and compounds **3** and **4** were

tested at 30, 60, and 90 μg/mL. The percentages of viable, early apoptotic, late apoptotic, and necrotic cells after 24 h of treatment with the AMTs **1-8** are shown in Figure 5.3.

Significant differences were observed between control and treated cells. As shown in Figure 5.3A, after 24 h 89.34% of vehicle alone-treated HT-29 cells were viable (Annexin V-PI-), 0.18% were early apoptotic cells (Annexin V+PI-) and 0.22% were late apoptotic (Annexin V+PI+). In contrast, HT-29 cells treated for 24 h with cystomexicone B (**3**), showed a progressive induction of the apoptosis process, with a significant increase at the dose of 90 μg/mL, both in the early (4.47%) and in the late (52.12%) apoptotic cells (total percentage of apoptotic cells, 56.6%). The AMT **2** also caused significant, although more moderated, apoptotic effect (57.7% of viable cells, 1.94 % early apoptotic, and 12.94 % late apoptotic). (Figure 5.3B). Compound **5** induced a percentage of apoptosis similar to **2**, but the most prominent effect was necrosis (72.75%).

In this line, although cell growth was not affected by the AMTs **1**, **6**, and **8** at concentrations up to 20 μg/mL, at the higher concentration of 30 μg/mL a strong necrotic effect was detected, with 31.22, 59.55 and 20.12 % of dead cells, respectively. After 24 h of treatment, the AMTs **4** and **7** did not induce neither apoptosis nor death of HT-29 cells.

5.3.3. Effects of the meroterpenoids 1-8 on cell cycle arrest in HT-29 cells

In an attempt to explore the effects of the AMTs **1-8** on the cell cycle progression of colon carcinoma cells HT-29, the cell cycle was analyzed by flow cytometry. The effects of increasing concentrations of usneoidone Z (**1**) on HT-29 cell progression through G0/G1-, S- and G2/M-phases are shown in Figure 5.4A. This compound was the most active among the tested AMTs and increasing concentrations (10, 20, 30 μg/mL) resulted both in a significant cell cycle arrest in the G2/M ($p<0.01$) and in the reduction of the number of cells in the G0/G1 phase ($p<0.01$).

The accumulation of cells at the G2/M phase was also significant with the AMTs **2**, **3**, **4**, **5** and **7** ($p<0.05$) and it was correlated with a subsequent significant decrease of cells in the G0/G1-phase (Figure 5.4B). Compounds **6** and **8** showed the same tendency in cell cycle progression but the changes were no significant.

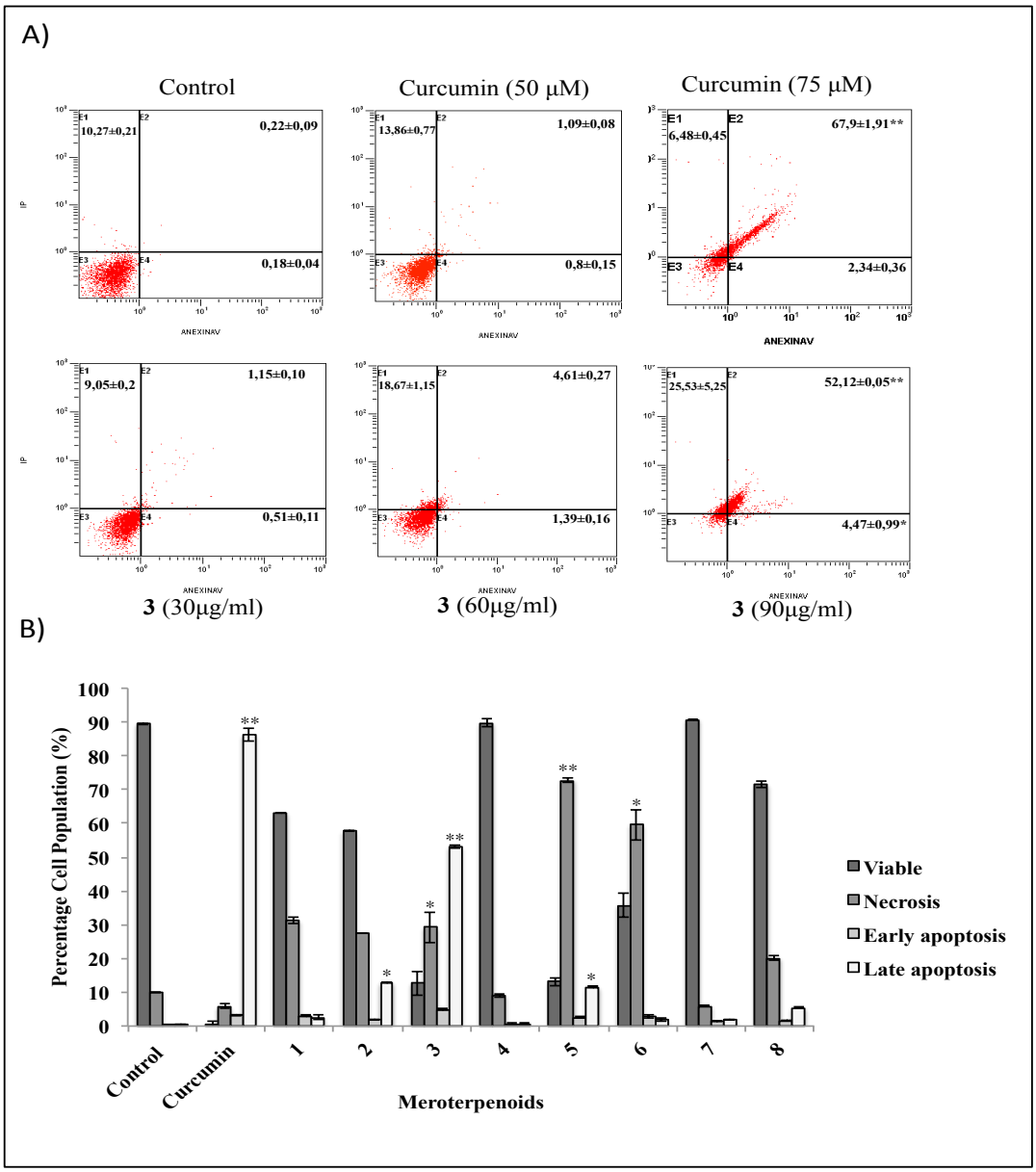

Figure 5.3. Apoptosis rates by flow cytometry of HT-29 colon cancer cells treated with the AMTs **1**-**8** for 24 h. Negative control cells received no treatment. Positive control received 50 and 75 µM of curcumin. **(A)** Flow cytometry histograms show the percentage of HT-29 cells treated with 30, 60, and 90 µg/mL of **3** undergoing early and late apoptosis. **(B)** Bar charts illustrate the percentage of viable, necrotic, early, and late apoptosis cells treated for 24 h with 30 µg/mL of **1**, **2**, **5**, **6**, **7** and **8**, and 90 µg/mL of **3** and **4**. Data represent mean ± SE from three independent experiments. Significant differences from control group: *p<0.05, and **p<0.01.

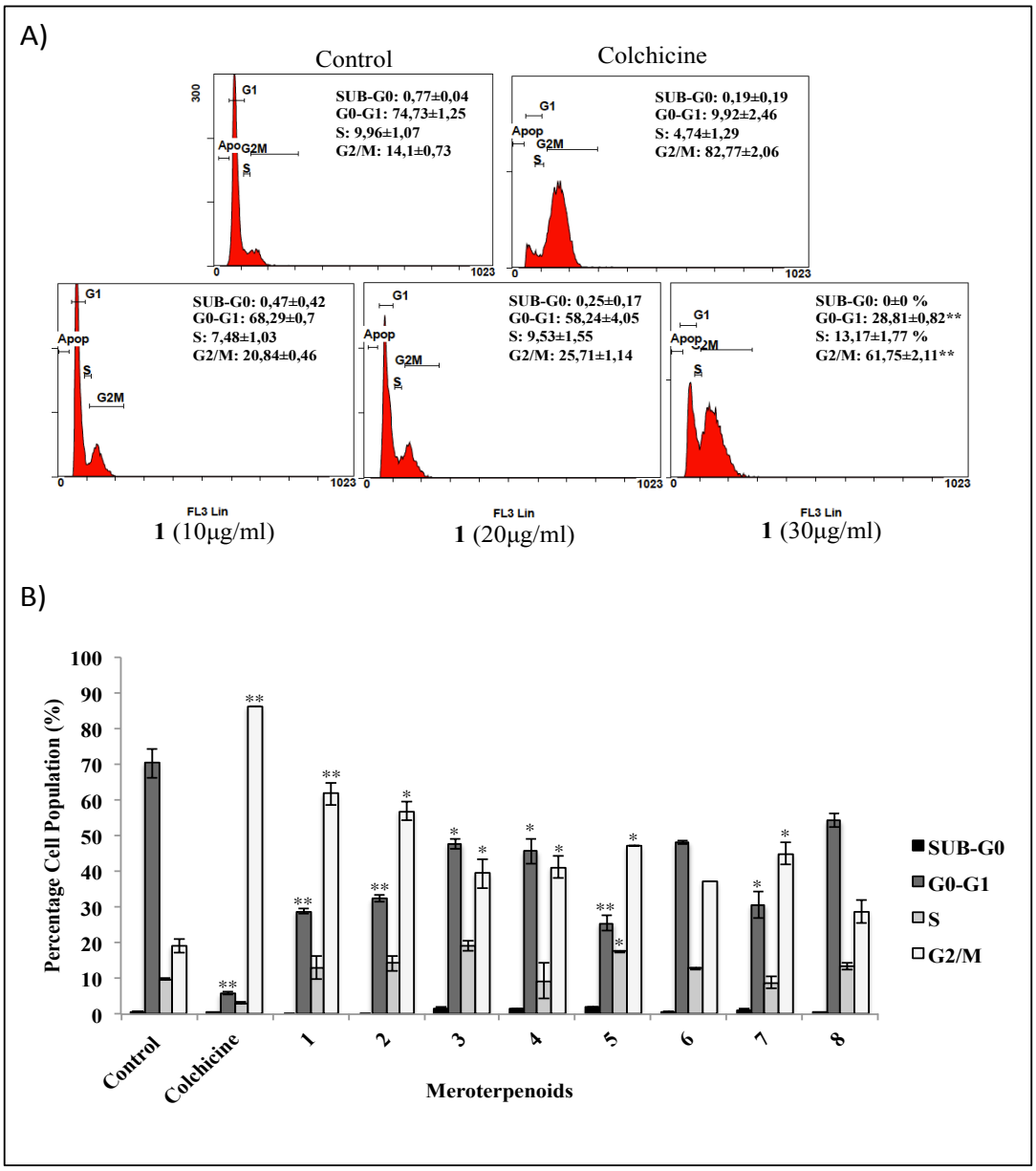

Figure 5.4. Flow cytometry analysis of cell cycle arrest in colon cancer cells HT-29 treated for 24 h with the AMTs **1**-**8**. Negative control cells received no treatment. Positive control received 0.2 µg/mL of colchicine. **(A)** Flow cytometry histograms showing HT-29 cells treated with 10, 20, and 30 µg/mL of compound **1**. **(B)** Bar charts for HT-29 cells treated with 30 µg/mL of **1**, **2**, **5**, **6**, **7,** and **8**, and 90 µg/mL of **3,** and **4**. Data represent mean ± SE from three independent experiments. Significant differences to control group: *p<0.05, and **p<0.01.

5.3.4. Effects of the AMTs 1-8 on the migration and invasion of HT-29 cells

Cell migration is a measure of the metastatic potential of cancer cells. To examine whether the AMTs **1-8** had any inhibitory effect on cell migration process, HT-29 cells were incubated for 24 h in the absence or presence of the compounds (10 μg/mL) in a wound-healing assay (Figure 5.5).

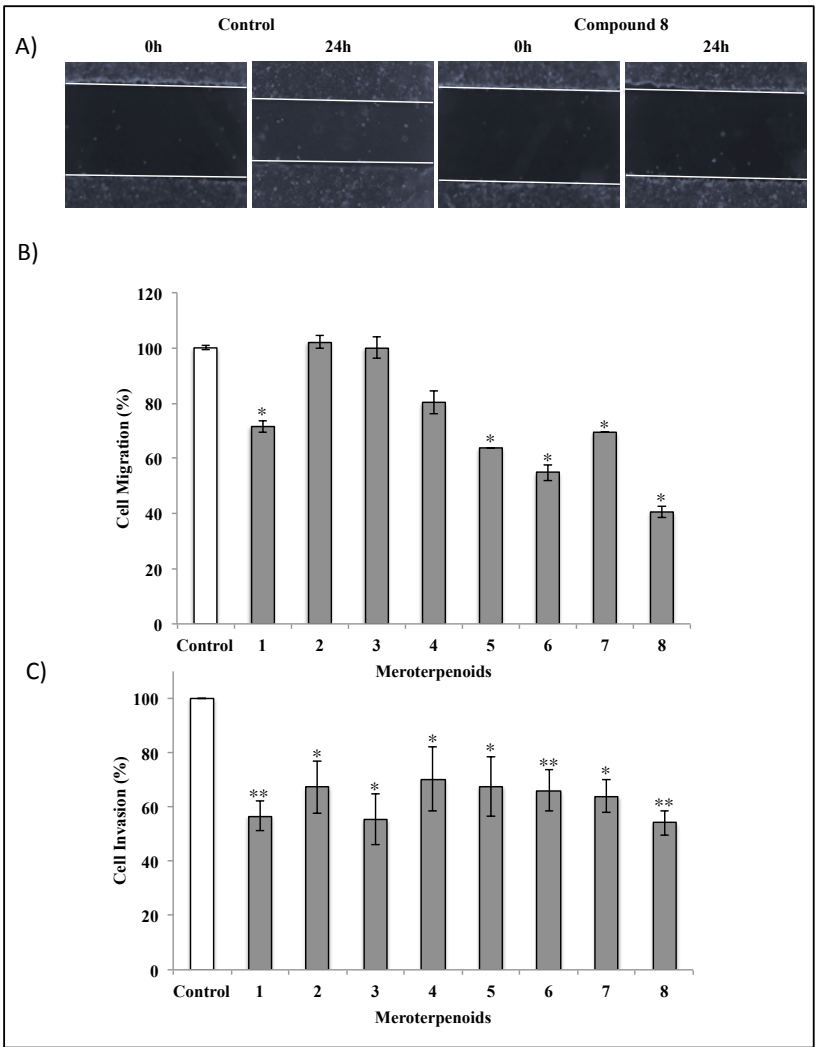

Figure 5.5. Effects of AMTs **1-8** on migration and invasion of HT-29 cells. **(A)** Seeded colon cancer cells in 6-well plates were wounded and imaged (0h). Untreated HT-29 cells and cells treated with compound **8** (10 μg/mL) were incubated for 24 h. **(B)** Bar charts show the percentage of migrated HT-29 cells after treatment for 24 h with **1**, **2**, **5**, **6**, **7**, and **8** at 10 μg/mL and with **3** and **4** at 30 μg/mL. **(C)** Anti-invasive activity of AMTs against HT-29 cells measured using a Cultrex assay kit. HT-29 cells were untreated or treated for 24 h with the AMTs (10 μg/mL for **1**, **2**, **5**, **6**, **7,** and **8**, and 30 μg/mL for **3,** and **4**). The data represent the means ± SE of three independent experiments. Significant differences to control group: *$p<0.05$ and **$p<0.01$.

According to the quantitative assessment, cystodione B (**8**) was the most active (Figure 5.5), causing at 10 µg/mL 59.1% inhibition of cell migration after 24 h ($p<0.05$).

As shown in Figure 5.5B, HT-29 cell migration to the wounded area was also significantly inhibited by 28.42%, 36.19%, 45.26% and 30.72% ($p<0.05$) in the presence of 10 µg/mL of compounds **1**, **5**, **6**, and **7**, respectively. However, compounds **2, 3**, and **4** showed no significant effects on cells migration. Overall, these data demonstrated that most of the merterpenoids of *C. usneoides* have significant inhibitory effects on the migration of HT-29 cells.

Another important characteristic of metastasis is the invasive ability of cancer cells. To determine the inhibitory effect of the AMTs **1-8** on the invasion of HT-29 cells, we used Cultrex® 96 well basement membrane extract (BME) cell invasion assay kit. The range of inhibition caused by the AMTs at 10 µg/mL was 30-45% (Figure 5C) when cells were incubated for 24 h. Among the tested compounds, usneoidone Z (**1**), cystomexicone B (**3**), and cystodione B (**8**), were the most active inhibiting cell invasion by more than 40% ($p<0.01$ for compounds **1** and **8**, and $p<0.05$ for compound **3**). These results demonstrated that all the tested AMTs can directly inhibit the invasive potential of colon cancer cells, thus indicating the interesting anticancer potential of these NPs.

5.3.5. The AMTs 1-8 inhibit phosphorylation of ERK, JNK and AKT

Since the previous findings showed that the AMTs **1-8** significantly inhibit migration and/or invasion of HT-29 cells, the underlying mechanism was further investigated, in particular the cell signaling pathways. Various studies suggest that MAPKs (ERK 1/2, JNK 1/2, and p38) and AKT are important players in cancer cell migration and invasion (Chen et al., 2005; Turner et al., 2007). In view of this evidence, the effects of the AMTs **1-8** on the phosphorylation of ERK1/2, JNK, and AKT were examined on HT-29 cells. The cancer cells were treated for 24 h with various concentrations of the AMTs and the phosphorylation of ERK1/2, JNK, and AKT were measured by western blot analysis.

The compounds **1**, **2**, **5**, **6**, **7**, and **8** significantly reduced the p-ERK1/2 (Figure 5.6) with the maximum inhibitory effect observed in cells treated with **5** and **8** at the highest concentration (20 µg/mL).

As shown in Figure 5.7, all the tested AMTs, except for the meroditerpenes **1** and **6**, significantly inhibited phospho-JNK, and the compound that had the maximum inhibitory effect was **4** at the highest concentration (60 μg/mL).

The data also showed that the expression of p-AKT protein was significantly downregulated in cells treated with **1**, **2**, **3**, **4**, **7**, and **8** (Figure 5.8), and there was no significant reduction of p-AKT production on cells treated with the AMTs **5** and **6**.

Based on these results, the mechanism for the inhibition of the metastatic activity on HT29 cells caused by the AMTs **1-8** could be partly explained by inducing the suppressions of ERK1/2, JNK or AKT pathways.

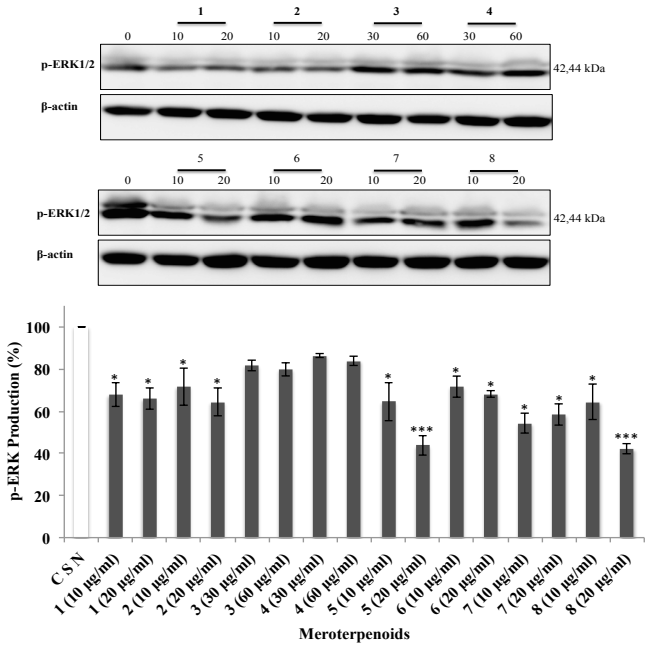

Figure 5.6. Effect of AMTs **1-8** on the activation of ERK by measuring the expression levels of the phosphorylated form (p-ERK) in HT-29 cells. The cells were treated for 24 h with the compounds (10 and 20 μg/mL for **1**, **2**, **5**, **6**, **7,** and **8**; 30 and 60 μg/mL for **3,** and **4**). The levels of p-ERK were measured by western blot analysis and quantified with an Image J analysis software. The data shown are the means ± SE of three independent experiments. Significant differences from control group: *p<0.05, **p<0.01 and, ***p<0.001.

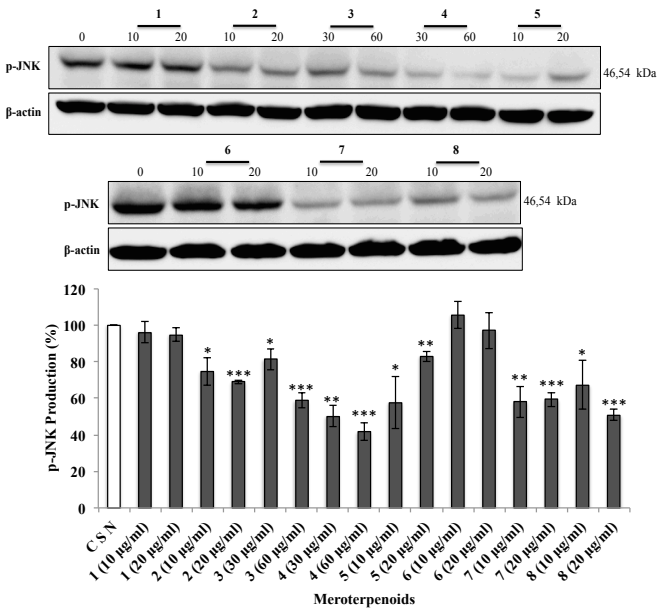

Figure 5.7. Effect of AMTs **1-8** on the activation of JNK by measuring expression levels of the phosphorylated form (p-JNK) in HT-29 cells. The cells were treated for 24 h with the compounds (10 and 20 μg/mL for **1**, **2**, **5**, **6**, **7,** and **8**; 30 and 60 μg/mL for **3,** and **4**). The levels of p-JNK were measured by western blot analysis and quantified with an Image J analysis software. The data shown are the means ± SE of three independent experiments. Significant differences from control group: *p<0.05, **p<0.01, and ***p<0.001.

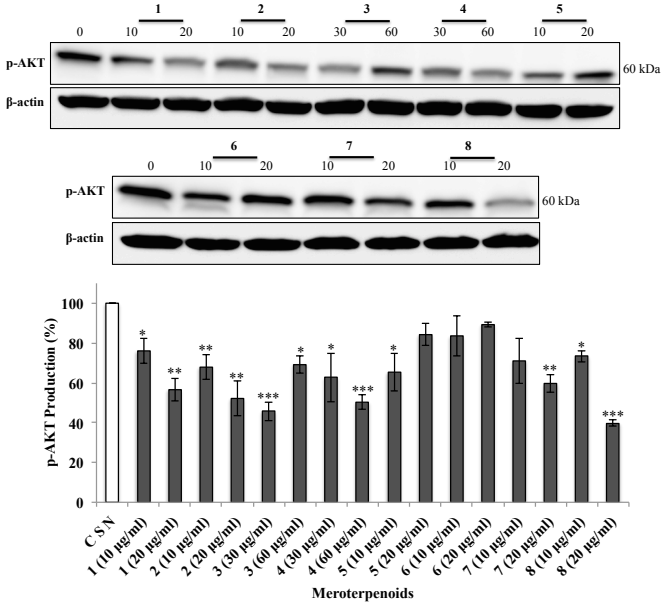

Figure 5.8. Effect of AMTs **1-8** on the activation of AKT by measuring expression levels of the phosphorylated form (p-AKT) in HT-29 cells. The cells were treated for 24 h with the compounds (10 and 20 μg/ml for **1**, **2**, **5**, **6**, **7** and **8**, and 30 and 60 μg/mL for **3** and **4)**. The levels of p-AKT were measured by western blot analysis and quantified with an Image J analysis software. The data shown are the means ± SE of three independent experiments. Significant difference from control group, *p<0.05, **p<0.01 and ***p<0.001.

5.4. Discussion

In this study various assays were used to investigate the antitumor effects on human colon HT-29 cells caused by eight AMTs isolated from the bioactive extract of the alga *C. usneoides*. We first determined that the AMTs **1**, **2**, **5**, **6**, **7**, and **8**, exhibited growth inhibitory activity against HT-29 cells with IC_{50} values in the range 7.8 to 14.0 μg/mL while compounds **3** and **4** were less potent (IC_{50} = 36.9 and 34.3 μg/mL, respectively). Interestingly, all the AMTs showed IC_{50} values significantly higher against the non-cancer cells CCD 841 CoN, with selectivity index of 5.26 for compound **1** and 5.23 for **5**. We have also investigated if the growth suppression induced by the AMTs **1**-**8** is mediated by apoptosis and cell cycle arrest. Our results showed that the compounds isolated from *C. usneoides* (except for **6** and **8**) induced significant anticancer effects against HT-29 cells through G2/M cell progression arrest, although only compounds **2, 3** and **5** produced apoptosis of the colon cancer cells. Moreover, we have shown the significant inhibitory effects of most of the tested AMTs on migration and invasion of the human colon cancer HT-29 cell line.

This is the first report on the antitumor activity of the AMTs **1-8** against colon cancer cells. Moreover, among the tested compounds, only there were previous antitumor data for usneoidone Z (**1)** (Urones et al. 1992). From the point of view of the structure-activity relationships the results of growth inhibition of HT-29 cells evidence the higher activity of compounds displaying a terpenoid chain of twenty carbon atoms (**1**, **2**, **5**, **6**, **7**, and **8**) upon comparison with those with a chain of fourteen carbon atoms (**3** and **4**). On the other hand, the similar IC_{50} values shown by compounds **1**, **2**, **5**, **6**, and **8** suggest that other structural features such as the configuration of the double bond at C-6, C-7 and the presence of an additional hydroxy group at C-3 or C-11, do not affect significantly to the growth inhibitory activity on HT-29 cells.

There are few previous data on the growth inhibitory activity of AMTs against colon cancer cells HT-29. In particular, it has recently been reported that the AMTs sargachromanols J (**Ss-16**) and R (**Ss-18**) (Figure 5.9), from the alga *Sargassum siliquastrum* (Lee et al., 2014), and zonaquinone acetate (**Sz-1**) (Figure 5.9), from *Stypopodium zonale* (Penicooke et al., 2013), inhibited the growth of HT-29 cells with IC_{50}

values of 29.3 μg/mL, 3.4 μg/mL, and 17.3 μM (7.8 μg/mL), respectively, which are comparable to those obtained in our study.

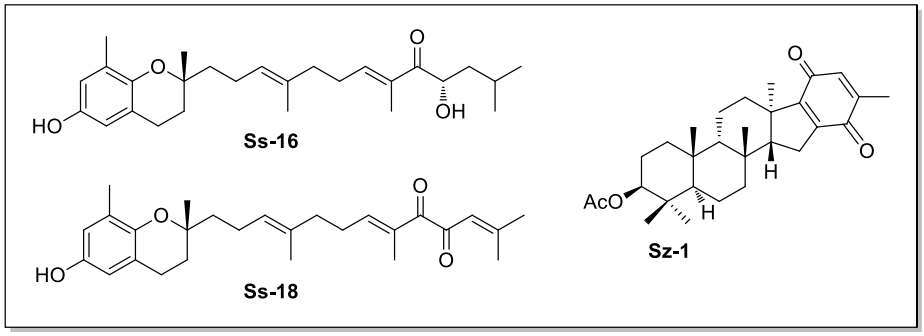

Figure 5.9. Chemical structures of AMTs previously reported to possess antitumor activity against HT-29 cells (Lee et al., 2014, Penicooke et al., 2013).

In our study, we were able to demonstrate that the antitumor activity of the meroterpene cystomexicone B (**3**) is exerted through induction of apoptosis. This finding was consistent with previous reports that demonstrated the apoptotic effects caused by various AMTs (Choi et al., 2017; Heo et al., 2011). In particular, the meroditerpene tuberatolide B (**Sm-1**) (Figure 5.10), isolated from the alga *Sargassum macrocarpum* (Choi et al., 2017), has been shown to inhibit the viability of various cancer cell lines, including breast cancer (MDA-MB-231), lung cancer (A549), and colon cancer (HCT116), by inducing apoptotic cell death, and sargachromanol E (**Ss-10**) (Figure 5.10), from *Sargassum siliquastrum*, has been reported to induce apoptosis in the colon cancer cell line HL-60 (Heo et al., 2011).

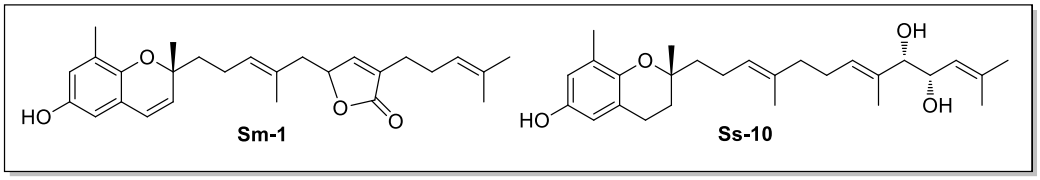

Figure 5.10. Chemical structures of the AMTs tuberatolide B (**Sm-1**) and sargachromanol E (**Ss-10**) previously reported to cause apoptosis in HCT-116 and HL-60 colon cancer cells, respectively (Choi et al., 2017; Heo et al., 2011).

On the other hand, in the last years a variety of algal terpenoids have been reported to induce apoptosis in several cancer cells, including HT-29 (Tarhouni-Jabberi et al., 2017), Jurkat leukemic cells (Cen-Pacheco et al., 2011), melanoma B16F10 cells (Velatooru et al., 2016; Campos et al., 2012), and human TNBC cells (Lakshmi et al., 2018).

Cancer is a complex pathology where the cells undergo different transformations, among which uncontrolled cell division stands out. Cell cycle deregulation is the hallmark of cancer progression and the control of the cell cycle helps to regulate cell growth. This is one of the most critical alterations during tumor progression and play an important role in apoptosis (Williams and Stoeber, 2012). The G2/M checkpoint is a known target for cell cycle inhibition (Dominguez-Brauer et al., 2015), which marks a barrier before entry into M phase (Palmer et Kaldis, 2016); in this way it is critical to prevent progression through mitosis when cells progress into G2 with an unrepaired DNA during the previous S or G1 phases, or when they possess incompletely replicated chromatin from S phase (Yang, 2012). A consequence is that cells with DNA damage can initiate an apoptotic program, that leads to the phenotypic manifestation of mitotic failed during the metaphase (Castedo et al., 2004). In this study, we have demonstrated that the growth inhibitory effect of the AMTs **1**, **2**, **3**, **4**, **5**, and **7** on HT-29 cancer cells is associated with a G2/M arrest and cell cycle progression. These results are in line with an earlier report that demonstrated that the algal halogenated monoterpene mertensene induced similar response with G2/M arrest from HT-29 cells (Tarhouni-Jabberi et al., 2017). However, other algal terpenes have been described to induce cell cycle arrest in G1 phase in different types of cell lines (Lakshmi et al., 2018; Campos et al., 2012).

Cancer metastasis is a leading cause of death in cancer patients. The migration and invasion of cancer cells allow them to detach from the primary tumor to the surrounding tissues and colonize the target organs (Hood and Cheresh, 2002). Interestingly, the present study has demonstrated that the treatment of cells with the AMTs **1**-**8** decreases migration and/or invasion of the colon cancer cells.

MAPK signaling pathway that consists of extracellular signal-related kinase 1 and 2 (ERK1/2), c-JUN N-terminal kinase/stress activated protein kinase (JNK/SAPK), and p38 (Kajanne et al., 2007), is involved in cell survival, cell-cycle progression, programmed cell

death, and metastasis of cancer cells (Go et al., 2011). In colorectal carcinoma, the MAPK pathway is aberrantly activated (Shan et al, 2009) and, therefore, the inhibition of this pathway is a potential therapeutic approach (Go et al., 2011).

It has been shown that the ERK promotes growth, differentiation, and proliferation of cancer cells (Jiang et al., 2018). It has also been reported that transient ERK activation might be linked to cellular proliferation while strong and persistent activation may lead to programmed cell death (Park et al., 2014). ERK promote either intrinsic or extrinsic apoptotic pathways by induction of mitochondrial cytochrome c release or caspase-8 activation (Cagnol and Chambard, 2010). ERK pathway not only participates in the regulation of apoptosis, but also controls G2/M cell cycle phase. ERK has been reported to regulate cyclin B1 transcriptional induction and also controls the assembly of cyclin-CDK complex via the CDK translocation (Li et al., 2008; Abrieu et al., 1997), which play pivotal roles in regulating cell cycle progression. Moreover, ERK1/2 regulates focal adhesion and cytoskeletal reorganization via the phosphorylations of specific cytoskeletal and focal adhesion proteins, including paxillin, FAK, and myosin light chain kinase, which are crucial signalling components to control cell migration, invasion, and cell cycle progression (Wu et al., 2008; Kuphal, 2005). In this study, we have examined the effect of compounds **1**-**8** on the ERK pathway. A decreased protein expression of phosphorylated ERK was observed in HT-29 cells treated with compounds **1**, **2**, **5**, **6**, **7**, and **8**, which support the crucial role of ERK in the regulation of proliferation, cycle progression, and metastasis processes in colon cancer cells.

Activation of JNK has been involved in the regulation of various cellular processes, including cell survival, proliferation, differentiation, and cell death (Tournier, 2013). However, few papers have been published regarding to the potential role of JNK in the cell cycle. Mingo-Sion et al., 2004 reported that the induced G2/M arrest may be due to the inability of some cells to sustain $p21^{Cip1/Waf1}$, a JNK substrate, in the absence of JNK activity. When $p21^{Cip1/Waf1}$ expression is increased in response to DNA damage, cyclin B/Cdk1 kinase activity is inhibited causing G2/M phases arrest (Bates et al., 1998). In this study, we have found that compounds **2**, **3**, **4**, **5**, and **7** inhibit cell proliferation through inducing a G2/M phase arrest in HT-29 cells via JNK pathway. Regarding to programed cell death, JNK play an active role in the regulation of both the intrinsic and extrinsic

apoptotic pathways (Dhanasekaran and Reddy, 2017). These findings suggest that p-JNK may be involved in the activation of cell apoptosis after the treatment with compound **3**.

JNK plays also a crucial role in cell migration and invasion. The oncogenic functions of JNK are particularly based on its ability to phosphorylate c-Jun and to activate transcriptional factor Activator Protein-1 (AP-1). Matrix metalloproteinases (MMPs), a key role for degrading the basement membrane, have an AP-1 consensus sequence that regulates tumour progression by enhancing tumour-induced angiogenesis and destroying local tissue architecture and basement membranes to allow tumor invasion and metastasis (Cai et al., 2017). The AMTs showing anti-migration (**5**, **7**, and **8**) and anti-invasion (**2**, **3**, **4**, **5**, **7**, and **8**) activities also decreased phosphorylation of JNK in colon cancer cells. suggesting that these compounds may have efficacy in the prevention of the metastasis of colon cancer cells.

Alteration of the PI-3K/AKT pathway has been detected during tumor formation in numerous cancers, including colorectal cancer (Jung et al., 2017). Many studies have reported that PI3K activation stimulates the downstream target AKT, which plays various and important roles in regulating cell proliferation, cell cycle, apoptosis, and cell invasion (Shant et al., 2009; Hollborn, 2007; Chang et al., 2003). AKT pathway has been shown to be involved in the cell cycle progression by down-regulating Cdk1 and Cyclin B1 expression, both of which can ultimately lead to the arrest of G2/M transition (Hiraoka et al., 2016). On the other hand, AKT modulate apoptosis signaling by inducing expression of multiple pro-apoptotic members of the Bcl2-family of mitochondria-targeting proteins. These pro-apoptotic proteins translocate in the mitochondria leading to caspase activation thus leading to apoptosis (Agarwal et al., 2013). AKT is also known to regulate the expression of FAK (focal adhesion kinase) proteins mediating colorectal cancer metastasis. In response to extracellular pressure, AKT and FAK bind directly, thus phosphorylating AKT at three serine residues. The phosphorylation of the three serine residues consequently phosphorylate the tyrosine residue (Tyr397) thus activating it. It therefore induces cell adhesion by increasing the binding of integrins to matrix, which finally lead to increased metastasis (Wang and Basson, 2011). Hence, inhibiting AKT may be an important therapeutic target for regulating cell cycle progression, apoptosis, and preventing cancer metastasis. In the present study, we have found that the AMTs **1**, **2**, **3**, **4**, **7**, and **8** reduce the

protein levels of p-AKT in HT-29 cells, indicating the role of these AMTs in the down-regulation of proliferation, cell cycle, apoptosis, and metastasis in colon cancer cells through the regulation of MAPK and AKT pathways. These results are in line with a previous study where the algal halogenated monoterpene mertensene was shown to induce G2/M cell cycle arrest and apoptosis in human colon adenocarcinoma HT-29, through the modulation of ERK-1/-2 and AKT signaling (Tarhouni-Jabberi et al., 2017). Nonetheless, some studies on the mechanism of action of other algal terpenoids have also demonstrated the intervention of other signaling pathways. For example, the sesquiterpene guai-2-en-10α-ol, from *Ulva fasciata,* was reported to induce apoptosis and cell cycle arrest in G1 phase of triple-negative breast cancer (TNBC) cell line (MDA MB-231) via regulation of EGFR/PI3 K/Akt pathway (Lakshmi et al., 2018) and laurinterol, from *Laurencia okamurae*, showed anticancer activity against melanoma cells (B16F1) through the p53-dependent pathway (Kim et al., 2008).

5.5. Conclusion

In summary, the present study demonstrates for the first time that various AMTs obtained from the alga *C. usneoides* inhibit *in vitro* the proliferation of colon cancer cells, while being significantly less cytotoxic against normal cells, induce cell cycle arrest, and decrease migration and invasion of HT-29 cells. Moreover, with cystomexicone B (**3**), apoptosis in HT-29 cells was detected. Our results provide proof that the tested AMTs promote strong anticancer effects through down-regulation of signaling pathways by ERK, JNK, and/or AKT. On the basis of the activity observed for the AMTs **1**, **2**, **5**, **7** and **8** in most of the assays performed in this study, these AMTs could be promising as agents for the prevention and treatment of colon cancer, although the potential of these NPs to act as chemopreventive and therapeutic agents for colorectal carcinomas needs to be previously evaluated in animal models.

5.6. References

Abrieu, A.; Fisher, D.; Simon, M.N.; Doree, M.; Picard, A. MAPK inactivation is required for the G2 to M-phase transition of the first mitotic cell cycle. *EMBO J.* **1997**, *16*, 6407–6413.

Agarwal, E.; Brattain, M.G.; Chowdhury, S. Cell survival and metastasis regulation by akt signalling in colorectal cancer. *Cell Signal.* **2013**, *25*, 1711–1719.

Amico, V. Marine brown algae of family Cystoseiraceae: Chemistry and chemotaxonomy. *Phytochemistry* **1995**, *39*, 1257−1279.

Atanasov, A.G.; Waltenberger, B.; Pferschy-Wenzig, E.M.; Linder, T.; Wawrosch, C.; Uhrin, P.; Temml, V.; Wang, L.; Schwaiger, S.; Heiss, E.H.; Rollinger, J.M.; Schuster, D.; Breuss, J.M.; Bochkov, V.; Mihovilovic, M.D.; Kopp, B.; Bauer, R.; Dirsch, V.M.; Stuppner, H. Discovery and resupply of pharmacologically active plant-derived natural products: A review. *Biotechnol. Adv.* **2015**, *33*, 1582–1614.

Bates, S.; Ryan, K.M.; Phillips, A.C.; Vousden, K.H. Cell cycle arrest and DNA endoreduplication following p21Waf1/Cip1 expression. *Oncogene* **1998,** *17*, 1691–1703.

Bézivin, C.; Tomasi, F.; Lohézie-Le, D.; Boustie, J. Cytotoxic activity of some lichen extracts on murine and human cancer cell lines. *Phytomedicine* **2003**, *10*, 499–503.

Cagnol, S.; Chambard, J.C. ERK and cell death: mechanisms of ERK-induced cell death--apoptosis, autophagy and senescence. *FEBS J.* **2010**, *277*, 2–21.

Cai, J.; Du, S.; Wang, H.; Xin, B.; Wang, J.; Shen, W.; Wei, W.; Guo, Z.; Shen, X.; Tenascin-C induces migration and invasion through JNK/c-Jun signalling in pancreatic cancer. *Oncotarget* **2017**, *8*, 74406–74422.

Campos, A.; Souza, C.B.; Lhullier, C.; Falkenberg, M.; Schenkel, E.P.; Ribeiro-do-Valle, R.M.; Siqueira, J.M. Anti-tumour effects of elatol, a marine derivative compound obtained from red algae *Laurencia microcladia*. *J. Pharm. Pharmacol.* **2012**, *64*, 1146-1154.

Castedo, M.; Perfettini, J.L.; Roumier, T.; Andreau, K.; Medema, R.; Kroemer, G. Cell death by mitotic catastrophe: a molecular definition. *Oncogene* **2004**, *23*, 2825–2837.

Cen-Pacheco, F.; Villa-Pulgarin, J.A.; Mollinedo, F.; Martín, M.N.; Fernández, J.J.; Daranas, A.H. New polyether triterpenoids from *Laurencia viridis* and their biological evaluation. *Mar. Drugs* **2011**, *9*, 2220–2235.

Chang, F.; Lee, J.T.; Navolanic, P.M.; Steelman, L.S.; Shelton, J.G.; Blalock, W.L.; Franklin, R.A.; McCubrey, J.A. Involvement of PI3K/Akt pathway in cell cycle progression, apoptosis, and neoplastic transformation: a target for cancer chemotherapy. *Leukemia* **2003**, *17*, 590–603.

Chen, P.N.; Hsieh, Y.S.; Chiou, H.L.; Chu, S.C. Silibinin inhibits cell invasion through inactivation of both PI3K-Akt and MAPK signaling pathways. *Chem. Biol. Interact*. **2005**, *156*, 141–150.

Choi, Y.K.; Kim, J.; Lee, K.M.; Choi, Y.J.; Ye, B.R.; Kim, M.S.; Ko, S.G.; Lee, S.H.; Kang, D.H.; Heo, S.J. Tuberatolide B Suppresses Cancer Progression by Promoting ROS-Mediated Inhibition of STAT3 Signaling. *Mar. Drugs* **2017,** *15*, pii: E55.

Cragg, G.M.; Newman, D.J. Natural products: a continuing source of novel drug leads. *Biochim. Biophys. Acta* **2013**, *1830*, 3670–3695.

De los Reyes, C.; Zbakh, H.; Motilva, V.; Zubía, E. Antioxidant and anti-inflammatory meroterpenoids from the brown alga *Cystoseira usneoides*. *J. Nat. Prod*. **2013**, *76*, 621−629.

Dhanasekaran, D.N.; Reddy, E.P. JNK-signaling: A multiplexing hub in programmed cell death. *Genes Cancer* **2017**, *8*, 682–694.

Dominguez-Brauer, C.T.; Thu, K.L.; Mason, J.M.; Blaser, H.; Bray, M.R.; Mak, T.W. Targeting mitosis in cancer: Emerging strategies. *Mol. Cell.* **2015**, *60*, 524–536.

Ferlay, J.; Soerjomataram, I.; Dikshit, R. et al. Cancer incidence and mortality worldwide: Sources, methods and major patterns in GLOBOCAN 2012. *Int. J. Cancer* **2015**, *136*, 359–386.

Go, H.; Hwang, H.J.; Kim, I.H.; Nam, T.J. Anoikis induction by glycoprotein from *Laminaria japonica* in HT-29 cells. *Prev. Med.* **2011**, *1*, 49−61.

Gouveia, V.; Seca, A.M.L.; Barreto, M.C.; Pinto, D.C.G.A. Di- and sesquiterpenoids from *Cystoseira* genus: Structure, intra-molecular transformations and biological activity. *Mini-Rev. Med. Chem.* **2013a**, *13*, 1150−1159.

Gouveia, V.L.M.; Seca, A.M.L.; Barreto, M.C.; Neto, A.I.; Kijjoa, A.; Silva, A.M.S. Cytotoxic meroterpenoids from the macroalga *Cystoseira abies-marina*. *Phytochemistry Lett.* **2013b**, *6*, 593–597.

Greiner, A.K.; Papineni, R.V.; Umar, S. Chemoprevention in gastrointestinal physiology and disease. Natural products and microbiome. *Am. J. Physiol Gastrointest. Liver Physiol*. **2014**, *307*, 1–15.

Heo, S.J.; Kim, K.N.; Yoon, W.J.; Oh, C.; Choi, Y.U.; Affan, A.; Lee, Y.J.; Lee, H.S.; Kang, D.H. Chromene induces apoptosis via caspase-3 activation in human leukemia HL-60 cells. *Food Chem. Toxicol*. **2011**, *49*, 1998–2004.

Hiraoka, D.; Aono, R.; Hanada, S.; Okumura, E.; Kishimoto, T. Two new competing pathways establish the threshold for cyclin-B–Cdk1 activation at the meiotic G2/M transition. *J. Cell. Sci.* **2016**, *129*, 3153–3166.

Hollborn, M.; Stathopoulos, C.; Steffen, A.; Wiedemann, P.; Kohen, L.; Bringmann, A. Positive feedback regulation between MMP-9 and VEGF in human RPE cells. *Invest. Ophthalmol. Vis. Sci.* **2007**, *48*, 4360–4367.

Hood, J.D.; Cheresh, D.A. Role of integrins in cell invasion and migration. *Nat. Rev. Cancer* **2002**, *2*, 91–100.

Huang, M.; Lu, J.J.; Huang, M.Q.; Bao, J.L.; Chen, X.P.; Wang, Y.T. Terpenoids: Natural products for cancer therapy. *Expert Opin. Investig. Drugs* **2012**, *21*, 1801−1818.

Jiang, H.; Zhu, Y.; Zhou, Z.; Xu, J.; Jin, S.; Xu, K.; Zhang, H.; Sun, Q.; Wang, J.; Xu J. PRMT5 promotes cell proliferation by inhibiting BTG2 expression via the ERK signaling pathway in hepatocellular carcinoma. *Cancer Med.* **2018***, 7,* 869–882.

Jung, S.K.; Jeong, C.H. Dehydroglyasperin D inhibits the proliferation of HT-29 human colorectal cancer cells through direct interaction with phosphatidylinositol 3-kinase. *J. Cancer Prev.* **2016**, *21*, 26–31.

Kajanne, R.; Miettinen, P.; Mehlem, A.; Leivonen, S.K.; Birrer, M.; et al. EGFR regulates MMP function in fibroblasts through MAPK and AP-1 pathways. *J. Cell Physiol*. **2007**, *212*, 489–497.

Kavousipour, S.; Khademi, F.; Zamani, M.; Vakili, B.; Mokarram, P. Novel biotechnology approaches in colorectal cancer diagnosis and therapy. *Biotechnol. Lett.* **2017,** *39*, 785–803.

Kim, M.M.; Mendis, E.; Kim, S.K. *Laurencia okamurai* extract containing laurinterol induces apoptosis in melanoma cells. *J. Med. Chem*. **2008**, *11*, 260–266.

Kuphal, S.; Bauer, R.; Bosserhoff, A.K. Integrin signaling in malignant melanoma. *Cancer Metastasis Rev.* **2005**, *24*, 195−222.

Lakshmi, P.T.; Vajravijayan, S.; Moumita, M.; Sakthivel, N.; Gunasekaran, K.; Krishna, R. A novel guaiane sesquiterpene derivative, guai-2-en-10α-ol, from *Ulva fasciata* Delile inhibits EGFR/PI3K/Akt signaling and induces cytotoxicity in triple-negative breast cancer cells. *Mol. Cell Biochem.* **2018**, *438*,123–139.

Leal, M.C.; Munro, M.H.G.; Blunt, J.W.; Puga, J.; Jesus, B.; Calado, R.; Rosa, R.; Madeira, C. Biogeography and biodiscovery hotspots of macroalgal marine natural products. *Nat. Prod. Rep*. **2013**, *30*, 1380–1390.

Lee, J.I.; Park, B.J.; Kim, H.; Seo, Y. Isolation of Two New Meroterpenoids from *Sargassum siliquastrum*. *Bull. Korean Chem. Soc.* **2014**, *35*, 2867–2869.

Li, Z.; Li, J.; Mo, B.; Hu, C.; Liu, H.; Qi, H.; Wang, X.; Xu, J. Genistein induces G2/M cell cycle arrest via stable activation of ERK1/2 pathway in MDA-MB-231 breast cancer cells. *Cell. Biol. Toxicol.* **2008**, *24*, 401–409.

Lisiak, N.; Paszel-Jaworska, A.; Totoń, E.; Rubiś, B.; Pakuła, M.; Bednarczyk-Cwynar, B.; Zaprutko, L.; Rybczyńska, M. Semisynthetic oleanane triterpenoids inhibit migration and invasion of human breast cancer cells through downregulated expression of the ITGB1/PTK2/PXN pathway. *Chem. Biol. Interact*. **2017,** *268*, 136–147.

Mayer, R.J. Targeted therapy for advanced colorectal cancer–more is not always better. *New Engl. J. Med*. **2009**, *360*, 623–625.

Mingo-Sion, A.M.; Marietta, P.M.; Koller, E.; Wolf, D.M.; Van Den Berg, C.L. Inhibition of JNK reduces G2/M transit independent of p53, leading to endoreduplication, decreased proliferation, and apoptosis in breast cancer cells. *Oncogene* **2004**, *23*, 596–604.

Moghadamtousi, S.Z; Karimian, H.; Rouhollahi, E.; Paydar, A.; Fadaeinasab, M.; AbdulKadi, H. *Annona muricata* leaves induce G1 cell cycle arrest and apoptosis through mitochondria-mediated pathway in human HCT-116 and HT-29 colon cancer cells. *J. Ethnopharmacol.* **2014**, *156*, 277–289.

Newman, D.J.; Cragg, G.M. Marine-sourced anti-cancer and cancer pain control agents in clinical and late preclinical development. *Mar. Drugs* **2014**, *12*, 255-278

Newman, D.J.; Cragg, G.M. Natural products as sources of new drugs from 1981 to 2014. *J. Nat. Prod.* **2016**, *79*, 629-661.

Nicoletti, I.; Migliorati, G.; Pagliacci, M.; Grignani, F.; Riccardi, C. A rapid and simple method for measuring thymocyte apoptosis by propidium iodide staining and flow cytometry. *J. Immunol. Methods.* **1991**, *139*, 271–279.

Palmer, N.; Kaldis, P. Chapter One - Regulation of the Embryonic Cell Cycle During Mammalian Preimplantation Development. *Curr. Top. Dev. Biol*. **2016**, 120, 1–53.

Park, J.I. Growth arrest signaling of the Raf/MEK/ERK pathway in cancer. *Front. Biol. (Beijing)* **2014**, *9*, 95–103.

Penicooke, N.; Walford, K.; Badal, S.; Delgoda, R.; Williams, L.A.D.; Joseph-Nathan, P.; Gordillo-Román, B.; Gallimore, W. Antiproliferative activity and absolute configuration of zonaquinone acetate from the Jamaican alga *Stypopodium zonale*. *Phytochemistry* **2013**, *87*, 96–101.

Rocha, D.H.A.; Seca, A.M.L.; Pinto, D.C.G.A. Seaweed secondary metabolites in vitro and in vivo anticancer activity. *Mar. Drugs* **2018**, *16*, 410.

Ruiz-Torres, V.; Encinar, J.A.; Herranz-López, M.; Pérez-Sánchez, A.; Galiano, V.; Barrajón-Catalán, E.; Micol, V. An updated review on marine anticancer compounds: the use of virtual screening for the discovery of small-molecule cancer drugs. *Molecules* **2017**, *22*, article 1037; doi:10.3390/molecules22071037.

Shan, J.Z.; Xuan, Y.Y.; Zheng, S.; Dong, Q.; Zhang, S.Z. Ursolic acid inhibits proliferation and induces apoptosis of HT-29 colon cancer cells by inhibiting the EGFR/MAPK pathway. *J. Zhejiang Univ. Sci. B.* **2009**, *10*, 668−674.

Shant, J.; Cheng, K.; Marasa, B.S; Wang, J.Y.; Raufman, J.P. Akt-dependent NF-kappaB activation is required for bile acids to rescue colon cancer cells from stress-induced apoptosis. *Exp. Cell Res.* **2009**, *315*, 432–450.

Skehan, P.; Storeng, R.; Scudiero, D.; Monks, A.; McMahon, J.; Vistica, D.; Warren, J. T.; Bokesch, H.; Kenney, S.; Boyd, M.R.J. New colorimetric cytotoxicity assay for anticancer-drug screening. *J. Natl. Cancer Inst.* **1990**, *82*, 1107−1112.

Suffness, M.; Pezzuto, J.M. Assays related to cancer drug discovery. In: *Methods in Plant Biochemistry: Assays for Bioactivity*, Hostettmann, K. (Ed.), Academic Press: London,

1990; pp. 71–133.

Sunasee, S.N.; Davies-Coleman, M.T. Cytotoxic and antioxidant marine prenylated quinones and hydroquinones. *Nat. Prod. Rep.* **2012**, *29*, 513-535.

Tarhouni-Jabberi, S.; Zakraoui, O.; Ioannou, E.; Riahi-Chebbi, I.; Haoues, M.; Roussis, V.; Kharrat, R.; Essafi-Benkhadir, K. Mertensene, a halogenated monoterpene, induces G2/M cell cycle arrest and caspase dependent apoptosis of human colon adenocarcinoma HT29 cell line through the modulation of ERK-1/-2, AKT and NF-κB signaling. *Mar. Drugs* **2017**, *15*, E221. doi: 10.3390/md15070221.

Tournier, K. The 2 Faces of JNK signaling in cancer. *Genes & Cancer* **2013**, *4*, 397–400.

Turner, N.A.; Aley, P.K.; Hall, K.T.; Warburton, P.; Galloway, S.; Midgley, L.; O'regan, D.J.; Wood, I.C.; Ball, S.G.; Porter, K.E. Simvastatin inhibits TNF-α induced invasion of human cardiac myofibroblasts via both MMP-9-dependent and -independent mechanisms. *J. Mol. Cell Cardio*. **2007**, *43*, 168–176.

Urones, J.G.; Basabe, P.; Marcos, I.S.; Pineda, J.; Lithgow, A.M.; Moro, R.F.; Brito Palma, F.M.S.; Araujo, M.E.M.; Gravalos, M.D.G. Meroterpenes from *Cystoseira usneoides. Phytochemistry* **1992**, *31*, 179−182.

Valls, R.; Piovetti, L. The chemistry of the Cystoseiraceae (Fucales: Pheophyceae): Chemotaxonomic relationships. *Biochem. Syst. Ecol.* **1995**, *23*, 723−745.

Velatooru, L.R.; Baggu, C.B.; Janapala, V.R. Spatane diterpinoid from the brown algae, *Stoechospermum marginatum* induces apoptosis via ROS induced mitochondrial mediated caspase dependent pathway in murine B16F10 melanoma cells. *Mol. Carcinog*. **2016**, *55*, 2222–2235.

Vermes, I.; Haanen, C.; Steffens-Nakken, H.; Reutellingsperger, C. Anovel assay for apoptosis flow cytometric detection of phosphatidyl serine expression on early apoptotic cells using fluorescein labeled annexinV. *J. Immunol. Methods* **1995**, *184*, 39–51.

Vizetto-Duarte, C.; Custódio, L.; Acosta, G.; Lago, J.H.G.; Morais, T.R.; Bruno de Sousa, C.; Gangadhar, K.N.; Rodrigues, M.J.; Pereira, H.; Lima, R.T.; Vasconcelos, M.H.; Barreira, L.; Rauter, A.P.; Albericio, F.; Varela, J. Can macroalgae provide promising anti-tumoral compounds? A closer look at *Cystoseira tamariscifolia* as a source for antioxidant and anti-hepatocarcinoma compounds. *Peer J.* **2016**, *4*, 1704, doi 10.7717/peerj.1704.

Wang, S.; Basson, M.D. AKT directly regulates focal adhesion kinase through association and serine phosphorylation: implication for pressure-induced colon cancer metastasis. *Am. J. Physiol. Cell Physiol.* **2011**, *300*, 657–670.

Williams, G.H.; Stoeber, K. The cell cycle and cancer. *J. Pathol*. **2012**, *226*, 352–364.

Wu, W.S.; Wu, J.R.; Hu, C.T. Signal cross talks for sustained MAPK activation and cell migration: the potential role of reactive oxygen species. *Cancer Metastasis Rev*. **2008**, *27*,

303–314.

Yang, V.W. *The Cell Cycle. Physiology of the Gastrointestinal Tract (Fifth Edition)*. Academic Press: USA, 2012; chapter 15, p.451–471.

6. Meroterpenoids from the brown alga *Cystoseira usneoides* as potential anti-inflammatory and anticancer agents

On the basis of the anti-inflammatory properties of the extract of *C. usneoides*, the pharmacological screening of the isolated AMTs was continued by testing *in vitro* the profile of anti-inflammatory activity in stimulated THP-1 human macrophages. Moreover, the promising anticancer activity observed for the AMTs against colon cancer cells encouraged us to perform further studies in new cell models, specifically in human lung adenocarcinoma A549 cells. Taken together, these results could evidence the potential preventive role of the AMTs in the chronic inflammation and tissue damage for cancer development, including lung cancer.

Abstract: The anti-inflammatory and anticancer properties of eight meroterpenoids isolated from the brown seaweed *Cystoseira usneoides* have been evaluated. The algal meroterpenoids (AMTs) **1**-**8** were tested for their inhibitory effects on the production of the pro-inflammatory cytokines tumor necrosis factor (TNF-α), interleukin-6 (IL-6), and interleukin-1β (IL-1β), and the expression of cyclooxygenase-2 (COX-2) and inducible nitric oxide synthase (iNOS) in LPS-stimulated THP-1 human macrophages. The anticancer effects were assessed by cytotoxicity assays against human lung adenocarcinoma A549 cells and normal lung fibroblastic MRC-5 cells, together with flow cytometry analysis of the effects of these AMTs on different phases of the cell cycle. The AMTs **1**-**8** significantly reduced the production of pro-inflammatory cytokines TNF-α, IL-6, and IL-1β, and suppressed the COX-2 and iNOS expression in LPS-stimulated cells ($p<0.05$). The AMTs **1**-**8** displayed higher cytotoxic activities against A549 cancer cells than against MRC-5 normal lung cells. Cell cycle analyses indicated that most of the AMTs caused the arrest of A549 cells at the G2/M and S phases. The AMTs **2** and **5** stand out by combining significant anti-inflammatory and anticancer activities while **3** and **4** showed interesting selective anticancer effects. These findings suggest that the AMTs produced by *C. usneoides* may have therapeutic potential in inflammatory diseases and lung cancer.

6.1. Introduction

Inflammation is a physiologic process in response to invading pathogens or endogenous signals such as tissue injury. It is initiated by migration of immune cells from blood vessels and release of mediators, followed by recruitment of inflammatory cells and secretion of increased amounts of cytokines and chemokines to eliminate invading pathogens and to repair damaged tissues (Pan et al., 2009; Medzhitov, 2008; Lu et al., 2006).

During the past decade, numerous epidemiological studies have consistently linked the immune system with tumorigenesis (Todoric et al., 2016). However, the role of inflammation in cancer is not new. Virchow in 1863 postulated that tumors arise in areas of chronic inflammation and that inflammation cells were present in the resected tumors (Bremnes et al., 2011; Balkwill and Mantovani 2001). These observations led him to hypothesize that inflammation is a predisposing factor of carcinogenesis (Lu et al., 2006; Balkwill and Mantovani, 2001). It is now becoming clear that the immune system contributes to all stages of tumorigenesis, from initiation to invasion and metastasis of tumors, by providing abundant molecules to the tumor microenvironment. These molecules include growth factors, cytokines, and chemokines that increase mutagenesis, promote unregulated cell proliferation, limit apoptosis, and favor angiogenesis, invasion, and metastasis (Conway et al., 2015; Ben-Baruch, 2006).

Lung cancer causes 19% of all cancer deaths worldwide (Bray et al., 2018): it is the most commonly diagnosed cancer and the leading cause of cancer-related mortality both in males and females (Ma et al., 2016; Torre et al., 2015). The lung, as organ of the respiratory system exposed to the outer environment, is a place predisposed for infections and chronic inflammatory injuries (Cho et al., 2011; Engels, 2008). The chronic airway inflammation contributes to DNA damage, mutation, and pathological/molecular alterations in the bronchial epithelium and microenvironment, through the production of different cytokines, chemokines, and transcription factor networks, which increase lung tumor development and progression (Cho et al., 2011; Engels, 2008; Azad et al., 2008). Hence, a strategy for the prevention and treatment of lung cancer could involve the regulation of inflammatory molecules, including pro-inflammatory cytokines, and inflammatory enzymes, such as cyclooxygenase-2 (COX-2) and inducible nitric oxide synthetase (iNOS).

Brown algae are a promising group of seaweeds known to be a rich source of bioactive compounds (Hussain et al., 2014). Among brown algae, the genus *Cystoseira*, which currently encompasses about fifty species widespread along the northeastern Atlantic ocean and the Mediterranean Sea (Guiry, 2018), has been one of the most studied genera, from both chemical and biological points of view (Bruno de Sousa al., 2017). In particular, many algae of the genus *Cystoseira* have been described to contain a variety of natural products of the meroditerpene class (Gouveia et al 2013a; Amico et al. 1995; Valls and Piovetti, 1995) some of which have been shown to possess anticancer, antimicrobial, antioxidant or antileishmanial properties (Bruno de Sousa et al., 2017 ;, Vizetto-Duarte et al., 2016; Gouveia et al., 2013a 2013b).

In the course of our research on bioactive metabolites from macroalgae, we addressed the study of the algal meroterpenoids (AMTs) **1**-**8** (Figure 6.1) isolated from the species *C. usneoides* (De los Reyes et al., 2013).

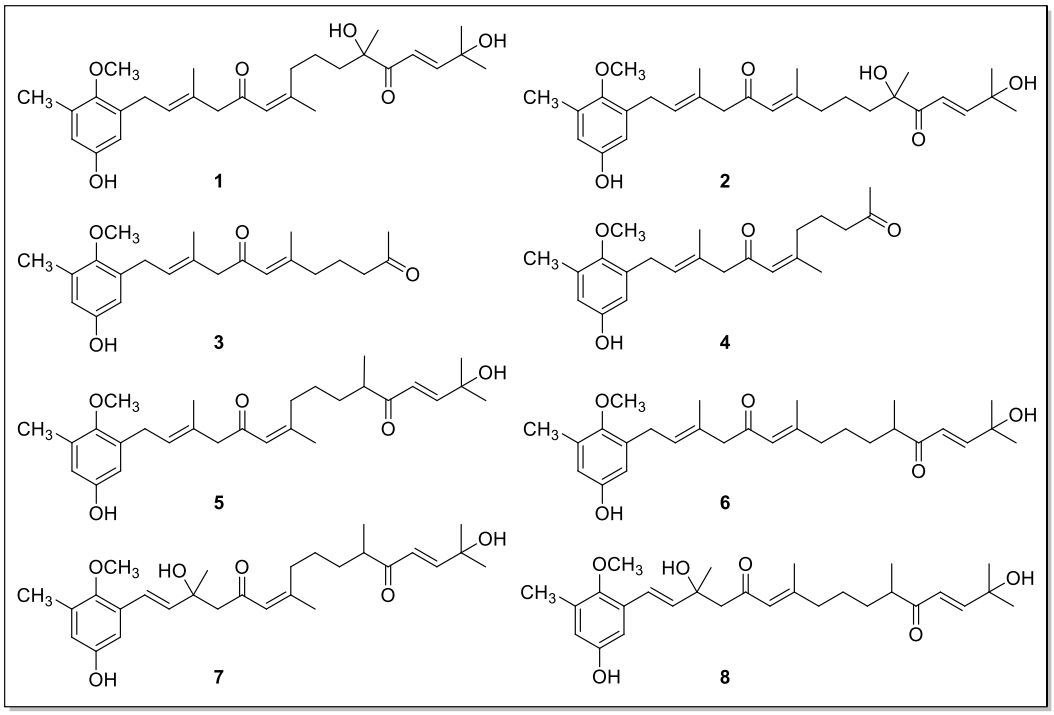

Figure 6.1. Chemical structures of the meroterpenes from *C. usneoides* subjected to anti-inflammatory and anticancer studies: usneoidone Z (**1**), 11-hydroxy-1′-*O*-methylamentadione (**2),** cystomexicone B (**3),** cystomexicone A (**4**), 6-*cis*-amentadione-1′-methyl ether (**5**), amentadione-1′-methyl ether (**6)**, cystodione A (**7**), and cystodione B (**8**).

As described in the previous chapter, the anticancer activity shown by the extract of *C. usneoides* against colon cancer cells HT-29 led us to study first the effects of the AMTs **1-8** on HT-29 cells. The compounds exhibited anticancer activity on HT-29 by inducing cell cycle arrest and apoptosis via the down-regulation of ERK/JNK/AKT signaling pathways.

On the other hand, the extract of *C. usneoides* had also shown promising anti-inflammatory activity as inhibitor of the production of the pro-inflammatory cytokine TNF-α. Thus, the first objective of the present study was to investigate the anti-inflammatory properties of the AMTs **1-8**. Secondly, taking into account the relationship between cancer and inflammation, this study also aimed to investigate the effects of the AMTs **1-8** on other types of cancer closely related to inflammatory processes such as lung cancer. We believe that investigating both activities and identifying compounds provided of both properties, anti-inflammatory and anticancer, could contribute to the understanding the relationship between cancer and inflammation.

Herein we demonstrate that the AMTs **1-8** exhibit anti-inflammatory activities through the inhibition of both the production of pro-inflammatory cytokines (TNF-α, IL-6, and IL-1β) and the protein expressions of COX-2 and iNOS in the LPS-stimulated THP-1 human macrophages as well as that the AMTs **1-8** also possess selective anticancer activity against human lung cancer cells A549 by inducing cell cycle arrest.

6.2. Material and Methods

6.2.1. Isolation and characterization of meroterpenoids 1-8

The collection of the alga samples, preparation of the extract, purification, and the structural characterization of the meroterpenoids **1-8** were described in the chemistry chapter (De los Reyes et al., 2013). Briefly, shade-dried samples of *C. usneoides* collected at the Gibraltar Strait were ground and extracted with acetone/methanol (MeOH). The resulting extract was subjected to column chromatography (CC) eluting with *n*-hexane/diethyl ether (Et_2O) mixtures of increasing polarity, then Et_2O, chloroform/MeOH mixtures, and finally MeOH. Repeated separation of selected fractions by CC and HPLC afforded the pure compounds **1-8**, whose structures were determined by NMR and MS.

6.2.2. Reagents for anti-inflammatory and anticancer assays

Sulforhodamine B (SRB), 3-(4,5-dimethylthiazol-2-yl)-2,5-diphenyl-tetrazolium bromide salt (MTT), dimethylsulfoxide (DMSO), Propidium Iodide (PI), Tris-base, acetic acid, trichloroacetic acid (TCA), and RNase were from Sigma-Aldrich (Munich, Germany); RPMI 1640 medium and fetal bovine serum (FBS) were from GIBCO (USA); phosphate buffer saline (PBS), streptomycine, penicillin, and trypsine-EDTA were from PAA (Laboratories GmbH, Austria). For western blotting, anti-COX-2 (Cayman, USA), anti-iNOS (ENZO, USA), anti-rabbit IgG antibody (Dako Cytomation, USA), anti-β-actin (Santa Cruz Biotechnology, USA) were pruchased.

6.2.3. Anti-inflammatory assays

Cell Culture

THP-1 human monocytic leukemia cell line was obtained from the American Type Culture Collection (TIB-202, ATCC, USA). The cells were cultured in RPMI 1640 medium containing 10% heat-inactivated FBS, 100 U/mL penicillin, and 100 mg/mL streptomycin, at 37 °C in humidified air containing 5% CO_2.

Cell Viability Assay

The viability of THP-1 cells was measured by the SRB assay (Skehan et al., 1990). The cells were seeded in 96-well plates with the growth medium at a density of 1×10^4 cells per well, and differentiation into macrophages was induced by 0.2 μM phorbol myristate acetate (PMA). Three days after differentiation into macrophages, the cells were treated with various concentrations (0, 3.125, 6.25, 12.5, 25, 50, 100 μg/mL) of the AMTs **1**-**8** in fresh medium and incubated for another 72 h. Then, the cells were fixed with 50 μL of trichloroacetic acid (TCA, 50%) and processed as described in the literature.

Determination of Pro-inflammatory Cytokines Production

THP-1 cells were plated at a density of 3×10^5 cells/mL in 24-well plates and incubated with PMA (0.2 μM) for 72 h in a humidified atmosphere of 5% CO_2 at 37°C. The macrophages were pre-treated for 1 h with AMTs **1**-**8** (8 μg/mL for compounds **1**, **2**, **3**, **4**, **7**, and **8,** and 4 μg/mL for **5** and **6**) and then stimulated with lipopolysaccharide (LPS, 1

μg/mL) for another 24 h. Dexamethasone (Dex) was used as positive reference compound at 1 μM. The viability of cells was greater than 95% throughout the experiment. The levels of TNF-α, IL-6, and IL-1ß in supernatants were measured with enzyme-linked immune-sorbent assay (ELISA) kits (Diaclone GEN-PROBE) according to the manufacturer's protocols. The absorbance was determined at 450 nm using a microplate reader. To calculate the concentration of cytokines, a standard curve was constructed using serial dilutions of cytokine standards provided with the kit.

Western Blotting Analysis

Western blotting was used to measure the protein levels of COX-2 and iNOS. THP-1 macrophages were plated at a density of 1×10^6 cells/mL in 6-well plates, treated for 1 h with compounds **1**-**8** (8 μg/mL for compounds **1**, **2**, **3**, **4**, **7**, and **8**, and 4 μg/mL for compounds **5** and **6**), and then stimulated with 1 μg/mL of LPS in medium at 37 °C. After 24 h the cells were washed with ice-cold PBS, collected, suspended in the lysis buffer (250 mM NaCl, 50 mM Tris (pH 7.5), 0.5 mM EDTA, 5 mM EGTA, 8 mM $MgCl_2$, 1 mM PMSF, 0.01 mg/mL pepstatin A, 0.01 mg/mL leupeptin, 0.01 mg/mL aprotinin, 1% Triton X-100) and centrifuged at 12,000g at 4 °C for 3 min to yield cell lysates. Protein concentration in cell lysates was determined by Bio-Rad Protein Assay (BioRad, Richmond CA, USA). Cytosolic proteins (50 μg) were separated with 10% SDS-polyacrylamide gel electrophoresis and transferred on PVDF membranes. The membranes were then blocked with 5% (w/v) non-fat dry milk in Tris-buffered saline containing 0.1% Tween-20 (pH 7.4) (TBST) buffer at room temperature for 1 h. The membranes were washed three times (10 min) in TBST buffer and incubated with specific primary antibodies anti-COX-2 (1:3000) or anti-iNOS (1: 1000) diluted in 5% (w/v) non-fat dry milk in TBST buffer, at 4 °C overnight. Then, the membranes were incubated with peroxidase-conjugated bovine peroxidase-conjugated goat anti-rabbit IgG (1: 1000) for 1h at room temperature. To ascertain that blots were loaded with equal amounts of protein lysates, they were also incubated in the presence of the antibody against β-actin protein (1:10,000). After washing the membrane again with TBST buffer (10 min) three times, the antibody was visualized using an enhanced chemiluminescence light-detecting kit (Super-Signal West Pico Chemiluminescent Substrate, Pierce, IL, USA), according to the manufacturer's

instructions and exposed to an X-ray film (GE Healthcare Ltd., Amersham, UK). The protein band densities were quantified using ImageJ v. 1.45 software (NIH, EEUU).

6.2.4. Anticancer assays

Cell line and cell culture

The human fetal lung fibroblastic MRC-5 cell line and the human lung adenocarcinoma A549 cell line were obtained from European Collection of Cell Cultures and maintained in Dulbecco's Modified Eagle's Medium (DMEM) supplemented with 2 mM glutamine, 100 U/mL penicillin, 100 µg/mL streptomycin and 10% FBS. Cell lines were cultured at 37º C in a humidified atmosphere containing 5% CO_2.

Cell proliferation assay

Cell proliferation was evaluated by a modified MTT assay, which measures the mitochondrial dehydrogenase activity (Calderón-Montaño et al., 2018). A total of 5×10^3 cells/well (MRC-5 cells) and 3×10^3 cells/well (A549 cells) were cultured in a 96-well plate for 24 h. Then, treatments were added to the cell culture. After 72 h of incubation, the medium was removed and 125 µL of MTT (1 mg/mL in medium) was added to each well and incubated for 4 h. Next, 80 µL of 20% sodium dodecyl sulphate (SDS) was added and incubated for 5 h at 37 ºC. The optical density of each well was measured at 540 nm (Synergy HT multiwell plate spectrophotometer reader, BioTek Instruments Inc., Winooski, VT, USA) to quantify cell viability. Cell survival (%) was expressed as percentage of viability compared to the control (non-treated cells).

Cell cycle analysis

For cell cycle analysis by flow cytometry, A549 cells were seeded at 1×10^6 cells/well in 6-well plates and incubated for 24 h followed by treatment with the AMTs, at concentration of IC_{50} (Table 6.3), and further incubation for 24 h. Cells were harvested after trypsinization and washed once with PBS. Then, the cells were centrifuged at 1500 rpm for 5 min (25 °C), the pellet was fixed with 1 mL of ice-cold 70% ethanol, and the samples were stored at −4 °C overnight. Then the cells were washed with PBS and incubated in the darkness with PBS containing 5 mg/mL of RNase A for 48 h at 4 °C. Subsequently, 50 µL

of 0.1 mg/mL of propidium iodide was added to the cells and were incubated for 1 h at 4°C. The relative DNA content per cell was analyzed using a Bekhman Coulter FC500 flow cytometer (Cytomics, MPL, USA). The data acquisition was performed with the DML program. The analysis of the acquired data was performed with the CXP cytometer.

6.2.5. Statistical Analysis

The results are presented as the mean ± Standard Error (SE) of at least three independent experiments. Data were evaluated with GraphPad Prism® Version 5.00 software. Differences between two groups were analyzed by the Student's *t*-test. Difference with $P < 0.05$ (*), $P < 0.01$ (**) or $P < 0.001$ (***) were considered statistically significant.

6.3. Results

The algal meroterpenoids (AMTs) usneoidone Z (**1**), 11-hydroxy-1'-*O*-methylamentadione (**2**), cystomexicone B (**3**), cystomexicone A (**4**), 6-*cis*-amentadione-1′-methyl ether (**5**), amentadione-1′-methyl ether (**6**), cystodione A (**7**), and cystodione B (**8**) (Figure 5.1) isolated from the alga *C. usneoides* have been investigated for their anti-inflammatory and anticancer activities.

6.3.1. Anti-inflammatory activity

Effects of AMTs 1-8 on the viability of THP-1 cells

The cytotoxic effect of AMTs **1-8** on LPS-stimulated THP-1 macrophages was determined at different concentrations and incubation times (0–100 µg/mL, 48 and 72 h) using the SRB assay. The results of this analysis demonstrated that none of the molecules affect cell viability at concentrations up to 10 µg/mL for AMTs **1**, **2**, **3**, **4**, **7**, **8**, and up to 6 µg/mL for AMTs **5** and **6** (data not shown). Therefore, in order to rule out cytotoxic effects, compounds **1**, **2**, **3**, **4**, **7**, and **8** were tested on THP-1 cells at maximum concentration of 8 µg/mL while **5** and **6** were tested at maximum concentration of 4 µg/mL.

Effects of AMTs 1-8 on TNF-α, IL-6, and IL-1ß expression in LPS-stimulated THP-1 macrophages

To determine the effects of the AMTs **1-8** on the production of TNF-α, IL-6, and IL-1ß, THP-1 macrophaghes were pretreated with the compounds and then stimulated with LPS, as the triggering factor to stimulate the cytokines production. The levels of proinflammatory cytokines in the cell supernatants were determined using the ELISA kits.

Upon comparison with control cells, TNF-α, IL-6, and IL-1ß levels were significantly increased in LPS stimulated cells up to 282.06, 389.47 and 181.8 ng/mL, respectively (Table 6.1). However, LPS-stimulated THP-1 macrophages pre-treated with the AMTs **1-8** showed a significant reduction of the production of pro-inflammatory cytokines (Table 6.1, Figure 6.2).

Table 6.1. Inhibitory effects of AMTs **1-8** on the production of TNF-α, IL-6, and IL-1ß in LPS-stimulated THP-1 macrophages.

	Cytokines production (ng/mL)		
	TNF-α	**IL-6**	**IL-1β**
Control	77.69±7.6	59.07±1.7	53.35±4.2
Control + LPS	282.06±2.1^{+++}	389.48±20.1^{++}	181.81±9.6^{+++}
Dexamethasone[a]	55.58±6.9***	28.18±2.3***	105.94±5.7**
AMTs:			
1[b]	75.85±15.5**	112.16±16.1***	46.25±2.6***
2[b]	101.15±19.5**	74.75±14.4***	28.30±5.7***
3[b]	120.91±17.5**	120.04±2.7**	117.67±11.4*
4[b]	163.1±13.9**	221.97±8.1**	141.83±9.5
5[c]	125.96±7.3***	125.3±12.1***	25.46±2.4***
6[c]	161.48±10.6**	191.07±5**	70.78±3.4**
7[b]	159.86±7.8**	196.42±10.1**	100.26±7.5**
8[b]	133.82±24.1**	160.18±18**	100.73±7.5*

[a] 1 μg/mL; [b] 8 μg/mL; [c] 4 μg/mL; Values are the mean ± SE of triplicate experiments; +++ $p < 0.001$ vs Control; *$p < 0.05$, **$p < 0.01$, ***$p < 0.001$ vs Control+LPS.

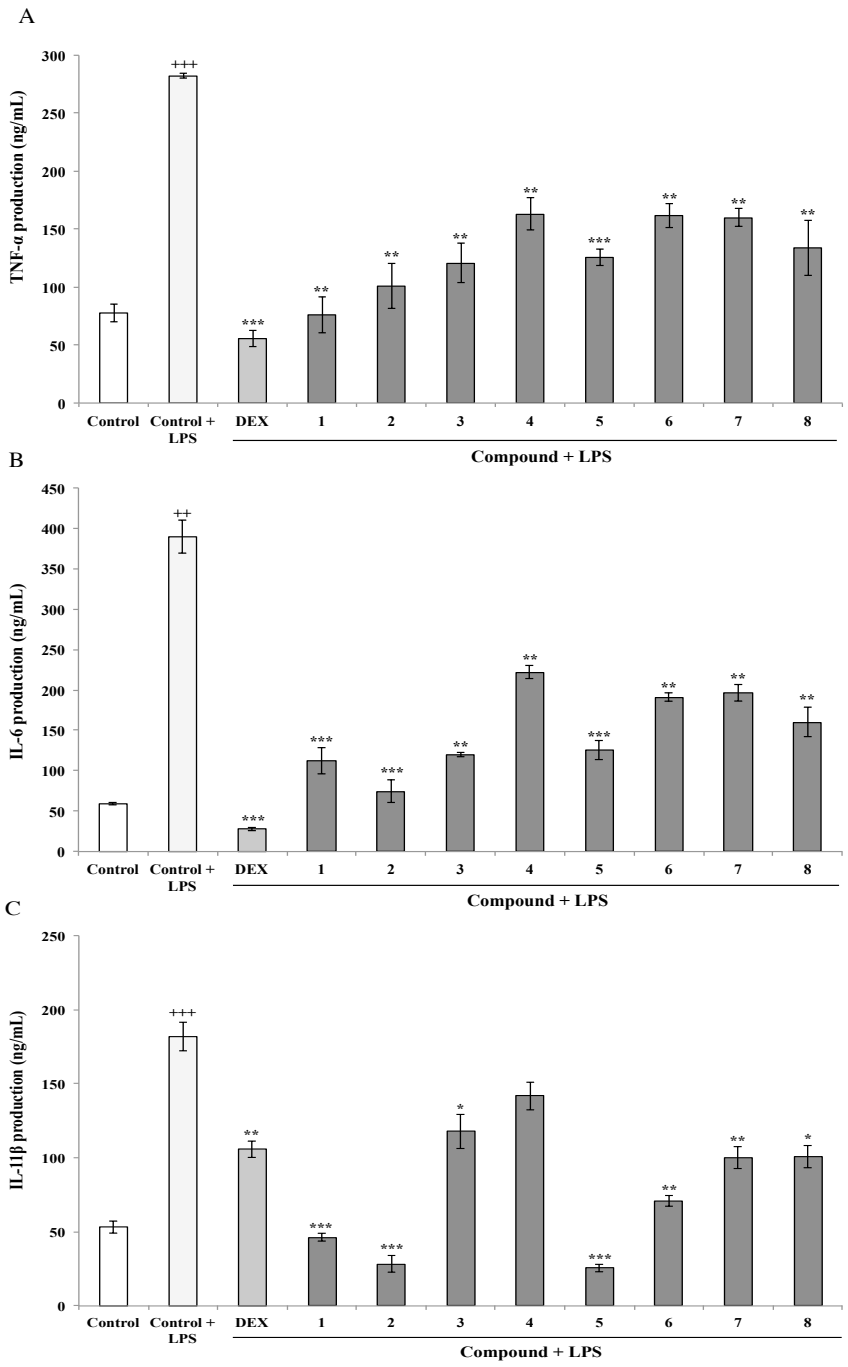

Figure 6.2. AMTs **1**-**8** inhibit LPS-induced expression of TNF-α, IL-6, and IL-1β in THP-1 macrophaghes (**A**, **B** and **C**) respectively. Cells were pretreated for 1 h with the AMTs (**1**, **2**, **3**, **4**, **7** and **8** at 8 μg/mL; **5** and **6** at 4 μg/mL), followed by 24 h treatment with LPS. TNF-α (**A**), IL-6 (**B**) and IL-1β (**C**) contents in the culture medium were determined by ELISA. Data are expressed as means ± SE from three independent experiments. Statistical significance is indicated ($^{+++}p < 0.001$ vs Control; $*p < 0.05$, $**p < 0.01$, $***p < 0.001$ vs Control+LPS).

Regarding to TNF-α, although all compounds induced a significant reduction of the level of this cytokine in THP-1, the meroditerpenes **1** and **2**, at 8 μg/mL, showed the higher suppressive effect causing 73% and 64% inhibition (Table 6.1 and Figure 6.2A). Compounds **3**, **5**, and **8** also induced more than 50% of inhibition (57%, 55%, and 52%, respectively), while compounds **4**, **6**, and **7** were less active, reducing the production of TNF-α by 42-43% ($P<0,01$).

As shown in Table 6.1 and in Figure 6.2B, among the eight AMTs, compound **2** markedly inhibited LPS-induced IL-6 production in THP-1 macrophages by 81% and compounds **1**, **3,** and **5** caused strong inhibitions of 71%, 69% and 67%, respectively.

The treatment of cells with compounds **4**, **6**, **7**, and **8** also significantly inhibited the production of IL-6 upon comparison with LPS-stimulated THP-1 control cells, although to a lesser extent (43%, 51%, 50% and 59%, respectively).

With regard to IL-1ß production, the pretreatment of cells with the AMTs **1-8** resulted in significant inhibition of this cytokine (Table 6.1 and Fig. 6.2C). The most marked effects were observed in the cells treated with compounds **2** (8 μg/mL) and **5** (4 μg/mL), which blocked the effect of 1 μg/mL LPS by 84% and 86%, respectively.

Moreover, pretreatment with the AMTs **1** (8 μg/mL) and **6** (4 μg/mL) also strongly inhibited LPS-induced IL-1ß production by 74% and 61%, respectively. The AMTs **3**, **7**, and **8** displayed inhibitory activity, causing IL-β decreases of 50%, 44%, and 35%, respectively.

Effects of AMTs 1-8 on the expression of COX-2 and iNOS proteins in LPS-stimulated THP-1 cells

COX-2 is the key enzyme regulating the production of prostaglandins, which are the central mediators of inflammation. On the other hand, iNOS enzyme represent an important molecular target closely involved in inflammatory responses. Thus, the effect of the AMTs **1-8** on LPS-induced COX-2 and iNOS protein expression was investigated by western blot analysis. As shown in Figure 6.3 and in Table 6.2, the expression of COX-2 and iNOS proteins was markedly augmented upon LPS treatment in THP-1 macrophages.

The pretreatment with the AMTs **2**, **3**, **4**, **5**, **6,** and **7** significantly down-regulated

the expression of COX-2, while no significant effect was observed for compounds **1** and **8**. The more active compounds were **3**, **5**, **6**, and **7** which decreased COX-2 levels by 53, 53, 64, and 58 % respectively. On the other hand, all AMTs **1-8** effectively suppressed LPS-induced iNOS expression, decreasing iNOS levels in the range 40-54 %.

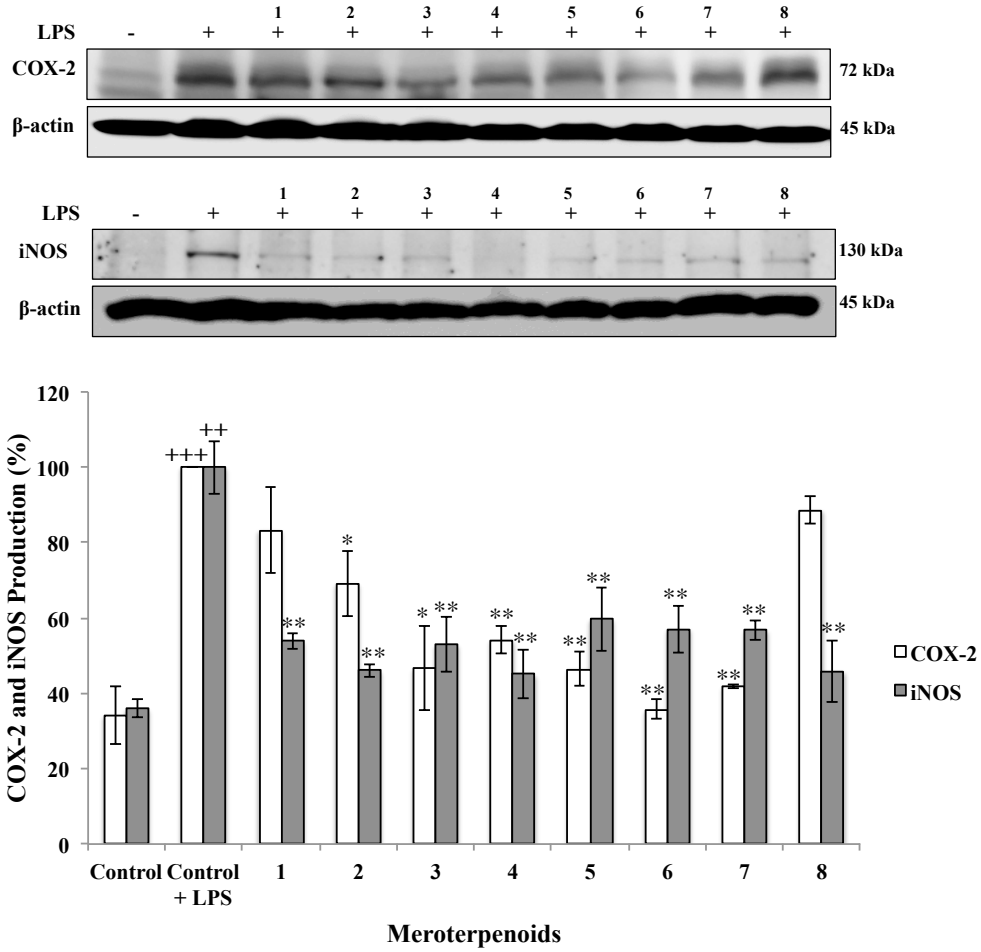

Figure 6.3. Effect of AMTs **1-8** on LPS-induced COX-2 and iNOS protein expression in THP-1 macrophages. Cells were pretreated for 1 h with the AMTs (**1**, **2**, **3**, **4**, **7** and **8** at 8 μg/mL; **5** and **6** at 4 μg/mL) and then stimulated with LPS (1 μg/mL). Cytosolic lysates from 24 h-stimulated cells were separated on 10% SDS-PAGE. COX-2, iNOS, and β-actin were detected by western blot analysis. Data are expressed as means ± SE from three independent experiments. Statistical significance is indicated ($^{+++}$ $p < 0.001$ and $^{++}$ $p < 0.01$ vs Control; *$p < 0.05$, **$p < 0.01$, ***$p < 0.001$ vs Control+LPS).

Table 6.2. Inhibitory effects of AMTs **1-8** on the production of COX-2 and iNOS in LPS-stimulated THP-1 macrophages.

	Percentage of production	
	COX-2	**iNOS**
Control	34.26±7.7	35.95±2.29
Control + LPS	100.00±0.2^{+++}	100.00±7.04^{++}
AMTs:		
1[a]	83.29±11.37	53.96±2.15**
2[a]	69.18±8.68*	46.06±1.68**
3[a]	46.65±11.3*	52.95±7.31**
4[a]	54.16±3.63**	45.07±6.37**
5[b]	46.48±4.46**	59.69±8.4**
6[b]	35.77±2.5**	57.12±6.3**
7[a]	41.98±0.61**	56.77±2.57**
8[a]	88.61±3.59	45.91±8.19**

[a]8 μg/mL; [b]4 μg/mL. Values are the mean ± SE of triplicate experiments;
+++ $p < 0.001$ vs Control; *$p < 0.05$, **$p < 0.01$, ***$p < 0.001$ vs Control+LPS.

6.3.2. Anticancer activity

Cytotoxic effects and selectivity of the AMTs 1-8

The effects of the AMTs **1-8** on cell survival was investigated in the human lung cancer cell line A549. The results, shown in Figure 6.4, indicated that all the AMTs inhibited the A549 cell growth after 72-h incubation in a dose-dependent manner. The most active compounds were **1**, **2**, **5** and **6** with IC_{50} values of 8.68, 6.61, 4.56, and 6.19 μg/mL, respectively (Table 6.3).

Since the AMTs **1-8** showed an interesting cytotoxic activity towards A549 cells, the compounds were similarly evaluated in a normal cell line (human fetal lung fibroblastic MRC-5 cells) to determine the selectivity index (SI).

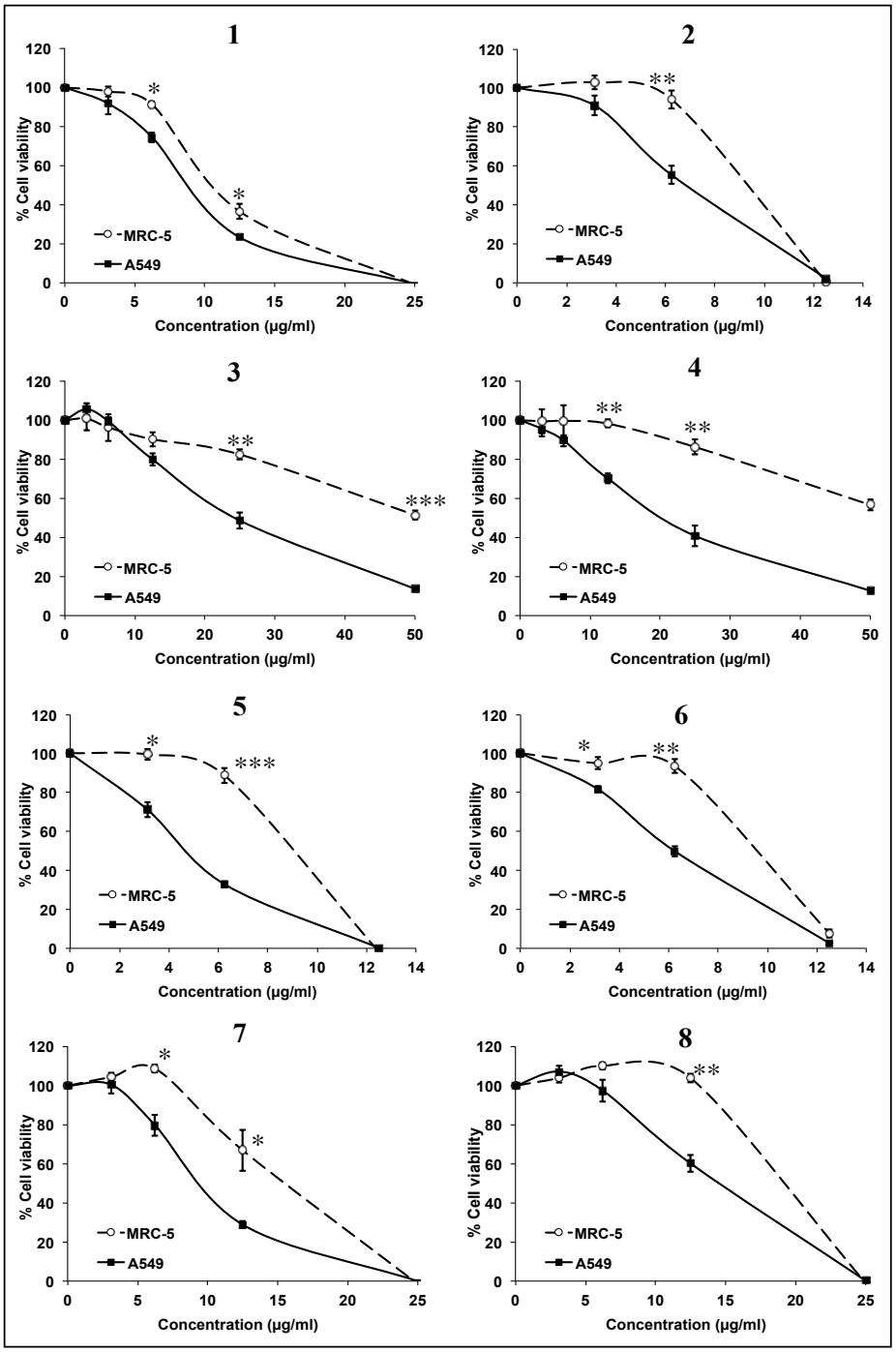

Figure 6.4. Effects of different concentrations of AMTs **1**-**8** on the viability of human lung cancer cell line A549 and the human fetal lung fibroblastic MRC-5 cells, using MTT assay and after 72 h of treatment. Results are expressed as percentage of viable cells (% cell viability). Data are mean ± SE from three independent experiments. *$p<0.05$, **$p<0.01$ and ***$p<0.01$ compared with the untreated group.

Table 6.3. IC_{50} values (μg/mL) of AMTs **1**-**8** against the normal lung cells MRC-5 and the lung cancer cells A549, after 72 h of treatment.

Compound	Cell lines		Selectivity Index
	MRC-5	**A549**	**SI**
1	10.64±0.50	08.68±0.15	1.22
2	08.65±0.18	06.61±0.38	1.30
3	51.91±2.76	24.42±1.71	2.12
4	58.38±3.30	21.00±1.79	2.78
5	08.39±0.14	04.56±0.21	1.83
6	08.87±0.05	06.19±0.25	1.43
7	14.46±1.14	09.31±0.33	1.55
8	17.83±0.09	13,96±0.55	1.28

SI = IC_{50} values for normal cells/ IC_{50} values for cancer cells. Data are means ± SE from three independent experiments.

It has been reported that compounds with SI value higher or equal to 2.0 are potentially selective (Suffness and Pezzuto, 1990). According to the data in Table 6.3, all AMTs showed selective cytotoxicity against the cancer cells; especially compounds **3** and **4** which at increasing concentrations maintained higher toxicity against A549 cancer cells than against MRC-5 non-malignant cells (Figure 6.4). It is worth noting that after treatment with 50 μg/mL of these two AMTs the cell viability was lower than 15% for cancer cells and higher than 55% for normal cells. On the other hand, **1** was the less selective compound; its SI was 1.22.

In view of the high incidence of harmful side effects induced by most existing anticancer drugs, the selective *in vitro* cytotoxicity exhibited by of **3** and **4** suggest that these compounds could be promising and interesting anticancer agents.

Effects of AMTs 1-8 on A549 cell cycle progression

We next investigated whether the treatment with AMTs **1**-**8** caused any cell cycle-related event which inhibit the viability of A549 cell line. Thus, the cells were treated with the AMTs (at concentrations of IC_{50} (Table 6.3)) or with colchicine (at 0.2 μg/mL) for 24 h, and then subjected to flow cytometry analysis to evaluate the distribution of cells in the

different phases of the cell cycle (Figure 6.5).

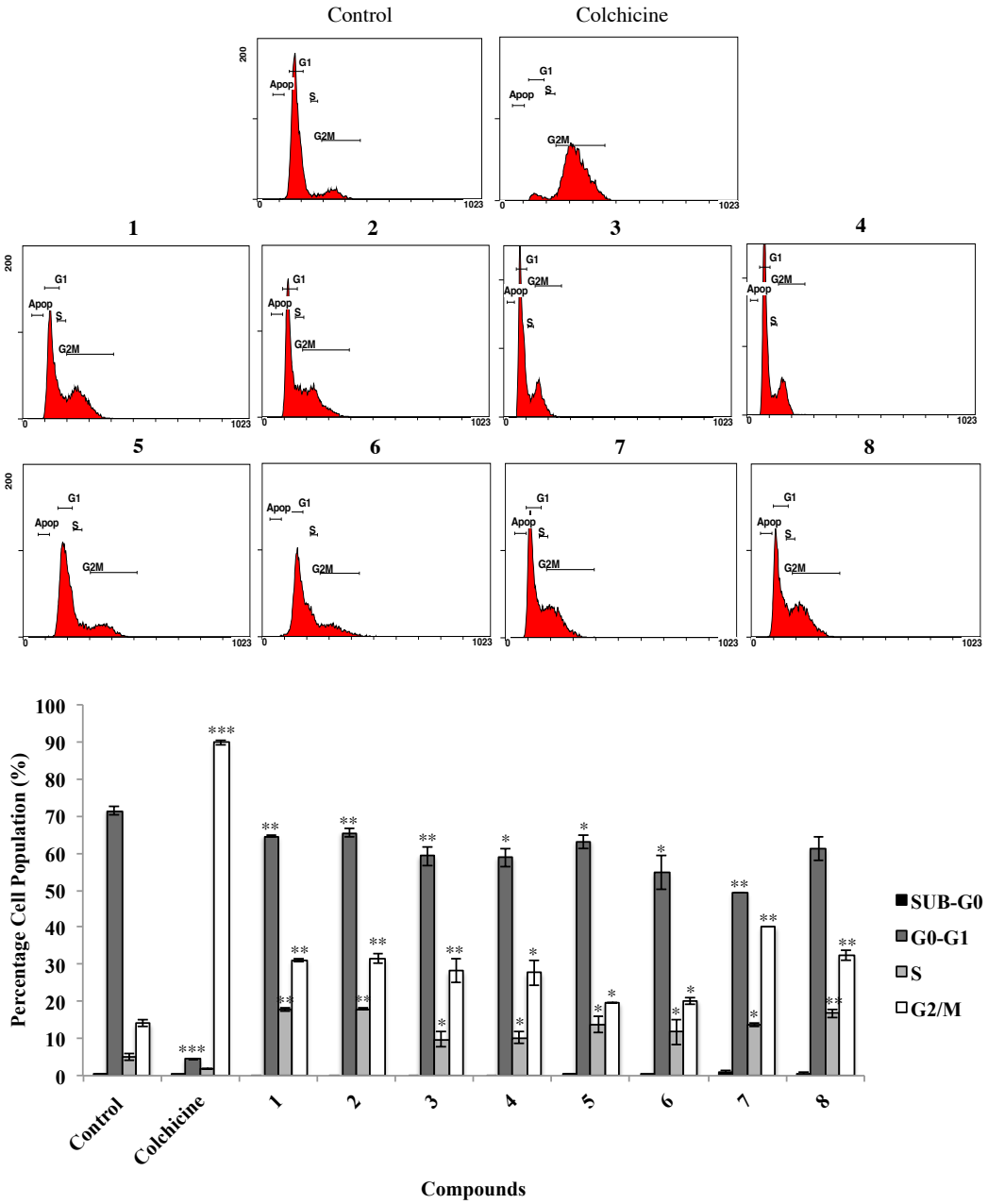

Figure 6.5. Effects of AMTs **1-8** on cell cycle distribution of A549 cells. Cells were incubated with IC_{50} doses of AMTs for 24 h. (**A**) Cells were harvested to measure the cell cycle distribution by flow cytometry. (**B**) Quantitative analysis of cell cycle distribution after treatment with AMTs. Data represent mean ± SE from three independent experiments. **p<0.01 and ***p<0.01 compared with the untreated group.

The results showed that most of the assayed AMTs induced a significant accumulation of cells at the G2/M phase (20-40%) and at the S phase (10-18%) of the cell cycle, with a parallel depletion of the percentage of cells in G0/G1 phase (49-65%) (Figure 6.5). The AMTs **1**, **2**, **7** and **8** were the most active and caused a remarkably increase of cells at G2/M phase (31.15, 31.62, 40.19, and 32.50%, $p<0.01$, respectively) compared with the control group (14.06 %) and at S phase (17.75, 17.90, 13.69, and 16.73%, $p<0.01$, respectively) compared with the control group (4.99 %). In parallel, a decrease of the population at G0/G1 phase was observed in the cells treated with these compounds (64.52, 65.42, 49.3, and 61.3%, $p<0.01$, respectively) in comparison with the control group (71.4 %).

6.4. Discussion

As a part of our ongoing project aimed to evaluate the biomedical potential of marine natural products, in the present study we have demonstrated the in vitro anti-inflammatory and anticancer activities of eight meroterpenoids (AMTs **1**-**8**) isolated from the brown alga *C. usneoides*.

First we investigated the anti-inflammatory effects of the AMTs **1**-**8** and their molecular mechanisms in LPS-induced THP-1 macrophages. The production of pro-inflammatory mediators including TNF-α, IL-6, and IL-1β by macrophages exposed to endotoxins is well established (Li et al., 2016; Rios et al., 2016). TNF-α plays a major role in initiating and regulating the release of adhesion molecules and the expression of inflammatory mediators during inflammatory responses (McCoy et al., 2011). IL-6 is a multifunctional cytokine that plays a role in inflammatory responses through the stimulation of acute phase responses, hematopoiesis, and immune reactions (Tanaka et al., 2014). Moreover, inhibition of IL-6 signaling has been successfully translated into the clinic as a powerful anti-inflammatory strategy (Baran et al., 2018). IL-1β is one of the most potent proinflammatory cytokines, which affects a large number of cellular responses and mediates inflammatory processes at local and systemic levels (Dinarello, 2018; Borthwick, 2016). These proinflammatory mediators can induce cell and tissue damage and also activate macrophages in various inflammation-associated diseases (Yoon et al., 2009).

The protein COX-2 is an important inflammatory enzyme responsible of the high prostaglandin levels widely observed in inflammatory pathology (Murakami and Ohigashi 2007). The enzyme iNOS is greatly expressed in macrophages and its activation leads to organ destruction in some inflammatory and autoimmune diseases (Pansanit et al., 2013). Therefore, treatment aimed to suppressing proinflammatory cytokines and enzymes is regarded as an effective therapeutic strategy for the control of several disorders, including the inflammatory diseases.

In this study, we found that the AMTs **1**-**8** significantly reduced the secretion of the proinflammatory cytokines TNF-α, IL-6, and IL-1β, as well as inhibited the protein expressions of COX-2 and iNOS in LPS-induced THP-1 macrophages. These findings are in line with other results from our group showing that other AMTs of *C. usneoides* reduce TNF-α expression in LPS-stimulated THP-1 cells (De los Reyes et al., 2016) and indicate that the meroterpenoids are responsable of the anti-inflammatory properties of the extract of the alga. Morevover, the results obtained for the AMTs **1**-**8** represent the first account on the activity of this class of meroterpenoids as inhibitors of the proinflammatory mediators IL-6, IL-1ß, COX-2 and iNOS.

Overall, the AMTs **1** and **2** were the most potent inhibitors of the production of the three proinflammatory cytokines, causing decreases in the range 71-84% at 8 μg/mL. At this concentration, compound **2** also significantly inhibited COX-2 and iNOs. These inhibitory effects observed for compound **2** (11-hydroxy-1′-*O*-methylamentadione or AMT-E) on THP-1 cells are consistent with the *in-vivo* study described in the next chapter, which shows that compound **2** exerts intestinal anti-inflammatory activity in the colitis by down-regulating TNF-α, IL-1ß, and IL-10, as well as suppressing COX-2 and iNOS expression in the mouse colon tissue (Zbakh et al., 2016).

Recent reports from other groups have also demonstrated the anti-inflammatory potential of a variety of algal terpenes and meroterpenes (Bruno de Sousa et al., 2017). A number of compounds have been assayed on LPS-stimulated RAW264.7 macrophages (Wijesinghe et al., 2014, Yoon et al. 2012, Chatter et al., 2011). Thus, the diterpenoid nerogioltriol (**Lg-1**) (Figure 6.6) from the alga *Laurencia glandulifera* was found to inhibit the activation of NFκB and the production of NO, TNF-α, and COX-2 (Chatter et al., 2011)

while the sesquiterpene 5β-hydroxypalisadin B (**Ls-1**) from *L. snackeyi* (Wijesinghe et al., 2014) and the meroterpene sargachromanol G from *Sargassum siliquastrum* (**Ss-19**) (Yoon et al. 2012) were shown to inhibit the production of NO, TNF-α, IL-6, and IL-1β, as well as reduce the COX-2 and iNOS expression in LPS-stimulated RAW264.7 macrophages.

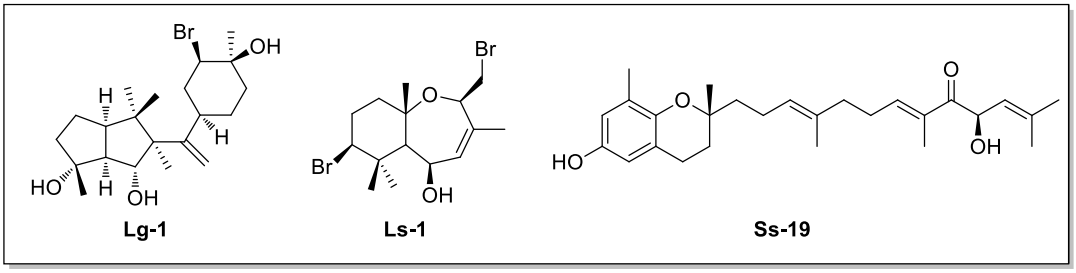

Figure 6.6. Chemical structres of algal terpenoids and AMTs which inhibit the production of proinflammatory mediators in LPS-stimulated RAW264.7 macrophages (Wijesinghe et al., 2014, Yoon et al. 2012, Chatter et al., 2011).

Other terpenes from *Dictyota plectens* showed anti-inflammatory effects by inhibiting the LPS-induced NO production in mouse peritoneal macrophages (PEMΦ) (Zhao et al., 2015) and, more recently, several terpenes from the red alga *L. tristicha* and from the brown alga *Homoeostrichus form*osana, showed an interesting anti-inflammatory ability by inhibiting the FMLP/CB-induced generation of superoxide anion and elastase release in human neutrophils (Fang et al., 2015; Chen et al., 2016). The results obtained for the AMTs **1-8** are in line with the anti-inflammatory activities above described, and show that the terpenoids from *C. usneoides* have potent inhibitory effects on the LPS-induced production of TNF-α, IL-6, and IL-1β, and on COX-2 and iNOS expression.

We next investigated the effects of the anti-inflammatory AMTs **1-8** on the viability of the lung cancer cells A549. It is well known that chronic inflammation is associated with several chronic diseases including cancer (Gupta et al., 2018; Makvandi et al., 2017). Cancer is the second leading cause of death worldwide, being lung cancer one of the most mortal cancer type (OMS). The metastatic cancer is an incurable disease for most patients because the current anticancer therapies lack of enough selective cytotoxicity to kill cancer cells without affecting healthy tissues (Siegel et al., 2018). Therefore, the development of new drugs with higher selectivity towards cancer cells is vital to advance towards the cure to this deadly disease. Nature, has provided useful anticancer drugs (*e.g.* the vinca alkaloids

and the diterpene paclitaxel) and is still a source of new agents (Martin-Cordero et al., 2012). In this line, along the last decades, an array of new anticancer compounds have also been isolated from marine organisms (Ercolano et al., 2019).

In this study, we have shown the anticancer activity of eight meroterpenoids obtained from the alga *C. usneoides*. In particular, we studied the cytotoxicity of the AMTs **1**-**8** against lung cancer cells and lung normal cells. All AMTs significantly inhibited the growth of A549 cancer cells. Interestingly, the compounds exhibiting a chain of twenty carbon atoms (**1**, **2**, **5-8**) were more cytotoxic (IC_{50} ranging from 4.56 to 13.96 μg/mL) than those with a chain of fourteen carbon atoms (**3** and **4**), a characteristic that had also been previously observed in the assays against the colon cancer cells HT-29. Moreover, we found that the cancer cells were more sensitive to the cytotoxic effect of AMTs **1**-**8** than MRC-5 normal cells. Compounds **3** and **4** had the highest selectivity towards cancer cells, showing selective cytotoxic activity at several concentrations assayed (from 12 to 50 μg/mL).

Among algae-derived metabolites, a few terpenoids and meroterpenoids have also recently been reported to possess anticancer activity against lung cancer cells A549.

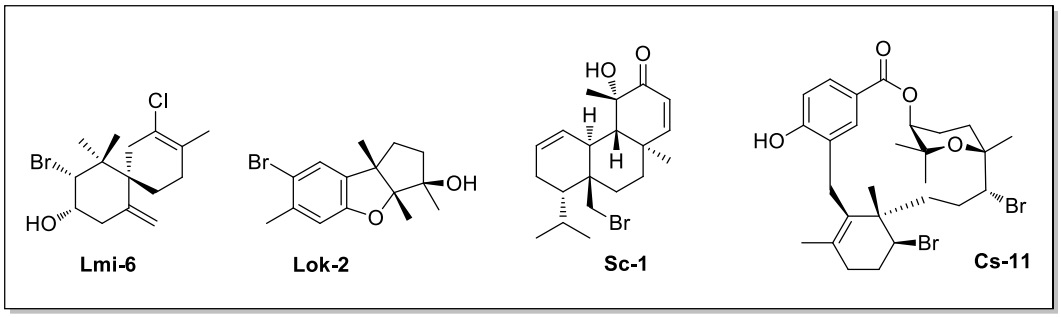

Figure 6.7. Chemical structures of algal terpenoids and AMTs with anticancer activity against A549 cells (Yu et al., 2014; Tesdale et al., 2014; Campos et al., 2012; Smyrniotopoulos et al., 2010; Lane et al., 2009).

Thus the sesquiterpenes elatol (**Lmi-6**) (Figure 6.7) from *Laurencia microcladia* together with 5β-hydroxyaplysin (**Lok-2**) and its hydroperoxy analogue from *L. okamurai* had cytotoxic effects towards A549 human cancer cell line (IC_{50} values of 4.8, 35.3 and 15.4 μM, rspectively) (Campos et al., 2012; Yu et al., 2014) while the diterpenes sphaerococcenol A (**Sc-1**) and two related analogues from *Sphaaerococcus coronopifolius*

inhibited the growth of A549 cells with IC_{50} values of 3.7, 19.0 and 18.0 μM (Smyrniotopoulos et al., 2010). Likewise meroditerpenoids from algae of the genus *Callophycus* exhibited cytotoxicity towards several human cancer cell lines, including A549 cells, with the higher activity observed for bromophycolides M, N, O, P, Q (**Cs-11**) and bromophycoic acid D (mean IC_{50} values of 3.1, 8.6, 9.7, 7.9, 2.0, and 6.8 μM, respectively) (Lane et al. 2009; Tesdale et al., 2014).

We have also demonstrated that most of the assayed AMTs suppress the proliferation of A549 by arresting cell cycle progression at the G2/M and S phases. The cell cycle checkpoints play a key role in the machinery that controls cell division by sensing defects occurring in vital processes, like DNA replication or chromosome segregation, inducing a cell cycle arrest till the repair of the detected defects (Malumbres 2012). The effect of algal terpenes on lung cancer and cell cycle distribution has been scarcely documented and less in A549 cells. Campos et al., 2012, demonstrated the anticancer properties of the sesquiterpene elatol (**Lmi-6** in Figure 6.7), isolated from *Laurencia microcladia*, by inducing cell cycle arrest in the G1 and the sub-G1 phases in several human cancer cell lines, including A549 cell line. Our results suggest, for the first time, that the meroterpenoids **1-8** affect the molecular pathways that control the A549 cell cycle progression by arresting the cells at the G2/M and S checkpoints.

6.5. Conclusion

In summary, most of the AMTs **1-8** were active in the performed anti-inflammatory and anticancer assays. Compounds **2** and **5** stand out by combining significant anti-inflammatory and anticancer properties while compounds **3** and **4** have an interesting anticancer profile because of their marked selective cytotoxicity. Literature offers strong evidence that chronic inflammation and tissue damage can cause cancer development including lung cancer (Conway et al., 2016). Hence, natural compounds that simultaneously possess anti-inflammatory and anticancer potentials are of great importance for cancer prevention and treatment. The anti-inflammatory and anticancer results above described for the AMTs **1-8** support the need to perform advanced biological activity studies with some selected AMTs in animal models of intestinal, lung, or skin inflammation and cancer.

6.6. References

Amico, V. Marine brown algae of family Cystoseiraceae: Chemistry and chemotaxonomy. *Phytochemistry* **1995**, *39*, 1257−1279.

Azad, N.; Rojanasakul, Y.; Vallyathan, V. Inflammation and lung cancer: roles of reactive oxygen/nitrogen species. *J. Toxicol. Environ. Health.* **2008**, *11*, 1–15.

Badisa, R.B.; Darling-Reed, S.F.; Joseph, P.; Cooperwood, J.S.; Latinwo, L.M.; Goodman, K.B. Selective cytotoxic activities of two novel synthetic drugs on human breast carcinoma mcf-7 cells. *Anticancer Res*. **2009**, *29*, 2993–2996.

Balkwill, F.; Mantovani, A. Inflammation and cancer: back to Virchow? *Lancet* **2001**, *357*, 539–545.

Baran, P.; Hansen, S.; Waetzig, G.H.; Akbarzadeh, M.; Lamertz, L.; Huber, H.J.; Ahmadian, M.R.; Moll, J.M.; Scheller, J. The balance of interleukin (IL)-6, IL-6·soluble IL-6 receptor (sIL-6R), and IL-6·sIL-6R·sgp130 complexes allows simultaneous classic and trans-signaling. *J. Biol. Chem*. **2018**, *293*, 6762–6775.

Ben-Baruch, A. Inflammation-associated immune suppression in cancer: the roles played by cytokines, chemokines and additional mediators. *Semin. Cancer Biol.* **2006**, *16*, 38–52.

Borthwick, L. A. The IL-1 cytokine family and its role in inflammation and fibrosis in the lung. *Semin. Immunopathol*. **2016**, *38*, 517–534.

Bray, F.; Ferlay, J.; Soerjomataram, I.; Siegel, R.L.; Torre, L.A.; Jemal, A. Global Cancer Statistics 2018: GLOBOCAN estimates of incidence and mortality worldwide for 36 cancers in 185 countries. *CA Cancer J. Clin*. **2018**, *68*, 394–424.

Bremnes, R.M.; Al-Shibli, K.; Donnem, T.; Sirera, R.; Al-Saad, S.; Andersen, S.; Stenvold, H.; Camps, C.; Busund, L.T. The role of tumor-infiltrating immune cells and chronic inflammation at the tumor site on cancer development, progression, and prognosis: emphasis on non-small cell lung cancer. *J. Thorac. Oncol*. **2011**, *6*, 824–833.

Bruno de Sousa, C.; Gangadhar, K.N.; Macridachis, J.; Pavão, M.; Morais, T.R.; Campino, L.; Varela, J.; Lago, J.H.G. *Cystoseira* algae (Fucaceae): update on their chemical entities and biological activities. *Tetrahedron: Asymmetry* **2017**, *28*, 1486–1505.

Calderón-Montaño, J.M.; Jiménez-Alonso, J.J.; Guillén-Mancina, E.; Burgos-Morón, E.;

López-Lázaro, M. A 30-s exposure to ethanol 20% is cytotoxic to human keratinocytes: possible mechanistic link between alcohol-containing mouthwashes and oral cancer. *Clin. Oral. Investig*. **2018**, *22*, 2943–2946.

Campos, A.; Souza, C.B.; Lhullier, C.; Falkenberg, M.; Schenkel, E.P.; Ribeiro-do-Valle, R.M.; Siqueira, J.M. Anti-tumour effects of elatol, a marine derivative compound obtained from red algae *Laurencia microcladia*. *J. Pharm. Pharmacol.* **2012**, *64*, 1146–1154.

Chatter, R.; Ben Othman, R.; Rabhi, S.; Kladi, M.; Tarhouni, S.; Vagias, C.; Roussis, V.; Guizani-Tabbane, L.; Kharrat, R. *In vivo* and *in vitro* anti-inflammatory activity of neorogioltriol, a new diterpene extracted from the red algae *Laurencia glandulifera*. *Mar. Drugs* **2011**, *9*, 1293–1306.

Chen, J.Y.; Huang, C.Y.; Lin, Y.S.; Hwang, T.L.; Wang, W.L.; Chiou, S.F.; Sheu, J.H. halogenated sesquiterpenoids from the red alga *Laurencia tristicha* collected in Taiwan. *J. Nat. Prod.* **2016**,*79*, 2315–2323.

Cho, W.C.; Kwan, C.K.; Yau, S.; So, P.P.; Poon, P.C.; Au, J.S. The role of inflammation in the pathogenesis of lung cancer. *Expert Opin. Ther. Tar.* **2011**, *15*, 1127–1137

Conway, E.M.; Pikor, L.A.; Kung, S.H.Y.; Hamilton, M.J.; Lam, S.; Lam, W.L.; Bennewith, K.L. macrophages, inflammation, and lung cancer. *Am. J. Respir. Crit. Care Med.* **2016**, *193*, 116–130.

De los Reyes, C.; Ortega, M.; Zbakh, H.; Motilva, V.; Zubía, E. *Cystoseira usneoides*: A Brown Alga Rich in Antioxidant and Anti-inflammatory Meroditerpenoids. *J. Nat. Prod*. **2016**, *79*, 395−405.

De los Reyes, C.; Zbakh, H.; Motilva, V.; Zubía, E. Antioxidant and anti-inflammatory AMTs from the brown alga *Cystoseira usneoides*. *J. Nat. Prod*. **2013**, *76*, 621−629.

Dinarello, C.A. Overview of the IL-1 family in innate inflammation and acquired immunity. *Immunol. Rev*. **2018**, *281*, 8–27.

Engels, E.A. Inflammation in the development of lung cancer: epidemiological evi- dence. *Expert Rev. Anticancer Ther.* **2011**, *8*, 605–615.

Ercolano, G.; De Cicco, P.; Ianaro, A. New Drugs from the Sea: Pro-Apoptotic Activity of

Sponges and Algae Derived Compounds. *Mar Drugs*. **2019**, *17*, 1–31.

Fang, H.Y.; Chokkalingam, U.; Chiou, S.F.; Hwang, T.L.; Chen, S.L.; Wang, W.L.; Sheu, J.H. Bioactive chemical constituents from the brown alga *Homoeostrichus formosana*. *Int. J. Mol. Sci.* **2015**, *16*, 736–746.

Gouveia, V.; Seca, A.M.L.; Barreto, M.C.; Pinto, D.C.G.A. Di- and sesquiterpenoids from *Cystoseira* genus: Structure, intra-molecular transformations and biological activity. *Mini-Rev. Med. Chem.* **2013a**, *13*, 1150−1159.

Gouveia, V.; Seca, A.M.L.; Barreto, M.C.; Neto, A.I.; Kijjoa, A.; Silva, A.M.S. Cytotoxic meroterpenes from the macroalga *Cystoseira abiesmarina*. *Phytochem. Lett*. **2013b**, *6*, 593−597.

Guiry, M.D. in Guiry, M.D. & Guiry, G. AlgaeBase. World-wide electronic publication. National University of Ireland, Galway. http://www.algaebase.org [searched 2018 Mar 20].

Gupta, S.C.; Kunnumakkara, A.B.; Aggarwal, S.; Aggarwal, B.B. Inflammation, a Double-Edge Sword for Cancer and Other Age-Related Diseases. *Front. Immunol*. **2018**, *27*, 9:2160.

Hussain, E.; Wang, L.; Jiang, B.; Riaz, S.; Butt, G.Y.; Shi, D. A review of the components of brown seaweeds as potential candidates in cancer therapy. *RSC Adv.* **2016**, *6*, 12592–12610.

Lane, A.L.; Stout, E.P.; Lin, A.S.; Prudhomme, J.; Le Roch, K.; Fairchild, C.R.; Franzblau, S.G.; Hay, M.E.; Aalbersberg, W.; Kubanek, J. Antimalarial bromophycolides J-Q from the Fijian red alga *Callophycus serratus*. *J. Org. Chem*. **2009**, *74*, 2736–2742.

Li, W.; Wang, Y.; Wang, X.; He, Z.; Liu, F.; Zhi, W.; Zhang, H.; Niu, X. Esculin attenuates endotoxin shock induced by lipopolysaccharide in mouse and NO production in vitro through inhibition of NF-κB activation. *Eur. J. Pharmacol.* **2016**, *791*, 726–734.

Lu, H.; Ouyang, W.; Huang, C. Inflammation, a key event in cancer development. *Mol. Cancer Res.* **2006**, *4*, 221–233.

Ma, Z. Yang, Y.; Fan, C.; Han, J.; Wang, D.; Di, S.; Hu, W.; Liu, D.; Li, X.; Reiter, R.J.; Yan, X. Melatonin as a potential anticarcinogen for non-small-cell lung cancer. *Oncotarget*. **2016***, 7*, 46768–46784.

Machado, F.L.; Ventura, T.L.; Gestinari, L.M.; Cassano, V.; Resende, J.A.; Kaiser. C.R.; Lasunskaia, E.B.; Muzitano, M.F.; Soares, A.R. Sesquiterpenes from the Brazilian Red

Alga *Laurencia dendroidea* J. Agardh. *Molecules* **2014**, *19*, 3181–3192.

Makvandi, M.; Sellmyer, M.A.; Mach, R.H. Inflammation and DNA damage: Probing pathways to cancer and neurodegeneration. *Drug Discov. Today Technol*. **2017**, *25*, 37–43.

Malumbres, M. Cell cycle-based therapies move forward. *Cancer Cell.* **2012**, *22*, 419–420.

Martin-Cordero, C.; Leon-Gonzalez, A.J.; Calderon-Montano, J.M.; Burgos-Moron, E.; Lopez-Lazaro, M. Pro-oxidant natural products as anticancer agents. *Curr. Drug Targets*. **2012**, *13*, 1006–1028.

McCoy, M.K.; Ruhn, K.A.; Blesch, A.; Tansey, M.G. TNF: a key neuroinflammatory mediator of neurotoxicity and neurodegeneration in models of Parkinson's disease. *Adv. Exp. Med. Biol.* **2011**, *691*, 539–540.

Medzhitov, R. Origin and physiological roles of inflammation. *Nature* **2008**, *454*, 428–435.

Murakami, A.; Ohigashi, H. Targeting NOX, INOS and COX-2 in inflammatory cells: chemoprevention using food phytochemicals. *Int. J. Cancer.* **2007**, *121*, 2357–2363.

Pan, M.H.; Lai, C.S.; Dushenkov, S.; Ho, C.T. Modulation of inflammatory genes by dietary flavonoids. *J. Agric. Food Chem*. **2009**, *57*, 4467–4477.

Pansanit, A.; Park, E.J.; Kondratyuk, T.P.; Pezzuto, J. M.; Lirdpra-pamongkol, K.; Kittakoop, P. Vermelhotin, an anti-inflammatory agent, suppresses nitric oxide production in RAW 264.7 cells via p38 inhibition. *J. Nat. Prod*. **2013**, *76*, 1824–1827.

Rios, E.C.; Soriano, F.G.; Olah, G.; Gerö, D.; Szczesny, B.; Szabo, C. Hydrogen sulfide modulates chromatin remodeling and inflammatory mediator production in response to endotoxin, but does not play a role in the development of endotoxin tolerance. *J. Inflamm (Lond)* **2016**, 13:10. DOI 10.1186/s12950-016-0119-2

Sansom, C.E.; Larsen, L.; Perry, N.B.; Berridge, M.V.; Chia, E.W.; Harper, J.L.; Webb, V.L. An antiproliferative bis-prenylated quinone from the New Zealand brown alga *Perithalia capillaris*. *J. Nat. Prod.* **2007**, *70*, 2042–2044.

Siegel, R.L.; Miller, K.D.; Jemal, A. Cancer statistics, 2018. *CA Cancer J. Clin*. **2018**, *68*, 7–30.

Skehan, P.; Storeng, R.; Scudiero, D.; Monks, A.; McMahon, J.; Vistica, D.; Warren, J. T.;

Bokesch, H.; Kenney, S.; Boyd, M.R.J. New colorimetric cytotoxicity assay for anticancer-drug screening. *Natl. Cancer Inst.* **1990**, *82*, 1107−1112.

Smyrniotopoulos, V.; Vagias, C.; Bruyère, C.; Lamoral-Theys, D.; Kiss, R.; Roussis, V. Structure and in vitro antitumor activity evaluation of brominated diterpenes from the red alga *Sphaerococcus coronopifolius*. *Bioorg. Med. Chem.* **2010**, *18*, 1321–1330.

Suffness, M.; Pezzuto, J.M. Assays related to cancer drug discovery. In: *Methods in Plant Biochemistry: Assays for Bioactivity* Hostettmann, K. (Ed.),; Academic Press, London, **1990**; vol. 6, pp. 71–133.

Tanaka, T.; Narazaki, M.; Kishimoto, T. IL-6 in inflammation, immunity, and disease. *Cold Spring Harb. Perspect Biol.* **2014**, *6*:a016295.

Teasdale, M.E.; Shearer, T.L.; Engel, S.; Alexander, T.S.; Fairchild, C.R.; Prudhomme, J.; Torres, M.; Le Roch, K.; Aalbersberg, W.; Hay, M.E.; Kubanek, J. Bromophycoic acids: bioactive natural products from a Fijian red alga *Callophycus sp*. *J. Org. Chem*. **2012**, *77*, 8000–8006.

Todoric, J.; Antonucci, L.; Karin, M. Targeting Inflammation in Cancer Prevention and Therapy. *Cancer Prev. Res. (Phila)* **2016**, *9*, 895–905.

Torre, L.A.; Bray, F.; Siegel, R.L.; Ferlay, J.; Lortet-Tieulent, J.; Jemal, A. Global Cancer Statistics, 2012. *CA Cancer J. Clin*. **2015**, *65*, 87–108

Valls, R.; Piovetti, L. The chemistry of the Cystoseiraceae (Fucales: Pheophyceae): Chemotaxonomic relationships. *Biochem. Syst. Ecol.* **1995**, *23*, 723−745.

Vizetto-Duarte, C.; Custódio, L.; Acosta, G.; Lago, J.H.G.; Morais, T.R.; Bruno de Sousa, C.; Gangadhar, K.N.; Rodrigues, M.J.; Pereira, H.; Lima, R.T.; Vasconcelos, M.H.; Barreira, L.; Rauter, A.P.; Albericio, F.; Varela, J. Can macroalgae provide promising anti-tumoral compounds? A closer look at *Cystoseira tamariscifolia* as a source for antioxidant and anti-hepatocarcinoma compounds. *Peer J*. **2016**, *4*, 1704, doi 10.7717/peerj.1704.

Wijesinghe, W.A.J.P.; Kang, M.C.; Lee, W.W.; Lee, H.S.; Kamada, T.; Vairappan, C.S.; Jeon, R.J. 5β-Hydroxypalisadin B isolated from red alga *Laurencia snackeyi* attenuates inflammatory response in lipopolysaccharide-stimulated RAW 264.7 macrophages. *Algae.* **2014**, *29*, 333–341.

Yoon, W.J.; Ham, Y.M.; Kim, S.S.; Yoo, B.S.; Moon, J.Y.; Baik, J.S.; Lee, N.H.; Hyun, C.G. Suppression of proinflammatory cytokines, iNOS, and COX-2 expression by brown algae *Sargassum micracanthum* in RAW264.7 macrophages. *Eurasia J. Biosci.* **2009,** *3*, 130–143.

Yoon, W.J.; Heo, S.J.; Han, S.C.; Lee, H.J.; Kang, G.J.; Kang, H.K.; Hyun, J.W.; Koh, Y.S.; Yoo, E.S. Anti-inflammatory effect of sargachromanol G isolated from *Sargassum siliquastrum* in RAW 264.7 Cells. *Arch. Pharm. Res.* **2012,** *35*, 1421–1430.

Yu, X.Q.; He, W.F.; Liu, D.Q.; Feng, M.T.; Fang, Y.; Wang, B.; Feng, L.H.; Guo, Y.W.; Mao, S.C. A seco-laurane sesquiterpene and related laurane derivatives from the red alga *Laurencia okamurai* Yamada. *Phytochemistry* **2014**, *103*, 162–170.

Zbakh, H.; Talero, E.; Avila, J.; Alcaide, A.; De los Reyes, C.; Zubía, E.; Motilva, V. The Algal Meroterpen 11-Hydroxy-11-O-Methylamentadione Ameloriates Dextran Sulfate Sodium-Induced Colitis in Mice. *Mar. Drugs.* **2016,** *14*, 1–14.

Zhao, M.; Cheng, S.; Yuan, W.; Dong, J.; Huang, K.; Sun, Z.; Yan, P. Further new xenicanes from a Chinese collection of the brown alga *Dictyota plectens*. *Chem. Pharm. Bull.* **2015**, *63*, 1081–1086.

7. The algal meroterpene 11-hydroxy-1′-*O*-methylamentadione ameloriates dextran sulfate sodium-induced colitis in mice

In this doctoral thesis we thought it was appropriate to complete our experiments by proving the responses of a selected AMT in an acute animal model of intestinal inflammation; this trial could also serve for a preliminary assessment of the potential acute systemic toxicity of the AMTs. These results have been published in: Zbakh et al., *Marine Drugs* **2016**, *14*, article 149.

Abstract: Inflammatory bowel disease (IBD) is a complex class of immune disorders. Unfortunately, a treatment for total remission has not yet been found, while the use of natural product-based therapies has emerged as a promising intervention. The present study was aimed to investigate the anti-inflammatory effects of the algal meroterpene 11-hydroxy-1′-*O*-methylamentadione (**2**, also AMT-E) in a murine model of dextran sodium sulphate (DSS)-induced colitis. AMT-E was orally administered daily (1, 10, and 20 mg/kg animal) to DSS treated mice (3% *w*/*v*) for 7 days. AMT-E prevented body weight loss and colon shortening and effectively attenuated the extent of the colonic damage. Similarly, AMT-E increased mucus production and reduced myeloperoxidase activity (marker for anti-inflammatory activity). Moreover, the algal meroterpene decreased the tumor necrosis factor (TNF)-α, interleukin (IL)-1β, and IL-10 levels, and caused a significant reduction of the expression of inducible nitric oxide synthase (iNOS) and cyclooxygenase-2 (COX-2). Our results demonstrate the protective effects of AMT-E on experimental colitis, provide an insight of the underlying mechanisms of this compound, and suggest that this class of marine natural products might be an interesting candidate for further studies on the prevention/treatment of IBD.

7.1. Introduction

Ulcerative colitis (UC) and Crohn's disease (CD) are two typical forms of inflammatory intestinal disease belonging to inflammatory bowel disease (IBD) (Mulder et al., 2014), which affect millions of people worldwide and carry a widespread health hazard

in modern society (Loftus et al., 2002). IBD is characterized by chronic and recurrent inflammatory disorders of the gastrointestinal tract (Papadakis et Targan, 200). Despite many years of extensive research, the aetiology and pathogenesis of IBD is not completely understood. It probably involves a complex interaction of several factors, including genetic susceptibility, immune disorders, bacterial flora within the intestinal environment, and environmental factors (Kaser et al., 2010). Therefore, the development of new, effective, and well-tolerated drugs for IBD therapy is necessary. Various models of experimental IBD have been developed to investigate the pathogenesis of this disease and may be used to test innovative approaches for therapy (Neurath et al., 2012). Among these models, experimental colitis induced by dextran sulphate sodium (DSS) has been widely used because it affords a high degree of uniformity and reproducibility of most lesions in the distal colon, and after 7 days of DSS administration the intestinal immune system is activated to generate, in a coordinated form, pro-inflammatory/anti-inflammatory cytokines (Talero et al., 2015). The pro-inflammatory cytokines amplify the inflammatory response by activating a cascade of immune cells such as neutrophils and macrophages. Infiltration of neutrophils results in the production of large amounts of cytotoxic reactive oxygen species, nitrogen metabolites, and lytic enzymes, which lead to severe inflammatory tissue injury, including mucosal disruption and ulceration (Yan et al., 2009).

Macroalgae produce a wide variety of bioactive compounds that offer great opportunities in the biomedical field (Hussain et al., 2016; Ioannou et Roussis, 2000; Smit, 2004). Although most research on the pharmacological potential of algal natural products has focused on cytotoxic and antimicrobial activities (Hussain et al., 2016; Murphy et al., 2014; Ioannou et Roussis, 2000), recent studies are also disclosing interesting properties of algae-derived extracts and natural products as anti-inflammatory agents (Dang et al., 2008; Na et al., 2005; Sansom et al., 2007; Tziveleka et al., 2005). Thus, we have recently described the *in vitro* anti-inflammatory activity of a series of meroterpenoids isolated from the brown alga *Cystoseira usneoides* (De los Reyes et al., 2016; De los Reyes et al., 2013). In particular, the meroditerpene 11-hydroxy-1′-*O*-methylamentadione (**2** or AMT-E) (Figure 7.1), which is one of the major natural products of this alga, showed significant activity as an inhibitor of the production of the pro-inflammatory cytokine TNF-α in LPS-stimulated THP-1 human macrophages (De los Reyes et al., 2013).

The promising *in vitro* activity exhibited by AMT-E led us to investigate the potential *in vivo* anti-inflammatory effect of this natural product on the experimental colitis induced by DSS. We have found that AMT-E exerts intestinal anti-inflammatory activity in the colitis by increasing mucus production, inhibiting neutrophil infiltration, down-regulating TNF-α, IL-1β, and IL-10, as well as suppressing COX-2 and iNOS expression in the mouse colon tissue.

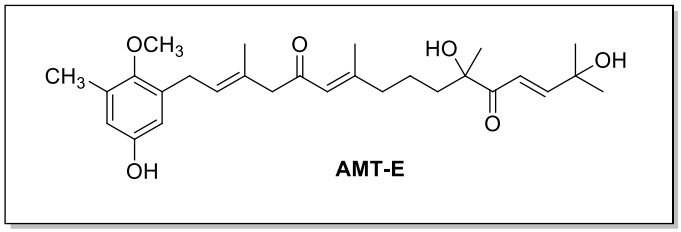

Figure 7.1. Chemical structure of the meroditerpene 11-hydroxy-1′-*O*-methylamentadione (AMT-E, **2**).

7.2. Materials and methods

7.2.1. Experimental animals

Seven-week-old female C57BL/6 mice weighing 18–20 g were purchased from Janvier Labs (France). Mice were housed on a regular 12 h light-dark cycle in a temperature (24–25 °C) and humidity (70%–75%) controlled room, and acclimated for 7 days. They were allowed free access to a laboratory diet (Panlab, Barcelona, Spain) and water *ad libitum*. The care and use of the animals and experimental protocol were approved by the Guidelines for the Animal Ethics Committee of the University of Seville, and all experiments in this study were carried out in accordance with the recommendations of the European Union regarding animal experimentation (Directive of the European Council 2010/63/EU).

7.2.2. Isolation of 11-hydroxy-1'-O-methylamentadione (AMT-E)

The meroditerpene AMT-E was isolated from the brown alga *Cystoseira usneoides* as previously described (De los Reyes et al., 2016). Briefly, the frozen alga was extracted with methanol, and after evaporation of the solution under reduced pressure, the aqueous residue was extracted with diethyl ether. The resulting extract was subjected to column

chromatography (CC) on silica gel eluted with a mixture of *n*-hexane/diethyl ether (50:50, *v*/*v*), diethyl ether, chloroform/methanol mixtures (90:10 and 80:20, *v*/*v*), and finally methanol. The fractions eluted with diethyl ether and chloroform/methanol (90:10, *v*/*v*) were further separated by CC using as eluents *n*-hexane/ethyl acetate mixtures (80:20 to 30:70, *v*/*v*), ethyl acetate, and finally methanol. Selected fractions were subjected to repeated separations in normal phase HPLC using as eluent *n*-hexane/ethyl acetate (60:40, *v*/*v*) and in reversed phase HPLC using as eluent methanol/water (70:30, *v*/*v*). The isolated compound was identified from its ^{1}H and ^{13}C NMR spectra (De los Reyes et al., 2013).

7.2.3. Induction of DSS colitis and treatments

Experimental colitis was induced by giving mice drinking water *ad libitum* containing 3% (*w*/*v*) DSS for 7 days. Mice of each of the groups were monitored carefully every day to confirm that they consumed an approximately equal volume of DSS-containing water. Animal body weights and water and food intake were recorded daily throughout all the experiments. On termination of the experiment on day eight, mice were killed by cervical dislocation. Colons were removed aseptically, slightly cleaned in physiological saline to remove faecal residues, weighed, and measured. Afterwards, the excised colons were cut longitudinally and small pieces from the middle to distal colon (areas of visible and inflammatory damage) were blotted dry, immediately frozen with liquid nitrogen, and stored at −80 °C until use.

Mice were divided randomly into five groups (twelve animals per group): (i) Sham group, which received drinking water, without DSS, throughout the experimental period (Sham); (ii) control group of induced colitis by DSS (DSS), and (iii–v) DSS groups treated with the compound AMT-E once a day during the 7 days at the doses of 1, 10 and 20 mg/kg body weight and named AMT-E (1), AMT-E (10) and AMT-E (20), respectively. AMT-E was dissolved in vehicle consisting of 0.9% saline solution and 1% Tween-80 (Sigma-Chemical Co., St. Louis, MO, USA) and was administered by oral gavage. Both Sham and DSS groups received equal vehicle (0.9% saline solution/1% Tween-80) on the same schedule as AMT-E. All efforts were made to minimize the animals suffering and to reduce the number of animals used. The doses of AMT-E were chosen on the basis of literature with marine meroterpenoids in animal models of inflammation (Ferrándiz et al., 1994;

Busserolles et al., 2005), including intestinal inflammation by DSS (Yamada et al., 2014), and also in a short-preliminary experiment in our lab to acquire safety and efficacy in the DSS model of colitis. Criteria about potential translation of results from animal to humans were considered (Reagan-Shaw et al., 2008).

7.2.4. Histological studies

For histological examination (4 animals per group), small sections (1 cm, approximately) from the middle to distal colon were excised and fixed in 4% paraformaldehyde in phosphate-buffered saline (PBS, pH 7.4), dehydrated by increasing concentrations of ethanol, and embedded in paraffin. Thereafter, sections of tissue were cut at 5 μm on a rotary microtome (Leica Microsystems, Wetzlar, Germany), mounted on clean glass slides and dried overnight at 37 °C. Sections were cleared, hydrated, and stained with haematoxylin and eosin, and Alcian blue for histological evaluation of colonic damage and mucus content, respectively, according to standard protocols; slides were coded to prevent observer bias during evaluation. All tissue sections were examined in an Olympus BH-2 microscope (GMI, Minnesota, USA) for characterization of histopathology changes. The tissues were analysed by a blinded observer to establish a composite Histological Score as previously described (Talero et al., 2015), where researchers do not know the origin of the sample, except the coordinator. Criteria included mucosal architecture (0, absent; 1, mild; 2, medium; 3, severe), cellular infiltration (0, none; 1, infiltrate around the crypt basis; 2, infiltrate reaching the muscularis mucosae; 3, infiltrate reaching the submucosa), and goblet cell depletion (0, absent; 1, present). The results were expressed as the average scores of the 3 colonic sections.

7.2.5. Myeloperoxidase activity assay

Myeloperoxidase (MPO) is an enzyme found in neutrophils and, in much smaller quantities, in monocytes and macrophages. The MPO activity according to the method of Grisham et al., 1990 was used as a convenient and valuable tool for evaluating neutrophil infiltration in the colon tissue. The colonic tissue samples were thawed, weighed, and homogenized in 10 volumes of 50 mM PBS, pH 7.4. The homogenate was centrifuged at 20,000× *g* for 20 min at 4 °C. The pellet was again homogenized in 10 volumes 50 mM PBS at pH 6.0, containing 0.5% hexadecyl trimethylammonium bromide (HETAB) and 10

mM EDTA. This homogenate was subjected to three cycles of freezing/thawing and a brief period of sonication. About 50 μL of homogenate sample was added to a 96-well microplate and incubated at 37 °C for 3 min with a mixture containing 0.067% *O*-dianisidine dihydrochloride, 0.5% HETAB, and 0.3 mM hydrogen peroxide. The changes in absorbance at 655 nm were measured with a microplate reader (Labysistem Multiskan EX, Helsinki, Finland). One unit of MPO activity was defined as the amount of enzyme present that produced a change in absorbance of 1.0 U/min at 37 °C in the final reaction volume containing the acetate. The results were expressed as U/mg tissue.

7.2.6. Cytokines assay

Colonic samples for cytokine determinations (TNF-α, IL-1β, and IL-10) were weighed and homogenized at 4 °C after thawing, in a lysis buffer (1:5 *w*/*v*) containing PBS (pH 7.2), 1% bovine serum albumin (BSA), 0.01 mg/mL leupeptin, 0.01 mg/mL pepstatin, 0.01 mg/mL aprotinin, and 1 mM phenylmethylsulfonyl fluoride (PMSF). Then, the tubes were centrifugated at 12,000× *g* for 10 min at 4 °C; the supernatants were frozen at −80 °C until assay. Cytokines levels in frozen colonic tissue biopsy samples were measured with a commercially available ELISA kit (Diaclone, Besançon, France) according to the manufacturer's instructions and then were expressed as nanograms per milligram of tissue.

7.2.7. Extraction of cytoplasmic proteins and western blot analysis

Frozen colonic tissues were weighed and homogenized in ice-cold lysis buffer (50 mM Tris HCl, pH 7.5, 8 mM MgCl2, 5 mM ethylene glycol bis (2-aminoethyl ether)-*N*,*N*,*N*′*N*′-tetraacetic acid (EGTA), 0.5 mM EDTA, 0.01 mg/mL leupeptin, 0.01 mg/ml pepstatin, 0.01 mg/mL aprotinin, 1 mM PMSF, and 250 mM NaCl). Homogenates were incubated for 10 min on ice and centrifuged (12,000× *g* for 15 min at 4 °C), and the supernatants were collected and stored at −80°C. Protein concentration in the supernants was determined following colorimetric method of Bradford with gamma globulin as the standard (Bradford, 1976). Equal amounts of protein (50 μg) were then separated on 10% acrylamide gel by sodium dodecyl sulphate-polyacrylamide gel electrophoresis. In the next step, the proteins were electrophoretically transferred onto nitrocellulose membrane at 120 mA for 90 min. The membranes were then blocked in PBS-Tween 20 containing 5% w/v defatted milk. Later, the membranes were incubated with specific primary antibodies, rabbit

anti-COX-2 and anti-iNOS (Cayman Chemical, Ann Arbour, MI), at 4 °C overnight and 1:1000 dilution. To prove equal loading, the blots were analysed for β-actin expression using an anti-β-actin antibody (Sigma-Aldrich, St. Louis, MO, USA). Each membrane was washed three times for 15 min and incubated with the secondary horseradish peroxidase-linked anti-rabbit (Pierce Chemical, Rockford, IL) for 60 min at room temperature. After washing the membranes again three times, the immunodetection was performed using an enhanced chemiluminescence light-detecting kit (Super-Signal West Pico Chemiluminescent Substrate, Pierce, IL, USA). Densitometric data were studied following normalization to the control (house-keeping gene). The signals were analysed and quantified with Scientific Imaging Systems (Biophotonics Image J Analysis Software).

7.2.8. Statistical analysis

All data are expressed as arithmetic means ± standard error of the mean (S.E.M.) Data were evaluated with GraphPad Prism® Version 5.00 software. The statistical significance of any difference in each parameter among the groups was evaluated by one-way analysis of variance (ANOVA) followed by Tukey test. p values of <0.05 were considered statistically significant. In the experiment involving histology, the figures shown are representative of at least three experiments performed on different days.

7.3. Results

7.3.1. AMT-E treatment protects mice against DSS-induced acute colitis

To determine the potential *in vivo* anti-inflammatory effect of AMT-E, we tested this compound using the DSS model of acute intestinal inflammation. It is worth noting that neither DSS nor the different AMT-E treatments caused changes in the relative weights and appearance of organs such as the liver, kidneys, and heart, which are highly susceptible to drug toxicity. However, as shown in Table 7.1, mice that were treated with DSS showed a marked colon shortening in relation to Sham animals ($p < 0.001$) (Table 7.1 and Figure 7.2. a,b). This effect is indicative of the presence of inflammation. AMT-E treatments modified this effect and the highest dose of the compound (20 mg/kg) was able to significantly prevent DSS-induced colon shortening ($p < 0.01$) (Table 7.1 and Figure 7.2e). Moreover, mice that were treated with DSS showed a progressive loss of body weight, with

fluctuations typical of this type of experiment, during the 7 days that the study lasted (Figure 7.2f). Mice treated with AMT-E were protected from this marked loss of body weight, with significant response from day three to the end, and for the three doses tested.

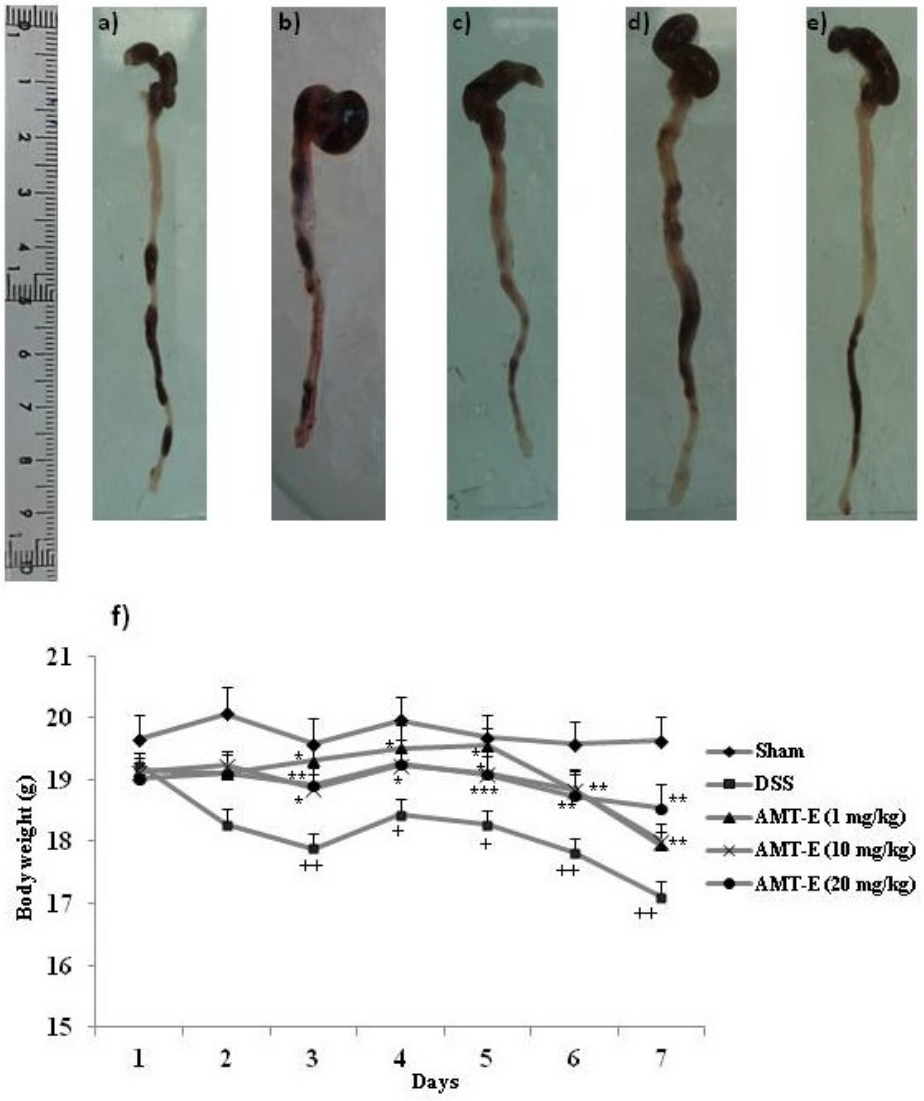

Figure 7.2. 11-hydroxy-1′-*O*-methylamentadione (AMT-E) protect mice against dextran sodium sulphate (DSS)-induced colitis. (**a**–**e**) Representative macroscopic appearance of the colon in (**a**) Sham group (**b**) mice treated with DSS and (**c**–**e**) mice receiving DSS plus AMT-E (1, 10, and 20 mg/kg p.o., respectively). (**f**) Change in bodyweight during the study. Data are expressed as the means ± SEM. Statistical significance between Sham and DSS groups was determined by Student's *t* test. The statistical differences between DSS and treatments groups were determined by oneway ANOVA followed by Bonferroni post-hoc test. $^{+}$ $p < 0.05$ and $^{++}$ $p < 0.01$ vs. Sham group; * $p < 0.05$, ** $p < 0.01$ and *** $p < 0.001$ vs. DSS group.

Table 7.1. Effects of AMT-E (1, 10, and 20 mg/kg p.o.) on colonic length in dextran sodium sulphate (DSS)-treated mice

Treatments (n = 12)	Sham [a]	DSS [b]	AMT-E [c] (1 mg/kg)	AMT-E [c] (10 mg/kg)	AMT-E [c] (20 mg/kg)
Colonic length (cm)	7.93 ± 0.16	6.02 ± 0.12 $^{+++}$	6.19 ± 0.10	7.00 ± 0.14	7.03 ± 0.16 **

[a] Sham group, receiving vehicle; [b] Group treated with DSS (3%) in drinking water, for 7 consecutive days; [c] Treated with DSS (3%) in drinking water and with AMT-E (1, 10, or 20 mg/kg, p.o.), for 7 consecutive days. Data are means ± S.E.M and were analysed by one-way ANOVA followed by Tukey test for comparison between groups. $^{+++}$ $p < 0.001$ vs. Sham group; ** $p < 0.01$ vs. DSS group.

7.3.2. AMT-E alleviates microscopic colon damage and increases mucus production

Histological examination and results from the histopathological score for all groups are shown in Figure 7.3 and Table 7.2. Colons from Sham mice revealed typical features of normal structure (Figure 7.3a). Consistent with the macroscopic changes, where DSS-treated mice showed inflammation in the medial-distal area of the colon, this was also evident after the microscopic analysis involving all layers of the bowel wall (score 3.93 ± 0.2, Table 7.2); extensive granulation tissue with the presence of a massive neutrophilic infiltration, fibroblasts and lymphocytes was also apparent, mainly in the mucosa and submucosa; necrosis of epithelium, distortion of crypts, and partial destruction of the glands were also detected (Figure 7.3c); Alcian blue staining, which detects acid mucin-positive goblet cells, revealed remarkable mucin depletion in ulcerative areas of DSS-treated animals (Figure 7.3d) compared with Sham mice (Figure 7.3b). By contrast, the histological sections of the AMT-E–treated animals (Figure 7.3e,g,i) showed an improvement in the microscopic features of colitis at all the doses used, evidenced by a preservation of the colonic mucosa structure and a reduction of inflammatory cells in the lamina propria when compared to DSS group. Moreover, Alcian blue-positive goblet cells were clearly observed in preserved regions of the mucosal layer in mice treated (Figure 7.3f,h,j). This analysis provides a score of 2.34 ± 0.1, 2.12 ± 0.2, and 1.82 ± 0.2 for AMT-E doses of 1, 10, and 20 mg/kg respectively ($p < 0.05$ vs. DSS group; Table 7.2).

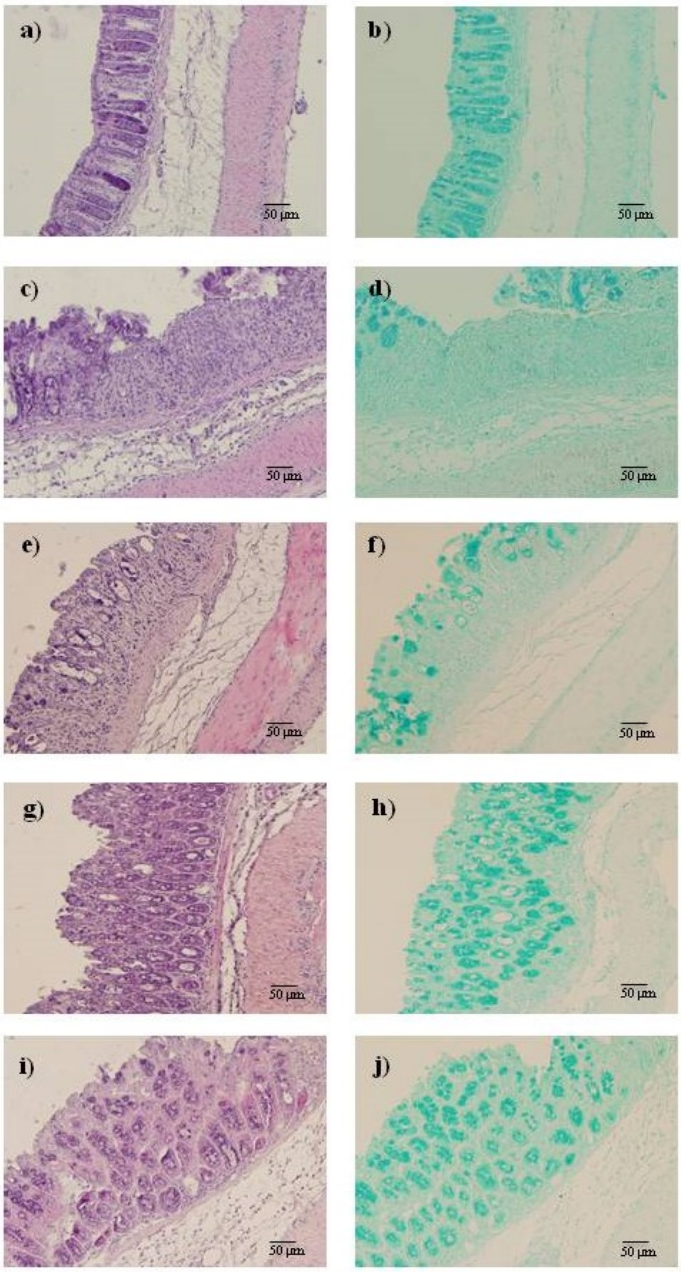

Figure 7.3. 11-hydroxy-1′-*O*-methylamentadione (AMT-E) administration attenuates microscopic colon damage induced by dextran sulfate sodium (DSS); this effect is detected in Haematoxylin/Eosin and also in Alcian Blue stain sections where positive goblet cells were more clearly observed in preserved regions of the mucosal layer in mice treated with different dose of AMT-E. Histological appearance of samples taken from middle to distal colon of mice: (**a**,**b**) Sham group; (**c**,**d**) DSS group; (**e**,**f**) DSS plus AMT-E (1 mg/kg, p.o.); (**g**,**h**) DSS plus AMT-E (10 mg/kg, p.o.) and (**i**,**j**) DSS plus AMT-E (20 mg/kg, p.o.). Original magnification X200.

Table 7.2. Effects of AMT-E on histological hcore in the dextran sodium sulphate (DSS) model

Treatments	Sham	DSS	AMT-E (1 mg/kg)	AMT-E (10 mg/kg)	AMT-E (20 mg/kg)
Colitis score	0	3.93 ± 0.2 *	2.34 ± 0.1 †	2.12 ± 0.2 †	1.82 ± 0.2 †

The criteria used for the histopathological scoring and immunostaining evaluation of colonic mucosa are described in the Experimental Section. Data are expressed as the means ± SEM. * $p < 0.05$ versus respective Sham group. † $p < 0.05$ versus DSS group.

7.3.3. AMT-E attenuates MPO levels in DSS-induced colitis in mice

The histopathology study indicated that a mechanism underlying the protective effects of AMT-E involved a reduced infiltration of inflammatory cells into the colonic mucosa. Thus, colon inflammation was quantitatively evaluated by MPO activity. As shown in Figure 7.4, DSS induced a significant increase in colon MPO activity from 0.07 ± 0.003, a basal concentration, to 0.11 ± 0.006 U/mg tissue ($p < 0.001$ vs. Sham group) after 7 days of DSS administration. The treatment with AMT-E at the doses of 10 and 20 mg/kg significantly suppressed the degree of polymorphonuclear neutrophil infiltration in colon tissue (0.09 ± 0.007 and 0.07 ± 0.0006 U/mg tissue, respectively, $p < 0.01$ vs. DSS group), Figure 7.4.

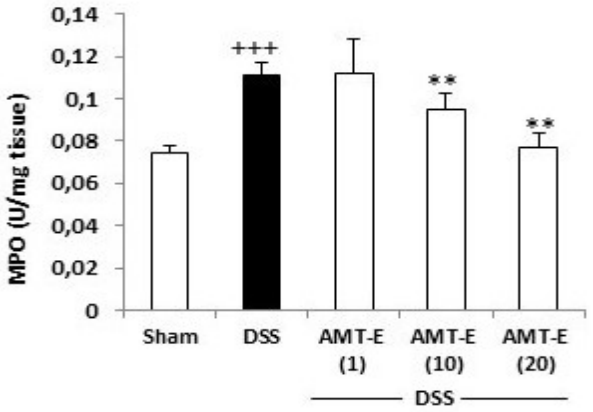

Figure 7.4. 11-hydroxy-1′-*O*-methylamentadione (AMT-E) administration reduces leukocyte infiltration. Myeloperoxidase activity (MPO, U/mg tissue) was quantified in mice treated with DSS alone or mice receiving DSS plus AMT-E (1, 10, and 20 mg/kg, p.o.). The Sham group received vehicle in an equal volume. Data are expressed as the means ± SEM. Statistical significance between Sham and DSS groups was determined by Student's t test. The statistical differences between DSS and AMT-E treated groups were determined by oneway ANOVA followed by Bonferroni *post-hoc* test. +++ $p < 0.001$ vs. Sham group. ** $p < 0.01$ vs. DSS group.

7.3.4. Effects of AMT-E on the production of cytokines in the colon of DSS-treated mice

To investigate the influence of AMT-E on cytokines production, we measured the levels of pro-inflammatory (TNF-α and IL-1β) and anti-inflammatory (IL-10) cytokines in the colonic tissue from different treatment groups. As shown in Figure 7.5, the levels of TNF-α and IL-1β were increased in the colon tissues from DSS-treated mice compared to that in control animals. Furthermore, the administration of AMT-E at a dose of 20 mg/kg significantly reduced the levels of these cytokines by 60% ($p < 0.01$) and 67% ($p < 0.001$), respectively, with respect to DSS group (Figure 7.5a,b). As regards IL-10, this cytokine was up-regulated in DSS-treated mice compared with Sham group. Interestingly, 10 and 20 mg/kg of AMT-E resulted in a significant decrease of IL-10 values compared with DSS group (Figure 7.5c).

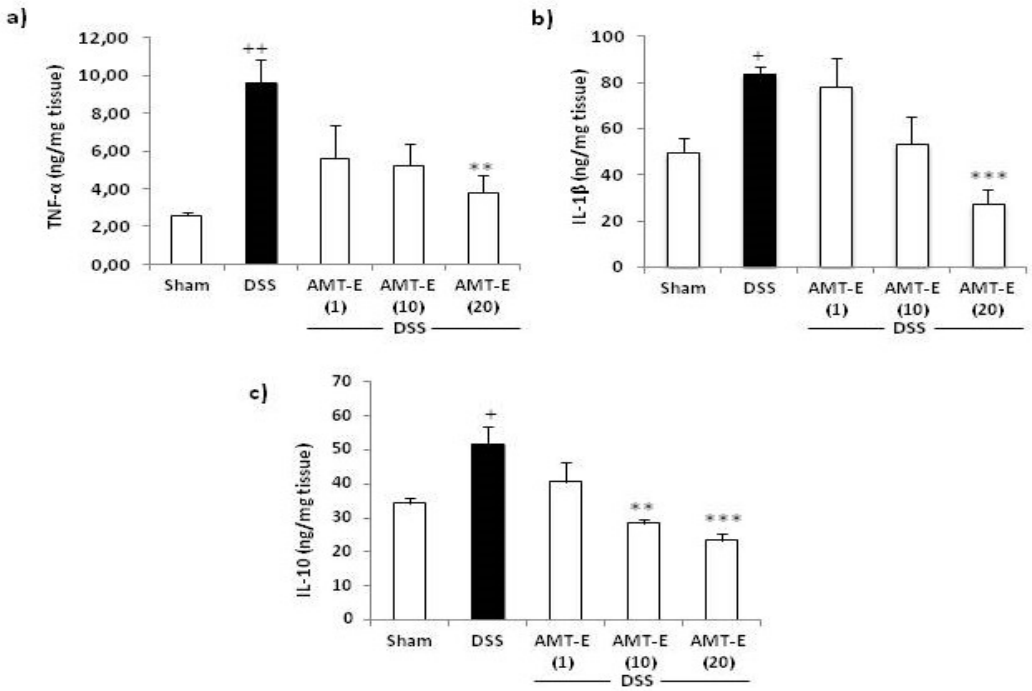

Figure 7.5. Effects of 11-hydroxy-1'-*O*-methylamentadione (AMT-E) administration on cytokine levels of colonic tissue in DSS-induced colitis. (**a**) TNF-α levels (ng/mg tissue); (**b**) IL-β levels (ng/mg tissue), and (**c**) IL-10 levels (ng/mg tissue), were quantified in mice treated with DSS alone and in those receiving DSS plus AMT-E (1, 10, and 20 mg/kg, p.o.). The Sham group received vehicle in an equal volume. Data are expressed as the means ± SEM. Statistical significance between Sham and DSS groups was determined by Student's t test. The statistical differences between DSS and AMT-E treated groups were determined by oneway ANOVA followed by Bonferroni *post-hoc* test. $^{+}$ $p < 0.05$ and $^{++}$ $p < 0.01$ vs. Sham. ** $p < 0.01$ and *** $p < 0.001$ vs. DSS group.

7.3.5. AMT-E downregulates the expression of COX-2 and iNOS in colonic mucosa

The effect of AMT-E on the expression levels of COX-2 and iNOS in cytosolic extracts from colonic mucosa was evaluated by Western blot analysis. The expression of both proteins was significantly increased in the colon tissues from DSS-treated mice compared with those in control mice ($p < 0.01$). However, administration of AMT-E significantly reduced the DSS-induced expression of COX-2 and iNOS that were decreased to basal levels with different doses of AMT-E (Figure 7.6).

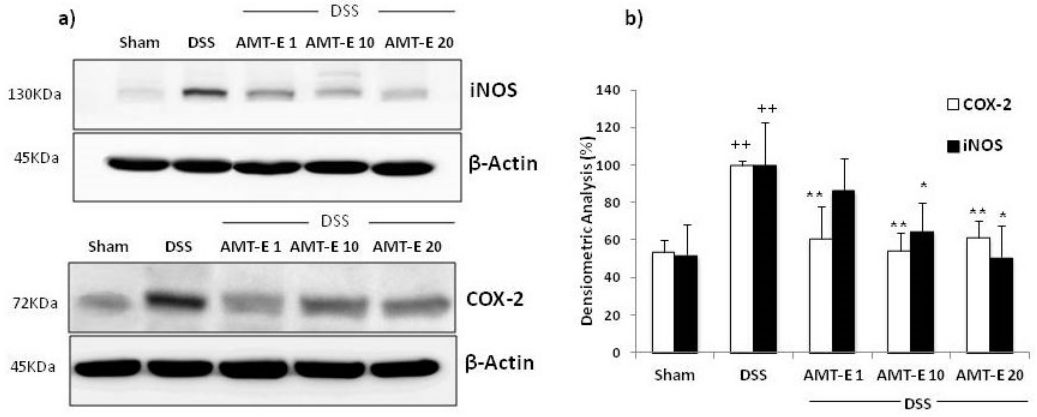

Figure 7.6. 11-hydroxy-1'-*O*-methylamentadione (AMT-E) administration reduces colonic protein levels of COX-2 and iNOS enzymes in DSS-induced colitis. (**a**) Representative western blot analysis of COX-2 ($n = 5$) and iNOS ($n = 4$) proteins. (**b**) Densitometric data were studied following normalization to the control (housekeeping gene, β-Actin). Data are expressed as the means ± SEM. Statistical significance between Sham and DSS groups was determined by Student's *t* test. The statistical differences between DSS and AMT-E treated groups were determined by oneway ANOVA followed by Bonferroni *post-hoc* test. $^{++}$ $p < 0.01$ vs. Sham group. * $p < 0.05$ and ** $p < 0.01$ vs. DSS group.

7.4. Discussion

IBD is a group of inflammatory conditions of the gastrointestinal tract with the two major types including ulcerative colitis (UC) and Crohn's disease (CD). The standard therapy for IBD includes mainly immunomodulatory agents, although their use entails severe side effects such as hormonal disturbance, peptic ulcer, liver dysfunction, and psychological problems (Baumgart et Sandborn, 2007). Therefore, the need for alternative therapeutic approaches is an emerging strategy.

Algae have been used in traditional medicine to treat a variety of diseases (Tseng et Chang, 1984), including gastrointestinal disorders such as vomiting, haemorrhoids, and dyspepsia (Ko et al., 2014). Further, the protective effects of the alga *Sargassum pallidum* (Lee et al., 2010) and of the extracts of the alga *Laminaria japonica* (Ko et al., 2014) on IBD have recently been reported. In this context, the *in vitro* anti-inflammatory activity detected for the natural products isolated from the brown alga *Cystoseira usneoides* (De los Reyes et al., 2016; De los Reyes et al., 2013) prompted us to evaluate the possible beneficial effects of AMT-E, one of the major active meroterpenoids of the alga, in an experimental model of colitis. The results have demonstrated that the treatment with this compound protected mice from the severity of DSS-induced colitis.

The DSS model mimics many of the features of human UC, such as diarrhoea, bloody faeces, body weight loss, mucosal ulceration, and shortening of colon length (Strober et al., 2002). In the current study, based in an induction of damage by DSS for seven days and finished on day eight, oral administration of AMT-E (1, 10, and 20 mg/kg) significantly suppressed DSS-induced colitis, preventing body weight loss, colon shortening, and the extent of intestinal inflammation, although we did not observe rectal bleeding in any group assayed, nor differences in diarrheal stool between groups that received DSS (control and treated). In addition, microscopic analysis of the colon confirmed data from the macroscopic study, reflecting attenuation of the mucosal disruption and oedema after treatment with AMT-E. The *in vivo* anti-inflammatory effects of a few marine meroterpenoids, including avarol, avarone, and a series of polyprenylhydroquinones, have been previously demonstrated by using the TPA-induced ear edema or the carrageenan-induced paw edema experimental models (Lucas et al., 2003; Terencio et al., 1998; Gil et al., 1995; Ferrándiz et al., 1994). More recently, the effects on experimental IBD have been described for bolinaquinone (Busserolles et al., 2005), a sesquiterpene quinone isolated from a sponge of the genus *Dysidea*, and zonarol (Yamada et al., 2014), a sesquiterpene hydroquinone isolated from the brown alga *Dictyopteris undulata* (Figure 7.7). In particular, zonarol has been described to protect mice against DSS-induced UC via the inhibition of both inflammation and apoptosis. In agreement with our findings, zonarol-treated mice (20 mg/kg/day) also exhibited significantly suppressed DSS-induced colon shortening (Yamada et al., 2014). On the other hand, bolinaquinone (20

mg/kg/day) was found to protect mice against trinitrobenzene sulphonic acid (TNBS)-induced colonic inflammation (Busserolles et al., 2005).

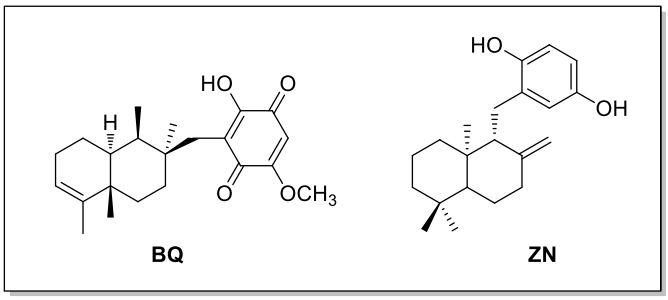

Figure 7.7. Chemical structures of marine meroterpenoids tested on inflammatory bowel disease (IBD) experimental models: bolinaquinone (BQ) (Busserolles et al., 2005) and zonarol (ZN) (Yamada et al., 2014)

Intestinal goblet cells produce the intestinal mucus, formed mainly by mucus glycoproteins or mucins. The intestinal mucus layer completely fills the crypts and acts both as a lubricant and as a physical barrier that protect the intestinal epithelial layer from injurious luminal stimulants (Ermund et al., 2013). Altered goblet cell physiology is considered as a hallmark of IBD pathology (Kaser et al., 2014). Further, clinical trials have indicated that IBD patients have decreased numbers of goblet cells and reduced mucus thickness (Oehlers et al., 2012). The histological findings from our study revealed mucin-depleted crypts in mice with DSS-induced colitis, as attested by the loss of Alcian blue-stained goblet cells. Interestingly, treatments with AMT-E allows an accumulation of mucus inside goblet cells, which suggests a protective effect of this compound on the colonic epithelial damage that occurs in colitis. Our results are in line with those reported for bolinaquinone, which given at a dose of 20 mg/kg ameliorated the signs of TNBS-induced colitis, as assessed by histological examination of the colon (Busserolles et al., 2005). However, the sesquiterpene hydroquinone zonarol did not significantly affect the number or size of mucus-producing goblet cells, as confirmed by Alcian blue or PAS staining (Yamada et al., 2014).

In IBD, the disruption of the epithelial barrier implies the deregulation of the innate immune system by commensal flora, but also defects in the adaptive immune system (Strober et al., 2002). One of the most prominent histological features observed in IBD is

neutrophil infiltration into the inflamed mucosa and subsequently into the intestinal lumen, resulting in the formation of the so-called crypt abscesses (Naito et al., 2007). During intestinal inflammation, neutrophils also contribute to the recruitment of other immune cells and facilitate mucosal healing by releasing inflammatory cytokines necessary for the resolution of inflammation (Soehnlein et Lindbom 2010]. In the present study, we have shown that MPO activity, an index of tissue-associated neutrophil accumulation, was significantly increased in the colonic mucosa after DSS administration. However, oral administration of AMT-E ameliorated polymorphonuclear infiltration into the colon, as evidenced by the suppression of colonic MPO activity as well as the improvement of histological features. These results suggest that inhibition of neutrophil accumulation by this meroterpene may be one of the protective mechanisms involved in reducing DSS-induced colonic mucosal injury.

To better understand the mechanism by which AMT-E ameliorates the DSS-induced colitis, we assessed the colonic production of the inflammatory cytokines TNF-α and IL-1β and the anti-inflammatory cytokine IL-10. Pro-inflammatory cytokines are known to play a pivotal role in the initiation and progression of the intestinal mucosa inflammation and immunity in IBD (Treiner, 2015). TNF-α may contribute to the induction of adhesion molecules and the expression of chemokines, resulting in an influx of inflammatory cells. Anti-TNF-α strategies are largely used in the clinical treatment of IBD (Scaldaferri et al., 2010), and the emerging data indicate that early use of anti-TNF-α antibodies leads to better long-term outcome in IBD patients by preventing mucosal damage (Gisbert et Chaparro 2015; Strober et al., 2002). The significance of increased IL-1β secretion in IBD has been also well-documented, and increased levels of IL-1β mRNA have been implicated in the production of many other inflammatory cytokines and also in the majority of IBD patients (Coccia et al., 2012; Häuser et al., 2011). In the present study, the administration of AMT-E potently down-regulated the expression of these pro-inflammatory cytokines. Our results on the anti-inflammatory capacity of AMT-E are related to previous findings for zonarol, which has also been shown to inhibit the production of the pro-inflammatory cytokine TNF-α in DSS mice (Yamada et al., 2014), and bolinaquinone, which was found to reduce the levels of IL-1β in the TNBS model of intestinal damage (Busserolles et al., 2005). Concerning IL-10, this cytokine is an essential immune component in the intestinal tract,

down-regulating the inflammatory process and helping to restore tissue homeostasis (Shah et al., 2012). In animal models, a paper by Kuhn et al., 1993 reported that IL-10-deficient mice developed chronic enterocolitis that can be prevented by administration of IL-10. Our group has also observed in this type of mice the spontaneous develop of chronic colitis and adenocarcinoma through a dysplasia sequence (Talero et al., 2016), and the reversal effects of experimental colitis by different treatments (Talero et al., 2008; Camacho-Barquero et al., 2007). In the present study, the levels of IL-10 in the colon were found to be significantly increased in DSS mice and reduced in animals with higher doses, comparable to sham. This response suggests that the lower presence of pro-inflammatory cytokines by treatment do not trigger IL-10 production, and confirms less inflammation and lower hyperactive immune response.

Previous research on IBD has demonstrated that Th1/Th2 derived cytokines not only regulate their own synthesis, but also the expression of mediators and enzymes, including cyclooxygenase-2 (COX-2) and inducible nitric oxide synthase (iNOS) (Neurath, 2012). COX-2 and iNOS enzymes represent important molecular targets in IBD prevention and treatment. In active inflammation, cell destruction and increased permeability allow bacteria to enter the lamina propria. Inflammatory cytokines and bacterial antigens induce and drive the transcription of both COX-2 and iNOS. These two pro-inflammatory enzymes are also up-regulated in experimental colitis (Talero et al., 2008) and in active human IBD (Cirillo et al., 2009). The expression and activity of these enzymes is associated with disease severity and involves them as potential anti-inflammatory drug targets. Our data clearly demonstrated that the colonic damage was associated with a higher expression of both COX-2 and iNOS proteins that were clearly reduced by AMT-E treatment. In line with our results, the marine meroterpenoid bolinaquinone has been reported to inhibit COX-2 and iNOS expression (Busserolles et al., 2005), while zonarol has only been shown to decrease the levels of iNOS expression in mice with DSS-induced UC (Yamada et al., 2014).

7.5. Conclusion

In summary, our results have demonstrated for the first time that AMT-E, a natural product isolated from the alga *C. usneoides*, is effective in the protection against

experimental colitis. The beneficial effects are mainly associated with macroscopic and microscopic data, and also with the markers of inflammation studied. Future studies are ensured, depending on the availability of AMT-E, that will investigate deeper into the molecular mechanism by which AMT-E decreases intestinal inflammation as well as into the preventive ability of the compound in a nutraceutical approach, or the responses in chronic intestinal inflammation models. In any case, the set of effects allows us to assess the *in vivo* pharmacological properties of AMT-E, providing valuable information toward the development of new therapeutic molecules from macroalgae with potential benefits in inflammatory bowel disease.

7.6. References

Baumgart, D.C.; Sandborn, W.J. Inflammatory bowel disease: Clinical aspects and established and evolving therapies. *Lancet* **200**, *369*, 1641–1657.

Bradford, M.M. A rapid and sensitive method for the quantitation of microgram quantities of protein utilizing the principle of protein-dye binding. *Anal. Biochem.* **1976**, *72*, 248–254.

Busserolles, J.; Payá, M.; D'Auria, M.V.; Gomez-Paloma, L.; Alcaraz, M.J. Protection against 2,4,6-trinitrobenzenesulphonic acid-induced colonic inflammation in mice by marine natural products bolinaquinone and petrosaspongiolide. *Biochem. Pharmacol.* **2005**, *69*, 1433–1440.

Camacho-Barquero, L.; Villegas, I.; Sanchez-Calvo, J.M.; Talero, E.; Sanchez-Fidalgo, S.; Motilva, V.; Alarcón de la Lastra, C. Curcumin, a *Curcuma longa* constituent, acts on MAPK p38 pathway modulating COX-2 and iNOS expression in chronic experimental colitis. *Int. Immunopharmacol.* **2007**, *7*, 333–342.

Cirillo, C.; Sarnelli, G.; Esposito, G.; Grosso, M.; Petruzzelli, R.; Izzo, P.; Calì, G.; D'Armiento, F.P.; Rocco, A.; Nardone, G.; Iuvone, T.; Steardo, L.; Cuomo, R. Increased mucosal nitric oxide production in ulcerative colitis is mediated in part by the enteroglial-derived S100B protein. *Neurogastroenterol. Motil.* **2009**, *21*, 1209–1112.

Coccia, M.; Harrison, O.J.; Schiering, C.; Asquith, M.J.; Becher, B.; Powrie, F.; Maloy, K.J. IL-1β mediates chronic intestinal inflammation by promoting the accumulation of IL-17A secreting innate lymphoid cells and CD4+ Th17 cells. *J. Exp. Med.* **2012**, *209*, 1595–1609.

Dang, H.T.; Lee, H.J.; Yoo, E.S.; Shinde, P.B.; Lee, Y.M.; Hong, J.; Kim, D.K.; Jung, J.H. Anti-inflammatory constituents of the red alga *Gracilaria verrucosa* and their synthetic analogues. *J. Nat. Prod.* **2008**, *71*, 232–240.

De los Reyes, C.; Ortega, M.J.; Zbakh, H.; Motilva, V.; Zubía, E. *Cystoseira usneoides*: A brown alga rich in antioxidant and anti-inflammatory meroditerpenoids. *J. Nat. Prod.* **2016**, *79*, 395–405.

De los Reyes, C.; Zbakh, H.; Motilva, V.; Zubía, E. Antioxidant and anti-inflammatory meroterpenoids from the brown alga *Cystoseira usneoides*. *J. Nat. Prod*. **2013**, *76*, 621–629.

Ermund, A.; Schutte, A.; Johansson, M.E.; Gustafsson, J.K.; Hansson, G.C. Studies of mucus in mouse stomach, small intestine, and colon. I. Gastrointestinal mucus layers have different properties depending on location as well as over the Peyer's patches. *Am. J. Physiol. Gastrointest. Liver Physiol.* **2013**, *305*, 341–347.

Ferrándiz, M.L.; Sanz, M.J.; Bustos, G.; Payá, M.; Alcaraz, M.J.; De Rosa, S. Avarol and avarone, two new anti-inflammatory agents of marine origin. *Eur. J. Pharmacol.* **1994**, *253*, 75–82.

Gil, B.; Sanz, M.J.; Terencio, M.C.; De Giulio, A.; De Rosa, S.; Alacaraz, M.J.; Payá, M. Effects of marine 2-polyprenyl-1,4-hydroquinones on phospholipase A2 and some inflammatory responses. *Eur. J. Pharmacol.* **1995**, *285*, 281–288.

Gisbert, J.P.; Chaparro, M. Use of a third anti-TNF after failure of two previous anti-TNFs in patients with inflammatory bowel disease: Is it worth it? *Scand. J. Gastroenterol.* **2015**, *30*, 1–8.

Grisham, M.B.; Benoit, J.N.; Granger, D.N. Assessment of leukocyte involvement during ischemia and reperfusion of intestine. *Methods Enzymol.* **1990**, *186*, 729–742.

Häuser, W.; Schmidt, C.; Stallmach, A.; Depression and mucosal proinflammatory cytokines are associated in patients with ulcerative colitis and pouchitis—A pilot study. *J. Crohns Colitis* **2011**, *5*, 350–353.

Hussain, E.; Wang, L.-J.; Jiang, B.; Riaz, S.; Butt, G.Y.; Shi, D.-Y. A review of the components of brown seaweeds as potential candidates in cancer therapy. *RSC Adv.* **2016**, *6*, 12592–12610.

Ioannou, E.; Roussis, V. Natural Products from Seaweeds. In *Plant-Derived Natural Products*; Osburn, A.E., Lanzotti, V., Eds; Springer: New York, NY, USA, 2009; pp. 51–81

Kaser, A.; Zeissig, S.; Blumberg, R.S. Inflammatory bowel disease. *Annu. Rev. Immunol.* **2010**, *28*, 573–621.

Ko, S.J.; Bu, Y.; Bae, J.; Bang, Y.M.; Kim, J.; Lee, H.; Beom-Joon, L.; Hyun, Y.H.; Park, J.W. Protective effect of *Laminaria japonica* with probiotics on murine colitis. *Mediators Inflamm.* **2014**, *2014*, doi:10.1155/2014/417814.

Kuhn, R.; Lohler, J.; Rennick, D.; Rajewsky, K.; Muller, D. Interleukin-10-deficient mice develop chronic enterocolitis. *Cell* **1993**, *75*, 263–274.

Lee, S.W.; Ryu, B.; Park, J.W. Effects of *Sargassum pallidum* on 2,4,6-trinitrobenzene sulfonic acid-induced colitis in mice. *J. Korean Orient. Intern. Med.* **2010**, *32*, 224–241.

Loftus, E.V., Jr.; Sandborn, W.J. Epidemiology of inflammatory bowel disease. *Gastroenterol. Clin. N. Am.* **2002**, *31*, 1–20.

Lucas, R.; Giannini, C.; D'Auria, M.V.; Payá, M. Modulatory effect of bolinaquinone, a marine sesquiterpenoid, on acute and chronic inflammatory processes. *J. Pharmacol. Exp. Ther.* **2003**, *304*, 1172–1180.

Mulder, D.J.; Noble, A.J.; Justinich, C.J.; Duffinc, J.M. A tale of two diseases: The history of inflammatory bowel disease. *J. Crohns Colitis* **2014**, *8*, 341–348.

Murphy, C.; Hotchkiss, S.; Worthington, J.; McKeown, S.R. The potential of seaweed as a source of drugs for use in cancer chemotherapy. *J. Appl. Phycol.* **2014**, *26*, 2211–2264.

Na, H.J.; Moon, P.D.; Ko, S.G.; Lee, H.J.; Jung, H.A.; Hong, S.H.; Seo Y.; Oh, J.M.; Lee, B.H.; Choi, B.W.; Kim, H.M. *Sargassum hemiphyllum* inhibits atopic allergic reaction via the regulation of inflammatory mediators. *J. Pharmacol. Sci.* **2005**, *97*, 219–226.

Naito, Y.; Takagi, T.; Yoshikawa, T. Molecular fingerprints of neutrophil-dependent oxidative stress in inflammatory bowel disease. *J. Gastroenterol.* **2007**, *42*, 787–798.

Neurath, M.F. Animal models of inflammatory bowel diseases: Illuminating the pathogenesis of colitis, ileitis and cancer. *Dig. Dis.* **2012**, *30*, 91–94.

Oehlers, S.H.; Flores, M.V.; Hall, C.J.; Crosier, K.E.; Crosier, F.S. Retinoic acid suppresses intestinal mucus production and exacerbates experimental enterocolitis. *Dis. Model. Mech.* **2012**, *5*, 457–467.

Papadakis, K.A.; Targan, S.R. Role of cytokines in the pathogenesis of inflammatory bowel disease. *Annu. Rev. Med.* **2000**, *51*, 289–298.

Reagan-Shaw, S.; Nihal, M.; Ahmad, N. Dose translation from animal to human studies revisited. *FASEB J.* **2008**, *22*, 659–661.

Sansom C.E.; Larsen, L.; Perry, N.B.; Berridge, M.V.; Chia, E.W.; Harper, J.L.; Webb, V.L. An antiproliferative bis-prenylated quinone from the New Zealand brown alga *Perithalia capillaris*. *J. Nat. Prod.* **2007**, *70*, 2042–2044.

Scaldaferri, F.; Correale, C.; Gasbarrini, A.; Danese, S. Mucosal biomarkers in inflammatory bowel disease: Key pathogenic players or disease predictors? *World J. Gastroenterol.* **2010**, *16*, 2616–2625.

Shah, N.; Kammermeier, J.; Elawad, M.; Glocker, E.O. Interleukin-10 and interleukin-10-receptor defects in inflammatory bowel disease. *Curr. Allergy Asthma Rep.* **2012**, *12*, 373–379.

Smit, A.J. Medicinal and pharmaceutical uses of seaweed natural products: A review. *J. Appl. Phycol.* **2004**, *16*, 245–262.

Soehnlein, O.; Lindbom, L. Phagocyte partnership during the onset and resolution of inflammation. *Nat. Rev. Immunol.* **2010**, *10*, 427–439.

Strober, W.; Fuss, I.J.; Blumberg, R.S. The immunology of mucosal models of inflammation. *Annu. Rev. Immunol.* **2002**, *20*, 495–549.

Talero, E.; Alcaide, A.; Ávila-Román, J.; García-Mauriño, S.; Vendramini-Costa, D.; Motilva, V. Expression patterns of sirtuin 1-AMPK-autophagy pathway in chronic colitis and inflammation-associated colon neoplasia in IL-10-deficient mice. *Int. Immunopharmacol.* **2016**, *35*, 248–256.

Talero, E.; Bolivar, S.; Ávila-Román, J.; Alcaide, A.; Fiorucci, S.; Motilva, V. Inhibition of chronic ulcerative colitis-associated adenocarcinoma development in mice by VSL#3. *Inflamm. Bowel Dis.* **2015**, *21*, 1027–1037.

Talero, E.; Sánchez-Fidalgo, S.; de la Lastra, C.A.; Illanes, M.; Calvo, J.R.; Motilva, V. Acute and chronic responses associated with adrenomedullin administration in experimental colitis. *Peptides* **2008**, *29*, 2001–2012.

Terencio, M.C.; Ferrándiz, M.L.; Posadas, I.; Roig, E.; de Rosa, S.; De Giulio, A.; Payá, M.; Alcaraz, M.J. Suppression of leukotriene B4 and tumor necrosis factor α release in acute inflammatory responses by novel prenylated hydroquinone derivatives. *Naunyn Schmiedebergs Arch. Pharmacol.* **1998**, *357*, 565–572.

Treiner, E. Mucosal-associated invariant T cells in inflammatory bowel diseases: Bystanders, defenders, or offenders? *Front. Immunol.* **2015**, *6*, 27.

Tseng, C.K.; Chang, C.F. Chinese seaweeds in herbal medicine. *Hydrobiologia* **1984**, *116/117*, 152–154.

Tziveleka, L.A.; Abatis, D.; Paulus, K.; Bauer, R.; Vagias, C.; Roussis, V. Marine polyprenylated hydroquinones, quinones, and chromenols with inhibitory effects on leukotriene formation. *Chem. Biodivers.* **2005**, *2*, 901–909.

Yamada, S.; Koyama, T.; Noguchi, H.; Ueda, Y.; Kitsuyama, R.; Shimizu, H.; Tanimoto, A.; Wang, K.Y.; Nawata, A.; Nakayama, T.; et al. Marine hydroquinone zonarol prevents inflammation and apoptosis in dextran sulfate sodium-induced mice ulcerative colitis. *PLoS ONE* **2014**, *9*, e113509.

Yan, Y.; Kolachala, V.; Dalmasso, G.; Nguyen, H.; Laroui, H.; Sitaraman, S.V.; Merlin, D. Temporal and spatial analysis of clinical and molecular parameters in dextran sodium sulfate induced colitis. *PLoS ONE* **2009**, *4*, e6073.

8. Conclusions

Marine algae produce a variety of secondary metabolites with novel structures that possess interesting biological properties for drug discovery purposes. In this regard, the primary objective of this thesis was to investigate the chemical and pharmaceutical properties of the brown alga *Cystoseira usneoides*, with attention focused on identifying compounds capable of targeting oxidative stress, cancer, and inflammation. The research performed has led us to the following conclusions:

1. The acetone/methanol extract of the brown alga *Cystoseira usneoides* exhibits potent radical scavenging activity. The extract also inhibits the growth of HT-29 human colon cancer cells in dose- and time-dependent manners, causes apoptosis, and induces cell cycle arrest in G2/M phase. In addition, the extract shows significant activity as inhibitor of the production of the pro-inflammatory cytokine TNF-α, in LPS-stimulated THP-1 human macrophages.

2. The chemical study of the alga *Cystoseira usneoides* has allowed the isolation of six known meroterpenoids: usneoidone Z (**1**), 11-hydroxy-1′-*O*-methylamentadione (**2**), cystomexicone B (**3**), cystomexicone A (**4**), 6-*cis*-amentadione-1′-methyl ether (**5**), and amentadione-1′-methyl ether (**6**), together with six new related compounds: cystodiones A (**7**), B (**8**), C (**9**), D (**10**), E (**11**), and F (**12**).

3. The AMTs **1**-**10** display radical-scavenging activity in the ABTS assay; the more active compounds are **5**, **6**, **7**, and **8** which show an antioxidant capacity equal or superior to that of the standard (Trolox).

4. The AMTs **1-8** exhibit significant cytotoxic activity against human colon cancer cells (HT-29) and lower cytotoxicity against non-malignant cells; compounds **1**, **2**, **5**, **6**, and **8** show the highest indexes of cytotoxic activity and selectivity. Treatment of HT-29 cells with the AMTs **2**, **3**, and **5** induce to apoptosis, and the compounds **1**, **2**, **3**, **4**, **5**, and **7** arrest the cell

cycle in G2/M phase. In addition, the AMTs **1**-**8** produce inhibitory effects on the migration and invasion of such type of cells.

5. The mechanistic analysis revealed that the anticancer effects of the AMTs **1**-**8** on human colon cancer cells occur through the down-regulation of p-ERK, p-JNK, and p-AKT signaling pathways. These results may provide novel clues as to how meroterpenes of *Cystoseira usneoides* play a role in the prevention/treatment of colon cancer.

6. The *in vitro* anti-inflammatory assays showed that the AMTs **1**-**8** reduce the production of pro-inflammatory cytokines in stimulated human macrophages; the meroditerpenes **1** and **2** display the higher inhibitory effect for TNF-α, IL-6, and IL-1β. In addition, compounds **2, 3**, **4**, **5**, **6**, and **7** significantly down-regulate the expression of COX-2, and all compounds suppress the iNOS expression.

7. The AMTs **1**-**8** display cytotoxic activity against human lung cancer cells (A549); the most active compounds are **1**, **2**, **5**, and **6**. Cell cycle analyses indicate that most of AMTs cause the arrest of A549 cells at the S and G2/M phases.

8. The selected meroterpene 11-hydroxy-1′-*O*-methylamentadione (**2**, AMT-E) effectively ameliorates the dextran sulfate sodium-induced colitis parameters in mice, by increasing mucus production, inhibiting neutrophil infiltration, down-regulating TNF-α, IL-1β, and IL-10, as well as suppressing COX-2 and iNOS expression in the colon tissue. These findings provide valuable information toward the development of new molecules from macroalgae with potential therapeutic benefits in inflammatory bowel disease.

Currently it is well established that oxidative stress, chronic inflammation, and cancer are closely related (Figure 8.1). Oxidative stress leads to DNA damage, mutagenesis, and destruction of diverse biological macromolecules. These changes may contribute to cancer through distinct mechanisms including inhibition of apoptosis, increase of cellular proliferation, angiogenesis, and disruption of DNA repair mechanism. Cancer cells and

inflammatory cells themselves liberate free radicals and a number of soluble mediators, including metabolites of arachidonic acid, cytokines, and chemokines, which leads to release and accumulation of reactive species. These, in turn, intensely recruit inflammatory cells in a vicious circle. Moreover, it is known that pathways that are regulated by ROS lead to the pathogenesis of cancer and inflammation, and include: modulation of numerous main molecular players such as prostaglandins and cytokines, various transcription factors, and kinase pathways including, NF-κB, MAPK and PI3K/Akt pathways, among others.

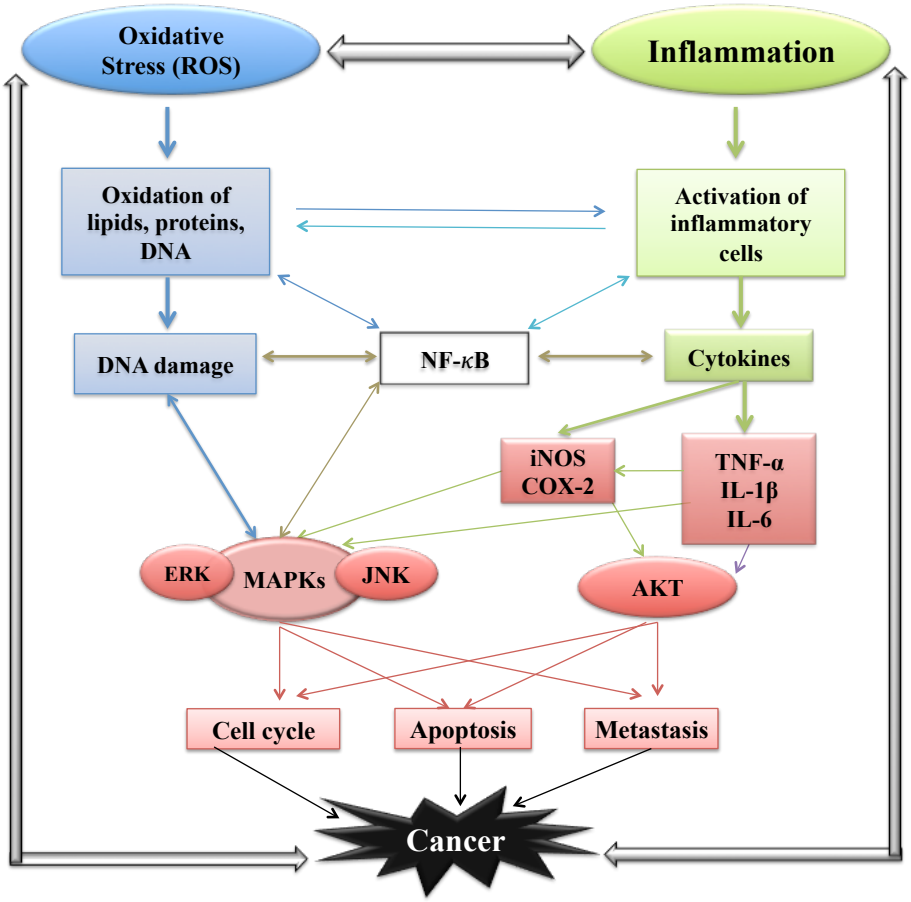

Figure 8.1. Schematic representation indicating the interdependence between oxidative stress, inflammation, and cancer. The targets assayed with positive response after treatment with AMTs **1**-**8** are colored in red.

The research conducted in this thesis has demonstrated that the meroterpenoids produced by the brown alga *Cystoseira usneoides* possess significant antioxidant, antitumor, and anti-inflammatory properties (Figure 8.2).

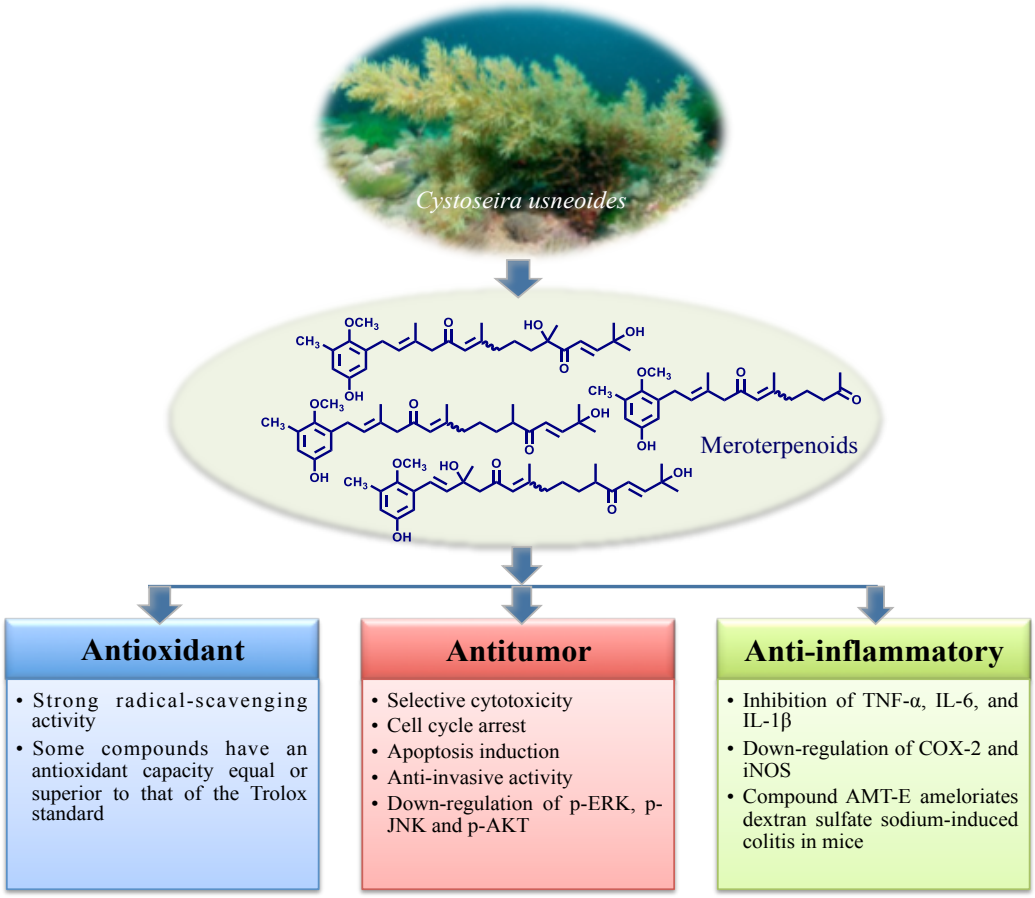

Figure 8.2. Biological properties identified in this thesis for the meroterpenoids of the alga *C. usneoides*.

These results encourage the continuation of studies for the use of this seaweed as valuable source for generating new health products, such as functional ingredients, or for the pharmaceutical industries. Hopefully, the results herein described may provide inspiration for the development of novel drugs from marine macroalgae, which could be used in inflammation/cancer prevention and treatment.